



UNIVERSIDADE CATÓLICA PORTUGUESA

**MATHEMATICAL MODELLING OF
SHELF LIFE LIMITING FACTORS
DURING STORAGE OF ORANGE JUICE**

Thesis submitted to the *Universidade Católica Portuguesa* to attain the degree of
PhD in Biotechnology with specialisation in Food Science and Engineering

by

Maria da Conceição Antas de Barros Menéres Manso



ESCOLA SUPERIOR DE BIOTECNOLOGIA

July 2000

UNIVERSIDADE CATÓLICA PORTUGUESA

**MATHEMATICAL MODELLING OF
SHELF LIFE LIMITING FACTORS
DURING STORAGE OF ORANGE JUICE**

Thesis submitted to the *Universidade Católica Portuguesa* to attain the degree of
PhD in Biotechnology with specialisation in Food Science and Engineering

by

Maria da Conceição Antas de Barros Menéres Manso

Under the supervision of Fernanda A. R. Oliveira, Professor

ESCOLA SUPERIOR DE BIOTECNOLOGIA

July 2000

Aos meus pais...

To my parents...

Sumário / Abstract

Sumário

O sumo de laranja é comercializado e consumido em todo o mundo e a sua qualidade não pode ser definida numa base subjectiva. Para fazer uma avaliação objectiva é necessário definir vários parâmetros da qualidade. O tempo de vida útil de alimentos é o tempo ao fim do qual se verifica que o producto se torna inaceitável sob o ponto de vista de segurança, sensorial /ou nutricional. Este período depende das características do produto, da embalagem e das condições de armazenamento. O tempo de vida útil de sumo de laranja pasteurizado é basicamente determinado por alterações químicas e a sua previsão carece da selecção de indicadores da qualidade adequados, bem como da identificação de indicadores críticos, isto é, aqueles que primeiro atingem o seu limite de aceitabilidade e por isso limitam a vida do produto. A técnica usual para determinar o tempo de vida de sumos processados assepticamente consiste na avaliação da qualidade em condições que simulam as reais. Testes acelerados, realizados em condições de armazenamento abusivas (por ex., temperatura elevada, concentrações de oxigénio elevadas), de forma a que a velocidade de deterioração do alimento seja mais rápida e, portanto os testes mais curtos, podem também ser utilizados e são particularmente interessantes neste caso, devido ao longo tempo de vida do produto.

O trabalho desenvolvido no contexto desta tese tem como objectivo contribuir para uma melhor compreensão das características que limitam o tempo de vida útil de sumo de laranja pasteurizado e, particularmente, para a modelagem das cinéticas dos indicadores da qualidade em condições de armazenamento normais e abusivas. Os objectivos específicos são (i) identificar os indicadores da qualidade críticos, (ii) analisar o efeito da temperatura e da concentração de oxigénio dissolvida após embalagem como factores de aceleração das reacções de formação ou degradação dos indicadores da qualidade e verificar a fiabilidade dos testes acelerados e (iii) desenvolver modelos matemáticos genéricos para descrever alterações da qualidade (ácido ascórbico (L-AA), acastanhamento, 5-hidroximetil-2-furfuraldeído, 2-furfuraldeído, 4-vinil-guaiacol) em sumo de laranja pasteurizado e embalado assepticamente, armazenado em condições normais e abusivas (temperatura e oxigénio). Tendo-se verificado que o ácido ascórbico é o factor crítico que limita o tempo de vida útil, os objectivos da tese integraram ainda: (i) a análise do efeito da adição de L-AA no tempo de vida do sumo de laranja e o estudo cinético do(s) indicador(es) da qualidade crítico(s) nestas condições e (ii) o estudo cinético desse(s) indicador(es) em sumo de laranja com e sem adição de vitamina C, em condições aeróbicas e anaeróbicas, numa gama de temperaturas alargada.

Experiências realizadas com sumo de laranja embalado assepticamente em pacotes Tetra Brik Aseptic (TBA), em condições de armazenamento isotérmicas, numa gama alargada de temperaturas (4 a 50 °C), mostraram que a degradação de L-AA, o escurecimento não enzimático e a alteração de compostos aromáticos são muito afectados pela temperatura, enquanto que a

concentração inicial de oxigénio dissolvida (1.0 a 10.2 ppm) não tem um efeito significativo. Este resultado limita o uso de elevadas concentrações iniciais de oxigénio como factor de aceleração para estudos de tempo de vida útil.

Foram desenvolvidos modelos matemáticos empíricos para descrever a cinética de degradação ou formação de indicadores da qualidade durante a armazenagem de sumo de laranja nas condições acima descritas. O escurecimento não enzimático e o 2-furfuraldeído foram bem descritos por um modelo de ordem zero, enquanto que o 4-vinil-guaiacol seguiu um modelo de primeira ordem. A formação do 5-hidroxi-metil-2-furfuraldeído mostrou uma descontinuidade com o tempo, que foi modelizada por duas reacções consecutivas de ordem zero, sendo a segunda muito mais rápida que a primeira. O inverso foi verificado para o L-AA (duas reacções consecutivas de primeira ordem), cuja velocidade de degradação foi muito mais rápida para tempos curtos. Isto foi atribuído a dois mecanismos reaccionais diferentes: um mecanismo aeróbico que domina enquanto há oxigénio disponível, seguido por uma reacção mais lenta quando a concentração de oxigénio é muito baixa. No entanto, verificou-se que este último mecanismo não é verdadeiramente anaeróbico, já que na completa ausência de oxigénio o L-AA parece não se degradar. O modelo de Weibull também descreve bem a degradação do L-AA, com a vantagem de ser muito mais simples e necessitar de um menor número de parâmetros. As constantes de reacção dos modelos acima descritos aumentam com a temperatura de acordo com equações do tipo lei de Arrhenius, em alguns casos com uma menor sensibilidade à temperatura (energia de activação) para temperaturas inferiores a aproximadamente 30 °C, do que a temperaturas acima deste valor.

Verificou-se que o indicador da qualidade crítico era o L-AA, seguido pelo escurecimento não enzimático. A adição de L-AA ao sumo de laranja permite aumentar o tempo de vida útil, porque a adição deste composto diminui a sua velocidade de degradação. No entanto, o L-AA continuou a ser o factor limitante do tempo de vida do sumo de laranja, excepto quando quantidades razoáveis deste composto eram adicionadas.

Tanto o modelo de Weibull como o de duas reacções consecutivas de primeira ordem provaram descrever bem a degradação de L-AA em armazenamento de sumo com adição de L-AA em condições de temperatura normais e abusivas. No entanto, o modelo de Weibull mostrou ser mais aplicável no caso de testes acelerados de vida útil, porque a constante de reacção não apresenta descontinuidades com a temperatura. A segunda reacção do modelo de duas reacções consecutivas de primeira ordem mostrou uma maior sensibilidade à temperatura em condições abusivas (35 a 45 °C) do que a temperaturas de armazenamento normais, o que impede a sua utilização em testes acelerados. A constante de reacção do escurecimento aumentou com a adição de L-AA e este foi bem descrito por um modelo de ordem zero.

Estudos relativos à degradação de L-AA e de ácido dehidroascórbico (DA) em sumo de laranja, com excesso de oxigénio, permitiram o desenvolvimento de um modelo mecanístico que descreve

o efeito estabilizante da adição do L-AA na sua degradação. Este mecanismo assume que a conversão de L-AA em DA é reversível, sendo a reconversão de DA em L-AA dependente da concentração de L-AA, e que o DA se degrada irreversivelmente. A constante de reacção destas reacções aumenta com a temperatura de acordo com uma lei de Arrhenius, sendo que a reacção de reconversão de DA em L-AA é mais sensível à temperatura. A degradação do L-AA nestas condições, foi também descrita pelo modelo de Weibull, mas este necessita um maior número de parâmetros para ter em conta o efeito da temperatura e da adição de L-AA. O escurecimento não enzimático segue um modelo de Weibull que tende para um valor de equilíbrio, mas não foi possível testar este modelo detalhadamente porque na maior parte das situações o escurecimento foi demasiado pequeno para permitir uma análise detalhada dessa cinética. O escurecimento aumentou linearmente com o nível de adição de L-AA.

Abstract

Orange juice is traded and consumed worldwide and its quality cannot be determined solely by subjective assessments. To make assessments more objective, several quality parameters have to be defined. The shelf life of food and beverages is the time after which the product becomes unacceptable from a safety, sensorial and/or nutritional perspectives. It depends on the product characteristics, packaging and storage conditions. The shelf life of pasteurised orange juice is primarily determined by chemical changes. For forecasting shelf life of a product, it is imperative to select adequate shelf life indicators, and to identify the critical ones, that is, those that first reach the respective threshold level and thus limit product shelf life. The usual technique for determination of shelf life of aseptically processed juices consists on the quality evaluation during storage in simulated real conditions. Accelerated Shelf Life Tests (ASLT), which are tests carried out at abusive storage conditions (e.g. high temperature, high oxygen content), so that food deterioration rate is much faster and thus tests are much shorter, may also be used and are of particular interest in this case because of the long-shelf life of the product.

The work developed in the framework of this thesis aims at contributing to the understanding of the characteristics that limit the shelf life of pasteurised orange juice, and particularly at the modelling of quality indicators kinetics in both normal and abusive conditions. Specific objectives included (i) to identify critical quality indicators, (ii) to analyse the effect of temperature and initial dissolved oxygen content as accelerating factors of the reactions of formation or degradation of the quality indexes, and to assess the reliability of ASLT, and (iii) to develop general mathematical models to describe quality changes (L-ascorbic acid, browning, 5-hydroxymethyl-2-furfuraldehyde, 2-furfuraldehyde, and 4-vinyl-guaiacol) in pasteurised orange juice stored in normal and abusive conditions (temperature and oxygen). As ascorbic acid was found to be the critical factor limiting shelf life, the work objectives were extended to: (i) assess the effect of supplementing orange juice with ascorbic acid on shelf life and to study the kinetics of the critical quality indicator(s) in these conditions and (ii) further study the kinetics of the critical quality indicator(s) in both ascorbic acid supplemented and non-supplemented juice, under aerobic and anaerobic conditions, in a range of temperatures.

Experiments carried out with orange juice packed in Tetra Brik Aseptic cartons, under isothermal conditions covering a wide range of temperatures (4 to 50 °C), showed that L-AA, browning, and flavour compounds were greatly affected by temperature whereas initial dissolved oxygen content (1.0 to 10.2 ppm) did not show a significant effect during storage. This limits the use of high initial oxygen contents as an accelerating factor for shelf life studies.

Empirical mathematical models were developed to describe the degradation kinetics of a number of quality indicators during storage of orange juice in the conditions above described. Browning and 2-furfuraldehyde were well described by a zero-order model whereas 4-vinyl-guaiacol

followed a first-order model. Formation of 5-hydroxymethyl-2-furfuraldehyde showed a discontinuity with time, which was modelled by two consecutive zero-order reactions, the second being much faster than the first. The reverse was observed for L-ascorbic acid (two consecutive first-order reactions), which degradation rate was much faster at short times. This was attributed to two different reactive pathways: an aerobic mechanism dominating while oxygen was available, followed by a slower anaerobic reaction when oxygen concentration was very small. It was however found that the later mechanism was not truly anaerobic, as in the complete absence of oxygen L-AA does not degrade. The Weibull model was also found to provide a good description of L-AA degradation, with the advantage of being much simpler and requiring less model parameters. The rate constants of the models above described, increased with temperature according to an Arrhenius-type equation, in some case with a lower sensitivity to temperature (activation energy) at temperatures below approximately 30 °C than at temperatures above this value.

L-AA was found to be the critical shelf life quality indicator, closely followed by browning. Supplementation of orange juice with L-AA led to increased shelf life, as addition of L-AA to orange juice slows down its degradation rate. However, L-AA remained the critical factor that limits orange juice shelf life, except when reasonable amounts of L-AA were added to the juice. Both the Weibull and the two consecutive first-order models provided a good description of the kinetics of degradation of L-AA during storage of L-AA supplemented juice under normal and abusive temperature conditions. Nevertheless, the Weibull model showed to be more suitable for accelerated shelf life testing, as the rate constant did not show any discontinuity with temperature. The second reaction of the two consecutive first-order reactions model shows a much higher sensitivity to temperature in abusive conditions (35 to 45 °C) than in normal storage temperatures, which hinders its use in ASLT. Browning rate increased with added L-AA content and was well described by zero-order kinetics.

Studies on L-AA and dehydroascorbic acid (DA) degradation in orange juice with excess oxygen allowed to develop a mechanistic model that could describe the stabilizing effect of added L-AA on its degradation. This mechanism assumes that L-AA conversion into DA is reversible, the reconversion of DA into L-AA being dependent on L-AA concentration, and that DA decomposes irreversibly into degradation products. The rate constants of these reactions were found to increase with temperature according to an Arrhenius-type relationship, being the reaction of reconversion of DA into L-AA more sensitive to temperature than the others. L-AA degradation in these conditions could also be well described by the Weibull model, although it would require a large number of parameters to account for temperature and added L-AA effects. Browning appears to follow a Weibull model levelling off to an equilibrium value, although this model could not be thoroughly tested because in most situations the extension of browning was too small to allow to a detailed analyses of its kinetics. Browning rate increased linearly with initial L-AA contents.

Acknowledgements

I wish to express my thanks to *Escola Superior de Biotecnologia* of the Catholic University of Portugal (ESB-UCP) for accepting me as a PhD student and providing the necessary conditions for my work.

To *Fundação para a Ciência e Tecnologia* for the support of this research work through program PRAXIS XXI (grant BD/16024/98). I am also grateful to *Fundação Caloust Gulbenkian*, *Fundação Luso-Americana para o Desenvolvimento* and ESB-UCP for providing me with additional financial support that allowed me a continuous exposure to different levels of food research.

To my supervisor, Professor Fernanda Oliveira, my very special gratitude and admiration for believing in my abilities. She always helped and encouraged me, and besides being a very good supervisor she became a very good friend.

To Dr. Rikard Öste for receiving me in the department of Applied Nutrition and Food Chemistry- Lund University (Sweden) as well as to Dr. Lília Arhné for all her support and help in Tetra Pak (Research & Development AB - Lund, Sweden). They both provided the environment necessary to conduct the experimental work presented in Part II of this thesis.

I thank Professor João Lourenço for receiving me at the Inter-University Institute of Macau, Macao, where I had excellent facilities to perform my work.

I thank Professor Fernanda Oliveira for receiving me at the department of Food Engineering, University College Cork, and all staff members and postgraduate researchers. They all created a warmfull environment that helped me to complete this thesis.

To Professor Vassilis Gekas, Professor Jorge Oliveira, Dr. Luís Cunha and Dr. Jesús Frías for their ideas, and helpful knowledgement that showed me the way to solve various problems, and added a valuable contribution to improve manuscripts and communications.

I am grateful to the Oliveira family, the Freire family, José and Luís for their help and friendship during my stay in Macao. These thanks are renewed to the Oliveira family during my stay in Cork.

I am also grateful to Cristina (and family) for her (their) friendship through many years.

To my friends and colleagues for their support and motivation (I won't discriminate names as each one of you had a very special contribution to the accomplishment of this work).

Finally, to my parents and brother, and all those in my family that have given me constant encouragement and love, my most deep and sincere thanks.

Maria da Conceição Manso

21st of July 2000

TABLE OF CONTENTS

Sumário	v
Abstract	viii
Acknowledgements	xi
Table of Contents	xiii
List of Symbols	xix
List of Equations	xxiv
List of Figures	xxxiii
List of Tables	xl
General Introduction	2

PART I

INTRODUCTION

Chapter 1. State-of-the-art	8
1.1. Introduction	8
1.2. Orange Juice Categories	9
1.2.1. Ready to Drink Orange Juice	9
1.2.1.1. Fresh squeezed orange juice	10
1.2.1.2. Not-from-concentrate juice (NFC)	10
1.2.1.3. From concentrate	11
1.2.1.4. Fortified orange juice	11

1.2.1.4.1. Juice with added floating pulp	11
1.2.1.4.2. Vitamin enriched	12
1.2.1.4.3. Calcium enriched	12
1.2.1.4.4. Fibre enriched	12
1.2.2. Concentrate Orange Juice	12
1.2.2.1. Frozen concentrated orange juice (FCOJ)	12
1.2.2.2. Concentrate at approximately 52 °brix	13
1.2.3. RTD Orange Products that should not be Called Orange Juice	13
1.2.3.1. Orange nectar	15
1.2.3.2. Orange juice drinks	15
1.2.3.3. Orange flavour drinks	15
1.3. Regulations Governing Juice Origin	15
1.4. Aspects that Fix the Limits of Product Shelf Life	16
1.4.1. Microbiology of Orange Juice	16
1.4.2. Nutrient Loss	19
1.4.2.1. Vitamin C	19
1.4.2.2. Vitamin B complex	23
1.4.3. Colour Stability	23
1.4.4. Flavour/Off-Flavour Development	25
1.5. Factors that Influence Product Shelf Life	28
1.5.1. Processing Treatment (Pasteurisation)	28
1.5.1.1. Inactivation of enzymes	29
1.5.1.2. Inactivation of microorganisms	30
1.5.2. Storage Temperature	32

1.5.3. Oxygen Content	32
1.5.4. Light	34
1.5.5. Packaging System - Properties of and Type of Containers	35
1.6. Mathematical Modelling of Quality Characteristics Decay	40
1.6.1. Simple Kinetic Models	42
1.6.1.1. Zero-order	43
1.6.1.2. First-order	43
1.6.1.3. Second-order	43
1.6.1.4. Probabilistic models – Weibull model	44
1.6.2. Dependence of Rate Constants on Temperature	46
1.6.2.1. Arrhenius law	46
1.6.2.2. Q ₁₀ concept	48
1.6.3. Modelling of Ascorbic Acid Degradation, Browning, Off-Flavour Development and Oxygen Consumption	49
1.6.3.1. Ascorbic acid	50
1.6.3.2. Browning	61
1.6.3.3. Off-flavour development	64
1.6.3.4. Oxygen	64
1.7. Shelf life Estimation	66
1.7.1. Shelf-life Estimation and Product Development	66
1.7.2. Methods for Shelf Life Estimation	67
1.7.3. Accelerated Tests for Shelf Life Estimation	69
1.7.3.1. Accelerated tests at elevated temperatures	69
1.7.3.2. Accelerated tests at high oxygen pressures	69

PART II
ANALYSIS OF THE CHANGES OF QUALITY
CHARACTERISTICS OF ASEPTICALLY PACKAGED ORANGE
JUICE DURING STORAGE

Chapter 2. Selection of quality indicators and identification of suitable conditions for accelerated storage tests of aseptically packaged orange juice	72
2.1. Introduction	73
2.2. Material and Methods	75
2.2.1. Product, packaging material and processing conditions	75
2.2.2. Experimental design	76
2.2.3. Analytical determinations	77
2.3. Results and Discussion	80
2.3.1. Effect of temperature and initial dissolved oxygen content on degradation of quality characteristics	80
2.3.2. Selection of shelf life indicators	82
2.4. Conclusions	88
Chapter 3. Modelling oxygen changes during storage of aseptic packaged orange juice	89
3.1. Introduction	90
3.2. The Mathematical Model	92
3.3. Material and Methods	95
3.3.1. Processing, packaging and experimental design	95
3.3.2. Package permeability measurements	95

3.3.3. Dissolved oxygen concentration measurement	96
3.3.4. Data for validation of the model	96
3.4. Results and Discussion	97
3.4.1. Modelling of dissolved oxygen concentration	97
3.4.2. Validation of the model	100
3.5. Conclusions	104
Chapter 4. Modelling ascorbic acid, browning and flavours changes during storage of aseptic packaged orange juice	105
4.1. Introduction	106
4.2. Mathematical Modelling	108
4.3. Material and Methods	109
4.4. Results and Discussion	109
4.4.1. L-Ascorbic acid	109
4.4.2. Browning index	121
4.4.3. Hydroxymethyl-2-furfuraldehyde	126
4.4.4. 2-Furfuraldehyde	132
4.4.5. 4-Vinyl-guaiacol	134
4.5. Conclusions	138

PART III

**MODELLING DEHYDROASCORBIC ACID, L-ASCORBIC ACID
AND BROWNING IN CONTROLLED CONDITIONS**

Chapter 5. Effect of ascorbic acid addition on L-ascorbic acid degradation and browning during storage in orange juice	141
5.1. Introduction	142
5.2. Material and Methods	143
5.2.1. Experimental design	143
5.2.2. Analytical determinations	144
5.2.3. Data analysis	146
5.3. Results and Discussion	147
5.3.1. L-Ascorbic acid degradation	147
5.3.2. Browning index	160
5.3.3. Shelf life prediction by accelerated testing	164
5.4. Conclusions	168
Chapter 6. Effect of continuous aeration on L-ascorbic acid, dehydroascorbic acid and browning kinetics	169
6.1. Introduction	170
6.2. Material and Methods	171
6.2.1. Experimental design	171
6.2.2. Analytical determinations	173
6.2.3. Data analysis	173

6.3. Results and Discussion	174
6.3.1. L-Ascorbic acid degradation under excess oxygen	174
6.3.2. Browning under excess oxygen	186
6.3.3. L-Ascorbic acid degradation in anaerobic conditions	190
6.4. Conclusions	191
Chapter 7. Effect of ascorbic acid addition on L-ascorbic acid degradation and browning under excess oxygen conditions	193
7.1. Introduction	194
7.2. Material and Methods	195
7.2.1. Experimental design	195
7.2.2. Analytical determinations	196
7.2.3. Data analysis	196
7.3. Results and discussion	197
7.3.1. L-Ascorbic acid degradation under excess oxygen	197
7.3.2. Browning under excess oxygen	210
7.3.3. L-Ascorbic acid degradation in anaerobic conditions	213
7.4. Conclusions	215
General Conclusions and Recommendations for Further Work	218
List of Communications based on thesis work	224
References	229

List of Symbols

Roman Symbol

A	reactant species A (in Chapter1) and package surface area (m^2) (in Chapter3) dehydroascorbic acid, in Figure 1.4
a_k	value of the rate constant for juice with with no added L-AA content (s^{-1}), Eq. 7.6
a_γ	Value of the constant γ for juice with no added L-AA, Eq. 7.3
$A_{k_{ref}}$	value of k_{ref} for juice with no added L-AA (s^{-1}), Eq. 5.1 to 5.3
B	reactant species B (in Chapter1)
b	constant of the dependence of the time of oxygen depletion with temperature ($^{\circ}C^{-1}$) Eq. 4.6 and 5.4
b_k	slope of the linear dependence of the rate constant C_{add} , ($L/(^{\circ}C.mg)$), Eq. 7.6
b_γ	slope of the linear dependence of the constant γ with C_{add} ($L/(^{\circ}C.mg)$), Eq. 7.3
$B_{k_{ref}}$	constants of the dependence of the rate constant at a T_{ref} with C_{add} , Eq. 5.1 to 5.3
C	concentration (in Chapter1)
C_A	concentration of species A at any time t (in Chapter1)
C_A^i	concentration of species A at time zero (in Chapter1)
C_a	L-AA concentration at a time t (mg/L)
C_a^i	initial L-AA concentration (mg/L)
C_{add}	added L-AA content (mg/L)
C_B	concentration of species B at time t (in Chapter1)
C_B^i	concentration of species B at time zero (in Chapter1)
C_{Br}	browning “concentration” at any time t (Abs. 420 nm)
C_{Br}^c	browning “concentration” at the time when the zero-order kinetics starts (Abs. 420 nm), Eq. 4.12

C_{Br}^i	browning “concentration” at time zero (Abs. 420 nm)
C_{Br}^∞	browning “concentration” at the standstill period, Eq. 4.11-4.12, or browning concentration at the equilibrium, Eq. 6.11-6.12 (Abs. 420 nm)
C_{da}	concentration of dehydroascorbic acid at any time t (mg/L)
C_F	concentration of furfural at any time t (ppb)
C_{HMF}	concentration of HMF at any time t (ppb)
C_{O_2}	concentration of dissolved oxygen in the juice at a time t (ppm)
$C_{O_2}^\infty$	equilibrium concentration dissolved oxygen concentration (ppm)
$C_{O_2}^i$	initial concentration of dissolved oxygen in the juice (ppm)
$C_{O_2}^{out}$	concentration of oxygen in the storage atmosphere (ppm)
C_P	concentration of PVG at any time t (ppb)
C_P^i	concentration of PVG at time zero (ppb)
C_P^∞	concentration of PVG at the equilibrium (ppb)
D	diffusion coefficient of oxygen in the packaging material (m ² /s)
d	thickness of the packaging material (m)
$D_{t_{c,ref}}$	time for O ₂ depletion for juice with no added L-AA at the reference temperature, Eq. 5.4
Ea	activation energy (kJ/mole)
Ea ₀	activation energy of the batch with no added L-AA content (kJ/mol), Eq. 7.13
k	rate constant (s ⁻¹)
k ₀	pre-exponential factor of the Arrhenius equation (s ⁻¹), Eq. 1.11 rate constant for juice without added L-AA at the reference

	temperature (s ⁻¹), Eq. 5.6
k_D	oxygen mass transfer coefficient (s ⁻¹) defined in equations (3.3) and (3.5)
k_{int}	mass transfer coefficient inside the package (m/s)
k_{out}	mass transfer coefficient outside the package (m/s)
$k_{overall}$	overall mass transfer coefficient (m/s)
k_p^1	oxygen partition coefficient of the package material at the outside wall
k_p^2	oxygen partition coefficient of the package material at the inside wall
k_p'	ratio of the oxygen partition coefficients (k_p^2/k_p^1)
k_R	reaction rate constant (s ⁻¹), (Chapter 3)
k_{ref}	rate constant at a reference temperature T_{ref} (°C)
m	slope of the dependence of the shape constant with temperature (°C ⁻¹) Eq. 4.8 and 5.5
	slope of the dependence of the scale parameter at the highest temperature with added L-AA content (C_{add}) (s.L/mg), Eq. 7.2
$m_{(1/\alpha)}$	slope of the linear variation of the rate constant at a reference temperature T_{ref} with added L-AA concentration (C_{add}), Eq. 5.5
m_{Ea}	slope of the dependence of the activation energy with added L-AA content (kJ.L/(mol.mg)), Eq. 7.7
m_k	slope of the linear relation of the rate constant at a reference temperature with C_{add} , (L/(mg.s ⁻¹)), Eq. 5.6
• $\dot{M}_{Kinetics}$	reaction rate
• $\dot{M}_{Mass Transfer}$	mass transfer rate

$m_{t_c,ref}$	slope of the linear relation of time of oxygen depletion at T_{ref} with C_{add} , Eq. 5.4
R	universal gas constant (8.314 J/(mol K))
$R^2_{adj.}$	determination coefficient
t	time (s)
t_0	parameter of the Weibull model, Eq. 4.19
t_c	critical time of behaviour change (s), (in Chapter 4) time of oxygen depletion (s), Eq. 4.1 to 4.6 and 5.1 to 5.4
$t_{c,ref}$	time of oxygen depletion at a reference temperature (s)
T_{ref}	reference temperature (°C)
$t_{w_{max}}$	time of maximum degradation rate (s)
V	package volume (m ³)
w_{max}	maximum degradation rate

Greek Symbols

α	time parameter of the Weibull equation (s)
$1/\alpha$	rate constant of the Weibull equation (s ⁻¹)
$(1/\alpha)_0$	rate constant at the reference temperature when no L-AA is added (s ⁻¹), Eq. 5.5
$(1/\alpha)_{ref}$	rate constant (s ⁻¹) at a reference temperature, in equation 4.8
α^i	scale constants at the highest (initial) temperature (s), Eq. 7.2
α^∞	scale constants at the lowest (final) temperature (s), Eq. 7.2
$\alpha _{T=45}$	value of the dependence of the scale parameter at the highest temperature (s), Eq. 7.2
β	shape factor of the Weibull equation
β_a	parameter of Eq. 7.4
β_b	parameter of Eq. 7.4 (°C ⁻¹)
β_c	parameter of Eq. 7.4 (°C ⁻²)
β_{ref}	shape constant at the reference temperature

γ constant of the dependence on temperature in Eq. 7.3

Subscripts

a L-ascorbic acid
Br Browning
da Dehydroascorbic acid
F Furfural
HMF 5-Hydroxymethyl-2-furfural
PVG 4-Vinyl-guaiacol

Superscripts

c critical
i at time zero
out outside
 ∞ at equilibrium

Abbreviations

A Dehydroascorbic acid, in Figure 1.4
AA, L-AA L-Ascorbic acid
ASLT Accelerated shelf life testing
Br Browning index
DA Dehydroascorbic acid
F, Furf Furfural or 2-Furfuraldehyde
HMF 5-Hydroxymethyl-2-furfural
L-AA L-ascorbic acid
OJ Orange juice
PVG 4-Vinyl-guaiacol
SL Shelf life
TA Titrable acidity

List of Equations

Chapter 1

$$-\frac{dC}{dt} = k \quad (1.1)$$

$$C = C^i - k \times t \quad (1.2)$$

$$-\frac{dC}{dt} = k \times C \quad (1.3)$$

$$C = C^i \times e^{-k \times t} \quad (1.4)$$

$$-\frac{dC_A}{dt} = k \times C_A^2 \quad (1.5)$$

$$-\frac{dC_A}{dt} = k \times C_A \times C_B \quad (1.6)$$

$$C_A = \frac{1}{\frac{1}{C_A^i} + k \times t} \quad (1.7)$$

$$C_A = C_B \frac{C_A^i}{C_B^i} \times e^{-(C_A^i - C_B^i) \times k_2 \times t} \quad (1.8)$$

$$f(t) = \begin{cases} \frac{\beta}{\alpha} \left(\frac{t}{\alpha}\right)^{\beta-1} e^{-\left(\frac{t}{\alpha}\right)^\beta}, & t > 0 \\ 0 & , \text{elsewhere} \end{cases} \quad (1.9)$$

$$F(t) = \int_0^t f(t) dt = 1 - e^{-\left(\frac{t}{\alpha}\right)^\beta} \quad (1.10)$$

$$k = k_0 \times e^{-\frac{Ea}{R} \times \frac{1}{T}} \quad (1.11)$$

$$k = k_{ref} \times e^{-\frac{Ea}{R} \times \left(\frac{1}{T} - \frac{1}{T_{ref}}\right)} \quad (1.12)$$

$$k_{ref} = k_0 \times e^{-\frac{Ea}{R} \times \frac{1}{T_{ref}}} \quad (1.13)$$

$$Q_{10} = \frac{\theta_s \text{ at } T}{\theta_s \text{ at } T+10} = \frac{\text{rate at } T+10}{\text{rate at } T} \quad (1.14)$$

$$Q_{10}^{\Delta/10} = \frac{Q_s(T_1)}{Q_s(T_2)} \quad (1.15)$$

$$\theta_{20} = \theta_{35} \times Q_{10}^{\Delta/10} = 6 \times 3^{15/10} = 31.2 \text{ months} \quad (1.16)$$

Chapter 3

$$V \frac{d(C_{O_2})}{dt} = \dot{M}_{\text{Mass Transfer}} + \dot{M}_{\text{Kinetics}} \quad (3.1)$$

$$\frac{1}{k_{\text{overall}}} = \frac{k_p^2}{k_p^1} \frac{1}{k_{\text{int}}} + \frac{1}{k_p^1} \frac{d}{D} + \frac{1}{k_{\text{out}}} \quad (3.2)$$

$$\left(\frac{dC_{O_2}}{dt}\right)_{\text{Mass Transfer}} = k_D \times (C_{O_2}^{\text{out}} - k'_p \times C_{O_2}) \quad (3.3)$$

$$k'_p = \frac{k_p^2}{k_p^1} \quad (3.4)$$

$$k_D = \frac{A}{V} k_{\text{overall}} \quad (3.5)$$

$$\left(\frac{dC_{O_2}}{dt}\right)_{\text{kinetics}} = k_R C_{O_2} \quad (3.6)$$

$$C_{O_2} = C_{O_2}^{\infty} + (C_{O_2}^i - C_{O_2}^{\infty}) \times e^{-kt} \quad (3.7)$$

$$C_{O_2}^{\infty} = \frac{k_D C_{O_2}^{\text{out}}}{k_R + k'_p k_D} \quad (3.8)$$

$$k = k_R + k'_p k_D \quad (3.9)$$

Chapter 4

$$C_a = C_a^i \times e^{-k_1 \times t} \quad t \leq t_c \quad (4.1)$$

$$C_a = C_a^i \times e^{-k_1 \times t} \times e^{-k_2 \times (t - t_c)} \quad t > t_c \quad (4.2)$$

$$C_a = C_a^i \times e^{-k_{1ref} \times t} \times e^{-\frac{Ea_1}{R} \left(\frac{1}{273.15+T} - \frac{1}{273.15+T_{ref}} \right)} \times t \quad t \leq t_c \quad (4.3)$$

$$C_a = C_a^i \times e^{-k_{1ref} \times t} \times e^{-\frac{Ea_1}{R} \left(\frac{1}{273.15+T} - \frac{1}{273.15+T_{ref}} \right) \times t_c} \times e^{-k_{2ref} \times (t-t_c)} \times e^{-\frac{Ea_{21}}{R} \left(\frac{1}{273.15+T} - \frac{1}{273.15+T_{ref}} \right) \times (t-t_c)} \quad t > t_c \text{ and } T \geq T_{ref} \quad (4.4)$$

$$C_a = C_a^i \times e^{-k_{1ref} \times t} \times e^{-\frac{Ea_1}{R} \left(\frac{1}{273.15+T} - \frac{1}{273.15+T_{ref}} \right) \times t_c} \times e^{-k_{2ref} \times (t-t_c)} \times e^{-\frac{Ea_{22}}{R} \left(\frac{1}{273.15+T} - \frac{1}{273.15+T_{ref}} \right) \times (t-t_c)} \quad t > t_c \text{ and } T < T_{ref} \quad (4.5)$$

$$t_c = e^{t_{c,ref}} \times e^{b \times (T - T_{ref})} \quad (4.6)$$

$$C_a = C_a^i \times e^{-\left(\frac{t}{\alpha}\right)^\beta} \quad (4.7)$$

$$C_a = C_a^i \times e^{-\left[\left(\left(\frac{1}{\alpha} \right)_{ref} \times e^{-\frac{Ea}{R} \left(\frac{1}{273.15+T} - \frac{1}{273.15+T_{ref}} \right) \times t} \right)^{\beta_{ref} + m \times (T - T_{ref})} \right]} \quad (4.8)$$

$$C_{Br} = C_{Br}^i + k \times t \quad (4.9)$$

$$C_{Br} = C_{Br}^i + k_{ref} \times e^{-\frac{Ea}{R} \left(\frac{1}{273.15+T} - \frac{1}{273.15+T_{ref}} \right) \times t} \quad (4.10)$$

$$C_{Br} = C_{Br}^\infty + (C_{Br}^i - C_{Br}^\infty) \times e^{-k_1 \times t} \quad t \leq t_c \quad (4.11)$$

$$C_{Br} = C_{Br}^c + k_2 \times (t - t_c) \quad t > t_c \quad (4.12)$$

$$C_{HMF} = k_1 \times t \quad t < t_c \quad (4.13)$$

$$C_{HMF} = k_1 \times t_c + k_2 \times (t - t_c) \quad t \geq t_c \quad (4.14)$$

$$C_{HMF} = k_{1ref} \times e^{-\frac{Ea_{11}}{R} \times \left(\frac{1}{273.15+T} - \frac{1}{273.15+T_{ref}} \right)} \times t \quad T < T_{ref} \text{ and } t < t_c \quad (4.15)$$

$$C_{HMF} = k_{1ref} \times e^{-\frac{Ea_{12}}{R} \times \left(\frac{1}{273.15+T} - \frac{1}{273.15+T_{ref}} \right)} \times t \quad T \geq T_{ref} \text{ and } t < t_c \quad (4.16)$$

$$C_{HMF} = k_{1ref} \times e^{-\frac{Ea_{11}}{R} \times \left(\frac{1}{273.15+T} - \frac{1}{273.15+T_{ref}} \right)} \times t_c +$$

$$+ k_{2ref} \times e^{-\frac{Ea_{21}}{R} \times \left(\frac{1}{273.15+T} - \frac{1}{273.15+T_{ref}} \right)} \times (t - t_c) \quad T < T_{ref} \text{ and } t \geq t_c \quad (4.17)$$

$$C_{HMF} = k_{1ref} \times e^{-\frac{Ea_{12}}{R} \times \left(\frac{1}{273.15+T} - \frac{1}{273.15+T_{ref}} \right)} \times t_c +$$

$$+ k_{2ref} \times e^{-\frac{Ea_{22}}{R} \times \left(\frac{1}{273.15+T} - \frac{1}{273.15+T_{ref}} \right)} \times (t - t_c) \quad T \geq T_{ref} \text{ and } t \geq t_c \quad (4.18)$$

$$t_c = t_0 \times e^{-\left(\frac{T}{\alpha}\right)^\beta} \quad (4.19)$$

$$C_F = k \times t \quad (4.20)$$

$$C_F = k_{ref} \times e^{-\frac{Ea_{11}}{R} \times \left(\frac{1}{273.15+T} - \frac{1}{273.15+T_{ref}} \right)} \times t \quad T < T_{ref} \quad (4.21)$$

$$C_F = k_{ref} \times e^{-\frac{Ea_{12}}{R} \times \left(\frac{1}{273.15+T} - \frac{1}{273.15+T_{ref}} \right)} \times t \quad T \geq T_{ref} \quad (4.22)$$

$$C_P = C_P^\infty + (C_P^i - C_P^\infty) \times e^{-k \times t} \quad (4.23)$$

$$C_P = C_P^\infty + (C_P^i - C_P^\infty) \times e^{-k_{ref} \times t} \times \frac{Ea}{R} \left(\frac{1}{273.15+T} - \frac{1}{273.15+T_{ref}} \right) \quad (4.24)$$

Chapter 5

$$C_a = C_a^i \times e^{\left[- \left(A_{k1ref} \times e^{-B_{k1ref} \times C_{add}} \right) \times e^{-\frac{Ea1}{R} \left(\frac{1}{273.15+T} - \frac{1}{273.15+T_{ref}} \right) \times t} \right]} \quad t \leq t_c \quad (5.1)$$

$$C_a = C_a^i \times e^{\left[- \left(A_{k1ref} \times e^{-B_{k1ref} \times C_{add}} \right) \times e^{-\frac{Ea1}{R} \left(\frac{1}{273.15+T} - \frac{1}{273.15+T_{ref}} \right) \times t_c} \right]} \times$$

$$\times e^{\left[- \left(A_{k2ref} \times e^{-B_{k2ref} \times C_{add}} \right) \times e^{-\frac{Ea21}{R} \left(\frac{1}{273.15+T} - \frac{1}{273.15+T_{ref}} \right) \times (t-t_c)} \right]} \quad t > t_c, T \geq T_{ref} \quad (5.2)$$

$$C_a = C_a^i \times e^{\left[- \left(A_{k1ref} \times e^{-B_{k1ref} \times C_{add}} \right) \times e^{-\frac{Ea1}{R} \left(\frac{1}{273.15+T} - \frac{1}{273.15+T_{ref}} \right) \times t_c} \right]} \times$$

$$\times e^{\left[- \left(A_{k2ref} \times e^{-B_{k2ref} \times C_{add}} \right) \times e^{-\frac{Ea22}{R} \left(\frac{1}{273.15+T} - \frac{1}{273.15+T_{ref}} \right) \times (t-t_c)} \right]} \quad t > t_c, T < T_{ref} \quad (5.3)$$

$$t_c = e^{\left(D_{t_c,ref} + m_{t_c,ref} \times C_{add} \right) \times e^{b \times (T - T_{ref})}} \quad (5.4)$$

$$C_a = C_a^i \times e^{-\left\{ \left[\left(\frac{1}{\alpha} \right)_0 + m_{1/\alpha} \times C_{add} \right] \times e^{-\frac{E_a}{R} \left(\frac{1}{273.15+T} - \frac{1}{273.15+T_{ref}} \right)} \right\} \times t}^{\beta_{ref} + m \times (T - T_{ref})} \quad (5.5)$$

$$C_{Br} = C_{Br}^i + (k_0 + m_k \times C_{add}) \times e^{-\frac{E_a}{R} \left(\frac{1}{273.15+T} - \frac{1}{273.15+T_{ref}} \right)} \times t \quad (5.6)$$

Chapter 6

$$C_a = C_a^i \times e^{-\left\{ \left[\left(\frac{1}{\alpha} \right)_{ref} \times e^{-\frac{E_a}{R} \left(\frac{1}{273.15+T} - \frac{1}{273.15+T_{ref}} \right)} \right] \right\} \times t}^{\beta_{ref} - m \times (T - T_{ref})} \quad (6.1)$$

$$t_{w_{max}} = \alpha \left[\frac{(\beta - 1)}{\beta} \right]^{\frac{1}{\beta}} \quad (6.2)$$

$$w_{max} = -C_a^i \times \frac{\beta}{\alpha} \times e^{-\left(\frac{\beta - 1}{\beta} \right)} \times \left(\frac{\beta - 1}{\beta} \right)^{\left(\frac{\beta - 1}{\beta} \right)} \quad (6.3)$$

$$C_a = C_a^i \times e^{-k_{ref} \times t} \times e^{-\frac{E_a}{R} \left(\frac{1}{273.15+T} - \frac{1}{273.15+T_{ref}} \right)} \quad (6.4)$$



$$\frac{dC_a}{dt} = -k_1 C_a + k_2 C_a C_{da} \quad (6.6)$$

$$\frac{dC_{da}}{dt} = k_1 C_a - k_2 C_a C_{da} - k_3 C_{da} \quad (6.7)$$

$$\frac{dC_a}{dt} = -k_1 C_a + k_2 C_a^2 C_{da} \quad (6.8)$$

$$\frac{dC_{da}}{dt} = k_1 C_a - k_2 C_a^2 C_{da} - k_3 C_{da} \quad (6.9)$$

$$\begin{aligned} \frac{dC_a}{dt} = & -k_{1ref} \times e^{-\frac{Ea1}{R} \left(\frac{1}{273.15+T} - \frac{1}{273.15+T_{ref}} \right)} \times C_a + \\ & + k_{2ref} \times e^{-\frac{Ea2}{R} \left(\frac{1}{273.15+T} - \frac{1}{273.15+T_{ref}} \right)} \times C_a^2 \times C_{da} \end{aligned} \quad (6.10)$$

$$\begin{aligned} \frac{dC_{da}}{dt} = & k_{1ref} \times e^{-\frac{Ea1}{R} \left(\frac{1}{273.15+T} - \frac{1}{273.15+T_{ref}} \right)} \times C_a - k_{2ref} \times e^{-\frac{Ea2}{R} \left(\frac{1}{273.15+T} - \frac{1}{273.15+T_{ref}} \right)} \times \\ & \times C_a^2 \times C_{da} - k_{3ref} \times e^{-\frac{Ea3}{R} \left(\frac{1}{273.15+T} - \frac{1}{273.15+T_{ref}} \right)} \times C_{da} \end{aligned} \quad (6.11)$$

$$\frac{C_{Br} - C_{Br}^{\infty}}{C_{Br}^i - C_{Br}^{\infty}} = 1 - e^{-\left[\left(\frac{t}{\alpha} \right)^{\beta} \right]} \quad (6.12)$$

$$\frac{C_{Br} - C_{Br}^{\infty}}{C_{Br}^i - C_{Br}^{\infty}} = 1 - e^{-\left\{ \left[\left(\frac{1}{\alpha} \right)_{ref} \times e^{-\frac{Ea}{R} \left(\frac{1}{273.15+T} - \frac{1}{273.15+T_{ref}} \right)} \times t \right]^{\beta} \right\}} \quad (6.13)$$

Chapter 7

$$\alpha = \alpha^i + (\alpha^{\infty} - \alpha^i) \times (1 - e^{-\gamma \times (45 - T)}) \quad (7.1)$$

$$\alpha^i = \alpha|_{T=45} + m \times C_{add} \quad (7.2)$$

$$\gamma = a_\gamma + b_\gamma \times C_{add} \quad (7.3)$$

$$\beta = \beta_a + \beta_b \times (T - T_{ref}) + \beta_c \times (T - T_{ref})^2 \quad (7.4)$$

$$C_a = C_a^i \times e \left\{ \left[t \times \frac{1}{(\alpha|_{T=45} + m \times C_{add}) + [\alpha^\infty - (\alpha|_{T=45} + m \times C_{add})]} \right] \times \frac{1}{\left[1 - e^{-(a_\gamma + b_\gamma \times C_{add}) \times (45 - T)} \right]} \right\}^{\beta_a + \beta_b \times (T - T_{ref}) + \beta_c \times (T - T_{ref})^2} \quad (7.5)$$

$$C_a = C_a^i \times e \left[(a_k - b_k \times C_{add}) \times e^{-\frac{E_a}{R} \left(\frac{1}{273.15 + T} - \frac{1}{273.15 + T_{ref}} \right)} \times t \right] \quad (7.6)$$

$$C_{Br} = C_{Br}^i + k_{ref} \times e^{-\frac{E_{a0} + m E_a \times C_{add}}{R} \left(\frac{1}{273.15 + T} - \frac{1}{273.15 + T_{ref}} \right)} \times t \quad (7.7)$$

List of Figures

Chapter 1

- Figure 1.1 Theoretical thermal destruction curves of PME, ascospores and vegetative cells of *Sacharomyces cerevisiae* in orange juice. From TetraPak (1998). The grey rectangle shows the time/temperature conditions usually applied commercially. 31
- Figure 1.2 Examples of some packages for orange juice. Source: Tetra Pak (2000). 36
- Figure 1.3 Multilayer structure of the Tetra Brick Aseptic carton (TBA). Reproduced with kind permission from Tetra Pak. 37
- Figure 1.4 Schematic representation of degradation pathways of ascorbic acid. Adapted from Tannenbaum *et al.* (1995) and Villota & Hawkes (1992). Dashed arrows represent simplification of several distinct reactional steps, here grouped as a single one. 51

Chapter 2

- Figure 2.1 Schematic representation of the processing conditions used to fill the Tetra Brik Aseptic cartons. The initial oxygen concentrations are represented between brackets. 76
- Figure 2.2 Schematic representation of the storage conditions used for the experimental design. 77
- Figure 2.3 Changes of concentration with time at 50 °C, (a) L-ascorbic acid, (b) browning, (c) HMF, (d) furfural and (e) PVG, for the different initial oxygen content batches: (◆) A-10.25 ppm, (◇) B-6.47 ppm, (▲) C-2.04 ppm, (△) D-1.36 ppm, (○) E-1.04 ppm. 83
- Figure 2.4 Changes of concentration with time for batch A (10.25 ppm), (a) L-ascorbic acid, (b) browning, (c) HMF, (d) furfural and (e) PVG, at different temperatures: (◆) 50, (◇) 40, (▲) 30, (△) 20, (●) 8 and (○) 4 °C. 84
- Figure 2.5 Decay of quality indexes: (■) L-AA, (◆) Browning, (○) HMF, (▲) Furfural and (●) PVG, at (a) 50 °C, (b) 40 °C, (c) 30 °C, (d) 20 °C, (e) 8 °C and (f) 4 °C. Zero represents the threshold value for acceptability of orange juice, with values above zero corresponding to acceptable concentrations. 87

- Figure 2.6 Relation between orange juice shelf life at accelerated, ambient and refrigerated conditions, considering browning as the shelf life indicator. 88

Chapter 3

- Figure 3.1 Schematic representation of the mass transport of oxygen from the atmosphere into a packaged liquid food product. 93
- Figure 3.2 Depletion of dissolved oxygen concentration during time in packaged orange juice at (◆) 20°C- batch A (initial O₂ content of 10.2 ppm), and model fit (solid line). 97
- Figure 3.3 Arrhenius plot for the reaction rate constant of oxygen consumption. 99
- Figure 3.4 Depletion of dissolved oxygen concentration during storage, experimental data at 4 (◇), 20 (●), 37 (▲), 76 (□) and 105 °C (◆), from Roig *et al.* (1994) and model fit (solid line). 101
- Figure 3.5 Depletion of dissolved oxygen concentration during storage of apple juice at 25°C, experimental data (◆) from Barron *et al.* (1993) and model fit (solid line). 103

Chapter 4

- Figure 4.1 Fits of the two consecutive first-order reaction models kinetic to L-ascorbic acid data at (◆) 50, (○) 40 and (●) 20 °C. The dashed and the solid line indicate, respectively the individual and global fit. 110
- Figure 4.2 Dependence of the reaction rate constants of the two consecutive first-order reaction kinetics for L-ascorbic acid on temperature: (a) rate constant of the first reaction (k_1); (b) rate constant of the second reaction (k_2). The symbol ◆ represents parameters estimated by individual fits and the solid lines indicate the global fit. 112
- Figure 4.3 Relation of the time required for oxygen depletion with temperature. The ◆ symbol represents parameters obtained with each individual fit and the solid line indicates the global fit. 113
- Figure 4.4 Fit of the Weibull model to L-ascorbic acid data at (◆) 50, (○) 40 and (●) 20 °C. The dashed and the solid line indicate, respectively the individual and global fit. 117

- Figure 4.5 Dependence of the Weibull model parameters on temperature for ascorbic acid: (a) rate constant ($1/\alpha$); (b) shape constant (β). The \blacklozenge symbols represent parameters estimated by individual fitting, the \bullet symbol represents β calculated when an Arrhenius equation was used to describe the relation of the reaction rate constants with temperature, and the solid lines indicate the global fit. 119
- Figure 4.6 Fit of the zero-order reaction model to browning data, at (\blacklozenge) 50, (\circ) 40, (\blacktriangle) 30, and (\triangle) 4 °C. The dashed and the solid line indicate, respectively the individual and global fit. 122
- Figure 4.7 Dependence of the rate constant of the zero-order model on temperature, for browning. The \blacklozenge symbols represent parameters obtained with the individual fit and the solid line indicates the global fit. 123
- Figure 4.8 Fit of Equations 4.11 and 4.12 (solid line) to browning at (\blacklozenge) 40 °C. 125
- Figure 4.9 Fit of the two consecutive zero-order reactions kinetic model to HMF data, at (\blacklozenge) 50, (\triangle) 40, (\square) 30, and (\circ) 4 °C. The dashed and the solid line indicate, respectively, the individual and global fit. 127
- Figure 4.10 Dependence of the reaction rate constants of the two consecutive zero-order reaction kinetics on temperature for HMF formation: (a) rate constant of the first reaction (k_1); (b) rate constant of the second reaction (k_2). The \blacklozenge symbols represent parameters estimated by individual fits and the solid line indicates the global fit. 128
- Figure 4.11 Relation of the time at which the reaction behaviour (HMF) changes with temperature. The \blacklozenge symbols represent parameters estimated with individual fits and the solid line indicates the global fit. 129
- Figure 4.12 Fit of the zero-order model to furfural data, at (\blacklozenge) 50, (\circ) 40, (\blacktriangle) 30, and (\triangle) 4 °C. The dashed and the solid line indicate, respectively the individual and global fit. 132
- Figure 4.13 Dependence of the rate constants of the zero-order model on temperature, for furfural. The \blacklozenge symbols represent parameters obtained with the individual fit and the solid line indicates the global fit. 133
- Figure 4.14 Fit of the first-order model to PVG data at (\blacklozenge) 50, (\circ) 40, (\blacktriangle) 30 and (\triangle) 20 °C. The dashed and the solid line indicate, respectively the individual and global fit. 135

- Figure 4.15 Dependence of the equilibrium PVG concentration on temperature. The \blacklozenge symbols represent parameters obtained with each individual fit and the solid line indicates the global fit. 137
- Figure 4.16 Dependence of the reaction rate constant of the first-order reaction kinetics on temperature for PVG. The \blacklozenge symbols represent parameters estimated with individual fits and the solid line indicates the global fit. 137
- Chapter 5**
- Figure 5.1 Representation of the conditions used for the experimental design. 144
- Figure 5.2 Fractional decrease of L-ascorbic acid at 35 °C, for different levels of L-AA addition: (\blacklozenge) batch I- no addition, (\triangle) K- 200 mg/L, (\square) L- 300 mg/L, and (\bullet) N- 500 mg/L. 147
- Figure 5.3 Fits of the two consecutive first-order reaction model to L-ascorbic acid at (\circ) 45°C -batch I, (\bullet) 45°C -batch N (500 mg/L), (\triangle) 20°C-batch I (no added L-AA) and (\blacktriangle) 20°C -batch N (500 mg/L). The dashed and the solid lines indicate, respectively the individual and global fit. 148
- Figure 5.4 Dependence of the reaction rate constants of the two consecutive first order reaction model on temperature and added L-AA concentration, for L-AA degradation: (a) rate constant of the first reaction (k_1); (b) rate constant of the second reaction (k_2). The symbol \bullet represents parameters estimated with individual fits and the surface indicates the global fit. 149
- Figure 5.5 Dependence of the time required for oxygen depletion with temperature and added L-AA content. The symbol \bullet represents parameters estimated from individual fits and the surface indicates the global fit. 150
- Figure 5.6 Decrease of dissolved oxygen with time (batch I - no added L-AA) at: (\blacklozenge) 45, (\diamond) 40, (\blacksquare) 35, (\square) 30, (\bullet) 25 and (\circ) 20 °C. 151
- Figure 5.7 Fit of the Weibull model to L-ascorbic acid data at (\blacklozenge) 40°C-batch I (no added L-AA), (\triangle) 20°C-batch I (no added L-AA) and (\bullet) 20°C -batch N (500 mg/L). The dashed lines indicate the individual fit and the solid lines the global fit. 156
- Figure 5.8 Dependence of the Weibull model parameters on

- temperature and added L-AA content, for L-AA degradation: (a) rate constant ($1/\alpha$); (b) shape constant (β). Symbols \bullet and \blacklozenge represent parameters estimated with individual fits, and the solid line and surface indicate the global fit. 157
- Figure 5.9 Fits of the zero-order model to browning index data at (\circ) 45°C -batch I (no added L-AA), (\bullet) 45°C -batch N (500 mg/L), (\blacktriangle) 35°C -batch K (200 mg/L) and (\triangle) 20°C-batch I (no added L-AA). The dashed and the solid lines indicate, respectively the individual and global fit. 161
- Figure 5.10 Dependence of the rate constant of the zero-order model on temperature and added L-AA content, for browning index. The symbol \bullet represent parameters estimated with individual fits and the surface indicates the global fit. 162
- Figure 5.11 Comparison of “true” shelf life and shelf life estimated by accelerated testing at (a) 45, (b) 40, (c) 35, (d) 30, (e) 25 and (f) 20 °C. The dots represent the “true” shelf life, calculated with the mathematical models developed with the data gathered in the full range of temperatures tested (20 to 45 °C). The squares and diamonds represent the shelf life estimated using a mathematical model developed on the basis of data gathered in the high temperature range only (35 to 45 °C) considering, respectively, the Weibull or the two first-order consecutive reactions model for L-AA degradation. Open symbols indicate that L-AA is the factor limiting shelf life, whereas full symbols indicate that shelf life is limited by browning. 166
- Figure 5.12 Estimation errors (%) when the Weibull model and the zero-order reaction are applied for L-AA degradation (dark grey bars) and browning (light grey bars), respectively. 167
- Chapter 6**
- Figure 6.1 Schematic representation of the experimental set-up 172
- Figure 6.2 Fits of the Weibull model to L-ascorbic acid data at \blacklozenge 20, \circ 30 and \blacktriangle 45 °C. The dashed and the solid lines indicate, respectively, the individual and global fits. 175
- Figure 6.3 Dependence of the Weibull model parameters on temperature, for ascorbic acid degradation: (a) rate constant ($1/\alpha$); (b) shape constant (β). The \blacklozenge symbols indicate the parameters obtained with individual fits and the line indicates the global fit. 176

-
- Figure 6.4 Evolution of experimental data of L-AA (●), DA (▲), browning (○) and pH (△) at 40 °C. 179
- Figure 6.5 Fits of the first-order model to L-ascorbic acid data for times smaller than 8 hours at ◆ 20, ○ 30 and ▲ 45 °C. The dashed and the solid lines indicate, respectively, the individual and global fits. 180
- Figure 6.6 Fits of the mechanistic model to (◆) L-ascorbic acid (C_a) and (□) dehydroascorbic acid (C_{da}) data at (a) 45, (b) 40, (c) 35, (d) 30, (e) 25 and (f) 20 °C. The dashed and the solid lines indicate, respectively, the global fit to C_{da} and C_a . 184
- Figure 6.7 Fit of the Weibull model to browning index data at (□) 20, (○) 30 and (◆) 45 °C. The dashed line indicates the individual fit and the solid line the global fit. 187
- Figure 6.8 Dependence of the Weibull model constants on temperature, for browning index (a) rate constant; (b) shape constant. The ◆ symbols represent parameters estimated with each individual fit and the line indicates the global fit. 188
- Figure 6.9 Effect of replacing aeration by N₂ flushing on L-AA degradation (T=45 °C): (●) after 2 hours, (△) after 4 hours (○) after 6 hours and (◆) control (continuous aeration). 190
- Chapter 7**
- Figure 7.1 Dependence of the parameter estimates, reaction rate at the reference temperature and activation energy, of Eq. 6.10 and 6.11 on added L-AA content (C_{add}). 198
- Figure 7.2 Fit of the mechanistic model to (◆) L-ascorbic acid (C_a) and (□) dehydroascorbic acid data (C_{da}) at 30 °C, for (a) batch I (no added L-AA), (b) batch J (100 mg/L), (c) batch K (200 mg/L), (d) batch L (300 mg/L), (e) batch M (400 mg/L) and (f) batch N (500 mg/L). The dashed and the solid lines indicate, respectively, the global fit to C_{da} and C_a . 200
- Figure 7.3 Fit of the Weibull model to ascorbic acid data at (◆) 45°C - Batch J (100 mg/L), (□) 45°C -N (500 mg/L), (○) 20°C -J (100 mg/L) and (●) 20°C -N (500 mg/L). The dashed and solid lines indicate, respectively, the individual and the global fit of the Weibull model. 201

-
- Figure 7.4 Dependence of the Weibull model parameters on temperature for L-ascorbic acid degradation: (a) scale constant (α); (b) shape constant (β). Symbols ● and ◆ represent parameters estimated with individual fits and the line and/or surface these estimated with the global fit. 205
- Figure 7.5 Fit of the first-order model to L-ascorbic acid data for times smaller than 8 hours: (◆) 45°C - Batch J (100 mg/L), (□) 40°C -L (300 mg/L), (△) 30°C -M (400 mg/L) and (●) 20°C -N (500 mg/L). The dashed and solid lines indicate, respectively, the individual and the global fit. 206
- Figure 7.6 Dependence of the reaction rate constant of the first-order model on temperature and added L-AA. The ● symbols represents parameters estimated with individual fits and the surface those estimated with the global fit. 208
- Figure 7.7 Fit of the zero-order model to browning at (△) 20 °C -batch I (no added L-AA), (▲) 20 °C -batch N (500 mg/L), (○) 45 °C -batch I (no added L-AA), and (●) 45 °C -batch N (500 mg/L). The dashed and solid lines indicate, respectively, the individual and global fits. 211
- Figure 7.8 Dependence of the zero-order model rate constants on temperature and added L-AA content, for browning. The ● symbol represent parameters estimated with individual fits and the solid surface/line indicates the global fit. 211
- Figure 7.9 Effect of continuous nitrogen flushing on (a) L-AA degradation and (b) dehydroascorbic acid formation/ degradation in orange juice, at △ 20 °C -batch I (no added L-AA), ▲ 20 °C -batch N (500 mg/L), ○ 45 °C -batch I (no added L-AA), and ● 45 °C -batch N (500 mg/L). 214

List of Tables

Chapter 1

Table 1.1	Summary of characteristics and shelf life expected for different fruit juices and juice drink products.	14
Table 1.2	Studies showing the influence of several factors on ascorbic acid degradation.	21
Table 1.3	Degradation products found in canned SSOJ after 12 weeks at 35°C. From Tatum <i>et al.</i> (1975).	27
Table 1.4	Ascorbic acid retention in orange juice packed in different containers at 1.1°C for 0, 1, 2, 3, 6 and 12 months storage. From Shaw <i>et al.</i> (1993b).	34
Table 1.5	Kinetic studies of ascorbic acid degradation.	53
Table 1.6	Kinetic studies of nonenzymatic browning.	62
Table 1.7	Kinetic studies of flavour (HMF, Furfural and PVG) formation.	63

Chapter 2

Table 2.1	Initial (after pasteurisation and packaging) and final contents of the quality indicators at the temperatures tested (*).	81
-----------	---	----

Chapter 3

Table 3.1	Permeability of the package, measured with the OXTRAN.	96
Table 3.2	Estimates of reaction rate constants, rate constant of oxidative reactions and oxygen mass transfer coefficient of oxygen in orange juice stored at different temperatures (“our data” and Roig <i>et al.</i> (1994)), and apple juice stored at 25 °C (Barron <i>et al.</i> , 1993).	102

Chapter 4

Table 4.1	Estimates of the parameters of the individual (Eq. 4.1 and 4.2) and global fitting (Eq. 4.3 to 4.6) of the two consecutive first-order model, for L-AA degradation.	115
-----------	---	-----

Table 4.2	Estimates of the parameters of the Weibull individual model (Eq. 4.7) and of the global model (Eq. 4.8), for L-AA degradation.	120
Table 4.3	Estimates of rate constant of the zero-order model, for the individual (Eq. 4.9) and global (Eq. 4.10) fitting of browning data.	124
Table 4.4	Estimates of the parameters for the two-consecutive reaction model (first followed by zero-order) fitting (Eq. 4.11 and 4.12) of browning data.	126
Table 4.5	Estimates of the parameters for two consecutive zero-order reaction model individual (Eq. 4.13 and 4.14) and global (Eq. 4.15 to 4.19) fitting of HMF data.	131
Table 4.6	Estimates of the parameters for the zero-order model individual (Eq. 4.20) and global (Eq. 4.21 and 4.22) fitting of furfural data.	134
Table 4.7	Estimates of the parameters for the first-order model individual (Eq. 4.23) and global (Eq. 4.24) fitting of PVG data.	138

Chapter 5

Table 5.1	Estimates of the parameters of the individual fitting of the two consecutive first order model (Eq. 4.1 and 4.2) to L-AA data.	154
Table 5.2	Dissolved oxygen concentration (ppm) at the time when reaction rate changes (t_c).	151
Table 5.3	Estimates of the parameters of the global fitting of the two consecutive first order model (Eq. 5.1 to 5.4) to L-AA data.	155
Table 5.4	Estimates of the parameters of the individual (Eq. 4.7) and global fitting (Eq. 5.5) of the Weibull model to L-AA data.	159
Table 5.5	Estimates of the parameters of the individual (Eq. 4.9) and global fitting (Eq. 5.6) of the zero-order model for browning data.	163

Chapter 6

Table 6.1	Estimates of the parameters of the individual (Eq. 4.7) and global fitting (Eq. 6.1) of the Weibull model to L-AA data.	178
Table 6.2	Estimates of the parameters of the individual (Eq. 4.1) and global fitting (Eq. 6.4) of the first-order model to L-AA data.	181
Table 6.3	Estimates of the parameters of the global fit of the mechanistic model (Eq. 6.10 and 6.11) to L-ascorbic acid and dehydroascorbic acid data.	185
Table 6.4	Estimates of the parameters of the individual (Eq. 6.12) and global fitting (Eq. 6.13) of the Weibull model to browning data, as well as the maximum growth rate and the time at which it occurs, calculated based on the global fitting parameters.	189

Chapter 7

Table 7.1	Estimates of the parameters of the global fit of the mechanistic model (Eq. 6.10 and 6.11) to L-ascorbic acid and dehydroascorbic acid data.	199
Table 7.2	Estimates of the parameters of the individual (Eq. 4.7) and global fitting (Eq. 7.5) of the Weibull model to L-AA data.	204
Table 7.3	Estimates of the parameters of the individual (Eq. 4.1) and global fitting (Eq. 7.6) of the first-order model to L-AA data.	209
Table 7.4	Estimates of the parameters of the individual (Eq. 4.9) and global fitting (Eq. 7.7) of the zero-order model to browning index data.	212

General Introduction

General Introduction

1. OBJECTIVES AND RATIONALE

The shelf life of a food is the time period for the product to become unacceptable from sensory, nutritional or safety perspectives (Fu & Labuza, 1993). From the viewpoint of the food industry, shelf life is based on the extent of quality loss that the food company will allow prior to product consumption while ensuring safety. For consumers, the end of shelf life is the time after which the food no longer has an acceptable look or taste. A universal definition of shelf life is virtually impossible to establish because one can never satisfy all parts involved (consumers and producers) and also because food systems have very complex mechanisms of deterioration. Despite this, shelf life of food products can be determined, and subsequently predicted, based on some primary mode of deterioration (Fu & Labuza, 1993).

The shelf life of citrus juices and related beverages is primarily determined by chemical changes and by microbial growth depending whether the juice is pasteurised or not. Chemical changes that lead to reduction in the marketability of the product include off-flavour development, product discoloration (caramelisation, nonenzymatic browning) and loss of important nutrients (Shaw *et al.*, 1993a). Legislation requirements regarding nutritional labelling, concentrate

primarily on the contents of vitamins and minerals, although citrus juices also contain carbohydrates, proteins and fats. For forecasting shelf life of a product, it is imperative to select adequate shelf life indicators, and to identify the critical ones. Critical shelf life indicators are those that first reach the respective threshold level and thus limit product shelf life.

Shelf life testing has been extensively reviewed by Gacula (1975), Mizrahi *et al.* (1977 a,b), Ragnarson & Labuza (1977), Karel (1979), Saguy & Karel (1980), Labuza (1982) and Labuza & Schmidl (1985). The usual techniques for determination of shelf life of aseptically processed juices consist on the quality evaluation during storage in simulated real conditions (temperature, oxygen content, and relative humidity of the air). However, this procedure is very time consuming since the shelf life of aseptically processed food is usually of some months, and consequently costly. Direct tests are also a major limitation in product development, as they delay the entry of the product in the market.

Accelerated Shelf Life Tests (ASLT) may overcome these problems. ASLT are tests carried out at abusive storage conditions (e.g. high temperature, high oxygen content), so that food deterioration rate is much faster and thus tests are much shorter. If the quality factors deterioration kinetics is known, then it is possible to use mathematical modelling to predict the quality of a product stored at ambient conditions. However, ASLT imply extrapolation of mathematical models to predict quality changes in conditions out of the range tested and thus are risky, as chemical reaction mechanisms may change with temperature and oxygen content.

The work developed in the framework of this thesis aims at contributing to the understanding of the characteristics that limit the shelf life of pasteurised orange juice, and particularly at the modelling of quality indicators kinetics in both normal and abusive conditions. Specific objectives included:

- To identify critical quality indicators.
- To analyse the effect of temperature and initial dissolved oxygen content as accelerating factors of the reactions of formation or degradation of the quality indexes, and to assess the reliability of ASLT.
- To develop general mathematical models to describe quality changes (L-ascorbic acid, browning, 5-hydroxymethyl-2-furfuraldehyde, 2-furfuraldehyde, and 4-vinyl-guaiacol) in pasteurised orange juice stored in ambient and abusive conditions (temperature and oxygen).

As ascorbic acid was found to be the critical factor limiting shelf life, the work objectives were extended to:

- Assess the effect of supplementing orange juice with ascorbic acid on shelf life and to study the kinetics of the critical quality indicator(s) in these conditions.
- Further study the kinetics of the critical quality indicators in both ascorbic acid supplemented and non-supplemented juice, under aerobic and anaerobic conditions, in a range of temperatures.

2. THESIS STRUCTURE

This thesis is written in seven chapters, divided in three parts. The first part of this work (Chapter 1) presents the basic characteristics of different categories of orange juice, quality characteristics that limit the acceptability of the product, and factors that influence product shelf life. General concepts of mathematical models are addressed, and kinetics of quality characteristics decay is reviewed. Also, basic concepts for shelf life estimation are presented.

The second part (Chapters 2, 3 and 4) deals with the selection of critical quality indicators, empirical modelling of a number of quality characteristics, and assessment of high temperature and initial dissolved oxygen contents as accelerating factors for shelf life.

The third part (Chapters 5, 6 and 7) addresses the effect of addition of ascorbic acid in the kinetics of two selected quality indicators: L-ascorbic acid and browning. Furthermore, Chapters 6 and 7 detail these kinetics under aerobic conditions.

Figure A.1 shows schematically the structure of the thesis, illustrating the interrelationships between the Chapters.

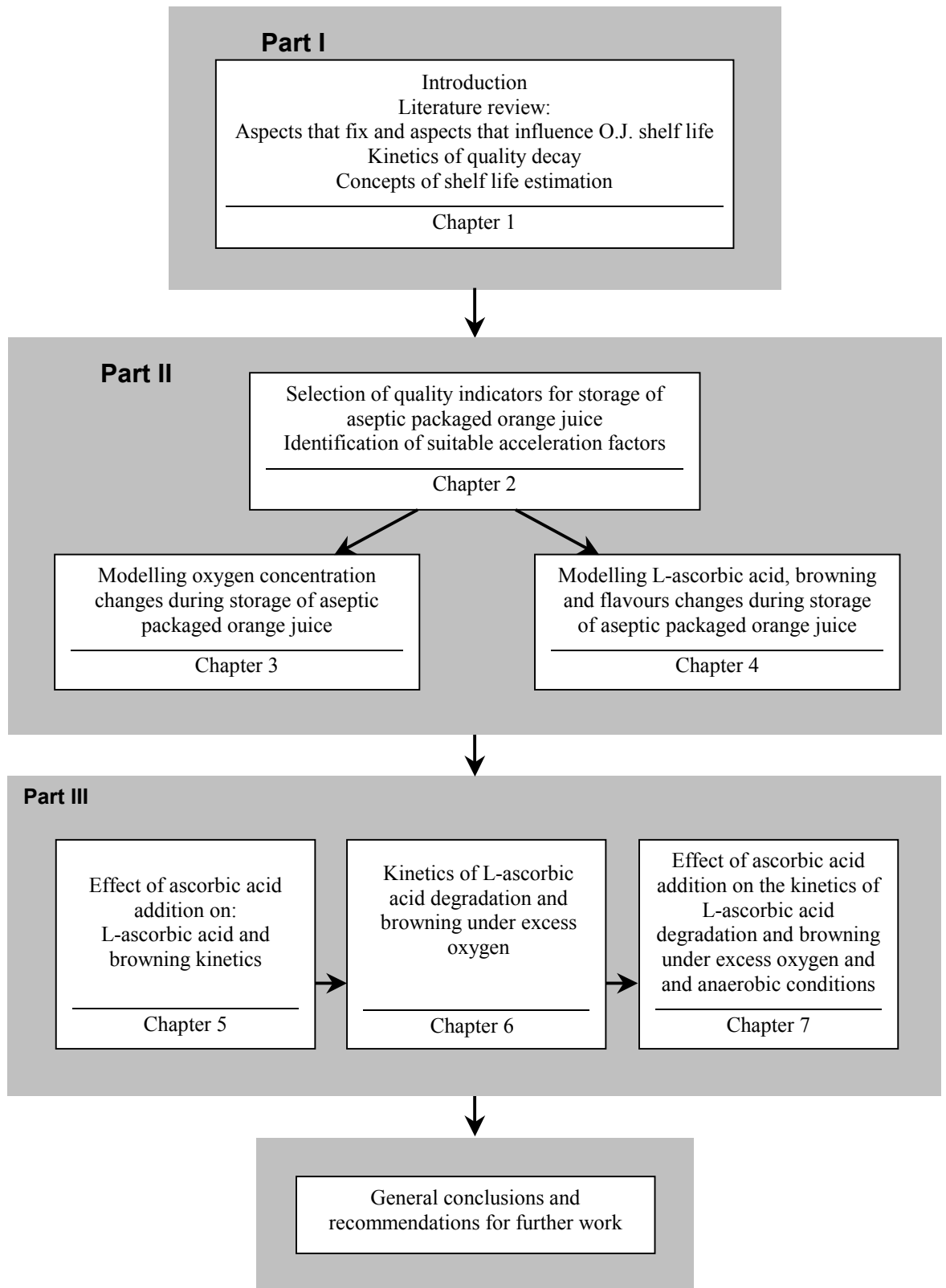


Figure A.1- Schematic structure of the thesis.

Part I

Introduction

CHAPTER 1

State-of-the-art

1.1- INTRODUCTION

As orange juice is produced on a seasonal basis, it must be stored between seasons to ensure a year-round supply to consumer markets. The most important compounds that influence the quality of orange juice are sugars and acids, flavour and colour components, and vitamin C. The deterioration of pasteurised juice quality is mainly related to flavour degradation, nonenzymatic browning and nutrient loss.

This chapter addresses particularly orange juice categories (characteristics and shelf life expected for different fruit juices and juice drink products), aspects that fix the limits of orange juice (microbiology, nutrient loss, colour stability, flavour/off-flavour development) and factors that influence product shelf life (processing treatment, storage temperature, oxygen content, light and packaging system). Mathematical models are also discussed, particularly in relation to quality characteristics decay. Finally, basic concepts of shelf life estimation are presented.

1.2-ORANGE JUICE CATEGORIES

Many different terms are used within orange juice marketing to describe various products. Several of these are not consistent and have different meanings in different countries, but there is a growing pressure to harmonise the terms used.

Orange juice products can be divided into two main categories – ready-to-drink (RTD) juices and concentrates. RTD juices are either not from concentrate (NFC) or reconstituted from concentrate. Concentrates require dilution with water before consumption.

A summary of the characteristics of different types of orange juices and orange juice drinks is presented in Table 1.1, namely the properties and the shelf life expected for those products.

1.2.1. READY-TO-DRINK ORANGE JUICE

Ready-to-drink orange juice can be also named after “ready-to-serve”, “single strength”, “pure” or “100%” juice. It is sometimes called “fresh orange juice”, but this term is misleading and should be avoided as it is used to mean either freshly squeezed orange juice or juice distributed chilled (NFC or made from concentrate).

RTD orange juice is at the strength at which it will be consumed. It is made either from concentrate juice (60 °brix bulk concentrate) reconstituted to single strength or from not from concentrate pasteurised juice (Shaw *et al.*, 1993b). It does not

require dilution before drinking. Some categories of RTD orange juice are described below.

1.2.1.1. Fresh squeezed orange juice

Juice packaged directly after extraction but without pasteurisation or any other physical or chemical treatment. Fresh squeezed non-pasteurised orange juice must be kept cold and, even then, has a relatively short shelf life. Off-flavours that develop in these unpasteurised products were described by Fellers (1988) as “stale” and of unknown cause. At 4.4°C and below, total microbiological counts were reported to decrease during storage in most juices. However, at 7.8°C they increased significantly, and those juices were unpalatable after one week (Shaw *et al.*, 1993b).

1.2.1.2. Not-from-concentrate juice (NFC)

Not-from-concentrate juice is a juice that has neither undergone a concentration step nor dilution during production. This pasteurised product is generally packaged in either plastic bottles or laminated board cartons. It is essential that these products be kept at refrigerated temperatures during storage, transportation and retail marketing in order to maintain quality. For unfrozen products without exception the lower the storage temperature, the better the flavour and vitamin C retention in the product. In the past, a one-month shelf life was typical for this product, but a 2-month shelf life is now possible due to newer packaging materials (Sadler *et al.*, 1992).

NFC is a term originated in the USA and is considered a premium quality product. “Premium juice” is a term that has also been used in the USA and Canada for NFC marketing purposes, and has also entered the EU market. In the EU the expression “not from concentrate” is felt to imply to consumers that the juice derived from concentrate is inferior to NFC and instead “direct juice” is the term proposed for use.

1.2.1.3. From concentrate

This product is also known as “orange juice made with concentrate”. The juice is prepared by dilution of concentrate with potable water. This pasteurised product is generally packaged in either plastic bottles or laminated board cartons (TetraPak, 1998) or aluminium cans (Anonymous, 2000). These products can be kept either at refrigerated (up to two months shelf life in plastic bottles and laminated board cartons) or at ambient temperatures (up to 6-8 months shelf life in laminated board cartons). In the case of canned juice its shelf life can be longer than 1 year.

1.2.1.4. Fortified Orange Juice

1.2.1.4.1. Juice with added floating pulp

This is juice with added floating cells, also known as pulp or fruit meat. The product is sometimes called “home style”, “natural”, etc. The added cells provide mouth feel and increase the natural fibre content of juice. Juice without pulp is referred to as “smooth”.

1.2.1.4.2. Vitamin enriched

Vitamins (both naturally occurring and manmade) can be added to increase the nutritional value of orange juice.

1.2.1.4.3. Calcium enriched

Calcium compounds, which are soluble in juice, are added to juice to increase its nutritional value.

1.2.1.4.4. Fibre enriched

Nutritional fibre (normally not from oranges) is added to increase the health value of juice.

1.2.2. CONCENTRATED ORANGE JUICE

Concentrated orange juice is diluted to single strength before consumption. The most common orange concentrate products for the trade and retail sectors are described below.

1.2.2.1. Frozen concentrated orange juice (FCOJ)

The term FCOJ may be misleading, as at such high concentrations it does not freeze solid but it is still pumpable. FCOJ is commercialised in different strength for different purposes. FCOJ has the longest shelf life of any 100% citrus juice product.

FCOJ 65-66 °brix: it is the standard product for trade orange juice concentrate. It is concentrated approximately 5.5 times (TetraPak, 1998). It is a bulk product only, stored at –6 to –25 °C in 55-gallon drums (≈280 L) (Morris, 1996).

FCOJ at approximately 55 °brix: this product is often referred as Dairy Pack. It is a bulk product only. It is 66 °brix concentrate cut back (re-diluted), e.g. with single strength juice and pulp, to the required concentration. No further additions are needed at the juice packer apart from water dilution. Dairies commonly use this product.

FCOJ at minimum 41.8 °brix: it is a retail product (mainly USA) for dilution with water (3 times) to single strength, and used at home, in restaurants, etc., and usually packed in cans (Anonymous, 2000).

1.2.2.2. Concentrate at approximately 52 °brix

It is a retail product aseptically packaged (mainly Europe) for dilution with water (4 times) to single strength, and used at home, in restaurants, etc.

1.2.3. RTD ORANGE PRODUCTS THAT SHOULD NOT BE CALLED ORANGE JUICE

As a general rule juice drinks are more stable than 100% juice products. Shaw *et al.* (1993b) reviewed the work of Potter *et al.* (1985), who had studied storage stability of a series of aseptically packaged orange drinks (laminated board cartons at ambient storage temperature) and found a 10% orange juice to be the most stable. It had an 8-month shelf life, which is 2-4 months longer than the shelf life of 100% orange juice.

Table 1.1- Summary of characteristics and shelf life expected for different fruit juices and juice drink products.

Type of Product	Thermal Treatment	Characteristics	Package	Storage Temperature (°C)	Shelf life		
<i>RTD or Single Strength Orange Juice</i>	Fresh squeezed	No	Must not have been frozen Must be unpasteurised Must not contain pulp wash solids	Polyethylene bottles	2	16-24 days	
					4.4	11 days	
					5.7	10 days	
	NFC Direct or Premium	Yes	Must be pasteurised Must not be made by reconstitution not concentrated juice	Glass bottles PET bottles Polyethylene containers Laminated board cartons	R T	21 - 42 days	
					Ambient temperature	10 months	
					Bulk stored in 1135 L bag (plastic) in box (wooden)	R T	> 1 year
					Bulk stored in 310 L drums	F T	> 2 years
	From concentrate	Yes	Must be pasteurised	Glass bottles Polyethylene containers Laminated board cartons Alu. Cans	R T	21 - 42 days	
					Ambient temperature	10 months	
						1 year	
Fortified	Yes		Glass bottles Laminated board cartons	R T Ambient temperature	21-42 days 8-10 months		
<i>Concentrated Orange Juice</i>	Frozen concentrate	Yes	Bulk stored in 310 L drums Laminated board cartons	F T [-25; -6]	5 years		
					1 year		
	Concentrate	Yes		Laminated board cartons Glass bottles	Ambient temperature	8-12 months	
<i>RTD Orange Products</i>	Nectars	Yes	Must have a minimum of 50% fruit juice (EU)	Glass bottles Tin cans Alu. Cans Aseptic laminated cartons	Ambient temperature	≈ 8 months	
	Drinks	Yes	usually 10% orange juice	PET bottles Aseptic laminated cartons Polyethylene Alu. cans	Ambient temperature	≈ 8 months	
Flavour drinks	Yes	Do not contain any genuine juice product	PET bottles Aluminium cans	Ambient temperature	≈ 8 months		

1.2.3.1. Orange nectar

Orange nectar is orange juice with added sugar, acids and/or water. The minimum fruit content varies according to legislation. For citrus nectar, EU regulations stipulate a minimum of 50% fruit juice content at RTD strength.

1.2.3.2. Orange juice drinks

Orange juice drinks have a juice content lower than nectars. They are not subject to juice legislation but to general food legislation. In some cases they may contain only peel oil and flavouring agents.

1.2.3.3. Orange flavour drinks

Orange flavour drinks are products tasting of orange but containing no genuine juice product.

1.3. REGULATIONS GOVERNING JUICE ORIGIN

In the EU, USA and several other countries, the term “orange juice” may only be used for juice extracted from sweet oranges, *Citrus sinensis* (Anonymous, 1949; Hui, 1999). Nevertheless, in the USA, regulations allow for up to 10% of tangerine or hybrid orange/tangerine juice to be included in orange juice, as it can improve the colour and flavour of the blended juices.

In principle, regulations governing direct juice, or NFC, require that nothing should be removed or added during juice extraction and further processing of the juice. For reconstituted orange juice, water should be added back to give the same

concentration as in the original juice. Pulp and essence may be added back to the same level as found in the original juice, but this is not valid in all countries.

In the EU directives for fruit juices, orange juice may only be extracted by mechanical means (water extraction is not allowed). In EU pulp wash and essences (flavours) may not be added to pure orange juice, a procedure that is allowed in the USA, up to 5% (Anonymous, 1949), and many other countries.

1.4. ASPECTS THAT FIX THE LIMITS OF PRODUCT SHELF LIFE

1.4.1. MICROBIOLOGY OF ORANGE JUICE

Despite documented evidence that specific pathogens are capable of survival in fruit juice, until recently it was widely accepted that most low pH/high acid foods were of minimal concern for food poisoning outbreaks. This was based on the knowledge that organic acids have an inhibitory and sometimes microbicidal effect on many bacteria (Parish, 1997). Recent outbreaks of food poisoning from *Salmonella* and *E. coli* O157:H7 were traced to nonpasteurised orange and apple juices, respectively (Parish *et al.*, 1996; Anonymous, 1995; Linton *et al.*, 1999).

Shelf stability of some 100% fruit juice products stored at room temperature is maintained by the combination of a heat process and low pH. The high acidity (pH \leq 4.5) limits the types of microorganisms that can grow in the juice, yet several have been isolated from orange juice (acid-tolerant bacteria, yeasts and moulds)

although few of them can cause spoilage (pathogenic) (McIntyre *et al.*, 1995). Therefore, in aseptically processed and packed food, microbial growth does not set the storage limit of the product, unless erroneously processed.

Saccharomyces cerevisiae, *Rhodotorula sp.* and *Zygosaccharomyces sp.* are the most common yeasts present in juice (TetraPak, 1998). *Saccharomyces cerevisiae* is the yeast most commonly associated with spoilage of pasteurised citrus juices. This organism produces an alcoholic fermentation resulting in a fermented off-flavour due to the presence of ethanol and carbon dioxide. Yeasts not capable of alcoholic fermentation may cause turbidity, flocculation and clumping in juice. *Zygosaccharomyces* is an osmophilic yeast and species of this yeast can readily survive the high osmotic pressures and low water activity of frozen concentrated orange juice (Shaw *et al.*, 1993b) and it is frequently associated with spoilage of concentrates (TetraPak, 1998). The presence of *Rhodotorula* may be indicative of poor post-pasteurisation hygiene.

Moulds that have been isolated from orange juice include *Aerobasidium pullulans*, *Aspergillus niger*, *Botrytis sp.*, *Fusarium sp.*, *Geotrichum sp.*, *Mucor sp.*, *Aspergillus fumigatus*, *Cladosporium sp.* and *Penicillium sp.*. Moulds are usually of small concern in processed citrus products because of their slow growth rates (Beuchat, 1982) and although they grow well in acid media, they require abundant oxygen and are generally sensitive to heat treatment and thus easily destroyed by pasteurisation. However isolated cases of mould spoilage by *Penicillium sp.*, *Aureobasidium pullulans* and *Cladosporium sp.* occasionally occur (Beuchat,

1982). With the introduction of long-term chilled storage of single strength orange juice in nonaseptic cartons with oxygen barriers, mould growth in citrus juice has become a more important issue (TetraPak, 1998).

Acid and acidified foods ($\text{pH} \leq 4.5$) generally are not heat processed sufficiently to destroy all bacterial spores because that process (sterilization) may adversely affect the quality of the product and is not necessary as most spores will not germinate and grow in such products. The major bacterial spoilage agents in citrus juices are *Lactobacillus* and *Leuconostoc* species (also termed lactic acid bacteria). These organisms are responsible for production of diacetyl, which imparts an undesirable buttery flavour to juice (Sadler *et al.*, 1992). *Leuconostoc* and many species of *Lactobacillus* also produce large amounts of CO_2 . A thermo-resistant spore-forming acidophilic bacteria was isolated from shelf-stable juices, named *Bacillus acidoterrestris* (Deinhard *et al.*, 1987), and later reclassified in a new genus called *Alicyclobacillus* (Wisotzkey *et al.*, 1992). *Alicyclobacillus* are of concern as they can germinate, grow, and cause spoilage of products with a pH previously considered below the range of spore-forming bacteria (Walls & Chuyate, 1998). This contamination is introduced into manufacturing process through unwashed or poorly washed fruit, and it causes a flat sour type of spoilage (no gas production was observed), producing an offensive-smelling compound, guaiacol, and other taint chemicals in orange and apple juices and juice-containing drinks (Pettipher *et al.*, 1997). Splittstoesser and coworkers (1998) also reported the detection of guaiacol in apple juice contaminated with *Alicyclobacillus*. The worldwide occurrence of *alicyclobacilli* in non-spoiled fruit juices and rapid

growth cycles culminating with sporulation of cells strongly indicate that spoilage of fruit juices by *alicyclobacilli* is incidental, requiring a combination of adequate conditions for growth of the organisms in the juice, such as low pH and high temperatures for long periods of time (Pinhatti *et al.*, 1998). Komitopoulou & coworkers (1999) reported that use of nisin is a potentially useful way of controlling this organism in fruit juice and fruit juice-containing products.

1.4.2. NUTRIENT LOSS

Nutrient loss in citrus juice products is essentially synonymous with vitamin loss. Since consumers derive major vitamin benefits from citrus juices, factors that impact on vitamin retention are of considerable importance (Shaw *et al.*, 1993b).

Vitamins can be grouped according to whether they are soluble in water or in nonpolar solvents. The water-soluble vitamins are vitamin C and a series known as vitamin B complex.

1.4.2.1. Vitamin C

Ascorbic acid (vitamin C) is the most important nutrient in orange juice. Some other fruits contain more ascorbic acid than oranges, such as kiwi, strawberries and blackcurrant, but fewer are as popular. Ascorbic acid is essential for the synthesis of collagen, the most abundant protein in mammals, and a lack of this vitamin leads to scurvy (Gregory, 1993).

Ascorbic acid is a natural antioxidant and its loss in juices is closely related to the availability of oxygen in packages. The loss of this vitamin in processed citrus juices is due to aerobic and anaerobic reactions of nonenzymatic nature (Shaw *et al.*, 1993b) or through catalysed or uncatalysed aerobic pathways (Villota & Hawkes, 1992). Several authors studied ascorbic acid decomposition, and several studies focusing on the influence of oxygen, packaging systems, and other chemicals on ascorbic acid contents (not on its kinetics) are presented in Table 1.2.

It is possible that the various mechanisms of deterioration can operate simultaneously. Which one predominates depends on the storage temperature and on the availability of oxygen, thus highly complicating the treatment of kinetic data (Villota & Hawkes, 1992).

The anaerobic pathway is independent of oxygen (as the name implies) and is mainly driven by the storage temperature. Losses caused by this pathway cannot be prevented by package type (TetraPak, 1998), being lower storage temperature the only way to minimise its rate (Trammel *et al.*, 1986). This mode of degradation is prevalent in hermetically sealed packages. Under anaerobic conditions ascorbic acid decomposes to 2,5-dihydro-2-furoic acid, 3-deoxy-D-pentosone, carbon dioxide and furfural (Huelin, 1953; Huelin *et al.*, 1971; Shaw *et al.*, 1993b).

The aerobic pathway needs oxygen and is therefore related to the presence of headspace oxygen, dissolved oxygen and the oxygen-barrier properties of the package (TetraPak, 1998). In cases where permeation of oxygen into package is considerable, headspace oxygen is present or oxygen is dissolved in the product,

Table 1.2- Studies showing the influence of several factors on ascorbic acid degradation.

Food or model food system	Package and Storage Conditions	Compounds under study	Compounds/factors affecting degradation	Atmospheric conditions	Retention (%)	Observations	Ref
Orange juice (pasteurised, made from concentrate) and Frozen concentrate orange juice	Glass bottles (7 oz): 12 months at 4, 10, 15, and 27°C Polyethylene bottles (64 oz): 6 months at -6.7, 1.1, and 10°C Polystyrene bottles (4 oz): 1.5 months at -6.7, 1.1, and 10°C Waxed cardboard cartons (64 oz): 2 months at -6.7, 1.1, and 10°C Foil-lined fiberboard cartons: 12 months at -20.5, -6.7, and 1.1°C Polyethylene lined fiber-board cans: 12 months at -20.5, -6.7, and 1.1°C	Ascorbic acid	Temperature	n.a.	≈ 65 (glass) ≈ 37 (polyethylene) ≈ 20 (polystyrene) ≈ 10 (waxed card.) >70 (foil-lined fib.) >30 (polyethylene lined fib.)	SSOJ packed in glass jars retained about 90% AA for over 4 months and 87% for 1 year at 4.4°C; AA retention was 67% after 8 months at 26.7°C (point after which the juice was unacceptable in flavour) Among the 4 types of containers used, crown capped glass bottles resulted in better AA protection even at higher storage temperatures. Hermetically sealed polyethylene containers were next, while losses were greater in polystyrene bottles and waxed cartons For the frozen juice, at higher temperatures, the foil barrier resulted in superior retention	Bissett & Berry (1975)
Guava puree	Bag-in-box aseptic package (1 gal) 9 months at -18, 10 and 23°C 2 initial dissolved oxygen content	Dissolved oxygen Headspace oxygen Ascorbic acid colour (Instrumental and visual measures) pH, °brix Taste tests	Temperature Deaeration	Aer./ Anaer.	42 (23°C) 58-61 (10°C) 73 (-18°C)	The quality of aseptically processed bag-in-box can best be assured by lowering product temperature during storage. Storage at 10°C will retard, but not prevent, colour change and loss of ascorbic acid Deaeration had almost no effect on the initial dissolved oxygen levels in this study, and little or no difference was observed between deaerated and nondeaerated purees	Chan & Cavalletto (1986)
Aqueous solutions	n.a.	Ascorbic acid Carbon dioxide Furfural	Ascorbic acid Carbon dioxide pH	Anaer.	n.a.	Foods with pH between 3.0 and 4.0 have a higher velocity of AA loss The yields of CO ₂ have been sufficient to suggest that AA decomposes anaerobically to CO ₂ and 5-carbon compounds. The reaction, which predominates below pH 2, gives furfural as the major product. The reactions occurring in the pH range of foods, i.e. the reaction with an optimum pH near the pK ₁ of AA and the fructose promoted-reaction may give 2,5-dihydro-2-furoic acid as the major product, but this has not been established	Huehn <i>et al.</i> (1971)

n.a.- not available; Aer.- aerobic; Anaer.- anaerobic.

Table 1.2 (cont.)- Studies showing the influence of several factors on ascorbic acid degradation.

Food or model food system	Package and Storage Conditions	Compounds under study	Compounds/factors affecting degradation	Atmospheric conditions	Retention (%)	Observations	Ref.
SSOJ and synthetic (10% V/V) orange drinks	retort pouch polyethylene whirl-pak (O ₂ permeation = 0) 20 weeks at 24°C 3 initial amino acid (a.a.) contents: 0.06, 0.66, 1.26% (w/w) 4 initial AA concentrations: 42, 380, 420, 718 mg/L	Ascorbic acid Browning	Browning Ascorbic acid Dehydroascorbic acid Aminoacids Oxygen	Aer./ Anaer.	56 (1.26% a.a.) 61 – 63 (0.06-0.66% a.a.)	Packaging in pouches (permeable to gases) accelerates the loss of AA due to higher oxygen and increases browning formation Loss of AA occurs in the preparation and processing of the samples (incorporation of air) Loss of AA occurs in the presence of aminoacids Aminoacids content had a linear effect on browning of orange drinks, within the conc used, but was more pronounced in the presence of high levels of AA	Kacem <i>et al.</i> (1987)
SSOJ (made from concentrate)	TB cartons (200 mL) Temperature (°C): 4, 20, 37, 76, 105 64 days Initial dissolved oxygen content= 4.45 ppm L-AA addition, Initial AA conc=330 mg/kg Sodium tiosulphate, sorbitol, etc...	L-Ascorbic acid Oxygen Browning HMF	Temperature	Aer./ Anaer.	n.a.	The fact that initial dramatic loss of O ₂ correlates with a greater decomposition of L-AA, and that after dissolved oxygen reached equilibrium further L-AA decomposition occurred independently of oxygen, is said to prove that aerobic and anaerobic pathways can operate simultaneously in the same system	Roig <i>et al.</i> (1994)
HTST-pasteurised SSOJ (made from concentrate)	700 mL glass bottles 5 months 22°C O ₂ conc= 0.6, 1.8, 6.5, 10.1 ppm	Oxygen	Ascorbic acid Browning Taste (off-flavour) Oxygen	Aer.	95% (0.6 O ₂) >70% (10.1 O ₂)	Linear relationship between ascorbic acid loss and initial dissolved oxygen concentration After 4 weeks, AA loss occurs independently of initial oxygen concentration AA loss and browning are linearly related to initial oxygen concentration Deaeration from 10.1 to 0.6 ppm improved taste during the first two months, but did not extend the shelf-life Findings consistent with the theory that oxygen-independent browning and AA loss are important on the mechanism of off-flavour formation	Trammell <i>et al.</i> (1986)
Carbonated beverages (Pepsi-Cola™ and Mandarin Orange Slice™) Bread Breakfast cereals Peanut butter Cooked beef roast	C.Bev: 250 mL glass bottles, 1 conc. AA, 15, 25, 35°C, 6 weeks in the dark Bread: 25°C, 3, 5, 8, 10 days B. Cereals: glass jars, 145 g, 25, 30, 40°C, 9 initial conc. of AA, 7 months P. Butter: glass jars with headspace, 63°C, 85 days	Free-Ascorbic acid Total-Ascorbic acid Peroxide value (butter) Hexanal (meat)	L- Ascorbic acid Sodium L-ascorbate L-ascorbate 2-mono-phosphate magnesium salt (AsMP)	Aer./ Anaer.	90 – 60 (15, 35 °C, cola bev.) 95 – 70 (15, 35 °C, orange bev.)	Carbonated bev.: Pepsi-Cola: rapid initial loss (5-10 days) of AA, after which the rate slowed Orange bev.: - AsMP was the most stable form of vitamin C Losses of L-AA in orange bev. (40% - 30 days) equalled those in Cola L- ascorbate 2-monophosphate is a stable form of vitamin C because it resists O ₂ -oxidation	Wang <i>et al.</i> (1995)

n.a.- not available; Aer.- aerobic; Anaer.- anaerobic.

the contribution of anaerobic degradation to the total vitamin C loss is small compared to aerobic degradation (Villota & Hawkes, 1992).

1.4.2.2. Vitamin B complex

The vitamin B complex group is composed of thiamine (vitamin B₁), riboflavin (vitamin B₂), niacin, a group comprised of pyridoxine, pyridoxal and pyridoxamine (vitamin B₆), pantothenic acid, biotin, folic acid and cobalamin (vitamin B₁₂). All B complex vitamins have been detected in citrus juice, except for vitamin B₁₂ (Shaw et al., 1993b).

Folic acid is the one found in more significant amounts (TetraPak, 1998). This vitamin is very important as it is required for DNA synthesis and its deficiency is first expressed in tissues with high rates of cell turnover (Gregory, 1993).

Limited studies have been conducted on the stability of the B complex vitamins in citrus juices (White et al., 1991). Folic acid is quite heat-sensitive, but the vitamin C in citrus juices protects it from degradation during heat treatment (TetraPak, 1998).

1.4.3. COLOUR STABILITY

Citrus juices colours are primarily due to carotenoids present in plastids located in the juice vesicles (Gross, 1977; Gross, 1987). Citrus carotenoids are C-40 compounds that can exist as either hydrocarbon carotenes or oxygenated xanthophylls and are primarily responsible for the red, orange and yellow pigments. The main carotenoids in orange juice are α -carotene, β -carotene, zeta-

carotene, α -cryptoxanthin, β -cryptoxanthin, antheraxanthin and violaxanthin (Stewart, 1980).

Juice colour is an important standard for determining quality of orange juice (Stewart, 1980). Legally, blending with more highly coloured juice is the only method for enhancing juice colour (Nagy et al., 1993).

Carotenes are relatively unstable and must be protected from oxygen, and stored under refrigerated conditions (Stein *et al.*, 1986). The colour of processed red and pink grapefruit fades during ambient temperature storage with a simultaneous darkening of the juice. The rate of colour degradation and browning are highly associated with storage temperature for aseptically prepared orange juice. The darkening of citrus juices during storage occurs most often in citrus juices that are stored at ambient temperature in containers that are not effective oxygen barriers and in the absence of antioxidants (Toledo, 1986).

Handwerk & Coleman (1988) reviewed browning as it occurs in citrus juices and model solutions. The role of amino acids, sugars, ascorbic acid, buffers and catalysts, sulphur dioxide and S-containing amino acids and thiols was discussed. According to the authors, sugar breakdown through the Maillard reaction is initiated by formation of hexose amines from amino acids and sugars present in citrus juice and proceeds through the Amadori or Heyns rearrangement to produce deoxy and amino hexoses. These deoxy compounds go through a series of reactions and through one of two pathways. One of these pathways produces furanones and pyrones, whereas the other produces furfurals and pyrroles. Both pathways are known to be operable because all four types of compounds have been

found in citrus juices. However the actual compounds responsible for browning, i.e., the brown pigments, were not identified.

Marcy et al. (1989) studied concentrate orange juice aseptically packed in flexible bags and stored at 4, 15, 22 and 30°C for 6 months. Nonenzymatic browning was measured monthly using a Hunter colour meter and absorbance at 420 nm. They found the greatest browning for high temperature stored samples and least browning in the samples stored at the lowest temperatures.

1.4.4. FLAVOUR / OFF-FLAVOUR DEVELOPMENT

Recent studies have involved quantification of 24 volatile constituents in samples of fresh Valencia and Temple orange juices (Moshonas & Shaw, 1987). Nispieros-Carrido & Shaw (1990) quantified 20 volatile constituents in 15 fresh orange juice samples. Their study is important because it compares volatile flavour compounds in different types of orange juices. Shaw *et al.* (1993a) used the same technique to quantify 19 volatile compounds in a different set of 4 fresh orange juice samples. Moshonas & Shaw (1994) quantified 46 volatile juice constituents in 13 fresh orange juice samples, hand and mechanically squeezed of 6 different cultivars. The results reported in their study provide the most complete database yet determined for quantities of volatile flavour compounds present in fresh orange juice. Nine of the 17 oil-soluble constituents present at higher levels in mechanical obtained juices include α -pinene, myrcene, limonene, octanal, nonanal, decanal, neral, geranial, and linalool. From these, only limonene has an established optimum level, and for processed orange juice it is about 135-180 ppm. The seven

water-soluble constituents quantified that are considered important for flavour of orange juice include ethyl acetate, ethyl propionate, methyl butanoate, ethyl butanoate, ethyl-3-hydroxyhexanoate, ethanol and (Z)-3-hexen-1-ol. Acetaldehyde and (E)-2-hexanol, two additional components considered important in orange flavour, were identified but not quantified. The components present at highest levels (10-fold or higher above their aroma thresholds) and important in orange flavour are limonene, myrcene, α -pinene, decanal, octanal, ethyl butanoate and linalool.

The highly desirable aroma and flavour of fresh squeezed citrus juices is difficult to stabilize and preserve. Once heat treatment has been applied to the juice to stabilize it from the microbiological and enzymatic point of view, certain chemical processes have been initiated which will ultimately degrade the flavour of the product due to the formation of off-flavours during storage.

Changes that occur during processing and storage of citrus juices can differ widely for the different products because of differences in starting material (juice), processing conditions, packaging materials and storage conditions. For instance, the initial flavour compound contents vary for different types of orange juice (Nispieros-Carriedo & Shaw, 1990).

Several factors have been recognized as contributing to the development of off-flavours during thermal processing and subsequent storage. Two aldehydes that are indicative of temperature abuse in fruit juice are 2-furaldehyde and 5-hydroxymethyl-2-furaldehyde (Wilkes *et al.*, 2000). Reduction or removal of oxygen from the headspace and minimization of initial dissolved oxygen in the

juice may partially reduce the short-term production of off-flavour (Shaw *et al.*, 1993b). However, other major off-flavours are formed from the acid-catalysed hydrolysis of citrus oil components, the formation of sulphur-containing juice components, and the chemical degradation of flavourless precursors to produce off-flavours.

Tatum *et al.* (1975) isolated 10 degradation compounds from canned single strength orange juice (SSOJ) stored at 35 °C for 12 weeks. These compounds were isolated with GLC and are listed in Table 1.3. Of the compounds identified, 4-vinyl guaiacol, 2,5-dimethyl-4-hydroxy-3(2H)-furanone and α -terpineol were found to be the most responsible for the malodorous properties of time-temperature abused juice. The first imparted an old fruit or rotten fruit aroma, the second imparted the pineapple-like aroma typically observed in aged orange juice and the last one was described as stale, musty or piny. Acid degradation of sugars was probably responsible for 2-hydroxyacetyl furan and 3-hydroxy-2-pyrone formation.

Table 1.3- Degradation products found in canned SSOJ after 12 weeks at 35°C. From Tatum *et al.* (1975).

Furfural	cis-1,8-p-menthadiol
α -terpineol	trans-1,8-p-menthadiol
3-hydroxy-2-pyrone	4-vinyl guaiacol
2-hydroxyacetyl furan	benzoic acid
2,5-dimethyl-4-hydroxy-3(2H)-furanone	5-hydroxymethyl furfural

These authors also state that furfural was formed from the degradation of ascorbic acid, fact mentioned previously in §1.4.2.1, via its anaerobic degradation pathway (Huelin, 1953; Huelin et al., 1971).

1.5. FACTORS THAT INFLUENCE PRODUCT SHELF LIFE

1.5.1. PROCESSING TREATMENT (PASTEURISATION)

Orange juice is a complex product. Therefore a good understanding of the basic nature and properties of orange juice is needed for processing and packaging orange juice. In fact, to ensure that high product quality is maintained during juice processing, such understanding is indispensable.

Processing steps to stabilise extracted orange juice with respect to enzyme and microbial activity are essential before concentration, bulk storage, packaging and distribution. Pasteurisation is the processing treatment used to make the product stable, and it is necessary in order to destroy the microorganisms capable of growing during storage and to inactivate enzymes to prevent cloud loss (TetraPak, 1998). Thermal resistance of microorganisms is traditionally expressed in terms of D and Z values. The D value is the time at a specific temperature for the microbial population to decrease by one log cycle (90%) (Villota & Hawkes, 1992), and may also be referred to as the decimal reduction time. The Z value is the change in temperature needed to alter the D value by one log cycle (Villota & Hawkes, 1992). The same concept may be extended to enzyme inactivation kinetics (Ramaswamy & Abbatemarco, 1996).

Orange juice is pasteurised at least twice before it reaches the consumer (TetraPak, 1998), with the exception of freshly squeezed single strength juice that is distributed chilled and has a shelf life inferior to 3 weeks. The first pasteurisation occurs immediately after extraction and before bulk storage, and is necessary to inactivate the enzyme pectin-methyl-esterase (PME) or pectinesterase (PE), which cause cloud loss of single-strength juice and gelation of concentrate during storage (Bruemmer, 1980). This process also destroys microorganisms, as a more intensive time-temperature treatment is necessary to inactivate PME than to destroy them. The second pasteurisation is aimed at destroying microorganisms that may have contaminated the juice after the first one, survived bulk storage and/or those which have contaminated the juice in subsequent stages of processing prior to package filling (Ramaswany & Abbatemarco, 1996).

1.5.1.1. Inactivation of enzymes

PME is mainly active in the temperature range from 5 to 65 °C and shows a maximum activity at 60 °C. Heat inactivation studies indicated a break in the inactivation curve near 70 °C but residual activity was not destroyed until temperatures around 90 °C were applied (Atkins *et al.*, 1953; Bisset *et al.*, 1953; Versteeg *et al.*, 1980; Wicker & Temelli, 1988; Cameron *et al.*, 1994; Castaldo *et al.*, 1997). The activity of the enzyme at temperatures below 5 °C is low, but it is still enough to cause cloud loss in single strength orange juice (Versteeg *et al.*, 1978), and at temperatures as low as -18 °C the reaction rate of this enzyme is

high enough to cause gelation of concentrates during storage (Atkins *et al.*, 1953; Guyer *et al.*, 1956).

Time-temperature conditions to inactivate PME are dependent on juice pH, juice pulp content, fruit variety/maturity (Snir *et al.*, 1996; Cameron *et al.*, 1997) and citrus peel (Cameron *et al.*, 1998). Typical commercial heat treatments vary from 98 to 90 °C for 10 to 60 seconds (Sadler *et al.*, 1992; Nagy *et al.*, 1993).

1.5.1.2. Inactivation of microorganisms

The heat resistance of microorganisms is affected by several factors, such as pH, water activity and oxygen. The reduction of microorganisms is more efficient under conditions not favourable for their growth. Moulds are less resistant to heat than yeasts and yeasts less resistant than bacteria, with some exceptions. The yeast *Sacharomyces cerevisiae* is one of these exceptions as it can produce ascospores that are much more heat resistant than its vegetative cells.

As mentioned previously, PME rather than microorganisms imposes time and temperature conditions for the primary pasteurisation. The second pasteurisation, carried out prior to juice packaging, is used for microbial destruction rather than enzyme inactivation, and as microorganisms are less heat resistant than enzymes, it can be carried out at lower temperatures. Temperatures and times ranging from 80 to 95 °C for 15 to 30 seconds are commonly used by the industry for the second pasteurisation of orange juice intended for storage at ambient temperature (TetraPak, 1998). However, the industry shows a growing concern in lowering the pasteurisation temperature and/or holding time.

The theoretical thermal destruction curves of PME, the vegetative cells and ascospores of *Sacharomyces cerevisiae* in orange juice are presented in Figure 1.1.

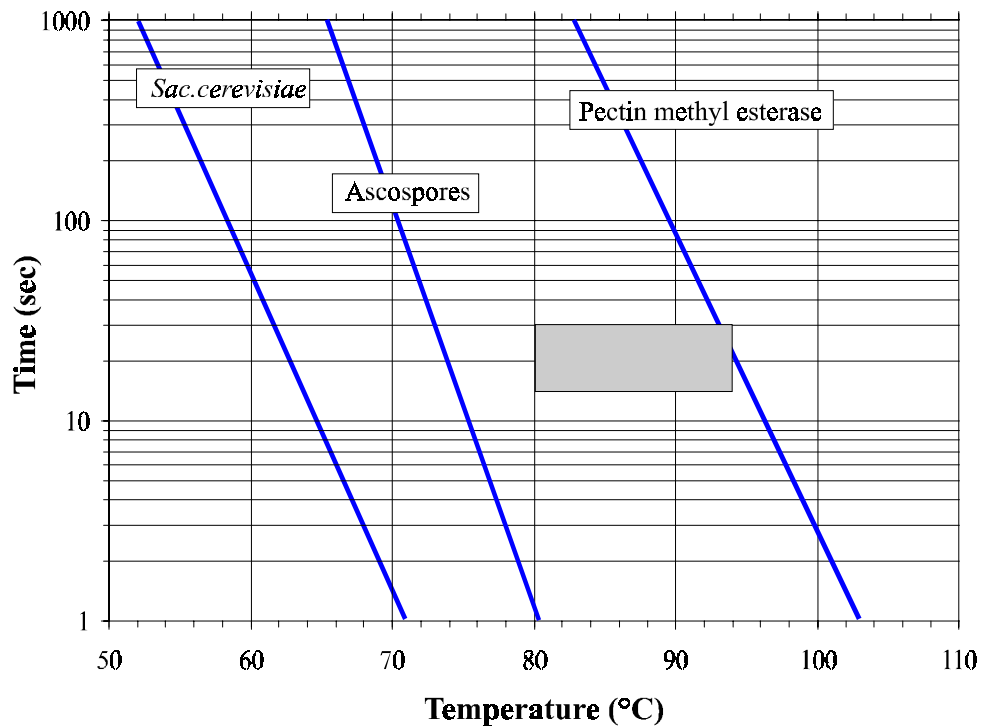


Figure 1.1- Theoretical thermal destruction curves of PME, ascospores and vegetative cells of *Sacharomyces cerevisiae* in orange juice. From TetraPak (1998). The grey rectangle shows the time/temperature conditions usually applied commercially.

All time/temperature combinations to the right of the ascospore curve are sufficient for 10 decimal reductions or more. The grey rectangle shows the time/temperature combinations usually applied commercially. Based on the heat resistance of the yeast *Sacharomyces cerevisiae* (and its ascospores), and considering that 10 decimal reductions will be sufficient to reduce the initial population, pasteurisation at 75 °C for 20 seconds is usually adequate for juice distributed nonaseptically at chilled temperatures (TetraPak, 1998).

Lower temperatures may also be sufficient for juice intended for chilled distribution and storage, but this is greatly influenced by the initial microflora as well as the desired shelf life.

1.5.2. STORAGE TEMPERATURE

Even when citrus juice is produced with good microbiological control and free from unwanted pectinesterase activity, chemical changes will occur during storage, which can influence its shelf life (Hendrix & Redd, 1995). Storage temperature is a major factor affecting chemical reaction rates and thus the shelf life of aseptically packed juice. In Southern countries, Africa or parts of South America, for example, where refrigerated storage of the product is considered too costly, aseptically packaged juices and juice drinks are often transported and sold in markets where the ambient storage temperature can reach 30°C. Under such storage temperatures, flavour deterioration occurs faster than is desired to maintain good flavour quality. Under these storage temperatures flavour changes due to production of furfural, hydroxymethylfurfural, α -terpineol, diacetyl, 3-methyl-2-butene-1-ol and other compounds (Nagy & Rouseff, 1986).

In a study published by Bisset & Berry (1975), single strength orange juice packed in glass jars retained about 90% ascorbic acid for over 4 months and 87% for 1 year at 4.4°C (acceptable flavour), and the retention was 67% after 8 months at 26.7°C (time after which the juice had unacceptable flavour).

1.5.3. OXYGEN CONTENT

As earlier described microbial growth does not set the storage limit of aseptically processed and packed products. Instead, certain chemical reactions will set the limit of the shelf life. Some of these deteriorative reactions are oxygen dependent, e.g., oxidative breakdown of nutrients like ascorbic acid, folacin and the sulphur containing amino acids, formation or loss of colour pigments and lipid oxidation with formation of off-flavours (Fennema, 1985).

At the fruit processor, the loss of vitamin C from orange fruit to frozen orange concentrate is generally negligible when the right processing conditions and short residence times before concentration and freezing are used (TetraPak, 1998). During reconstitution of the orange juice and further processing steps, the amount of oxygen present has an important impact on juice quality, the most dominant of which is the loss of vitamin C and consequent loss of nutritional value. The degradation of vitamin C leads then to formation of unwanted compounds (off-flavours and browning).

If air (oxygen) gains entry during the reconstitution steps or in any step of the process, it can cause problems. Dissolved and dispersed gases are removed in a deaerator. Problems with foaming can occur if the incoming product contains high concentrations of undissolved gas. When juice goes from a high pressure (in the pipes) to a lower pressure (in the deaerator), gas solubility decreases and bubbles of free gas form in the juice and build up foam (TetraPak, 1998), and if the deaerator is filled with foam, deaeration becomes insufficient. High concentration of dispersed oxygen may lead to ineffective pasteurisation (Hahn, 1988), due to

reduced residence time or inconsistent heating. Foaming causes decreased filling efficiency, which can lead to product losses and/or incorrect amounts of juice in packages (Hahn, 1988). Because oxygen takes part in many reactions it is crucial to protect the juice during storage and the extent of protection depends on how long and at what temperature it will be stored. Thus in packages that are not exceptionally tight (all except the metal cans) oxidative changes will have a crucial influence on shelf life. The type of container in which citrus juice is packaged has an important influence on retention of vitamin C. Table 1.4 shows the vitamin C retention for different package containers and for different periods of time.

Table 1.4- Ascorbic acid retention in orange juice packed in different containers at 1.1°C for 0, 1, 2, 3, 6 and 12 months storage. From Shaw *et al.* (1993b).

Container Types	Storage Times (months)					
	0	1	2	3	6	12
Ascorbic acid retention (%)						
Glass bottle ^a	100	97	94	91	85	88
Polyethylene bottle	100	90	79	70	43	-
Polystyrene container	100	41	10	-	-	-
Waxed cardboard	100	55	18	-	-	-
Foil-lined fiberboard	100	94	92	73	-	-
Polyethylene-lined fiberboard	100	97	94	45	23	-

^aNote: Glass bottles were stored at 4.4°C and not at 1.1°C.

1.5.4. LIGHT

Several authors reported that light has a negative effect on ascorbic acid content when oxygen is present (Singh *et al.*, 1976; Mack *et al.*, 1976). Ahmed *et al.* (1976) attributed the flavour changes and ascorbic acid losses in nonpasteurised

refrigerated orange juice to light exposure in combination with microbial growth and the presence of oxygen in the juice.

Similar findings were reported by Solomon *et al.* (1995) and Solomon (1994) showing that ascorbic acid content is not affected by light in airtight glass (tin lid) - high oxygen barrier - but it is in high light transparency polyethylene (when compared to low transparency)- low oxygen barrier material. In high light transmission polyethylene (low oxygen-barrier material), ascorbic acid content in orange juice stored at 8 °C showed a retention of 23.9% compared to 36.6% in low light transmission polyethylene, at the end of 38 days of storage. Therefore, light protection should be considered for use in packages for chilled distribution that have low oxygen-barrier properties.

1.5.5. PACKAGING SYSTEM - PROPERTIES OF AND TYPE OF CONTAINERS

The shelf life of pasteurised juice depends largely on container type and the flavour changes that occur during storage are markedly different depending on whether the container is glass, plastic, laminated flexible multi-layer carton or tin or aluminium can (Marshall *et al.*, 1986).

The two major types of packages used for orange juice are laminated carton packages (either aseptic or nonaseptic) and bottles (Figure 1.2). Glass bottles are the second most common orange juice package used worldwide, closely followed by plastic bottles. In USA, plastic bottles for chilled orange juice take a second place after laminated cartons and in Germany glass bottles are mainly used. A

very small amount of juice for consumption is sold in cans, which is the most popular package in Japan.

Permeability of the container to oxygen is an important factor limiting the shelf life of properly stored pasteurised orange and grapefruit juices. Newer packages containing barriers to oxygen permeability have led to increased storage times (Marshall *et al.*, 1986).



Figure 1.2- Examples of some packages for orange juice.

Source: Tetra Pak (2000).

Carton based packages are made from laminated carton material normally consisting of paperboard coated externally and internally with polyethylene, and a barrier layer. This barrier layer is usually aluminium foil, but there are other materials such as EVOH (ethylene vinyl alcohol), SiO_x on polyester, and PA (polyamide). The package oxygen barrier properties also depend on the barrier properties of strips, closures and the tightness of seals.

As an alternative to metal, plastic or glass containers, aseptic paperboard packaging must be as air-tight, opaque and taint-free (i.e., no migration from packaging material to filled product) as possible, to assure the natural quality and long shelf life of the product; it must be attractive and functional, i.e., easy to open

and to pour; and off course it must be cost effective. Examples of packages designed to meet this criteria are the Combibloc carton (PE/board/PE/AL/PE) (Reuter, 1988) and the Tetra Brik carton. Tetra Brik packaging material is mainly composed of printed-paper, coated with aluminium foil and several plastic layers. TBA cartons (Figure 1.3) are made of a multi-layer structure, combining low density polyethylene, paper board and aluminium foil and thus oxygen transmission takes place mostly through the package seam. The inner material side of the finished package is coated with a special layer facilitating the sealing process. The various layers are functional: the outer polyethylene protects the ink layer and enables the sealing process of the package flaps; the bleached paper serves as carrier of the decor and the unbleached gives the package the required mechanical rigidity; the laminated polyethylene binds the aluminium to the paper; the aluminium foil works as a gas barrier and guarantees that the filling product is protected against the influence of light; two inner polyethylene layers provide liquid barrier (Reuter, 1988).

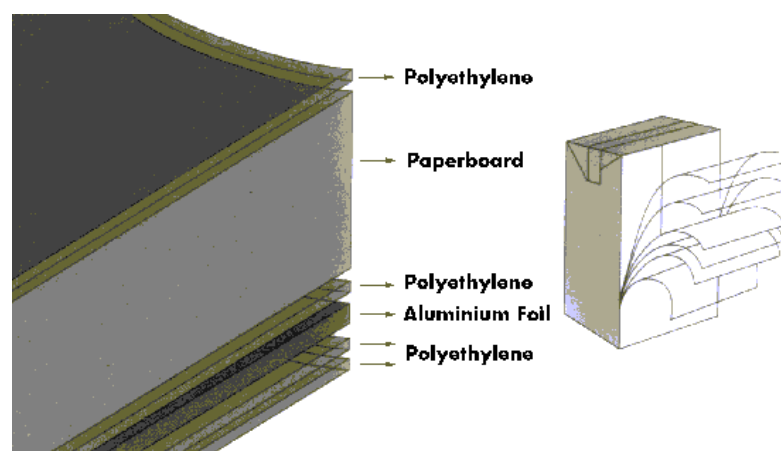


Figure 1.3- Multilayer structure of the Tetra Brick Aseptic carton (TBA). Reproduced with kind permission from Tetra Pak.

The comparative barrier properties of some materials are: LDPE < OPP < PET < NYLON < SARAN < EVOH < AL FOIL (Reuter, 1988).

Depending on the filled product and distribution period, the material might need to have a high oxygen resistance to limit oxidative deterioration to a minimum, especially in the case of fats and vitamin C reduction. On the other hand, inert gases, such as nitrogen and carbon dioxide which are often added to the filling product already during production, to reduce oxygen content, must be kept in the container as long as possible. This also applies to the gas evacuation process during filling and closing operations to reduce oxygen content in the headspace (Hahn, 1988). A certain amount of headspace is always advisable to ensure that the package can be opened and poured without spilling. Headspace is crucial when it is not possible to seal the filled package through the product, namely when it contains suspended solids, but when filling products with high vitamin C content such as citrus fruit juices, reducing headspace is necessary to prevent rapid degradation of ascorbic acid. However, for long shelf life it is often more vital to keep oxygen permeation (e.g., through the longitudinal seam) to a minimum (Reuter, 1988).

Of the package types used today for orange juice, glass bottles are normally considered to have the best gas barrier properties, preventing both oxygen ingress and the loss of carbon dioxide from sparkling drinks (Giles, 1998). Blow-moulded plastic bottles are an alternative to glass bottles. The most common are HDPE (high density polyethylene) bottles produced with the extrusion blow moulding process. These types of bottles have a low oxygen barrier and are used for chilled

juice with short shelf life (\approx 3 weeks). The oxygen barrier can be improved by adding polymers with better oxygen barrier, like EVOH (ethylene vinyl alcohol) or PA (polyamide). With these barriers, plastic bottles allow ambient storage for 6 months or longer. PET (polyethylene terephthalate) bottles are made by stretch blow moulding starting with a preform. These bottles are very robust but do not provide as good oxygen barrier as glass. Regular PET bottles give a shelf life for orange juice of 4 to 6 months, and adding a barrier may extend the shelf life up to one year.

Another characteristic to have in consideration, besides oxygen barrier properties, is the extent of loss of aroma compounds due to absorption or permeation in different package types. This mainly involves nonpolar aroma compounds and limonene is a key compound for monitoring flavour scalping (Nielsen, 1994; Nielsen & Giacini, 1994). Scalping of limonene does not seem to have a detrimental effect on sensorial quality of orange juice (Pieper et al., 1992).

Generally three main types/groups of packages are considered regarding loss of aroma compounds. Type 1 package has no efficient aroma barrier, such as carton packages without a barrier layer and LDPE and HDPE bottles. Type 2 package has an aroma barrier not in contact with the product, and a sealing layer (LDPE) in contact with the product. Most laminated cartons are type 2 packages. Type 3 package has an aroma barrier in contact with the product, such as glass and PET bottles (TetraPak, 1998).

There is another aspect to have in consideration, which has to do with how packaging is performed and/or intended for: aseptic vs. nonaseptic packaging.

Aseptic packaging is used for storage at ambient temperature, but in order to use this type of packaging there are some prerequisite conditions, such as: the orange juice has to be free of microorganisms when packed; packages should not recontaminate the product and must provide an effective barrier against external microorganisms (TetraPak, 1998). Therefore, product shelf life is not determined by microbiological factors but mainly by barrier properties against oxidative changes. Nonaseptic package is used for juice under chilled distribution (TetraPak, 1998). Microbial spoilage usually becomes the limiting factor of shelf life depending on heat treatment, packaging hygienic status and storage temperature (1-10 °C). In this case aroma and oxygen barriers are of less importance.

1.6. MATHEMATICAL MODELLING OF QUALITY CHARACTERISTICS DECAY

Chemical kinetics encompasses the study of reaction mechanisms and rates at which chemical reactions proceed. The area of kinetics in food systems has received a great deal of attention in past years, due primarily to efforts to optimise or at least reduce quality degradation of food products during processing and storage. Moreover, understanding the reactive mechanisms is important to obtain and report meaningful information that, in one hand can provide a better idea of how to formulate or fortify food products (to preserve the existing nutrients or components in a food system) or, on the other hand, to minimize the appearance of undesirable breakdown products (Villota & Hawkes, 1992).

The reaction pathway, also called the reaction mechanism, may be determined through proper experimentation. A chemical reaction may take place in a single step, as is the case of elementary reactions, or in a sequence of steps, as would be the case for most reactions occurring in food systems. Conditions such as temperature, oxygen availability, pressure, initial concentration, and the overall composition of the system may affect the mechanism of reaction.

Although traditionally one can apply reaction kinetics to model chemical changes occurring in a system, other physicochemical changes may also be described using a kinetic approach. One example of this is the description of textural changes and it is obvious that this kinetics represent the final effect caused by a number of complex phenomena (leading to an overall result).

Studies must be conducted under conditions identical to those prevailing during the actual commercial processing or storage conditions being modelled, because of the sensitivity of many nutrients to their chemical and physical environments. As summarized by Hill & Grieger-Block (1980) and Lenz & Lund (1980), reaction kinetics should be obtained at several temperatures to allow calculations of the dependence of rate constants on temperature. Additionally, the joint estimation of the rate constant (k) and equilibrium concentration (C^∞) becomes critical when experiments cannot be conducted in order to provide sufficient degradation/formation of the compound under study, because of the long times required to reach equilibrium or because the system degrades before reaching steady state (Machado et al., 1999a), as estimating C^∞ is essentially predicting

outside the range of the data (Seber & Wild, 1989). This was also well demonstrated by Cunha (1998) for first-order kinetics.

The usefulness of any model for descriptive or predictive purposes greatly depends on the precision and accuracy of the model parameter estimates. Rigorous parameter estimation requires an adequate statistical analysis of experimental data, and a careful experimental design (Cunha et al., 1998). As stressed by Bates and Watts (1988), even a very careful data analysis is unable to recover information that is not present in the experimental data.

1.6.1. SIMPLE KINETIC MODELS

1.6.1.1. Zero-order

In zero-order reactions the rate is independent of the concentration. For a degradation reaction:

$$-\frac{dC}{dt} = k \quad (1.1)$$

where C is the concentration, t the time, and k the zero-order reaction rate constant, which by integration results in:

$$C = C^i - k \times t \quad (1.2)$$

where C^i and C are, respectively, concentrations at time zero and any time t .

This may occur in two different situations: when intrinsically the reaction rate is independent of the concentration of reactants, and when the concentration of the reacting compound is so large that the overall reaction rate appears to be

independent of its concentration. The second case seems to be the most common situation when this order reaction is observed in food systems (Villota & Hawkes, 1992).

1.6.1.2. First-order

The mathematical expression for a first-order degradation reaction is as follows:

$$-\frac{dC}{dt} = k \times C \quad (1.3)$$

where k is the first-order reaction rate constant. By integration this equation becomes:

$$C = C^i \times e^{-k \times t} \quad (1.4)$$

Although a number of compounds follow this reaction order in a food product, most compounds in a model product will not follow true first-order reaction kinetics but rather, a pseudo-first-order reaction (Villota & Hawkes, 1992). For simplicity sake, pseudo- n^{th} -order reactions will be further referred to as simply n^{th} -order reactions.

1.6.1.3. Second-order

There are two important types of second-order kinetics: type I, $A + A \rightarrow P$:

$$-\frac{dC_A}{dt} = k \times C_A^2 \quad (1.5)$$

and type II, $A + B \rightarrow P$

$$-\frac{dC_A}{dt} = k \times C_A \times C_B \quad (1.6)$$

where C_A and C_B are concentrations of the reactant species A and B at time t, and k the second-order reaction rate constant. For type I, the integrated expression yields:

$$C_A = \frac{1}{\frac{1}{C_A^i} + k \times t} \quad (1.7)$$

and for type II, it becomes:

$$C_A = C_B \frac{C_A^i}{C_B^i} \times e^{[-(C_A^i - C_B^i) \times k_2 \times t]} \quad (1.8)$$

where C_A^i and C_B^i , C_A and C_B are the concentrations of species A and B at time zero and time t, respectively.

It should be stressed that in the case of type II reactions if one of the components is present in excess the reaction may follow pseudo first-order kinetics with respect to the other component.

1.6.1.4. Probabilistic models – Weibull model

The Swedish physicist Waloddi Weibull introduced the family of Weibull distributions in 1939 (Devore, 1995). Weibull (1951) discusses a number of applications in his paper. This distribution has been used extensively to deal with problems such as reliability and life testing (time to failure or life length of a component) and can be used to describe ecological, microbial, enzymatic and chemical degradation kinetics.

The probability density function of the Weibull distribution can be described as (Hahn & Shapiro, 1967):

$$f(t) = \begin{cases} \frac{\beta}{\alpha} \left(\frac{t}{\alpha}\right)^{\beta-1} e^{-\left(\frac{t}{\alpha}\right)^\beta}, & t > 0 \\ 0 & , \text{elsewhere} \end{cases} \quad (1.9)$$

with $\alpha > 0$ and $\beta > 0$. The corresponding cumulative distribution is:

$$F(t) = \int_0^t f(t) dt = 1 - e^{-\left(\frac{t}{\alpha}\right)^\beta} \quad (1.10)$$

where α is a scale constant (its inverse corresponds to the reaction time constant) and β is the shape constant, or behaviour index (Seber & Wild, 1989). It is evident from Equation 1.10 that α is the time when the concentration has decreased by one natural log cycle (app. 67%), and that the Weibull model corresponds to the first order model for the specific case of $\beta=1$ (Walpole & Myers, 1978). Equation 1.16 has a sigmoid shape for $\beta > 1$ and a monotonous decrease, steeper than exponential at low times, for $\beta < 1$ (Nelson, 1969).

The reaction time constant is temperature sensitive and this dependence can often be described by an Arrhenius-type relationship (Shepherd and Bhardwaj, 1988; Machado et al., 1999b). The β parameter, or shape constant, is related to the kinetic mechanisms and may be expected to be temperature independent, at least within a limited range of temperature, as found by Ilincau et al. (1995) and Machado et al. (1999a). This parameter gives the model a wide flexibility, making it a potential good model to describe different reaction kinetics.

The Weibull distribution was successfully applied to describe shelf life failure (Gacula Jr. & Kubala, 1975; Schmidt & Bouma, 1992). The Weibull model was

further used to model failure of apple tissue under cyclic loading (McLaughlin & Pitt, 1984), grape pomace elutriation (Peraza et al., 1986), water uptake and soluble solids losses during rehydration of dried apple pieces (Ilincanu et al., 1995) and breakfast cereals immersed in water (Machado et al., 1999a) or milk (Machado et al., 1999b). This model has also been used to describe enzyme inactivation under high pressure (Lemos et al., 1999), *Bacillus subtilis* death kinetics under high-pressure conditions (Heinz & Knorr, 1996), isothermal heat-resistance of *Bacillus cereus* (Fernández et al., 1999), and shrinkage of potato during frying (Costa et al., 2000). The Page model (similar to the Weibull model) was used to model thin-layer drying of pigeon pea (Shepherd & Bhardwaj, 1988) and the drying kinetics of Thompson seedless grapes (Sawhney et al., 1999).

Some examples of very recent application of this model to other fields of research are the successful modelling of fire-recurrence within a natural reserve (Palakow & Dunne, 1999), the survival from a specific disease process (Gamel *et al.*, 2000) and dose-response analyses of cancer data (Melnick & Kohn, 2000).

1.6.2. DEPENDENCE OF RATE CONSTANTS ON TEMPERATURE

1.6.2.1. Arrhenius Law

For a chemical reaction, the rate constant, k , is often related to temperature by an Arrhenius-type relation:

$$k = k_0 \times e^{-\frac{Ea}{R} \times \frac{1}{T}} \quad (1.11)$$

where k_0 is the pre-exponential rate constant, R is the gas constant (8.314 J/mol K), T is the absolute temperature (K), and E_a is the activation energy (J/mol) (Labuza & Kamman, 1983). Labuza & Riboh (1982) enumerated potential causes for non-linear Arrhenius plots when the food product is held at high abuse temperature. Furthermore, when reaction mechanisms change with temperature, the activation energy may be variable (Karel, 1983). The activation energy may also vary with concentration and other composition factors.

This form of Arrhenius model (Eq. 1.11) does not use a finite reference temperature and the value of the rate constant at an infinite temperature (k_0) is often very high. Besides the generation of values outside and far from the range of interest (usually a narrow temperature range), if an infinite reference temperature is used, the model parameters (k_0 and E_a) have a very high correlation (interdependence) coefficient that significantly obstructs the regression convergence. This problem has been pointed out by Nelson (1983), who suggested a transformation of the equation that corresponds to the use of a finite reference temperature. As Van Boekel (1996) explains, to reduce correlation between k_0 and E_a , the temperature can be centred about the mean value of temperatures studied (T_{ref} , reference temperature), and the Arrhenius equation can be reformulated:

$$k = k_{ref} \times e^{-\frac{E_a}{R} \times \left(\frac{1}{T} - \frac{1}{T_{ref}} \right)} \quad (1.12)$$

where k_{ref} is the reparameterised pre-exponential factor:

$$k_{ref} = k_0 \times e^{-\frac{Ea}{R} \times \frac{1}{T_{ref}}} \quad (1.13)$$

If the Arrhenius equation seems to be suitable to describe the temperature dependence, linearization followed by linear regression, to determine E_a and k_{ref} should not be automatic, because errors may not be distributed normally after transformation and the residuals weights are changed. Non-linear regression should be used instead. Also, if the dependence of the rate constants on temperature has been properly assessed, it is better to incorporate Eq. 1.12 directly into the rate equations by substituting the right hand side of Eq. 1.12 for the rate constant, rather than estimating each k at each temperature studied and subsequently determining E_a and k_{ref} via Eq. 1.12 (Van Boekel, 1996). This non-linear regression, often referred to as one-step methodology in opposition to the traditional 2-steps method, has shown not to introduce bias (Haralampu et al., 1985). Non-linear least square methods of analysis are thoroughly reviewed by Johnson & Frasier (1985).

1.6.2.2. Q_{10} concept

Mathematical models have been used in both the food and pharmaceutical sciences to describe how much faster a reaction will proceed if the product is held at some high abuse temperature. If the temperature-accelerating factor is known, then extrapolation to lower temperatures, such as those found in distribution, could be used to predict true product shelf life in those conditions. In the study of food shelf life, this accelerating factor is sometimes called the Q_{10} factor and is defined as:

$$Q_{10} = \frac{\theta_s \text{ at } T}{\theta_s \text{ at } T+10} = \frac{\text{rate at } T+10}{\text{rate at } T} \quad (1.14)$$

where T is the temperature (°C), and θ_s is the shelf life at the indicated temperatures (Labuza, 1982). For any temperature difference Δ , different from 10 °C, this becomes:

$$Q_{10}^{\Delta/10} = \frac{Q_s(T_1)}{Q_s(T_2)} \quad (1.15)$$

Thus, for example, if the Q_{10} is 3 and the published shelf life θ_s was 6 month at 35 °C, the shelf life at 20 °C would be:

$$\theta_{20} = \theta_{35} \times Q_{10}^{\Delta/10} = 6 \times 3^{15/10} = 31.2 \text{ months} \quad (1.16)$$

In many cases, the Q_{10} is not given, so one must establish the mathematical relationship (Labuza & Schmidl, 1985), which is done by means of kinetic modelling.

1.6.3. KINETIC OF NUTRIENT LOSSES AND DEPENDENCE ON ENVIRONMENTAL FACTORS AND FOOD COMPOSITION

In the following sections, a brief discussion of the mechanisms of deterioration of compounds of interest for the present study is presented, with reference to relevant studies reported in literature.

1.6.3.1. Ascorbic acid

Ascorbic acid degradation can follow an aerobic (catalysed or non-catalysed) and/or anaerobic pathway. The scheme shown in Figure 1.4 helps to visualise the influence of oxygen and heavy metals on the route and products of degradation reaction. In the presence of oxygen, ascorbic acid (H_2A) is degraded primarily via its monoanion (HA^-) to dehydroascorbic acid (A), involving the formation of a metal anion complex, which combines with oxygen to give a metal-oxygen-ligand complex ($MHAO_2^{(n-1)+}$). The exact pathway and overall rate is a function of concentration of metal catalysts ($M^{n+} = Cu^{2+}, Fe^{3+}$) in the system. The rate of formation of dehydroascorbic acid is approximately first-order with respect to $[HA^-]$, $[O_2]$ and $[M^{n+}]$. When the metal catalysts are Cu^{2+} and Fe^{3+} , the specific rate constants are several orders of magnitude greater than the spontaneous oxidation, and therefore even a few parts per million of these metals may cause serious losses of vitamin C in food products (Tannenbaum et al., 1985).

In the non-catalysed oxidative pathway the ascorbate anion (HA^-) is subjected to direct attack by oxygen in a rate-limiting step, to give first the radical anions (A^\bullet) and (H_2O^\bullet), followed rapidly by formation of dehydroascorbic (A) and H_2O_2 . Thus the catalysed and uncatalysed pathways have common intermediates and are undistinguishable by product analysis. Since dehydroascorbic acid is readily reconverted to ascorbate by mild reduction, the loss of vitamin activity comes only after hydrolysis of the lactone to form 2,3-diketogulonic acid (DKG).

Under anaerobic conditions ascorbic acid degradation yields furfural, 2-furoic acid and other acids (Villota & Hawkes, 1992). The maximum degradation occurs

at approximately pH 4, followed by a decrease upon a decrease in pH to 2, followed by a rate increase with an increase in acidity (Huelin et al., 1971).

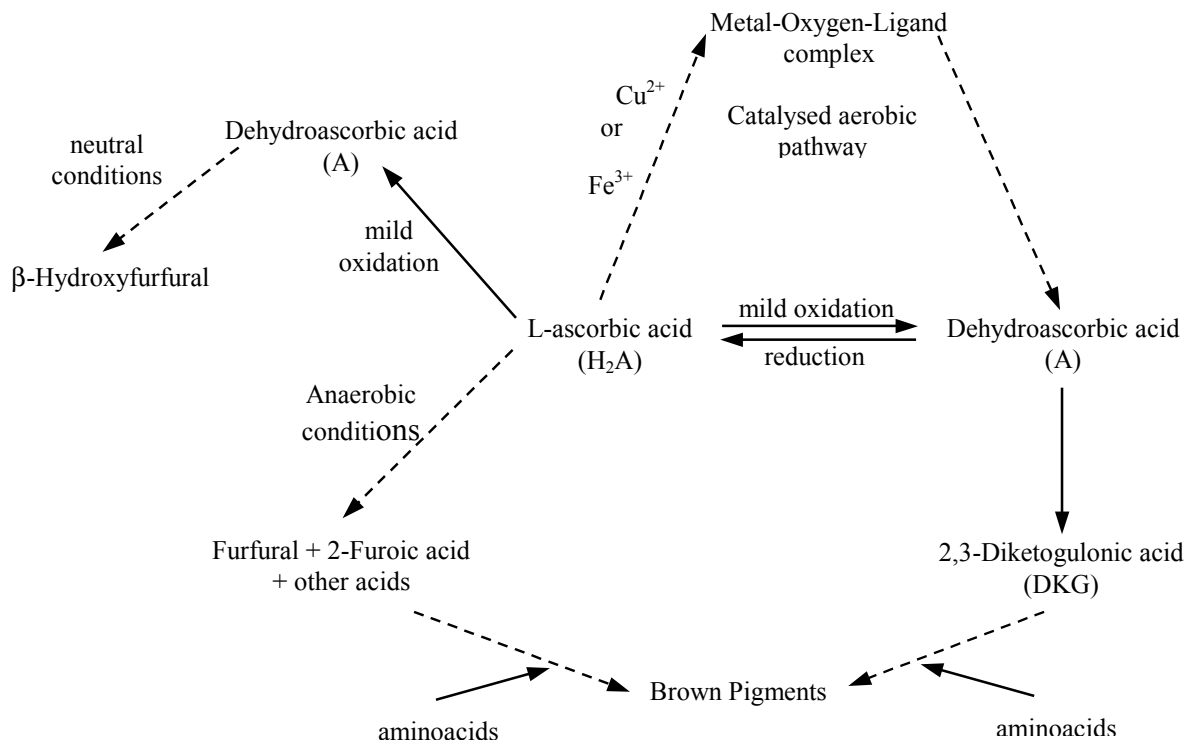


Figure 1.4- Schematic representation of degradation pathways of ascorbic acid. Adapted from Tannenbaum et al. (1995) and Villota & Hawkes (1992). Dashed arrows represent simplification of several distinct reactional steps, here grouped as a single one for simplicity sake.

Many researchers studied ascorbic acid degradation kinetics and factors that affected its rate in food or model food products. Hereafter, a summary table (Table 1.5) of published studies stressing the most important findings is displayed. Most studies report L-AA degradation to follow first-order kinetics. These studies cover a wide range of products (e.g. model food systems, fruit juices, peas, cereals) and conditions (anaerobic, aerobic non-catalytic and aerobic catalytic), as

well as different processes (e.g. thermal processing, concentration) and storage in different packages. In many cases the retention of ascorbic acid in the conditions and times tested is relatively high, what may explain the adequacy of this simple mathematical model to describe L-AA degradation.

A smaller number of researchers report L-AA degradation to follow zero-order kinetics (Kaanane et al., 1988; Laing et al., 1978) or second-order kinetics (Eison-Perchonok & Doves, 1982; Mohr Jr., 1980; Singh et al., 1976). Kanner et al. (1982) reported different reaction orders below 25 °C (first-order) and above 37 °C (different from first-order). More complex mechanisms have been suggested to describe L-AA degradation by Vieira et al. (2000), Sakai et al. (1987), Hughes (1985), Lee et al. (1977), Singh et al. (1976) and Khan & Martell (1967 a,b).

The dependence of the rate constants on temperature is reported to follow an Arrhenius-type equation. Nagy & Smoot (1977) reported two distinct Arrhenius profiles, with a critical transition region between 22 and 26.7 °C.

Hsieh & Harris (1993) reported that the mechanism of L-AA degradation in canned orange juice depends on oxygen concentration, being different above and below 2 ppm, and Kennedy et al. (1992), observed that after the dissolved oxygen in juice packed in TB cartons reaches an equilibrium, L-AA decomposition occurs independently of oxygen.

L-AA degradation during storage of lemon juice protected from light was reported to be independent of initial oxygen contents (Robertson & Samaniego, 1986).

Table 1.5 – Kinetic studies of ascorbic acid degradation.

Food/model system	Package/Storage Conditions	Compounds under study	Other compounds	Compounds/Factors affecting degradation	Atm. Cond.	Applied kinetic	Retention (%)	Fit quality	Observations	Ref.
Buffer solution	Packaging system: n.a.	Ascorbic acid		Catalytic metals: Fe(III) Cu(II)	Aer.	First-order	n.a.	n.a.	The first order rate constant in an air saturated catalytic metal free solution is less than $6 \times 10^{-7} \text{ s}^{-1}$ at pH=7 Ascorbate can be used in a quick and easy test to determine if the near-buffer solutions are indeed “catalytic metal free”	Buethner (1988)
Buffered model system (pH= 6.1)	Closed system with headspace and control of headspace gases temperatures: 30 to 55°C initial AA conc=30, 35, 40, 50, 65 g/L oxygen levels= 10, 15, 21%	Ascorbic acid		Temperature Ascorbic acid addition Oxygen	Aer.	Second-order	75	Good $0.96 < r^2 < 0.99$	Oxygen concentration was maintained through out the experiment Ascorbic acid autoxidation is dependent on dissolved oxygen concentration It appears that the rate of oxygen dissolution into the AA solution is dependent on both temperature and headspace oxygen levels	Eison-Perchonok & Doves. (1982)
Sucrose solution	BOD bottle (300 mL) Initial AA conc= 6.67 g/L $\approx 700 \text{ min (11.7 h)}$ pH: 3.0 to 5.0 3 temperatures: 26.5, 30, and 33°C	Ascorbic acid	Oxygen	Temperature Sucrose pH	Aer.	Second-order in relation to dissolved oxygen Dependent on T by Arrhenius Eq.	78.5 – 87	Good $0.98 < r^2 < 0.99$	Above 2 ppm of dissolved oxygen content there is one mechanism of reaction and below 2 ppm there is another Molar ratio between O ₂ and AA: $\equiv 1 \text{ mol of O}_2 \text{ per mol of AA}$ Ea (AA) was higher in presence of 10% sucrose than in non sucrose controls, and the addition of sucrose reduced the rate of reaction at the temperature tested Effects of sucrose on AA: pH independent physical effect retards AA oxidation; pH dependent catalytic effect accelerates AA oxidation	Hsieh & Harris (1993)
Aqueous solution with AA	Erlenmeyer flasks (open) 4 temperatures= 25, 62, 75, 86 °C Initial AA conc= 500 mg/L 90 minutes	Ascorbic acid Dehydro-ascorbic acid		Temperature Continuous aeration.	Aer.	Mechanism of degradation: $\begin{array}{ccccc} \text{Prod} & & \text{Prod} & & \text{Prod} \\ \uparrow k_3 & & \uparrow k_4 & & \uparrow k_5 \\ \text{AA} & \xrightleftharpoons[k_{-1}]{k_1} & \text{DHAA} & \xrightleftharpoons[k_{-2}]{k_2} & \text{DKA} \end{array}$ First-order (reversible) for DHA and diketogulonic acid. First-order reaction for AA loss	72.2 - 50	Good *	The AA-to-DHA-to-DKA mechanism fits the data reasonably well An irreversible path from AA to products appears to exist. The rate constant k ₃ appears to be large enough that it may be possible to degrade measurable amounts of AA without any DHA being formed	Hughes (1985)

*- By visual inspection of the graph; n.a.- not available; Aer.- aerobic; Anaer.- anaerobic.

Table 1.5 (cont.) – Kinetic studies of ascorbic acid degradation.

Food/model system	Package/Storage Conditions	Compounds under study	Other compounds	Compounds/Factors affecting degradation	Atm. Cond.	Applied kinetic	Retention (%)	Fit quality	Observations	Ref.
O.J. (var. early season Valencia) and O. J. serum	Concentrated during the study (180 minutes, 70.3 to 97.6°C, from 11.7 to 80.6°brix)	Ascorbic acid	Browning	Temperature °brix	Anaer.	First-order	> 60	Good 0.974 < r ² < 0.99	AA rate constants in orange juice serum did not differ from whole juice Ea (AA) ≈ 30 kcal/mol (125.4 kJ/mol) and were independent of solid content	Johnson <i>et al.</i> (1995)
Valencia O.J. (Pasteurised at 92°C for 30sec)	Glass bottles (200 mL) Temperature: 4, 22.5, 35 and 45°C	Ascorbic acid	Total solids pH, acidity Formol no. Reducing Sugars Furfural	Temperature	Anaer.	Zero-order	97- 47	Good *	At high temperature (45°C) furfural production relates very well to AA degradation (r= 0.96), but for lower T this relation is not so obvious	Kaanane <i>et al.</i> (1988)
SSOJ (var. Valencia) and OJ concentrate	Can (6 oz) 18 months 6 temperatures (°C)=18, 5, 12, 17, 25, 37 4 °brix= 11°, 34°, 44°, 58	Ascorbic acid	Browning Furfural Sensorial changes	Temperature °brix	Aer./ Anaer.	T ≤ 25° first-order T= 37°C different from first-order	95 – 10	Good *	AA loss depends on the degree of concentration of the O. J. (increase with °brix)	Kanner <i>et al.</i> (1982)
SSOJ (made from concentrate)	TB cartons 64 days Initial dissolved oxygen content= 4.45 ppm Temperature (°C): 4, 20, 37, 76, 75 L-AA addition (supplemented with 0.34M, 1mL)	Ascorbic acid		Ascorbic acid Oxygen Temperature	Aer./ Anaer.	Zero, first and second-order were applied (4 to 37°C) Impossible to say which fits best the data.	60.4 – 2	Zero-order: 0.97 < r ² < 0.985 1st-order: 0.93 < r ² < 0.99 2nd -order: 0.97 < r ² < 0.97	Initial sudden drop of oxygen, intensified at higher temperatures Initial drop correlates with AA degradation during initial stage of storage After the dissolved oxygen reaches the equilibrium, L-ascorbic acid decomposition occurs independently of oxygen	Kennedy <i>et al.</i> (1992)

*- By visual inspection of the graph; n.a.- not available; Aer.- aerobic; Anaer.- anaerobic.

Table 1.5 (cont.) – Kinetic studies of ascorbic acid degradation.

Food/model system	Package/Storage Conditions	Compounds under study	Other compounds	Compounds/Factors affecting degradation	Atm. Cond.	Applied kinetic	Retention (%)	Fit quality	Observations	Ref.
Aqueous solution	2 temperatures: 0.4, 25°C 7 O ₂ contents: 11.1, 8.9, 6.7, 4.5, 2.3, 1.1, 0.4 ppm 9 pH levels: 2-5.5	Ascorbic acid (H ₂ A)		Cu (II) Fe (III) Temperature Oxygen pH	Aer./ Anaer.	<ul style="list-style-type: none"> • Spontaneous Oxidation <ul style="list-style-type: none"> - First order, in relation to HA⁻ - [0.40; 1.0] atm O₂: $-\frac{dAA_{Total}}{dt} = k_1 [HA^-] [O_2]$ • Cu²⁺ Ion Catalysed Oxidation <ul style="list-style-type: none"> - First order, in relation to H₂A, pH= [1.5; 3.5] • Fe³⁺ Ion Catalysed Oxidation <ul style="list-style-type: none"> - First order, in relation to H₂A, pH= [1.5; 3.85] $-\frac{dAA_{Total}}{dt} = k_1' [H_2A] [M^{n+}] + k_2' [HA^-] [M^{n+}]$ 	n.a.	Good *	<p>The rate of the non-catalysed oxidation of AA was found to be proportional to oxygen concentration at 20% or higher. In the pH range investigated [2-5.5] only the monoionic species of AA was found to be reactive toward O₂</p> <p>A mechanism is proposed whereby O₂ takes part directly in the oxidation of the ascorbate anion, HA⁻</p> <p>The rates of the ferric and cupric anion catalysed oxidations were found to be 1st order with respect to O₂. A reaction path involving O₂ bound to metal-ascorbate complex is proposed</p> <p>The catalytic activity of cupric ion was found to be more than that of ferric ion toward the oxidation of the ascorbate anion; in the oxidation of the neutral species, ferric ion is a better catalyst than cupric ion</p> <p>The mechanistic implications of the catalysed and unanalysed reactions are discussed</p>	Khan & Martell (1967 a)
Aqueous solution	2 temperatures: 0.4, 25°C Oxygen: 80 - 5% 5 pH levels: 2.25-3.45	Ascorbic acid (H ₂ A)		Cu (II)-EDTA Cu (II)-HEDTA Cu (II)-NTA Cu (II)-HIMDA Cu (II)-IMDA Fe (III)-DTPA Fe (III)-CDTA Fe (III)-EDTA Fe (III)-HEDTA Fe (III)-NTA Fe (III)-HIMDA Temperature Oxygen pH	Aer./ Anaer.	<p>Catalytic activity of Cu(II)-IMDA > Cu(II)-HIMDA > Cu(II)-NTA > Cu(II)-HEDTA > Cu(II)-EDTA</p> <p>Catalytic activity of Fe(III)-HIMDA > Fe(III)-NTA > Fe(III)-HEDTA > Fe(III)-EDTA > Fe(III)-CDTA > Fe(III)-DTPA</p> $-\frac{dAA_{Total}}{dt} = k_1 [H_2A] [ML] + k_2 [HA^-] [ML]$	n.a.	Good	<p>The metal chelate catalyst is totally inactive for the oxidation of the un-ionised species of AA</p> <p>Mechanism proposed for metal chelate catalysed oxidation of AA: direct participation of metal chelate species in an electron-transfer process</p> <p>A mixed ligand chelate of ascorbate anion, HA⁻, and metal chelate, MLⁿ⁺, is formed in a pre-equilibrium step. This is followed by an electron transfer within the mixed ligand chelate, HAML⁽ⁿ⁻¹⁾⁺, then dissociates in a fast step to the lower valence metal chelate ML⁽ⁿ⁻¹⁾⁺ and a semiquinone. Oxidation of the lower valence metal chelate and semiquinone by molecular O₂ takes place in subsequent steps</p> <p>The catalytic activities of the cupric and ferric chelates were found to be independent of O₂ concentration, which is in agreement with this mechanism</p>	Khan & Martell (1967 b)

*- By visual inspection of the graph; n.a.- not available; Aer.- aerobic; Anaer.- anaerobic.

Table 1.5 (cont.) – Kinetic studies of ascorbic acid degradation.

Food/model system	Package/Storage Conditions	Compounds under study	Other compounds	Compounds/Factors affecting degradation	Atm. Cond.	Applied kinetic	Retention (%)	Fit quality	Observations	Ref.
Model system	Mixing bowl (with tight-fit cover); Steady-state experiment: 4 temperatures: 71, 79, 92, 105°C 25 min 3 a _w content: 0.69, 0.80, 0.90 Unsteady-state experiment; Extruder, 6.5 min.	Ascorbic acid		Water activity Temperature	n.a.	Zero-order	≈ 57.5	Good r ² >0.97 (Steady-state experiment)	Rates of AA degradation are dependent upon O ₂ availability, which is in turn dependent upon temperature and moisture content The equation derived to predict the amount of AA lost during an unsteady state heating process was successful when tested under conditions approximating a linear T rise (error for the final predicted value < 5%) The same equation yielded less accurate predictions of AA losses during extrusion (error for the final predicted value < 10%)	Laing <i>et al.</i> (1978)
Peas	TDT cans 5 temperatures: 110, 115, 121, 126, 132 °C 6 hours	Ascorbic acid	O ₂ monitored	Temperature	Aer./ Anaer.	First-order	30 - 96	Reasonable good *	Discussion on the values of E _a for this study and others, both for aerobic and anaerobic conditions, reaching the conclusion that the differences on E _a indicate that kinetic studies should be conducted for different food systems	Lathrop & Leung (1980)
Fresh squeezed O.J. Unpasteurised FROZEN	Polyethylene bottle 24 months storage Temperature (°C): -23 Initial AA= 406 mg/L pH=3.7 °brix: 11.4	Ascorbic acid		Temperature	n.a.	First-order	80.8	Good *	This study did not intended to characterize the kinetics of vitamin C loss Over the 24 month period, the rate of decline was 0.8% per month Based on this storage study, vitamin C content of frozen, fresh squeezed, unpasteurised OJ has been shown to provide 131% of the daily value of vitamin C requirements, even after 24 months of storage. The vitamin C was still within the label declaration which complies with the nutritional labelling law (FDA, 1993)	Lee & Coates (1999)

*- By visual inspection of the graph; n.a.- not available; Aer.- aerobic; Anaer.- anaerobic.

Table 1.5 (cont.) – Kinetic studies of ascorbic acid degradation.

Food/model system	Package/Storage Conditions	Compounds under study	Other compounds	Compounds/Factors affecting degradation	Atm. Cond.	Applied kinetic	Retention (%)	Fit quality	Observations	Ref.
Seaweed Mixed Cereal Orange Juice	Package system: n.a. 4 temperatures: 23, 35, 40, 45°C 7 a_w content: 0.32, 0.51, 0.67, 0.75, 0.84, 0.88, 0.93 10 moisture content: 1.1 to 33.3 gH ₂ O/100g sol	Ascorbic acid		Water activity Moisture content Temperature	n.a.	First-order the rate of AA loss increases with increasing a_w .	n.a. (a_w =0.93) 11 (a_w =0.84) 80 (a_w =0.32)	Good *	Ascorbic acid destruction rates increased with increasing a_w Ascorbic acid was more rapidly destroyed in the desorption system than in the adsorption system due to a decrease in viscosity and possible dilution of the aqueous phase	Lee & Labuza (1975)
Tomato Juice	Can (8 oz) 6.3 months 4 temperatures: 10, 18.3, 29.4, 37.8 °C Initial conc (Cu): 2.6 and 10 ppm pH: 3.53, 3.78, 4.06, and 4.36	Ascorbic acid		Temperature pH Metal catalyst - Cu	Aer.	AA loss is first order in relation to AA AA=f(T) Arrhenius relation Describes 3 reactions involved in the overall destruction of AA: $AH^- \xrightarrow{k_1} \text{Product}$; $AH_2 \xrightarrow{k_3} \text{Product}$ $AH_2 + AH^- \xrightarrow{k_1} AH_2.AH^- \xrightarrow{k_2} \text{Product}$ $AA_T \xrightarrow{k} \text{Product}$; $-\frac{d(AA)}{dt} = k(AA_T)$	≈ 60	Good *	The rate of AA destruction was influenced by pH, reaching a maximum near pK of AA The rate of copper-catalysed destruction of AA increased with copper conc. and was affected by pH. E_a changes with pH, with a minimum at pH 4.06 (3.3 kcal/mol) A mathematical model was developed for the rate of AA loss as function of T, pH and Cu A computer simulation program was developed to predict AA stability in tomato juice Predictions were in good agreement with results of the shelf-life tests	Lee <i>et al.</i> (1977)
Intermediate moisture food material	Jacketed, stirred reactor with air space above reactants Temperature: 60 to 110°C 3 a_w 's: 0.9, 0.8, 0.69	Ascorbic acid		Oxygen mass transfer a_w	Aer./Anaer.	Second-order	n.a.	n.a.	The effect of oxygen transport on degradation rate was determined by comparing the experimental observations with theoretical predictions for a four series of regimes (a regime is characterised by different relative rates of O ₂ mass transfer and chemical reaction) The most likely explanation for the experimental data is regime III- the chemical reaction rate is sufficiently fast that all the oxygen reacts in a thin film near the interface between the food and the gas phase, which enhances the mass transfer rate due to chemical reaction	Mohr Jr. (1980)

*- By visual inspection of the graph; n.a.- not available; Aer.- aerobic; Anaer.- anaerobic.

Table 1.5 (cont.) – Kinetic studies of ascorbic acid degradation.

Food/model system	Package/Storage Conditions	Compounds under study	Other compounds	Compounds/Factors affecting degradation	Atm. Cond.	Applied kinetic	Retention (%)	Fit quality	Observations	Ref.
SSOJ (Var. early, mid and late Valencia)	Can (6 oz) 11 temperatures: 4.4, 15.6, 21.1, 29.4, 32.2, 35, 37.8, 40.6, 43.3, 46.1, 48.9°C 12 weeks	Ascorbic acid		Temperature	Aer./Anaer.	First-order Two distinct Arrhenius profiles [4.4, 21.1] and [29.4, 46.1] °C Employment of orthogonal polynomials in the analysis of variance indicates that the mechanism of AA degradation was not the same at all temperatures	92 - 6	Good $0.97 < r^2 < 0.99$	Values of U. S. RDA of vitamin C are given At each specific temperature all 14 juices, regardless of plant or processing season, showed essentially similar percent vitamin C's retention The Arrhenius plot showed two distinct temperatures regions, with a critical transition region between 22 and 26.7°C	Nagy & Smoot (1977)
Lemon Juice	Glass flasks, 250 mL, covered with AL foil. Initial dissolved oxygen content: 0.41, 1.44 and 3.74 mg/L Temperature: 36°C	Ascorbic acid	Browning HMF Furfural	Initial dissolved oxygen content	Aer./Anaer.	First or second-order	47.1	1st order: $0.85 < r^2 < 0.87$ 2 nd -order: n.a.	Initial oxygen content did not affect significantly the rate of AA degradation and furfural formation Correlation between AA and the other compounds was between 0.8 and 0.9	Robertson & Samanigo (1986)
Sweet aqueous model system: $a_w = 0.94$ and pH = 3.5	Glass flasks: 60 mL (no headspace) ≈210 days at 24°C, 125 days at 33°C, 105 days at 45°C, 140 h at 70°C, 90 h at 80 and 90°C. Initial AA conc = 330 mg/kg Stored in the dark	Ascorbic acid	Browning	Temperature Humectants: gluco-se, sucrose, sorbi-tol Additives: potassi-um sorbate, sodi-um bissulfite	Aer./Anaer.	First-order	> 20	n.a.	At lower temperatures (24,33,45 °C) the humectants protected L-AA from destruction (sugars being the most effective due to the structure forming effect they have) At higher temperatures characteristic of processing (70, 80, 90°C) humectants with active carbonyls (glucose, sucrose) promoted AA destruction and nonenzymatic browning reactions AA destruction occurred mainly through anaerobic path as O ₂ was depleted in 15 h (70-90°C) or 25 days at low T	Rojas & Gerschenson (1997)
Grapefruit Juice	60 min Initial AA content: 34.8, 112.5, 204.8 mg/100 g ^o brix: concentrated during the study from 11 to 62 ^o brix	Ascorbic acid		Added AA concentration ^o brix	Anaer.	First-order Dependent on T by Arrhenius Eq. Ea = 5 kcal/mol (11 ^o brix) Ea = 11.3 kcal/mol (62 ^o brix) Arrhenius coeff. dependent on ^o brix Polynomial curve fitting, empirical kinetic equation correlating rate of reaction with temperature and degree of concentration.	< 85	Good $0.972 < r < 0.999$	Initial AA conc. has no significant effect either on rate of deterioration or mechanism A model combining kinetic data with process variables was developed and proved useful in predicting and optimising vit. C retention processes where grapefruit juice is subjected to any combination of thermal and concentration treatments	Saguy <i>et al.</i> (1978)

*- By visual inspection of the graph; n.a.- not available; Aer.- aerobic; Anaer.- anaerobic.

Table 1.5 (cont.) – Kinetic studies of ascorbic acid degradation.

Food/model system	Package/Storage Conditions	Compounds under study	Other compounds	Compounds/Factors affecting degradation	Atm. Cond.	Applied kinetic	Retention (%)	Fit quality	Observations	Ref.
Buffer solution	Temperature: 25°C Constant O ₂ content 4 pH levels: 2.5, 2.5, 4.5, 6	Ascorbic acid		Cu (II) - citrate complexes. pH	Aer.	First-order	n.a.	n.a.	The rate of cupric ion-catalysed oxidation was found to be first order with respect to ascorbic acid. The effects of cupric ion conc. and pH suggests a mechanism involving the formation of a transition complex between monoascorbate ion and Cu(II)-citrate chelate	Sahbaz & Somer (1993)
Aqueous solution with AA	Package system: n.a. 11 hours 2 Temperatures: 30 and 71°C Oxygen levels: saturation with air, oxygen, or 10% O ₂ - 90% N ₂ B-carotene: 80°C 2 initial AA conc. = 114, 266 mg/L	Ascorbic acid	β-carotene	Temperature Dissolved oxygen content AA addition Continuous aeration	Aer.	AA oxidation has a first-order kinetics at one time and zero-order at another time: $A \xrightarrow{k_a} B \xrightarrow{k_b} C$ First order: $k_a > k_b \times (A)_0$ Zero order: $k_a < k_b \times (A)_0$ First order reaction in respect to B-carotene	17.5 - 28	Good *	Rate constants are independent of initial AA content	Sakai <i>et al.</i> (1987)
Infant formula	Closed cells (boxes) 20 hours 3 initial dissolved oxygen content: 1.0, 4.86, and 8.71 ppm 5 light intensities: dark, 1071, 2142, 3213, and 4284 lux Temperature: 7.2 °C	Ascorbic acid		Temperature Oxygen Light intensity	Aer.	Second-order Describes reaction scheme: $AA + O_2 \xrightarrow{k} DHAA + H_2O$ $-\frac{d(AA)}{dt} = k(AA)(O_2)$ $\ln \left[\frac{AA}{O_2} \right] = [AA_0 - O_{20}]kt + \ln \left[\frac{AA_0}{O_{20}} \right]$	≈ 33	n.a.	In samples exposed to light an increase in initial dissolved oxygen content increased the second-order rate constants The rate constants under dark conditions for different initial dissolved oxygen concentration remain unchanged Increasing light intensity above 1756 lux did not increase the rate constant, and below that the rate constant increases linearly with light intensity	Singh <i>et al.</i> (1976)

*- By visual inspection of the graph; n.a.- not available; Aer.- aerobic; Anaer.- anaerobic.

Table 1.5 (cont.) – Kinetic studies of ascorbic acid degradation.

Food/model system	Package/Storage Conditions	Compounds under study	Other compounds	Compounds/Factors affecting degradation	Atm. Cond.	Applied kinetic	Retention (%)	Fit quality	Observations	Ref.
Cupuaçu nectar	TDT tubes (with headspace) 6 temperatures: 60, 70, 75, 80, 90, 99 °C 240 minutes	Ascorbic acid Dehydro-ascorbic acid		Temperature	Aer./Anaer.	<p>First-order</p> $AA \xrightleftharpoons[k_{-1}]{k_1} DHAA \xrightarrow{k_2} DKGA$ <p>After a transformation of variables ($C_{AA}^* = C_{AA} - C_{AA}^i$) the reaction was treated as two consecutive irreversible reactions:</p> $C_{AA}^* \xrightarrow{k_1} C_{DHAA} \xrightarrow{k_2} C_{DKGA}$ $C_{AA}^* = C_{AA}^{i*} \times e^{-k_1 \times t}$ $\frac{C_{DHAA}}{C_{DHAA}^i} = \left\{ \left[\left(\frac{C_{AA}^*}{C_{AA}^{i*}} \right)^{k_1} \left(-\frac{C_{AA}^{i*}}{C_{DHAA}^i} + \left(\frac{k_2}{k_1} - 1 \right) + \frac{C_{AA}^{i*}}{C_{DHAA}^i} \right) \right] \right\} \left(\frac{k_2}{k_1} - 1 \right)$	≈75	Good	<p>Reversible first order for AA ($E_a = 74 \pm 5 \text{ kJ/mol}$, $k_{80} = 0.032 \pm 0.003 \text{ min}^{-1}$)</p> <p>Mechanistic model for DHAA (with the second reaction having $E_a = 65 \pm 9 \text{ kJ/mol}$, $k_{80} = 0.013 \pm 0.003 \text{ min}^{-1}$)</p>	Vieira <i>et al.</i> (2000)
Orange Grapefruit Tangerine Lemon Lime	Whole fruit Can	Ascorbic acid		<ul style="list-style-type: none"> - Production factors - Climate - Position of fruit on the tree - Maturation - Rootstock effects - Citrus variety (and fruit parts) - Processed products: seasonal variability, processing effects, storage time and temperature - Vitamin C destruction: reaction order and reaction rates (aerobic and anaerobic mechanisms) - Effects of container - Influence of juice constituents 		First-order			<p>The variability of vitamin C in fresh fruit is due to variety, climate, horticultural practice, maturity stage and storage conditions</p> <p>Processing fruit into juice products results in minimal loss of vitamin C potency but subsequent storage of the finished product at higher temperatures results in considerable loss</p> <p>From the point of view of the consumer, numerous investigations have shown that fresh processed single strength and reconstituted citrus juices may be kept in a refrigerator for a reasonable length of time (4 weeks) without serious loss of vit C. Even when juice is stored at room temperature, storage time is limited more by loss of palability than by loss of vit C</p> <p>Aerobic and anaerobic mechanisms are mainly responsible for loss of vit C in processed products</p> <p>The mode of breakdown of vitamin C can best be explained by a 1st-order reaction but a significant quadratic time effect has been determined by polynomial regression calculations</p> <p>Plots of log rate (vit C loss) vs. 1/T for canned orange juice showed two distinct Arrhenius profiles, whereas canned grapefruit showed only one</p>	Nagy (1980) - A review

*- By visual inspection of the graph; n.a.- not available; Aer.- aerobic; Anaer.- anaerobic.

Similar results found by Singh et al. (1976) in infant formula protected from light, whereas in samples exposed to light increased initial oxygen led to faster L-AA degradation.

1.6.3.2. Browning

Browning compounds are formed during the Maillard reaction, which occurs between sugars and aminoacids, polypeptides, or proteins, and between polysaccharides and polypeptides or proteins (Kawamura, 1983). There are many pathways and literally thousands of compounds that might contribute to the formation of these coloured compounds, but when it comes to mathematically model of non-enzymatic browning, most authors use zero-order reaction kinetics. This linear model may not be the most adequate to describe the complex group of reactions involved in orange juice browning. Nevertheless, it is a very simple model and it proved to be effective to predict the browning of orange juice in a different range of temperatures. Table 1.6 summarises studies reported in literature. Rojas & Gerschenson (1997) reported a zero-order kinetic for browning in a sweet aqueous model system. The same order of reaction was reported by Robertson & Samaniego (1986) but these authors suggest the existence of a lag period, dependent on initial oxygen content, being greater for the lower initial concentrations. Nagy et al. (1990) reported that it is inaccurate to define browning by a simple zero or first-order reaction, especially within the temperature region of 30-50 °C.

Table 1.6 – Kinetic studies of nonenzymatic browning.

Food/model system	Package and Storage Conditions	Compounds/factors affecting formation	Atm. Cond.	Applied kinetic	Fit quality	Observations	Ref.
Grapefruit juice	Can, bottle 18 weeks 5 temperatures (°C): 10, 20, 30, 40, 50	Temperature	n.a.	Reaction order should be between zero and one, for temperatures < 30°C	n.a.	Browning in citrus juices involves a complex group of reactants that produce an assortment of brown pigments of highly unstable characteristics. Based on these reasons and results of other researchers, the authors believe that it is inaccurate to define browning by a simple zero or first-order reaction No simplistic models should be applied to define the complex series of events leading to brown discoloration of citrus juices, especially within the temperature region of 30-50 °C	Nagy <i>et al.</i> (1990)
Lemon Juice	Glass flasks, 250 mL, covered with AL foil. Initial dissolved oxygen content: 0.41, 1.44 and 3.74 mg/L Temperature: 36°C	Initial dissolved oxygen content Temperature	Aer./Anaer.	Zero-order with a lag period.	0.895 < r ² < 0.946	The lag period before browning increased depended on the initial dissolved oxygen concentration, being greater for the lower initial concentration Highly significant correlations were obtained between browning index, HMF and furfural (> 0.96), suggesting that all 3 would be suitable as chemical indices of storage temperature abuse in lemon juices. (Correlation between AA and the other compounds was between 0.8 and 0.9)	Robertson & Samaniego (1986)
Sweet aqueous model system. a _w = 0.94 and pH= 3.5	Glass flasks: 60 mL (no headspace) ≈210 days at 24°C, 125 days at 33°C, 105 days at 45°C, 140 h at 70°C, 90 h at 80 and 90°C. Initial AA conc.= 330 mg/kg Stored in the dark	Temperature Humectants (glucose, sucrose, and sorbitol) Additives (potassium sorbate, sodium bisulphite)	Aer./Anaer.	Zero-order	n.a.	At higher temperatures characteristic of processing (70, 80, 90 °C) humectants with active carbonyls (glucose, sucrose) promoted AA destruction and nonenzymatic browning reactions	Rojas & Gerschenson (1997)

n.a.- not available; Aer.- aerobic; Anaer.- anaerobic.

Table 1.7 – Kinetic studies of flavour (HMF, Furfural and PVG) formation.

Food/model system	Package and Storage Conditions	Compounds under study	Compounds/factors affecting formation	Atm. Cond.	Applied kinetic	Fit quality	Observations	Ref.
Valencia O.J. (Pasteurised at 92°C for 30sec)	Glass bottles (200 mL) Temperature (°C): 4, 22.5, 35 and 45°C	Furfural	Temperature	Anaer.	Zero-order	n.a.	At high temperature (45°C) furfural production relates very well with AA degradation ($r=0.96$), but for lower T this relation is not as obvious	Kanane <i>et al.</i> (1988)
Grapefruit juice	Vials (10mL) 4 Temperatures (°C): 90, 100, 110, 120 5 experimental times (20, 40, 60, 80, 100 min)	HMF	Temperature	n.a.	Reaction order, according to empirical kinetics of formation was 0.31	Good *	There was a lag phase in kinetics of HMF formation. $E_a=130\pm7$ kJ/mol, $k_r=0.0105\pm0.00040(\text{mg/L})^{0.69}\times\text{s}^{-1}$ (the used reference temperature is not mentioned)	Körmeny <i>et al.</i> (1994)
Orange juice	Culture tubes (15x1.5 cm) Abuse time/ temperature protocol Temperature (°C): 75, 85, 95 Time: 15, 30, 60 min pH: 3.1, 3.8, 4.5 Initial oxygen: 6.2, 0.6 ppm	Furfural 2-hexanal α -terpineol p-vinyl guaiacol	Temperature pH Initial oxygen	Aer./ Anaer.	Furfural: not modelled 2-hexanal: zero-order α -terpineol: zero-order p-vinyl guaiacol: zero-order Arrhenius equation was used to calculate E_a 's E_a (2-hexanal)= 14.831 kcal/mol E_a (α -terpineol)= 20.257 kcal/mol E_a (PVG)= 28.258 kcal/mol	Fit not shown r^2 (2-hex)= 0.994 r^2 (α -ter)= 0.981 r^2 (PVG)= 0.981	The pseudo zero order kinetics applied to 2-hexanal is not valid as concentration varies with time in a form far from a straight line. pH has the most significant effect on the increase of α -terpineol and PVG, as their concentration doubled at the low pH value for the same temperature. This is in agreement with previous studies from Lee & Nagy (1990) In reality it is the release of ferrulic acid (precursor of PVG) that is acid catalysed, and Blair <i>et al.</i> (1952)	Marcotte <i>et al.</i> (1998)
SSOJ (var. Hamlin, Pineapple, early and late Valencia)	Can (46 oz) 5 Temperatures (°C): -18, 4, 16, 21, 35	Furfural Flavour evaluation	Temperature	Anaer.	No kinetics for furfural, but by visual observation of the graphs a zero or first-order is not applicable	n.a.	Juices with lower pH the ones with higher % of citric acid produced more furfural at 35°C	Nagy & Dinmore (1974)
Lemon Juice	Glass flasks, 250 mL, covered with AL foil. Initial dissolved oxygen content: 0.41, 1.44 and 3.74 mg/L Temperature: 36°C	HMF Furfural	Temperature	Aer./ Anaer.	HMF: first-order reaction Furfural: zero-order reaction	HMF $0.965 < r^2 < 0.977$ Furfural $0.983 < r^2 < 0.988$	Initial oxygen content did not affect significantly the rate of furfural formation Highly significant correlations were obtained between browning index, HMF and furfural (>0.96), suggesting that all 3 would be suitable as chemical indices of storage temperature abuse in lemon juices. (Correlation between AA and the other compounds was between 0.8 and 0.9.)	Robertson & Samaniego (1986)

*- By visual inspection of the graph; n.a.- not available; Aer.- aerobic; Anaer.- anaerobic.

1.6.3.3. Off-Flavour Development

There is little information in literature regarding kinetic modelling of off-flavours, although a number of studies are published showing the effect of the temperature, pH and a_w , on sensorial properties (aroma, flavour and threshold values) of these compounds and formation/degradation chemical pathways. Studies on kinetic modelling of furfural, HMF and PVG are summarised in Table 1.7.

Robertson & Samaniego (1986) reported HMF formation in lemon juice to follow a first-order reaction, and Körmeny *et al.* (1994) reported a lag phase for the same kinetics. Furfural formation was reported to follow a zero-order kinetic both in orange juice (Kaanane *et al.*, 1988) and lemon juice (Robertson & Samaniego, 1986). The later researchers concluded that initial oxygen content did not affect the rate of furfural formation. Marcotte *et al.* (1998) reported PVG formation to follow a zero-order kinetic reaction. The mechanism of formation of PVG has been mainly studied by Fiddler *et al.* (1967) and later in citrus by Lee & Nagy (1990), Peleg *et al.* (1991, 1992), and Naim *et al.* (1988, 1993).

The dependence of the reaction rates of these compounds on temperature was considered to follow an Arrhenius-type relationship.

1.6.3.4. Oxygen

In some situations the amount of oxygen is limited to a level that causes no significant effect in the food. In other cases, the total amount of oxygen potentially able to react with nutrients is significant, and the effect of oxygen

concentration (or partial pressure) on the rate of oxidative reactions must be considered (Karel, 1974; Quast & Karel, 1972a; Saguy & Karel, 1980).

The mathematical modelling of oxygen uptake by packaged foods has been mainly applied to dried and fatty foods (Quast et al., 1972; Quast & Karel, 1972b; Ragnarsson & Labuza, 1977). For liquid foods, several studies report the effect of oxygen on quality degradation during storage, but few of them report changes of oxygen concentration. Scarcer are studies where the changes are mathematically modelled and even scarcer the ones that use a packaged liquid food (in a real package material). Singh (1976) developed a mathematical model to describe ascorbic acid and dissolved oxygen concentration changes in an infant formula packaged in glass bottles and stored at 7 °C. This model was based on Fickian diffusion of oxygen accompanied by a second order chemical reaction in the liquid food. Barron et al. (1993) reported a study where a finite element method was applied to the modelling of simultaneous oxygen diffusion and chemical reaction in packaged apple juice, stored at 25 °C, using a cylindrical high-density polyethylene package (top and bottom insulated). Hertlein et al. (1995) presented a study of prediction of steady state oxygen transmission from transient state measurements. Two models were tested, one with an equation describing the transient state, another using a partial pressure pulse instead of a constant change in partial pressure. The study included testing of both models in different films (mono and multilayers) and it was concluded that both models were valid only for ideal conditions.

No works were found on modelling of oxygen changes in liquid foods packaged in aseptic cartons.

1.7. SHELF LIFE ESTIMATION

Shelf life may be defined as the period of time during which the food product will remain safe, be certain to retain desired sensory, chemical physical and microbiological characteristics, and comply with any label declaration of nutrition data, when stored under recommended conditions (IFST, 1993). This definition adds one statement to that mentioned previously in the General Introduction, which is the obligation to comply with label declarations. The dependence of the kinetics of nutrient loss on environmental factors varies from product to product and process to process and must, therefore, be established for each specific case to be evaluated. It is the responsibility of the food manufacturer (together with the retailer for own label products) to determine shelf life of food.

For forecasting shelf life of a product it is imperative to select adequate shelf life indicators. Shelf life indicators are compounds that have a notorious influence on the product safety or quality (nutritional value, appearance or flavour characteristics). Critical shelf life indicators are those that first reach the respective threshold levels and thus limit the product shelf life.

1.7.1. SHELF-LIFE ESTIMATION AND PRODUCT DEVELOPMENT

There are different types of shelf life studies, in respect to the purpose they serve while the product is being developed:

- Initial shelf life studies (ISLS) are carried out once the concept of a new product has been agreed;
- Preliminary shelf life determinations (PSLD) are the first shelf life determination carried out to the whole product (including package).
- Confirmatory shelf life determinations (CSLD) are carried out at the end of the product development process;
- Routine shelf life determinations (RSLD) are conducted so that the shelf life of any existing product can be monitored and to check if it is still correct for different environmental conditions to which it can be subjected.

The exact test is often product-specific and is selected to measure the end-point of the shelf life. Because these tests are highly expensive (either in house or contracted tests) it is critical that companies use the most cost effective tests in their shelf life studies. Tests may involve one or a combination of sensorial, microbiological, chemical, and physical determinations.

Interpretation of shelf life data can only be done meaningfully if the shelf life determination has been conducted properly. It should take in consideration

scaling-up factors (any fluctuations that might occur in for a given product formulation), safety and quality aspects.

The final shelf life should be set to give a clear margin of safety, and particularly in the case of a high risk category product a date should be set based on data that relate to the “worst case” manufacturing and storage scenario, which later can be reviewed if necessary.

Documentation is one aspect that should be taken in consideration, as it is very important to keep clear reports (dated and initialled) with details of rationale, assumptions, methods and procedures.

1.7.2. METHODS FOR SHELF LIFE ESTIMATION

Shelf life estimation can be done by means of direct or indirect methods. Direct methods are usually used for products with short shelf life, as shelf life determination is based on monitoring quality factors, chemical and/or microbiological, in a situation that exactly replicates the real conditions of packaging, storage and distribution (Poças & Oliveira, 1998).

When the product shelf life is expected to be relatively long, it is possible that the product may be launched before any confirmatory shelf life determination can be completed. Because of this and economical aspects, it is highly desirable that faster methods for predicting shelf life are available. These indirect methods are generally based on the principles of accelerated shelf life determination.

Accelerated tests are done exposing the food product to abusive storage conditions, i.e., high temperature, high oxygen content, or others (humidity, light, etc.) relevant to the deteriorative reaction mechanism involved (IFST, 1993). Accelerated tests in complex food systems present a problem because published kinetic data are scarce or contradictory or even unavailable. Therefore, accelerated tests must be developed in face of many unknowns. In this respect, foods present more difficult problems than other chemical systems.

Accelerated tests have been used mostly for dried products. A number of reviews on accelerated tests may be found in literature (Mizrahi et al., 1970 a,b; Ragnarsson and Labuza, 1977; Karel, 1979; Saguy & Karel, 1980; Labuza & Schmidl, 1985).

1.7.3. ACCELERATED TESTS FOR SHELF LIFE ESTIMATION

1.7.3.1. Accelerated tests at elevated temperatures

Typically foods are subjected to storage at 37 and 51°C, and various correlations (usually based on the Arrhenius relation or simplifications of that relation, such as the Q_{10} concept) are used to extrapolate the results to the expected storage temperatures (Karel, 1979). When more accuracy is desired, several elevated storage temperatures (usually 5 to 6) are used and the Q_{10} value or activation energy is determined experimentally, based on the assumption that they are independent of temperature. However, this is often not the case, leading to

erroneous extrapolation. Usually reaction rates are more sensitive to temperature in the range used in accelerated tests, this implying that shelf life may be overestimated, which causes a major problem to food producers.

1.7.3.2. Accelerated Tests at High Oxygen Pressures

Conducting stability tests at high oxygen pressures can sometimes accelerate reactions involving oxidation. The potential for acceleration is not very great because oxidation reactions typically become independent from the oxygen concentration above some critical concentration level, which varies with temperature and other conditions (Karel, 1979). Nevertheless, traditional accelerated tests for oxidation-susceptible oils use exposure to high oxygen pressures to assess the relative stability of such oils.

One aspect on ASLT, which calls for certain precautions, is the change in the water solubility of oxygen by temperature. In oxygen sensitive products, this has to be corrected for by the use of increased partial oxygen pressure at elevated test temperatures.

PART II

Analysis of the changes of characteristics of aseptically packaged orange juice during storage

CHAPTER 2

Selection of quality indicators and identification of suitable conditions for accelerated storage tests of aseptically packaged orange juice

This study focus on the analysis of the influence of temperature and initial dissolved oxygen content on selected quality indexes: L-ascorbic acid concentration, browning index, titrable acidity, brix degree, pH, 5-hydroxymethyl-2-furfuraldehyde, 2-furfuraldehyde and 4-vinyl guaiacol. The main objective was to select critical quality indicator(s) for shelf life estimation and to assess temperature and initial dissolved oxygen content as accelerating factors for shelf life studies. Single strength Valencia orange juice (12° brix) with five different initial oxygen concentrations (1 to 10 ppm) was filled into 1L Tetra Brik Aseptic (TBA) cartons and stored at six temperatures (4 to 50 °C). Samples of juice were collected at different times up to 13 months and analysed for dissolved oxygen concentration and the selected quality characteristics. The results were statistically analysed, showing that temperature has a major effect on the loss of quality factors. There is not statistical evidence that initial dissolved oxygen concentration has an effect on any of the quality indicators, and thus it shows no potential as an accelerating factor for shelf life studies. Ascorbic acid and browning were found to be adequate shelf indicators.

2.1. INTRODUCTION

Aseptically processed orange juice may have a long shelf life: the low pH of the product in combination with the heat treatment usually provides an efficient mean to prevent microbial growth. Therefore, the shelf life of pasteurised juices is limited by deteriorative reactions that result in loss or degradation of flavour components and nutritive value (essentially ascorbic acid). The development of new products, the use of new packages and/or changes in processing conditions imposes the need of shelf life studies. Shelf life evaluation consists of conventional and accelerated storage studies (Gnanasekharan & Floros, 1993). Conventional studies may take years to complete depending on the product, package and objectives under study, being therefore a major obstacle both for the food manufacturer and the food packaging industries. Accelerated shelf life tests attempt to reduce testing time by accelerating deteriorative mechanisms through exposure to abusive conditions. Temperature is commonly used as an accelerating factor (Almonacid-Merino *et al.*, 1993; Mizrahi & Karel, 1977b; Singh & Heldman, 1976; Rogers, 1963) and it has also been suggested in literature that increased oxygen contents can increase the rate of oxidative reaction (Eison-Perchonok, & Downes, 1982; Karel, 1974; Quast *et al.*, 1972). Oxygen plays a major role in the loss of quality in orange juice during storage, mainly because of ascorbic acid degradation, through the aerobic pathway, and colour changes. The aerobic pathway of ascorbic acid degradation in packaged juice is related to the presence of headspace oxygen, dissolved oxygen in the juice, and the oxygen-

barrier properties of the package. Several publications also indicate the involvement of oxygen on off-flavour formation during storage of orange juice, but this is not yet fully understood.

A number of quality factors have been suggested in literature to monitor and estimate shelf life of juices.

Because L-AA is quite unstable, degrading both through aerobic and anaerobic pathways, its loss is usually used as an index of loss of overall quality in citrus juices (Shaw *et al.*, 1993).

HMF and furfural have been used to monitor citrus juice quality, as their content in freshly processed juice is virtually zero whereas large amounts accumulate in storage-abused juice (Nagy and Randall, 1973). Even in properly manufactured juice concentrates, HMF may be formed by acid catalysed sugar dehydration (Lee & Nagy, 1996) and fructose is the major potential source for the formation of this compound. It was noticed, particularly for orange juice, that HMF was related to nonenzymatic browning (Lee *et al.*, 1986), which makes it useful as a quality indicator (Graumlich *et al.*, 1986; Lee & Nagy, 1996). 2-Furfuraldehyde (Furfural) is obtained from decomposition of sugar, amino acid-reducing sugar condensation and ascorbic acid degradation (anaerobic pathway). It has been regarded as an index of product quality and a useful indicator of temperature abuse (Nagy and Randall, 1973) as it is established that the concentration of this compound in juice products increases over time, although it does not contribute to off-flavour (Nagy and Dinsmore, 1974; Lee & Nagy, 1996). 4-Vinyl-guaiacol (PVG) was identified by Tatum *et al.* (1975) as one of the most malodorous off-

flavour compounds in aged canned orange juice. PVG increases significantly during storage of orange juice (Lee & Nagy, 1990; Naim et al., 1988; Peleg et al., 1992) and its probably one of the first significant off-flavours to be noticed during storage of orange juice, particularly at ambient or higher temperatures. It imparts an old fruit or rotten flavour to orange juice (Lee & Nagy, 1990).

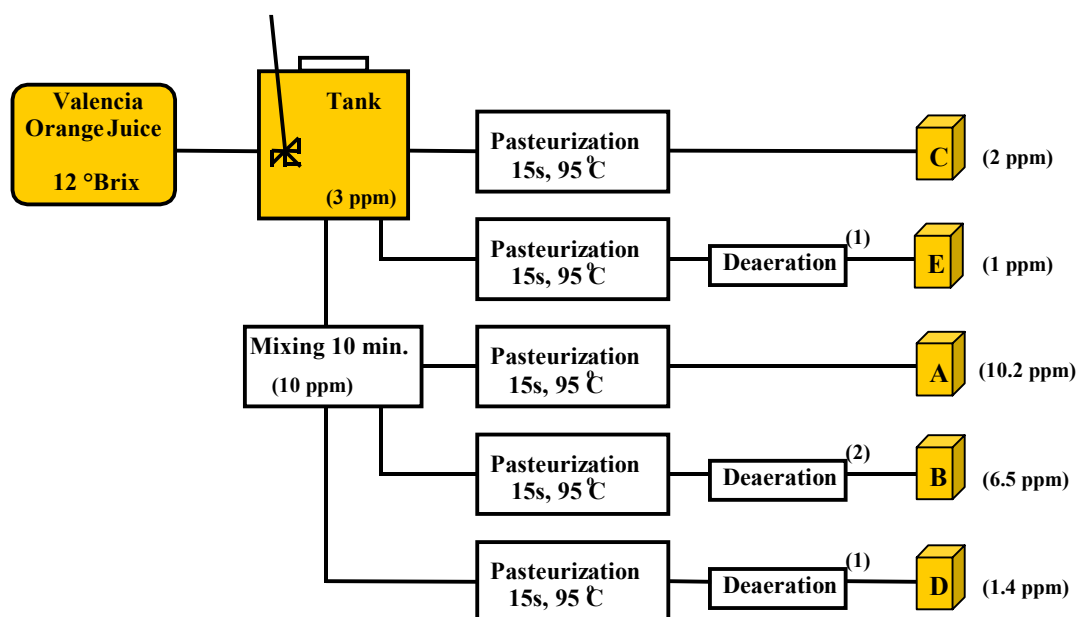
The main purpose of this study was to analyse the effect of temperature and initial dissolved oxygen content as accelerating factors of the reactions of formation or degradation of the quality indexes as well as to identify critical quality factors, i.e., the quality factor that first reaches the acceptability threshold.

2.2. MATERIAL AND METHODS

2.2.1. PRODUCT, PACKAGING MATERIAL AND PROCESSING CONDITIONS

Single Strength Valencia Orange Juice (12°Brix) was obtained from Cargill Citra-America, Inc. At Tetra Pak pilot plant (Lund, Sweden) the juice was homogenised, pasteurised at 95°C during 15 seconds and aseptically filled into 1 L Tetra Brik Aseptic (TBA) cartons with a LSE (Longitudinal Sealing Edge) strip and without headspace (see Figure 2.1).

The orange juice was stirred and/or deaerated prior to aseptic filling, in order to obtain batches with 5 different initial oxygen concentrations (10.25, 6.47, 2.08, 1.36 and 1.04 ppm, that will be referred to as batches A, B, C, D and E, respectively). A total of 700 TBA cartons were filled, 140 in each run, i.e. for each batch. The physical-chemical properties of the juice immediately after packaging are summarised in Table 2.1.



- (1) maximum pressure in the deaeration tank
 (2) partial pressure in the deaeration tank

Figure 2.1 – Schematic representation of the processing conditions used to fill the Tetra Brik Aseptic cartons. The initial oxygen concentrations are represented between brackets.

TBA cartons are made of a multilayer packaging material and the permeability of the package to gases is very low due to the presence of the aluminium layer, with exchanges occurring mainly through the seam (e.g., permeability to oxygen at 20°C is 0.014 cm³/(package*day) at 0.2 atm, 50% RH).

2.2.2. EXPERIMENTAL DESIGN

Storage experiments were conducted in temperature controlled walk-in rooms at 4, 8, 20, 30, 40 and 50 °C (±0.5 °C). A total of 5 x 140 TBA cartons were randomly distributed into six storage walk-in rooms (Figure 2.2).

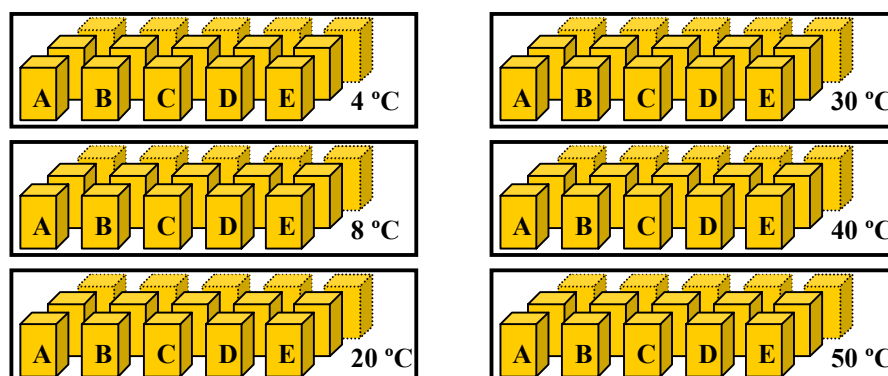


Figure 2.2 – Schematic representation of the storage conditions used for the experimental design.

Ten (2 samples x 5 batches) TBA cartons were randomly collected from each storage walk-in room at different time intervals, depending on temperature, and analysed for dissolved oxygen concentration (O_2), L-ascorbic acid concentration (L-AA), browning index, titrable acidity, brix degree, pH, 5-hydroxymethyl-2-furfuraldehyde (HMF), 2-furfuraldehyde (Furfural or Furf) and 4-vinyl-guaiacol (PVG). Results are summarised in Tables A.1 and A.2 (Appendix A).

2.2.3. ANALYTICAL DETERMINATIONS

The dissolved oxygen concentration in the juice was measured using a WTW Trioxmatic EO 200 oxygen electrode in combination with a WTW OXI 200 microprocessor. The electrode was calibrated with an one-point calibration using water vapour saturated air (WTW-Quick-Calibration) and equipped with a stirring device that allows a representative sample flow at the oxygen electrode. Before measurement, the packages were shaken. A small opening was made just large enough to fit the oxygen probe, which was immersed in the juice immediately

after opening. The concentration of dissolved oxygen (ppm) was recorded when a steady value was displayed (approximately 60 seconds).

Browning index was measured as the light absorbance at 420 nm (Meydav et al., 1977) using a DMS 100 UV-Visible spectrophotometer (Varian, Sweden). The brown pigments were extracted by dilution of the juice 1:1 (v/v) with 95% ethyl alcohol. Before measurements, the juice was filtered through a Munktell 00H analytical filter paper. Two measurements were performed in two replicate juice samples.

An enzymatic kit from Boeringer Mannheim (Sweden) was used for determination of L-ascorbic acid concentration in the juice (Boeringer cat. No 409677). Before analysis, the packages were shaken and 1 mL orange juice was collected in an eppendorf tube. The juice was then centrifuged at 400 rpm for 20 minutes and the supernatant was used for analysis as described by the manufacturer. When required, samples were diluted with 1.5% meta-phosphoric acid (pH 3.5-4.5).

Brix degree was measured by refractometry with an Atago hand refractometer, and pH was measured with an electrode HI 1310S, PMH 62 standard pH-meter instrument.

Titration acidity was measured as described by the Association of Official Analytical Chemists (AOAC, 1965): sodium hydroxide (NaOH) of known concentration was slowly added under agitation until a pH value in the range of 8.1 to 8.2 was reached. HMF, furfural and PVG concentrations were determined

using a Beckman System HPLC (Beckman Instruments, Inc. San Remo, California) equipped with a LiChrospher 100 RP-18 column (5 mL, 250 mm ×4 mm, Merck, Sweden) and a RP-18 precolumn (25 mm ×4 mm, Merck, Sweden), followed by a Beckman Photo Diode Array detector and by a HP 1046A Programmable Fluorescence Detector. Simultaneous quantification was performed using methods adapted from Lee et al. (1986) and Lee & Nagy (1990). Each sample was injected twice. Before HPLC analysis the juice samples were centrifuged for 10 minutes at 12,000 x rpm. One millilitre of supernatant was injected into a C-18 Sep-Pak cartridge (Varian, Sweden), which had been preconditioned with 2 mL of methanol followed by 3 mL of water. The compounds were eluted with 0.3 mL of acetonitrile followed by 0.7 mL of water. The eluted samples were filtered through a 0.45 µm Millipore filter (Millipore Corporation, Milford, MA, USA) before injection. HMF (5-hydroxymethyl-2-furaldehyde, H-9877, 99% pure, Sigma-Aldrich Sweden AB), Furf (2-furaldehyde, 18591-4, Sigma-Aldrich Sweden AB) and PVG (2-methoxy-4-vinylphenol, 98% pure, Lencaster Synthesis, LTD, UK) were used to prepare the standard solutions (external standards). A linear gradient and isocratic elution with 1% acetic acid in water (solvent A) and 1% acetic acid in acetonitrile (solvent B) was used with a flow rate of 1 mL/min, linear gradient, 90 to 68% of A, 10 to 32% of B, 20-25 min, isocratic, 68% of A; 25-35 min, linear gradient, 68 to 58% of A, 32 to 42% of B. The column was washed with 100% B for 10 minutes, and equilibrated with 90% A - 10% B for 10 minutes. Analysis was carried out at room temperature by injecting 80 µL of the sample or standard solution into the

column. The separated chromatographic peaks were identified (λ of 280 nm) and their areas were integrated with a Photo Diode Array detector (HMF, furfural and PVG). This detector was also used for peak purity determination. Furthermore, PVG was also quantified using a fluorescence detector (280nm for excitation, 340 nm for emission).

2.3. RESULTS AND DISCUSSION

2.3.1. EFFECT OF TEMPERATURE AND INITIAL DISSOLVED OXYGEN CONTENT ON DEGRADATION OF QUALITY CHARACTERISTICS

Brix degree (12.6 ± 0.1), pH (3.83 ± 0.01) and titrable acidity (2.35 ± 0.05) were found to remain unchanged during storage, for the temperatures and periods tested, whereas the remaining parameters studied showed to vary with time, particularly at the higher temperatures (see Table 2.1). An analysis of variance also showed that initial oxygen content, in the range tested, did not affect any of the quality indicators, with exception of L-AA degradation at 4 °C, HMF formation at 50 °C and browning at 4 and 8°C (95% significance level), where batches A and B were statistically different from C, D and E.

Dissolved oxygen concentration decreased rapidly and after the first sampling time (2 days) its concentration showed to be very low and fairly constant (Appendix A). It was expected that the dissolved oxygen content would have an influence on L-AA degradation but that was not evident from the experimental

Table 2.1- Initial (after pasteurisation and packaging) and final contents of the quality indicators at the temperatures tested (*).

time (day)	Juice Batch/T	HMF (ppb)	Furfural (ppb)	PVG (ppb)	Oxygen (ppm)	L-Ascorbic Acid (mg/l)	Browning (Abs.420nm)	°Brix	Titration acidity (g Citric Acid /100g OJ)	pH
0	Batch A	0	0	0	10.25 ± 0.01	333	0.149 ± 0.008	12.7 ± 0.1	2.36 ± 0.05	3.86 ± 0.01
0	Batch B	0	0	0	6.47 ± 0.02	362	0.142 ± 0.009	12.6 ± 0.1	2.34 ± 0.05	3.85 ± 0.01
0	Batch C	0	0	0	2.08 ± 0.01	396	0.135 ± 0.006	12.6 ± 0.1	2.35 ± 0.05	3.84 ± 0.01
0	Batch D	0	0	0	1.42 ± 0.01	427	0.134 ± 0.007	12.6 ± 0.1	2.36 ± 0.05	3.82 ± 0.01
0	Batch E	0	0	0	1.04 ± 0.00	437	0.132 ± 0.004	12.6 ± 0.1	2.36 ± 0.05	3.82 ± 0.01
84	50°C	21432 ± 425	874 ± 31	88.7 ± 5	0.11 ± 0.01	6 - 4	0.986 ± 0.002	12.6 ± 0.1	2.35 ± 0.05	3.82 ± 0.01
84	40°C	3975 ± 281	101.2 ± 7	65.5 ± 4	0.11 ± 0.01	63 - 110	0.466 ± 0.003	12.6 ± 0.1	2.33 ± 0.05	3.81 ± 0.01
395	30°C	4103 ± 9	148 ± 5	58.7 ± 5	0.11 ± 0.01	- 127	0.380 ± 0.003	12.6 ± 0.1	2.34 ± 0.05	3.83 ± 0.01
395	20°C	505 ± 26	96.5 ± 6	15.3 ± 2	0.11 ± 0.01	129 - 201	0.250 ± 0.002	12.6 ± 0.1	2.36 ± 0.05	3.84 ± 0.01
395	8°C	531 ± 27	42.3 ± 8	≈ 0	0.11 ± 0.01	148.6 - 173	0.154 ± 0.002	12.6 ± 0.1	2.35 ± 0.05	3.82 ± 0.01
395	4°C	378 ± 37	48 ± 4	≈ 0	0.11 ± 0.01	168.5 - 254	0.148 ± 0.002	12.6 ± 0.1	2.36 ± 0.05	3.83 ± 0.01

(*)Values at the end of storage refer to the average of the different batches tested, except for L-AA, where values represent concentrations for batch A and E. At 20°C, L-AA values refer to 359 days of storage.

results (Figure 2.3). The effect of initial dissolved oxygen content is negligible when compared to the effect of temperature, as can be seen in Figures 2.3 and 2.4. Further examples are presented, as graphic correlations for individual temperatures, on Figures A.1 to A.6 (Appendix A).

Dissolved oxygen content has however an effect on orange juice prior to packaging, as the initial values of L-AA concentration decrease with increasing initial dissolved oxygen content (333 mg/L of L-AA at 10.25 ppm of O₂, and 437 mg/L of L-AA at 1.04 ppm of O₂). This stresses the importance of low dissolved oxygen contents during processing if a high quality juice (nutrition quality) is to be obtained.

2.3.2. SELECTION OF SHELF LIFE INDICATORS

In order to select an adequate shelf life indicator, the rate of decay or formation of the parameters tested was analysed considering their threshold levels.

The threshold value for furfural is reported to be 80 ppm (Fors, 1983), for HMF this value is 200 ppm (Fors, 1983), whereas for PVG is 0.05 ppm (Tatum *et al.*, 1975). For browning there is no reported threshold value, but from sensory we found that a browning index of 0.2 might be used as a threshold level for the juice used in this work, as at this level a difference in colour can be noticed which leads to visual rejection (its not an attractive juice but is not repulsive as well). As far as ascorbic acid is concerned, its content has to be stated in the juice package.

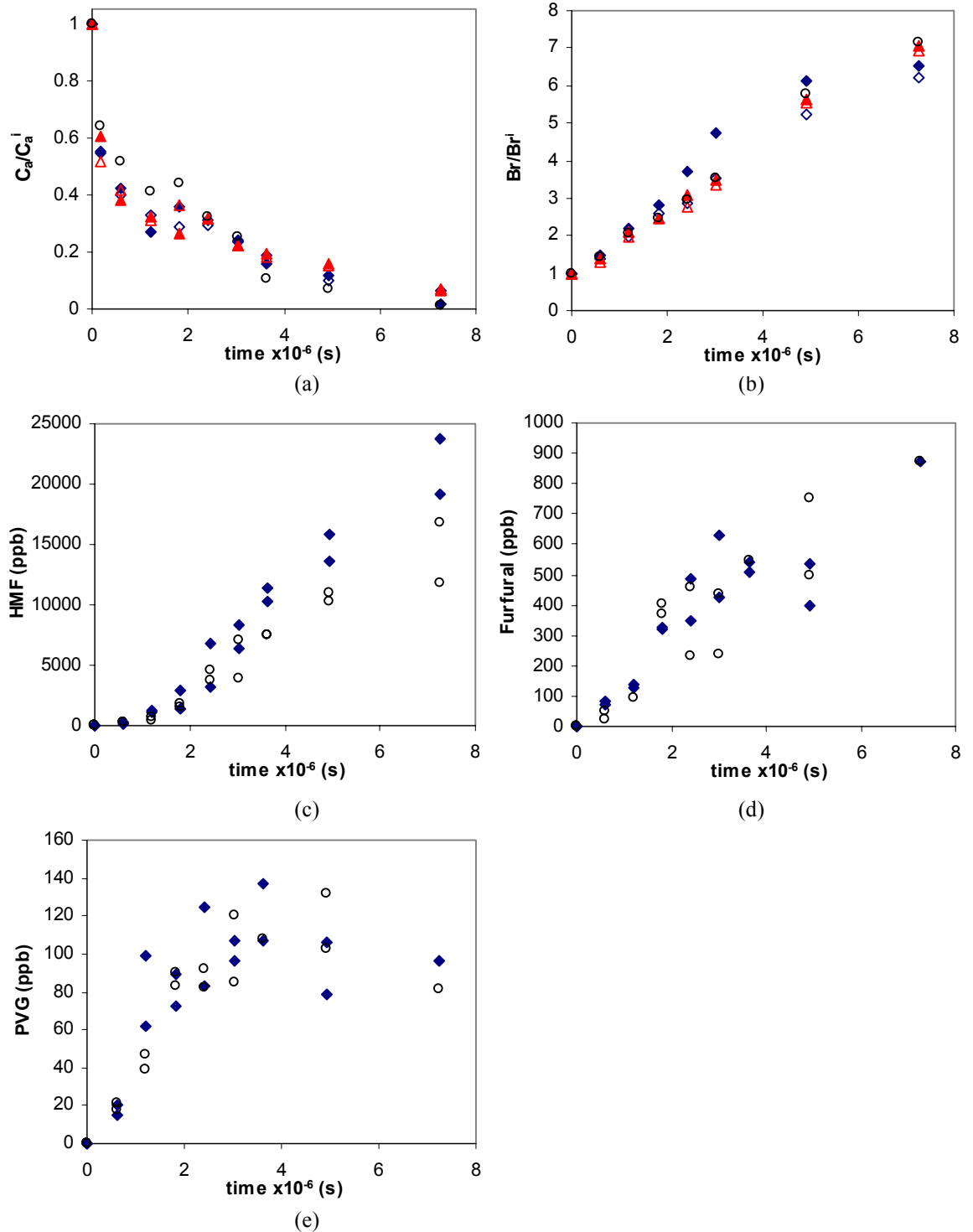


Figure 2.3- Changes of concentration with time at 50 °C, (a) L-ascorbic acid, (b) browning, (c) HMF, (d) furfural and (e) PVG, for the different initial oxygen content batches: (◆) A-10.25 ppm, (◇) B-6.47 ppm, (▲) C-2.04 ppm, (△) D-1.36 ppm, (○) E-1.04 ppm.

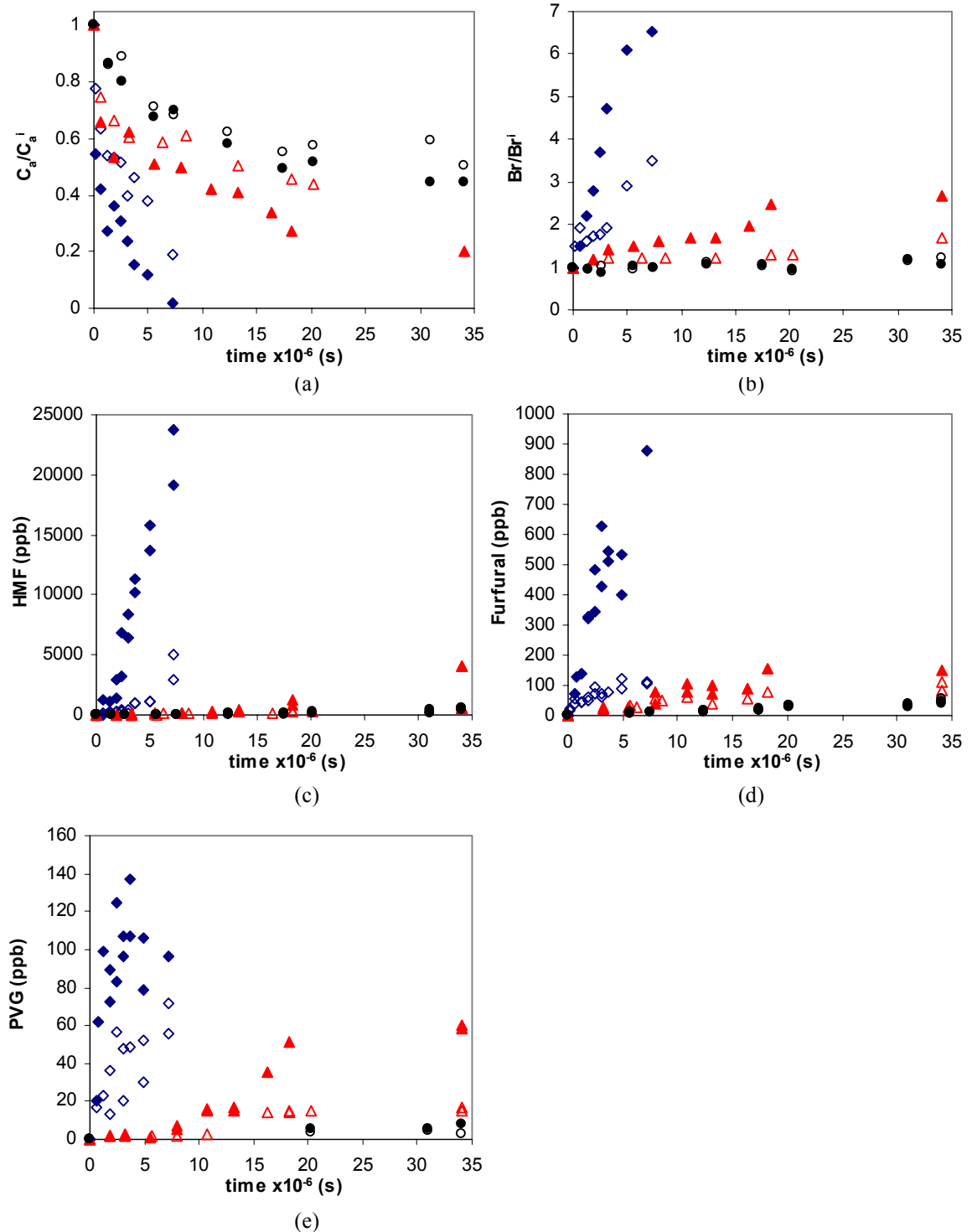


Figure 2.4- Changes of concentration with time for batch A (10.25 ppm), (a) L-ascorbic acid, (b) browning, (c) HMF, (d) furfural and (e) PVG, at different temperatures: (\blacklozenge) 50, (\diamond) 40, (\blacktriangle) 30, (\triangle) 20, (\bullet) 8 and (\circ) 4 °C.

The recommended value of AA for packaged juices varies very much from country to country, even within the EU. The EU Fruit Juice Directive based on the AIJN code of practice for the evaluation of fruit and vegetable juices states that, with regard to vitamins, EU countries may decide on their own rules. In the UK the recommended value is 100 mg/L, while the German RSK values (Richtwert, Schawkungsbreite, Kennzahlen: guide value, range, reference number) state that a minimum of 200 mg/L of L-AA is expected at the end of shelf life. Nevertheless packaged orange juices in general declare values of 200, 300 and sometimes up to 400 mg/L throughout Europe and USA. In some cases this value is conveyed as a % of the recommended daily allowance (RDA), which is a usual case in USA because of the nutrition labelling law (130% RDA) (FDA, 1993). The initial ascorbic acid content of high quality orange juice ranges from 400 to 600 mg/L (source: Tetra Pak). Provided that the production procedures are correct, only a small loss of vitamin C occurs during the initial processing and more significant losses may occur during processing at the juice packer and during storage. Typical values for orange juice when consumed range from 200 to 400 mg/L (source: Tetra Pak). In this work a concentration of 300 mg/L was chosen as threshold level.

Figure 2.5 shows clearly that for ambient and higher temperatures, browning and ascorbic acid are the first indicators of shelf life that decay below the respective thresholds (C_T) (values above 0 show that the compound has not reached its threshold yet), although it is also possible to note that PVG is a good indicator of

temperature abuse. At refrigerated temperatures the juice maintained good quality during all storage time tested.

Browning is often reported to follow zero-order model kinetics (§1.6.3), which greatly simplifies accelerated shelf life studies. Greater contents of L-AA during storage may be achieved by addition before packaging (Chapters 5 to 7). The kinetics of ascorbic acid losses is more complex to describe mathematically, as referred in §1.6.3, making trickier the choice of this compound as the potential shelf life indicator. Besides, L-AA determination involves much more work and expensive equipment than browning determination.

Figure 2.6 shows how the storage time required to reach the browning threshold level at a given temperature relates to the time required at other temperatures with accelerating factors of (approx.) x134 for real storage at 8 °C, of x19 for storage at 20 °C and of x4 at 30 °C. Using the shelf life time of 21 days for browning index at 40 °C to predict the end of shelf life at 30°C and 20 °C yielded errors of, respectively, 11 and 7%. The calculation of the accelerating factors was based on the rate constants of browning, presented in §4.3.

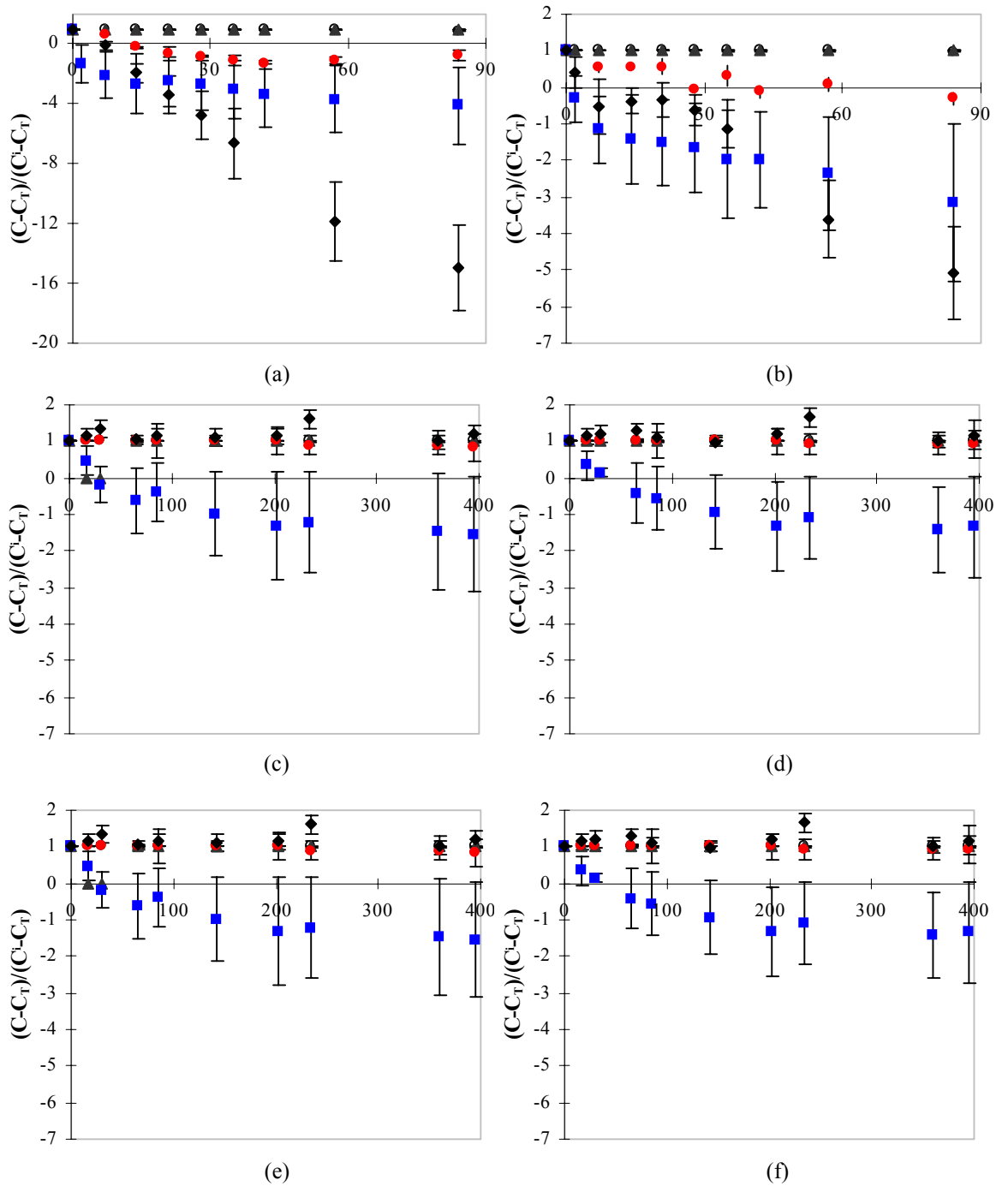


Figure 2.5- Decay of quality indexes: (■) L-AA, (◆) Browning, (○) HMF, (▲) Furfural and (●) PVG, at (a) 50 °C, (b) 40 °C, (c) 30 °C, (d) 20 °C, (e) 8 °C and (f) 4 °C. Zero represents the threshold value for acceptability of orange juice, with values above zero corresponding to acceptable concentrations.

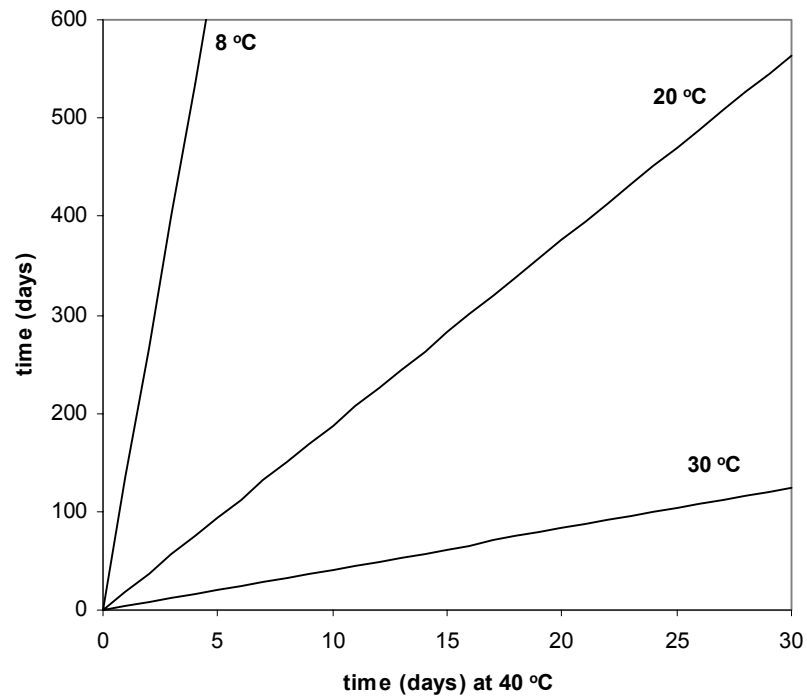


Figure 2.6- Relation between orange juice shelf life at accelerated, ambient and refrigerated conditions, considering browning as the shelf life indicator.

2.4. CONCLUSIONS

Results showed that TA, °brix and pH did not vary during the storage period tested. The other quality indexes were greatly affected by temperature whereas initial dissolved oxygen content did not show a significant effect during storage. This limits the use of high initial oxygen contents as an accelerating factor for shelf life studies. Browning and L-AA contents were considered to be adequate shelf life indicators.

CHAPTER 3

Modelling oxygen concentration changes during storage of aseptic packaged orange juice

In this chapter a mathematical model that combines oxygen uptake from the outside environment with oxygen consumption by first order oxidative reactions in packed juice during storage is presented. The model was applied to orange juice aseptically packaged in Tetra Brik Aseptic cartons, during storage up to 5 months at 4, 8, 20, 30, 40 and 50 °C (data reported in Chapter 2). The parameters of the model, the oxygen mass transfer coefficient and the rate constant of consumption reactions, were estimated by fitting the model to the experimental data. The value of the rate constant was three orders of magnitude greater than the value of the oxygen mass transfer coefficient. The influence of temperature on the reaction rate was well described by an Arrhenius type equation, with activation energy of 46 kJ/mole. This model was further tested with data reported in literature and it was found that it adequately describes the dissolved oxygen concentration changes during storage.

3.1. INTRODUCTION

For the purpose of package design and optimisation, it is important to consider the deteriorative reactions that take place in the food product. In many food products, these reactions are dependent on oxygen concentration, which directly affects the rate of oxidation of vitamins, lipids, pigments and proteins (Quast & Karel, 1972).

Oxygen permeates through many package materials and its concentration inside the package changes during storage. A mathematical model to describe the concentration of dissolved oxygen is therefore important for both food and packaging producers. For the food producer, because oxygen influences product shelf life, and for the packaging industry because the oxygen barrier of packaging materials can be optimised.

The mathematical modelling of oxygen uptake by packaged foods has been mainly applied to dried and fatty foods (Quast & Karel, 1971; Quast & Karel, 1972; Quast *et al.*, 1972; Ragnarsson & Labuza, 1977). For liquid foods, several studies report the effect of oxygen on quality degradation during storage, but few of them report changes of oxygen concentration. Roig *et al.* (1994) studied the effects of some additives in single strength orange juice stored in Tetra Brik Aseptic packages and dissolved oxygen concentration was measured as a function of time for several temperatures; however, no mathematical model was applied. Mack *et al.* (1976), Singh *et al.* (1976) and Hsieh & Harris (1993) studied the kinetics of oxygen uptake by liquid foods during storage considering the kinetics

of ascorbic acid degradation. These studies were carried out with unpacked products. Singh (1976) developed a mathematical model to describe ascorbic acid and dissolved oxygen concentration changes in an infant formula packaged in glass bottles and stored at 7°C; this model was based on Fickian diffusion of oxygen accompanied by a second order chemical reaction in the liquid food. Sadler (1984) using a similar model made a comprehensive study on the prediction of quality losses in a liquid food, considering various polymeric packaging materials. Methods for determination of oxygen solubility in the food and polymers, diffusion coefficients of oxygen in the food and polymers, as well as the oxygen permeation rate and the oxidation rate of the food, were also presented. Barron et al. (1993) reported a study where a finite element method was applied to the modelling of simultaneous oxygen diffusion and chemical reaction in packaged apple juice, stored at 25 °C, using a cylindrical high-density polyethylene package (top and bottom insulated). No works were found on modelling of oxygen changes in liquid products packaged in aseptic cartons.

This chapter presents the development of a mathematical model to describe the concentration of dissolved oxygen in packaged juice during storage, considering both oxygen transfer through the package and oxygen consumption by deteriorative reactions. This model was validated with experimental data regarding aseptically packaged orange juice stored at different temperatures (Chapter 2) as well as with data earlier reported in literature.

3.2. THE MATHEMATICAL MODEL

The oxygen concentration inside a packaged liquid food without headspace depends on (i) the initial concentration upon packaging, (ii) oxygen permeation through the package, including the seam, and (iii) oxygen consumption by deteriorative reactions. A mass balance leads to:

$$V \frac{d(C_{O_2})}{dt} = \dot{M}_{Mass\ Transfer} + \dot{M}_{Kinetics} \quad (3.1)$$

where V is the package or liquid volume, C_{O_2} is the dissolved oxygen concentration in the juice at a time t , $\dot{M}_{Mass\ Transfer}$ is the mass transfer rate and $\dot{M}_{Kinetics}$ is the reaction rate. The mass transport of oxygen from the atmosphere into the packaged food product may be described as a three step process (Figure 3.1): in the first step the molecules of oxygen are transported from the atmosphere to and dissolved in the packaging material; in the second step the oxygen diffuses through the packaging material moving towards the food, and the last step consists on the desorption of the molecules from the package and their solubilisation in the food. The partition coefficients at the outside and inside wall of the material (k_p^1 and k_p^2 respectively) may be different from unity and depend on the system characteristics; for instance, when k_p^1 is smaller than unity, the concentration at the package surface is smaller than that at the contacting gas layer, as shown in the example sketched in Figure 3.1.

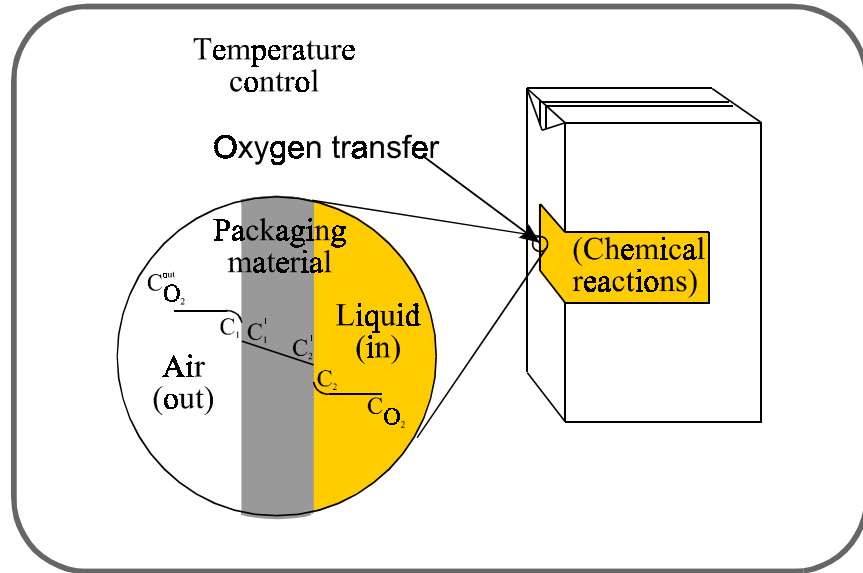


Figure 3.1 - Schematic representation of the mass transport of oxygen from the atmosphere into a packaged liquid food product.

Using the concept of resistances connected in series, an overall mass transfer coefficient ($k_{overall}$) can be defined:

$$\frac{1}{k_{overall}} = \frac{k_p^2}{k_p^1} \frac{1}{k_{int}} + \frac{1}{k_p^1} \frac{d}{D} + \frac{1}{k_{out}} \quad (3.2)$$

where D is the diffusion coefficient of oxygen in the packaging material, d is the thickness of the material, and k_{int} and k_{out} are the mass transfer coefficients inside and outside the package, respectively. It is important to note that the barrier properties of the package will influence the magnitude of D , k_{int} and k_{out} values.

When dealing with a high barrier material, the permeability properties of the package seam should be considered. The mass transfer rate through the package may then be described by:

$$\left(\frac{dC_{O_2}}{dt} \right)_{Mass\ Transfer} = k_D \times (C_{O_2}^{out} - k'_p \times C_{O_2}) \quad (3.3)$$

where:

$$k'_p = \frac{k_p^2}{k_p^1} \quad (3.4) \quad \text{and} \quad k_D = \frac{A}{V} k_{overall} \quad (3.5)$$

$C_{O_2}^{out}$ stands for oxygen concentration in the storage atmosphere, k_D is the oxygen mass transfer coefficient and A is the package surface area.

For simplicity sake, the consumption of oxygen may be assumed to follow a first order kinetic reaction with respect to oxygen (Barron *et al.*, 1993),

$$\left(\frac{dC_{O_2}}{dt} \right)_{kinetics} = k_R C_{O_2} \quad (3.6)$$

where k_R is the reaction rate constant. Substituting equations (3.3) and (3.6) into equation (3.1), rearranging and integrating the equation between the time zero ($C_{O_2} = C_{O_2}^i$) and time t, the concentration of dissolved oxygen in the food inside the package at a time t, C_{O_2} , is given by the following equation:

$$C_{O_2} = C_{O_2}^{\infty} + (C_{O_2}^i - C_{O_2}^{\infty}) \times e^{-kt} \quad (3.7)$$

where the equilibrium concentration, $C_{O_2}^{\infty}$, and the rate constant, k , are given by:

$$C_{O_2}^{\infty} = \frac{k_D C_{O_2}^{out}}{k_R + k'_p k_D} \quad (3.8) \quad \text{and} \quad k = k_R + k'_p k_D \quad (3.9)$$

3.3. MATERIAL AND METHODS

3.3.1. PROCESSING, PACKAGING AND EXPERIMENTAL DESIGN

Processing, packaging and the experimental design of the storage experiments were explained previously in §2.2.1 and §2.2.2.

3.3.2. PACKAGE PERMEABILITY MEASUREMENTS

TBA cartons are made of a multilayer packaging material: low density polyethylene/ paper board/ aluminium foil/low density polyethylene (from the outside to the inside). The permeability of the package to air is very low due to the presence of the aluminium layer (high oxygen barrier package), with gases exchanges occurring mainly through the seam.

The OXTRAN MH-2/20 was used to measure the oxygen transmission rate of the entire Tetra Brik Aseptic package. To test the package permeability a Package Environmental Chamber (PEC) was used in order to have humidity and temperature control inside and outside the package. Nitrogen was circulated continuously through the package that was exposed to an atmosphere with 21% oxygen and 50% RH. Permeability data at 10, 20, 30 and 40°C are reported on Table 3.1.

Table 3.1- Permeability of the package, measured with the OXTRAN.

Temperature (°C)	Permeability	
	as measured with Oxtran (cm ³ /(package×day) at 0.2 atm, 50% RH)	converted to k _D values ^(*) ×10 ¹⁰ (s ⁻¹)
10	0.009	4.97
20	0.014	7.72
30	0.023	12.73
40	0.038	20.95

$$(*) \quad k_D [s^{-1}] = F_{oxtran} \left[\frac{cm^3 \text{ of nitrogen}}{package \text{ area} \times day} \right] \times \frac{package \text{ area}}{package \text{ volume}} \left[\frac{cm^2}{cm^3} \right] \times \frac{1}{86400} \left[\frac{day}{s} \right]$$

3.3.3. DISSOLVED OXYGEN CONCENTRATION MEASUREMENT

The concentration of dissolved oxygen was measured as described in §2.2.3.

3.3.4. DATA FOR VALIDATION OF THE MODEL

In order to further validate the mathematical model, data from Roig et al. (1994) (Table C.1, Appendix C) and Barron et al. (1993) (Table C.2, Appendix C) were used. Roig et al. (1994) reported a storage experiment with a similar package material, and studied the effects of some additives on dissolved oxygen content changes during storage of reconstituted single strength orange juice packed in 200 mL Tetra Brik cartons. Barron et al. (1993) studied storage of apple juice packaged in a much more permeable packaging system (high-density polyethylene).

3.4. RESULTS AND DISCUSSION

3.4.1. MODELLING OF DISSOLVED OXYGEN CONCENTRATION

The concentration of dissolved oxygen during storage changes drastically during the first days of storage and then is kept approximately constant, as can be seen in Figure 3.2 (and Figures C1 to C.6, Appendix C).

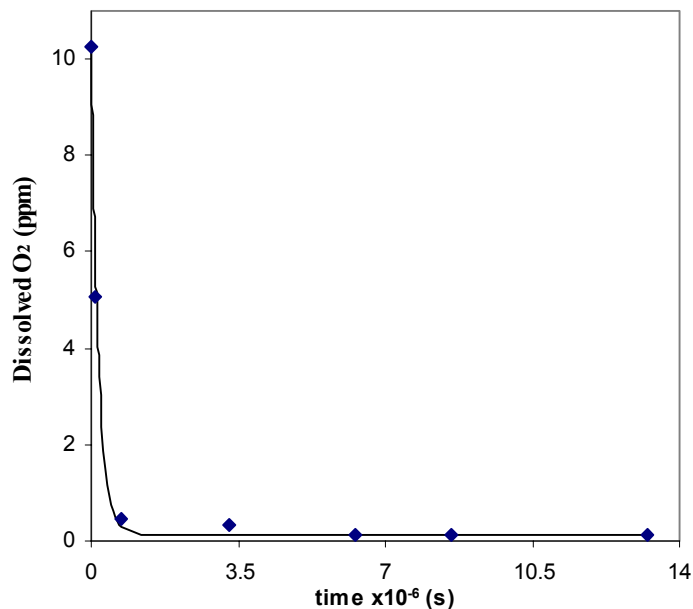


Figure 3.2 - Depletion of dissolved oxygen concentration during time in packaged orange juice at (◆) 20°C- batch A (initial O₂ content of 10.2 ppm), and model fit (solid line).

The changes observed during the first days of storage are caused by the rapid consumption of oxygen by oxidative reactions in the juice (Graumlich *et al.*, 1986). After this initial period, the oxygen transported through the package and

the consumption of oxygen by the oxidative reactions balance each other, keeping the level of oxygen in the product constant. There were no significant difference between batches (different initial oxygen contents) and the equilibrium oxygen concentration was found not to be significantly dependent on temperature and initial dissolved oxygen concentration (significance level of 95%) in the ranges tested. Furthermore its value was found to be significantly different from zero (significance level of 95%), with a value of 0.110 ± 0.008 ppm.

Changes in dissolved oxygen content in the packaged orange juice during storage were modelled for all the temperatures tested according to the model above described. The rate constant k was estimated by non-linear fitting of the Equation 3.7 to the experimental data, using the Kaleida Graph 3.0.1, 1993 Abelbeck software. This parameter showed values between 31.1×10^{-6} and $1.9 \times 10^{-6} \text{ s}^{-1}$ (Table 3.2). Reaction rate constant values of the same order of magnitude were reported for oxygen dependent reactions by Hsieh and Harris (1993) and by Mack *et al.* (1976), respectively in water and in a solution of sucrose in water (an infant food). The estimated rate constants (k) and the equilibrium concentration ($C_{O_2}^{\infty}$) values were further used to calculate the rate constant of the consumption reactions (k_R) and the mass transfer coefficient (k_D) (Equations 3.8 and 3.9), assuming k_p' equal to unity (Table 3.2). The values obtained show that the mass transfer coefficient is three orders of magnitude smaller than the consumption rate constant, what is in accordance with the fast decrease in oxygen concentration and the low level of oxygen at equilibrium. It was found that the influence of k_p' on

the estimated values of k_R was very small: assuming an error of $\pm 10\%$ (k_p' equal to 0.9 or 1.1), the estimated values of k_R were not statistically different from the value estimated considering $k_p'=1$. The dependence of the reaction rate constant (k_R) with temperature followed an Arrhenius type relationship (Figure 3.3) with activation energy (E_a) of 46 kJ/mole and pre-exponential factor (k_0) of 949 s^{-1} .

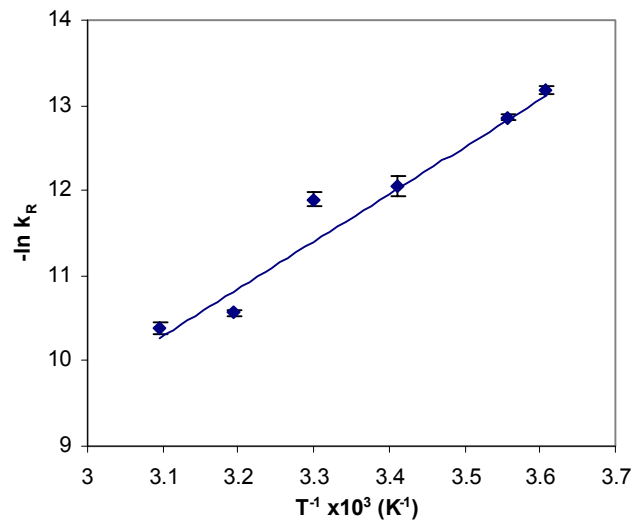


Figure 3.3 - Arrhenius plot for the reaction rate constant of oxygen consumption.

The mass transfer coefficients are three to four times smaller than the reaction rate constants, and their dependence on temperature is similar to the one observed for the reaction rate constants with an activation energy equal to 49 kJ/mol. This value reveals a sensitivity to temperature somewhat larger than the expected for diffusional processes (Garrote et al., 1988; Rodger et al., 1984), which may be due to the effect of temperature on oxygen solubility in the package and in the juice.

The estimates of the mass transfer coefficients are of the same order of magnitude as those measured with the OXTRAN, except at 40°C where the estimated k_D value is 5 times greater than the OXTRAN value.

3.4.2. VALIDATION OF THE MODEL

Because of the fast decrease in oxygen concentration, our data do not allow for a highly accurate assessment of the proposed mathematical model. Therefore, the adequacy of the model to predict oxygen concentration changes in stored orange juice was further checked using two additional sets of experimental data found in literature: Roig *et al.* (1994) and Barron *et al.* (1993).

Data from Roig *et al.* (1994) relate to dissolved oxygen content changes during storage at 4, 20, 37, 76 and 105 °C. The authors report a 0.2713 mL uptake of oxygen into a 200 mL carton, after one month, when the package is stored at 18°C (uptake rate $\approx 0.009 \text{ cm}^3 \text{ O}_2 /(\text{pack} \times \text{day})$ or $\approx 1.04 \times 10^{-7} \text{ cm}^3 \text{ O}_2 /(\text{pack} \times \text{day})$), that is similar to the results reported in the present work (Table 3.1). Using our model, a good correlation between experimental and predicted dimensionless oxygen concentration values was observed (Figure 3.4). Estimated values of the reaction rate constants, rate constant of oxidative reactions and oxygen mass transfer coefficients are presented on Table 3.2 (k values were estimated by simultaneous optimisation of several isothermal experiments, using a Fortran programme based on the Simplex method (Nelder & Mead, 1965). The oxidative reaction rate constants showed an Arrhenius type dependency on temperature with activation

energy of 46 kJ/mole (similar to the one reported in the present work) and a pre-exponential factor (k_0) of 144.7 (s^{-1}). The estimated equilibrium oxygen concentration was 0.582 ppm. This value is higher than the one obtained in our study. This difference may be related to the importance of the seal on oxygen exchanges: the smaller the package, the greatest the relative contribution of the seal to the total oxygen uptake.

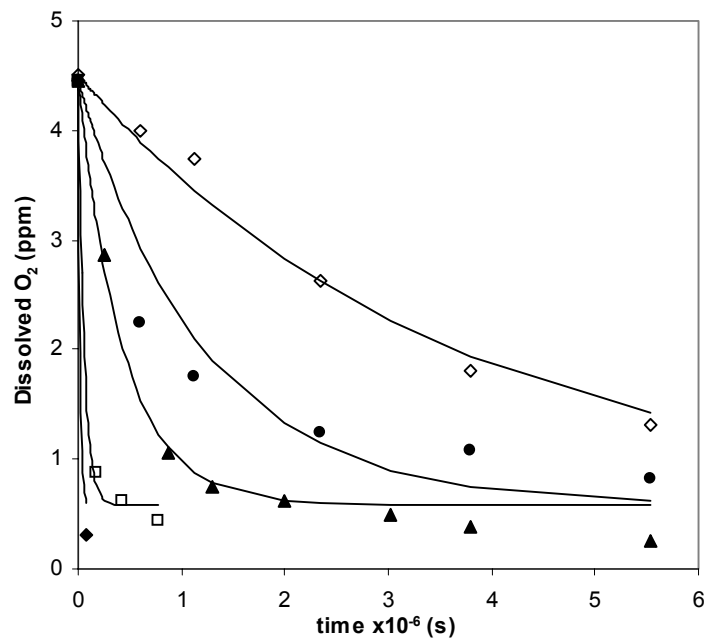


Figure 3.4- Depletion of dissolved oxygen concentration during storage, experimental data at 4 (\diamond), 20 (\bullet), 37 (\blacktriangle), 76 (\square) and 105 °C (\blacklozenge), from Roig *et al.* (1994) and model fit (solid line).

Data from Barron *et al.* (1993) relate to changes in dissolved oxygen content of apple juice samples stored at $25.0 \pm 0.2^\circ\text{C}$ and $45 \pm 3\%$ of RH (in a controlled atmosphere chamber), in 0.77 L HDPE cylindrical packages (top and bottom insulated). The authors reported an average oxygen permeability constant for

Table 3.2- Estimates of reaction rate constants, rate constant of oxidative reactions and oxygen mass transfer coefficient of oxygen in orange juice stored at different temperatures (“our data” and Roig *et al.* (1994)), and apple juice stored at 25 °C (Barron *et al.*, 1993).

(°C)	"Our data"				Roig <i>et al.</i> (1994)				Barron <i>et al.</i> (1993)			
	$k \times 10^6 (s^{-1})$	$k_R \times 10^6 (s^{-1})$	$k_D \times 10^{10} (s^{-1})$	R^2	$k \times 10^6 (s^{-1})$	$k_R \times 10^6 (s^{-1})$	$k_D \times 10^{10} (s^{-1})$	R^2	$k \times 10^6 (s^{-1})$	$k_R \times 10^6 (s^{-1})$	$k_D \times 10^6 (s^{-1})$	R^2
4	1.9 ± 0.1	1.9 ± 0.1	7.3 ± 0.7	0.992	0.28 ± 0.15	0.28 ± 0.15	5.4 ± 3.0	0.976				
8	2.6 ± 0.1	2.6 ± 0.1	9.7 ± 0.8	0.998								
20	5.8 ± 0.7	5.8 ± 0.7	23 ± 3	0.908	0.83 ± 0.45	0.83 ± 0.45	17.4 ± 9.4	0.878				
25									354 ± 32	349.5 ± 86.8	4.5 ± 0.5	0.998
30	6.8 ± 0.5	6.8 ± 0.5	28 ± 2	0.988								
37					2.3 ± 1.3	2.3 ± 1.3	51.7 ± 27.8	0.992				
40	25.9 ± 0.9	25.9 ± 0.9	110 ± 9	0.998								
50	31 ± 2	31 ± 2	139 ± 12	0.994								
76					17.4 ± 9.1	17.4 ± 9.1	432 ± 227	0.998				
105					59 ± 30	59 ± 30	1587 ± 821					

HDPE of $10600 \text{ cm}^3/(\text{m}^2 \cdot \text{atm} \cdot \text{day})$ ($\approx 98.2 \text{ ml of O}_2 /(\text{pack} \times \text{day})$ or $\approx 1.14 \times 10^{-3} \text{ cm}^3$ of $\text{O}_2/(\text{pack} \times \text{day})$). This material is much more permeable to oxygen than those tested before, and therefore the relative importance of the oxygen transfer through the package should be greater, allowing for a better test of the model proposed in the present work. Values of the rate constant, rate constant of oxidative reactions and oxygen mass transfer rate are shown on Table 3.2. The estimated equilibrium oxygen concentration was $3.49 \pm 0.23 \text{ ppm}$. Figure 3.5 show that the model fits very well the experimental data.

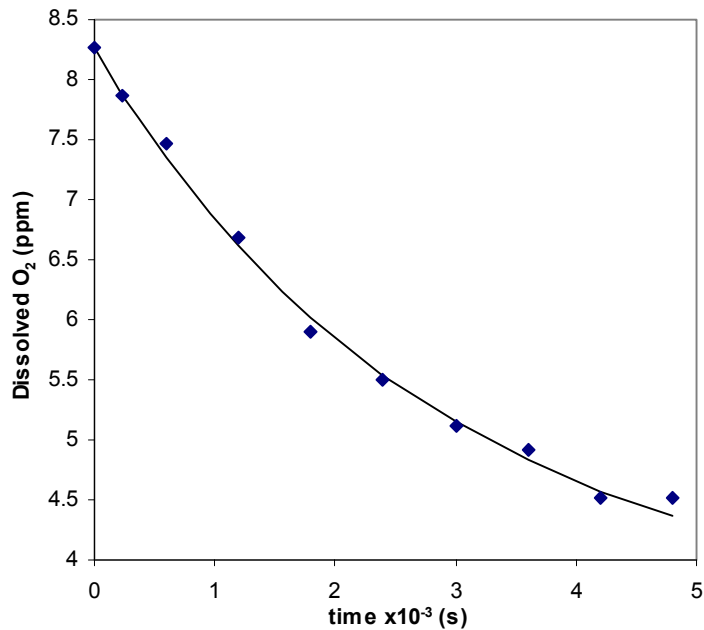


Figure 3.5- Depletion of dissolved oxygen concentration during storage of apple juice at 25°C , experimental data (\blacklozenge) from Barron *et al.* (1993) and model fit (solid line).

3.5. CONCLUSIONS

A model combining oxygen transfer through the package and oxygen consumption within the package, assuming no oxygen stratification in the juice described well the oxygen changes in packaged orange juice stored at temperatures from 4 to 50°C.

It was found that the oxidative reactions in juice packed in TBA are limited by the mass transfer through the package being high enough to maintain a residual oxygen concentration in the juice. The package permeability was much smaller than the oxidative rate constant.

The model was also applied to reported data, including packaging materials with a much lower barrier to oxygen, also with good results.

CHAPTER 4

Modelling ascorbic acid, browning and flavours changes during storage of aseptic packaged orange juice

This chapter presents the mathematical modelling of the changes with storage time of the quality factors reported in Chapter 2 (L-ascorbic acid (L-AA), browning (Br), 5-hydroxymethyl-2-furfuraldehyde (HMF), 2-furfuraldehyde (Furfural) and 4-vinyl guaiacol (PVG)) and their dependence on temperature. An empirical approach was applied and the kinetics were described with simple models: zero and first-order, two consecutive zero-order, two consecutive first-order, and Weibull models. In spite of their simplicity these models showed in general a fair agreement to experimental data. L-AA degradation was much faster at small than at longer times, due to oxygen depletion in the earlier stages of storage. The rate constants increased with temperature according to an Arrhenius type equation, in some cases with a lower sensitivity to temperature (activation energy) at temperatures below app. 30 °C than at temperatures above this value.

4.1. INTRODUCTION

In order to establish mathematical models for quality changes during storage and to predict the shelf life of packaged product, it is necessary: (i) to identify and quantify the orange juice quality characteristics that significantly change during storage; (ii) to identify the factors that influence the quality change and (iii) to develop mathematical models to describe the deterioration of quality and influence of the external factors. Chapter 2 highlighted the relevant quality indicators and this chapter focuses on the mathematical modelling of their kinetics during storage.

The mechanisms of degradation of ascorbic acid in processed citrus juices involve aerobic and anaerobic pathways of nonenzymatic nature (enzymatic reactions may be involved, but only if the pasteurisation was not correctly performed). These two pathways of ascorbic acid degradation - aerobic and anaerobic - can operate in the same system. In literature one can find different mathematical models to predict ascorbic acid concentration during storage, as earlier discussed (§1.6.3), and although first-order kinetics is the model most frequently applied to describe this degradation, more complex mathematical models have also been reported, as a model proposed by Sakai et al. (1987) consisting of two consecutive reactions (the first of order zero and the second of first-order). This model was used to describe the ascorbic acid oxidation in an aqueous solution, with different initial ascorbic acid concentration in which dissolved oxygen was held at a constant level. These authors showed that this reactive mechanism might be perceived as

either apparent first or zero-order kinetics, depending on the initial concentration of ascorbic acid and on the ratio of the rate constants of the sequential reactions.

Several authors (Eison-Perchonok & Dowes, 1982; Hsieh & Harris, 1993; Kennedy et al., 1992) reported that the levels of initial dissolved oxygen affect the rate of ascorbic acid oxidation (see Table 1.4 in §1.6.3). Others (Singh et al., 1976) showed that under dark conditions the rate constants of L-AA degradation for different initial dissolved oxygen concentration were not statistically different.

The colour changes, or rather the darkening of orange juice during storage are based on the appearance of brown coloured compounds caused by the chemical reaction of orange juice components present in the juice matrix. The brown compounds are formed in the end phase of the Maillard reaction (also known as nonenzymatic browning), which is a reaction between sugars and amino acids. This reaction is generally not dependent on oxygen, but is clearly temperature-driven (§1.6.3). Ascorbic acid can participate in that development via its degradation products resulting from both the aerobic and anaerobic pathways. In spite of its complexity, browning has been modelled as zero-order kinetics (Rojas & Gerschenson, 1997; Robertson & Samaniego, 1986).

HMF kinetics has been described either as a second order autocatalic reaction or a zero-order reaction, with or without induction period (Lee et al., 1986). Furfural formation was reported to follow zero-order kinetics (Kaanane et al., 1988; Robertson & Samaniego, 1986). The same order of reaction was used to model PVG formation (Marcotte et al., 1998). Initial oxygen content did not affect their

rate of formation and the dependence of their reaction rates on temperature was considered to follow Arrhenius-type relationships.

The main objectives of this work was to develop general models to predict ascorbic acid loss, and development of browning, HMF, Furfural and PVG in aseptically packaged orange juice, during storage at temperatures ranging from 4 to 50 °C.

4.2. MATHEMATICAL MODELLING

Selected mathematical models (kinetic equations) were fitted to the experimental data, either by linear or non-linear regressions, according to each particular case. Fits were performed for each experiment carried out at each temperature and for all batches to assess the quality of the fit of the models, and to analyse the dependence of the model parameters on temperature. These will be further referred to as individual fits.

In most situations the experimental data for the different batches (different initial dissolved O₂ contents), at each temperature, were not significantly different, and they were treated as replicates. The influence of temperature on reaction rate constants was described by Arrhenius-type relationships.

In order to improve parameter estimation, once the model was checked, the adopted procedure was to apply a single regression to the whole set of experimental data for a given kinetics, by combining the kinetic equations with

the equations that relate the model parameters to temperature. This will be further referred to as "global fitting".

The validity of the models was checked with the Statistica™ ('99Edition) software package.

4.3. MATERIAL AND METHODS

The material and methods are those described in Chapter 2 (§2.2).

4.4. RESULTS AND DISCUSSION

4.4.1. L-ASCORBIC ACID DEGRADATION

Modelling L-AA degradation with two consecutive first-order kinetics

Although most reported works describe ascorbic acid degradation as zero, first or second-order kinetics, these models did not fit well the experimental data of the current work. It was however found that L-AA degradation could be well described by two consecutive first-order reactions:

$$C_a = C_a^i \times e^{-k_1 \times t} \quad t \leq t_c \quad (4.1)$$

$$C_a = C_a^i \times e^{-k_1 \times t} \times e^{-k_2 \times (t - t_c)} \quad t > t_c \quad (4.2)$$

where C_a is the L-AA concentration at a time t , C_a^i is the initial L-AA concentration, k_1 and k_2 are the rate constants of the first and second reactions

and t_c is the time of oxygen depletion (change from the first to the second reaction).

This model assumes that two reactions with different rate constants, related to the aerobic and anaerobic pathways, are involved in ascorbic acid degradation during storage.

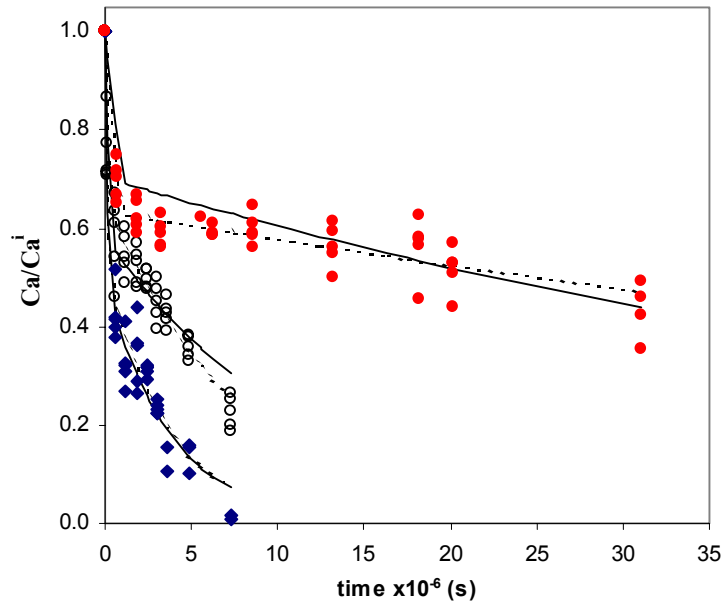


Figure 4.1- Fits of the two consecutive first-order reaction models kinetic to L-ascorbic acid data at (◆) 50, (○) 40 and (●) 20 °C. The dashed and the solid line indicate, respectively the individual and global fit.

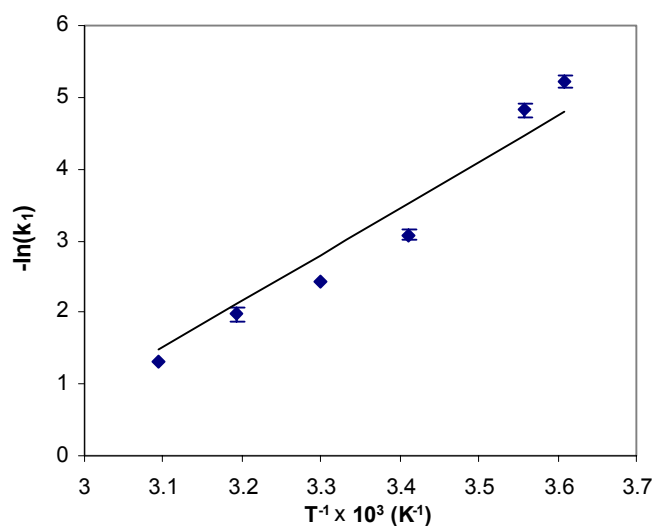
The first reaction was assumed to follow an aerobic pathway and therefore it would only proceed until depletion of oxygen, taking place for less than 3 days at 50°C and 71 days at 4 °C. The second reaction, slower, was assumed to correspond to the anaerobic pathway. As previously mentioned, dissolved oxygen content dropped quickly to an equilibrium value within a few days. Figure 4.1 shows typical examples of the fit of the two consecutive first-order reactions

model to the experimental data and the parameters of the individual model fit are presented in Table 4.1 ($R^2_{\text{adj}} > 0.942$, correlation coefficients < 0.939) (for further examples, see Figures C.1 and C.2, Appendix C, where the individual and global fits of the two consecutive first-order model are depicted).

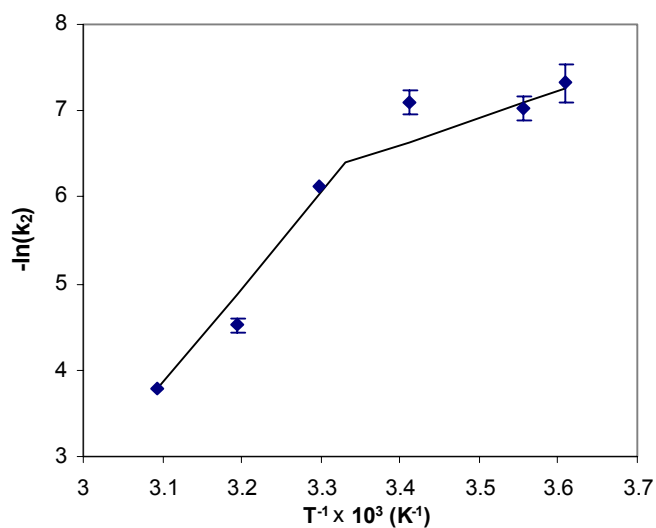
As previously mentioned, the effect of initial dissolved oxygen is in part accounted for in the initial L-AA concentration values. One should be aware that the data corresponding to the first reaction are scarce and thus, the analysis of its kinetics cannot be very accurate. Furthermore, it was assumed that the aerobic reaction was first-order in relation to L-AA, which is rather simplistic, as oxygen is the limiting factor in the degradation of ascorbic acid in this pathway. This model assumes that the aerobic reaction is brought to an end when a certain L-AA conversion is obtained, and so the anaerobic reaction depends not only on temperature but also on the dissolved oxygen content, though the later does not influence as much as the former.

The reaction rate constants from the first reaction follow an Arrhenius relation with temperature (see Figure 4.2a). Although two Arrhenius profiles might be perceived from the dependence of estimates of the reaction rate constants on temperature (Figure 4.2a), the global fit for that case produced estimates of activation energies that were not statistically different. Thus, a single Arrhenius relation was used to describe the variation of the first reaction rate constants on temperature. The reaction rate constants from the second reaction followed two distinct Arrhenius profiles, one for the temperature range 50 to 30 °C, and another for 20 to 4 °C (see Figure 4.2b).

The logarithm of the time required for oxygen depletion was found to decrease exponentially with temperature (Figure 4.3).



(a)



(b)

Figure 4.2- Dependence of the reaction rate constants of the two consecutive first-order reaction kinetics for L-ascorbic acid on temperature: (a) rate constant of the first reaction (k_1); (b) rate constant of the second reaction (k_2). The symbol \blacklozenge represents parameters estimated by individual fits and the solid lines indicate the global fit.

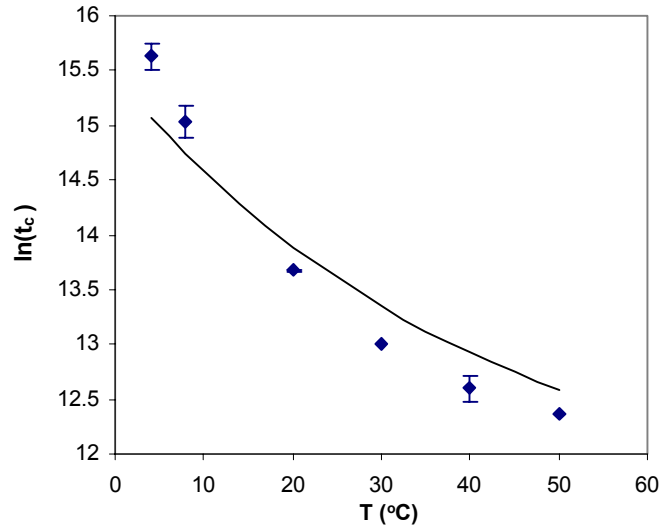


Figure 4.3- Relation of the time required for oxygen depletion with temperature. The \blacklozenge symbol represents parameters obtained with each individual fit and the solid line indicates the global fit.

The relationships of the rate constants and time of oxygen depletion with temperature were then incorporated in Equations 4.1 and 4.2 to build a global model:

$$C_a = C_a^i \times e^{-k_{1ref} \times t} \times e^{-\frac{Ea_1}{R} \left(\frac{1}{273.15+T} - \frac{1}{273.15+T_{ref}} \right) \times t} \quad t \leq t_c \quad (4.3)$$

$$C_a = C_a^i \times e^{-k_{1ref} \times t_c} \times e^{-\frac{Ea_1}{R} \left(\frac{1}{273.15+T} - \frac{1}{273.15+T_{ref}} \right) \times t_c} \times e^{-k_{2ref} \times (t-t_c)} \times e^{-\frac{Ea_{21}}{R} \left(\frac{1}{273.15+T} - \frac{1}{273.15+T_{ref}} \right) \times (t-t_c)} \quad t > t_c \text{ and } T \geq T_{ref} \quad (4.4)$$

$$C_a = C_a^i \times e^{-k_{1ref} \times t_c} \times e^{-\frac{Ea_1}{R} \left(\frac{1}{273.15+T} - \frac{1}{273.15+T_{ref}} \right) \times t_c} \times e^{-k_{2ref} \times (t-t_c)} \times e^{-\frac{Ea_{22}}{R} \left(\frac{1}{273.15+T} - \frac{1}{273.15+T_{ref}} \right) \times (t-t_c)} \quad t > t_c \text{ and } T < T_{ref} \quad (4.5)$$

and

$$t_c = e^{t_{c,ref} \times e^{b \times (T - T_{ref})}} \quad (4.6)$$

where k_{1ref} and k_{2ref} are rate constants at a reference temperature T_{ref} , Ea_1 , Ea_{21} and Ea_{22} are activation energies regarding the dependence of the rate constants with temperature, R is the universal gas constant, $t_{c,ref}$ is the time of oxygen depletion at a reference temperature and b is the constant of the dependence of the time of oxygen depletion with temperature. The equations describing the effect of temperature were written in terms of a reference finite temperature that in this case is also the temperature where the Arrhenius profile changes. The same concept was applied to the relation of time of oxygen depletion with temperature.

Equations 4.3 to 4.6 were fitted to the whole set of data and Table 4.1 shows the parameter estimates. This global fit had an R^2_{adj} of 0.943 and the collinearity between the model parameters was below 0.94. Values below 0.99 are considered acceptable (Bates & Watts, 1988; Van Boeckel, 1996). Further information on the quality of the fit is included in Appendix C (Figure C.6a illustrates the agreement between predicted and experimental data, Figure C.7a the lack of residual tendency for the predicted values, and Figure C.8a the frequency distribution of the residuals).

Table 4.1- Estimates of the parameters of the individual (Eq. 4.1 and 4.2) and global fitting (Eq. 4.3 to 4.6) of the two consecutive first-order model for L-AA degradation.

INDIVIDUAL FITTING							
T (°C)	t_c (s)	$k_1 \times 10^9$ (s ⁻¹)	$k_2 \times 10^9$ (s ⁻¹)				
4	6134400 ± 691200	63 ± 5	8 ± 1.2				
8	3369600 ± 518400	94 ± 9	10 ± 1				
20	864000 ± 69120	532 ± 35	93 ± 1				
30	449280	1018	25.5				
40	293760 ± 34560	1620 ± 116	126 ± 9				
50	233280	3125	266				

GLOBAL FITTING							
$t_{c,ref}$	b (°C ⁻¹)	T_{ref} (°C)	$k_{1ref} \times 10^9$ (s ⁻¹)	E_{a1} (kJ/mol)	$k_{2ref} \times 10^9$ (s ⁻¹)	E_{a21} (kJ/mol)	E_{a22} (kJ/mol)
2.13 ± 0.09	-0.024 ± 0.002	27 ± 2	579 ± 35	54 ± 2	20 ± 1	92 ± 4	26 ± 4

The model showed to fit well the experimental data and thus it can be used to describe the degradation of ascorbic acid in aseptically packaged liquid food during storage. However, it involves a great number of parameters and further studies are needed to better understand both reactions and to obtain better estimates of the model parameters.

Modelling L-AA degradation with the Weibull model

The Weibull model was initially developed to describe the failure of a given system subjected to stress conditions over time. This model is very flexible owing to the inclusion of a shape constant in addition to the rate constant, which allows for its application to a number of diverse situations and it has proved to have an

interesting potential for describing microbial, enzymatic and chemical degradation kinetics (Cunha et al., 1998). When applied to L-AA degradation, it can be described by the following equation:

$$C_a = C_a^i \times e^{-\left(\frac{t}{\alpha}\right)^\beta} \quad (4.7)$$

where C_a is the L-AA concentration at a time t , C_a^i is the initial L-AA concentration, α is a scale constant (its inverse corresponds to the reaction time constant) and β is the shape constant, or behaviour index (Seber & Wild, 1989). It is evident from Equation 4.7 that α is the time when the concentration has decreased by one natural log cycle (app. 67%), and that the Weibull model corresponds to the first-order model for the specific case of $\beta=1$. Equation 4.7 has a sigmoid shape for $\beta>1$ and a monotonous decrease, steeper than exponential at low times, for $\beta<1$ (Nelson, 1969). The reaction time constant is temperature sensitive and this dependence can often be described by an Arrhenius-type relationship (Shepherd and Bhardwaj, 1988; Machado *et al.*, 1999). The β parameter, or shape constant, is related to the kinetic mechanisms and may be expected to be temperature independent, at least within a limited range of temperature.

As referred in §2.3, L-AA data for the different batches (initial oxygen content effect) were not statistically different (with exception of data at 4 °C, where batches A and B were statistically different from C, D and E). Nevertheless, the model was fitted to the data, yielding reaction rate and shape constants for each

different set of batches and temperatures. Figure 4.4 shows typical examples of the fit of the Weibull model to the experimental data ($R^2_{\text{adj}} > 0.93$) (for further examples, see Figures C.1 and C.2, Appendix C, where the individual and global fits of the Weibull model are illustrated).

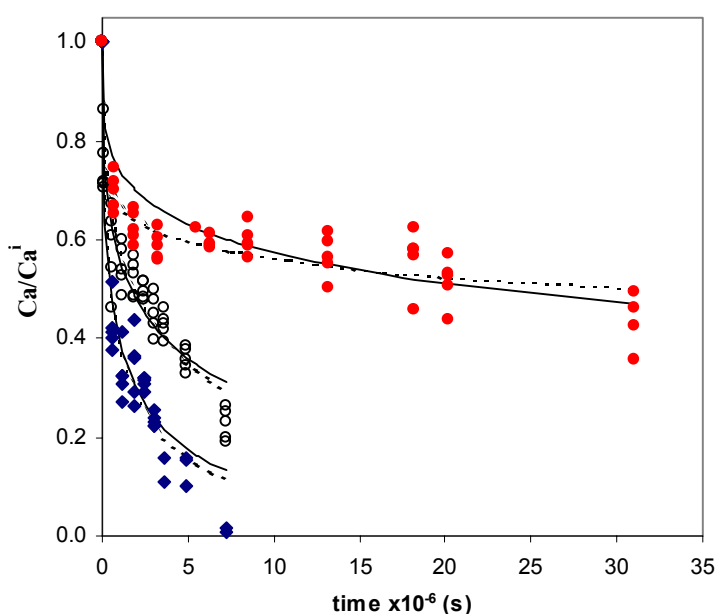


Figure 4.4- Fit of the Weibull model to L-ascorbic acid data at (\blacklozenge) 50, (\circ) 40 and (\bullet) 20 °C. The dashed and the solid line indicate, respectively the individual and global fit.

Although, there were significant differences (95% significance level) on the reaction rate constants for the different batches at the same temperature, there was not a common trend for all temperatures (see Figures C.3a and C.4, Appendix C). The shape constant showed significant differences both for temperature and batch, but while it increased with temperature, with the exception at 4 and 8 °C, it did not show a common trend with batch (see Figures C.3b and C.5). Therefore, both constants were considered to be temperature dependent only, and the different

batches were used as replicates. The estimates of the model parameters are presented in Table 4.2.

The reaction rate constant increased with temperature, following an Arrhenius-type relationship (Figure 4.5a). The data at lower temperatures showed some deviation to this pattern but also greater errors, which may be due to the correlation between the model parameter α and β . An Arrhenius-type equation was then imposed to describe the relationship of α with temperature and new estimates of β were calculated. These showed a clear linear increase of β with temperature (see Figure 4.5b), which shows that the degradation patterns differ with temperature. Kanner *et al.* (1982) reported changes in the degradation pattern at temperatures between 25 and 37°C, as well as Nagy & Smoot (1977), who reported a critical temperature transition region between 22 and 26.7°C.

The said relationships of $1/\alpha$ and β with temperature were then incorporated in Equation 4.7 to build a global model:

$$C_a = C_a^i \times e^{-\left[\left(\frac{1}{\alpha} \right)_{ref} \times e^{-\frac{Ea}{R} \left(\frac{1}{273.15+T} - \frac{1}{273.15+T_{ref}} \right)} \right] \beta_{ref} + m \times (T - T_{ref})} \quad (4.8)$$

where $(1/\alpha)_{ref}$ is the rate constant at a reference temperature T_{ref} , Ea is the activation energy regarding the dependence of the rate constant with temperature, β_{ref} is the shape constant at the reference temperature, m is the slope of the dependence of the shape constant with temperature and R is the universal gas constant.

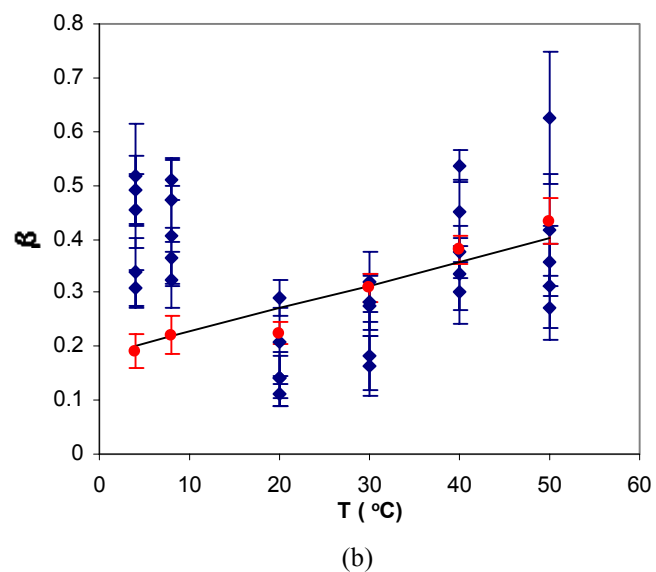
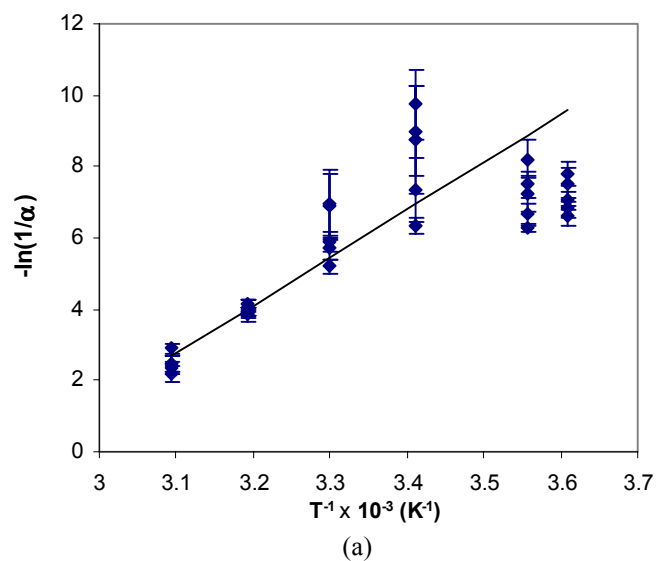


Figure 4.5- Dependence of the Weibull model parameters on temperature for ascorbic acid degradation: (a) rate constant ($1/\alpha$); (b) shape constant (β). The \blacklozenge symbols represent parameters estimated by individual fitting, the \bullet symbol represents β calculated when an Arrhenius equation was used to describe the relation of the reaction rate constants with temperature, and the solid lines indicate the global fit.

Table 4.2- Estimates of the parameters of the Weibull individual model (Eq. 4.7) and of the global model (Eq. 4.8), for L-AA degradation.

INDIVIDUAL FITTING			
T (°C)	$1/\alpha \times 10^9$ (s⁻¹)	β	
4	8.9 ± 1.5	0.40 ± 0.03	
8	9.6 ± 1.9	0.41 ± 0.04	
20	3.2 ± 1.5	0.16 ± 0.02	
30	27.7 ± 5.8	0.24 ± 0.03	
40	220 ± 12	0.40 ± 0.03	
50	880 ± 81	0.41 ± 0.04	
GLOBAL FITTING			
$1/\alpha_{\text{ref}} \times 10^9$ (s⁻¹)	Ea (kJ/mol)	β_{ref}	m (°C⁻¹)
33.6 ± 3.5	112 ± 4	0.30 ± 0.01	0.0044 ± 0.0005

$T_{\text{ref}} = 27$ °C

The Arrhenius equation was written in terms of a reference finite temperature rather than in terms of an infinite temperature in order to improve parameter estimation (Van Boeckel, 1996). The average temperature of the range tested, 27 °C (300.15 K), was chosen as the reference temperature.

Equation 4.8 was fitted to the whole set of data and Table 4.2 shows the parameter estimates. This global fit had a high R^2_{adj} (0.96) and the collinearity between the model parameters was below 0.86. Further information on the quality of the fit is included in Appendix C (Figure C.6b illustrates the agreement between predicted and experimental data, Figure C.7b the lack of residual tendency for the predicted values, and Figure C.8b the frequency distribution of the residuals).

The two models tested to describe AA degradation yielded fits statistically different (significance level of 95%). Both the residuals (1.130 for Weibull model and 0.816 for two-consecutive first-order model) and the goodness of fit (the AIC test (AKAIKE information criterion (Sakamoto et al., 1986)) revealed that the two-consecutive first-order has a slighter better result (higher value) than the Weibull model (two-consecutive: AIC=-866.27, Weibull: AIC=-772.64)). However, the Weibull model presents two advantages that must not be overlooked: it has a smaller number of parameters (half) and presents no discontinuity regarding the dependence of the rate constants on temperature, which makes it more suitable for accelerated shelf life tests.

When trying to decide which of several non-nested models is best, one should take into consideration that the primary aim of data analysis is to explain or account for the behaviour of the data, not simply to get the best fit (Bates & Watts, 1988).

4.4.2. BROWNING INDEX

As mentioned in §2.3, data of non-enzymatic browning was not affected by the initial level of dissolved oxygen (significance level of 95%), with the exception of data at 4 and 8 °C (batches A and B significantly different from C, D and E). At these two low temperatures data showed no significant increase with storage time (significance level of 95%), revealing mainly an increase in scatter with time.

As discussed earlier (§1.6.3), many authors use a zero-order kinetic reaction to model non-enzymatic browning. In spite of the simplicity of this model, particularly taking into consideration the complex group of reactions involved in orange juice browning, it has proved to be effective for predictive purposes. It can be described by the following equation:

$$C_{Br} = C_{Br}^i + k \times t \quad (4.9)$$

where C_{Br}^i and C_{Br} are concentrations at time zero and at any time t , and k is the rate constant of browning. This equation yielded good fits to the data ($R^2_{adj.} > 0.939$) and examples of the individual fits are depicted in Figure 4.6.

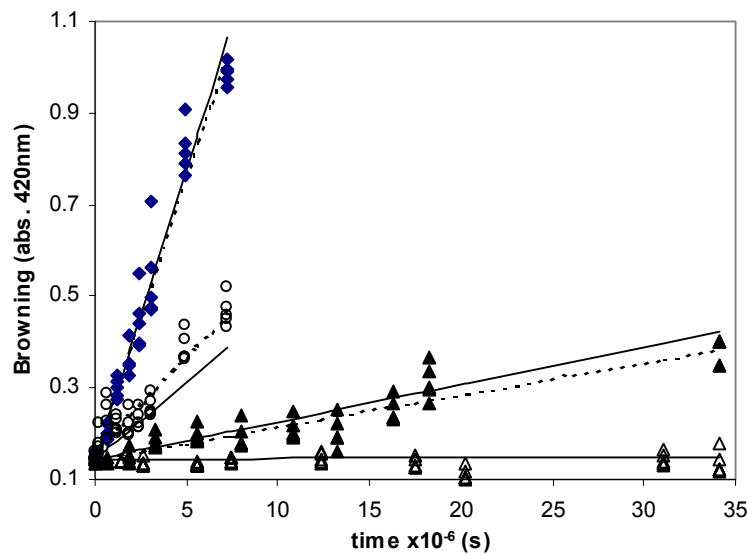


Figure 4.6- Fit of the zero-order reaction model to browning data, at (◆) 50, (○) 40, (▲) 30, and (△) 4 °C. The dashed and the solid line indicate, respectively the individual and global fit.

The estimates of the model parameter constant (see Table 4.3) increased with temperature according to an Arrhenius type equation in the range of temperature from 20 to 50 °C (Figure 4.7). As mentioned above no significant increase was noticed at 4 and 8 °C and the individual fit produced rate constants with no physical meaning for these two temperatures.

The said relationship of the rate constant with temperature was then incorporated in Equation 4.10 to build a global model:

$$C_{Br} = C_{Br}^i + k_{ref} \times e^{-\frac{Ea}{R} \left(\frac{1}{273.15+T} - \frac{1}{273.15+T_{ref}} \right)} \times t \quad (4.10)$$

where k_{ref} is the rate constant at a reference temperature T_{ref} , Ea is the activation energy regarding the dependence of the rate constant with temperature and R is the universal gas constant.

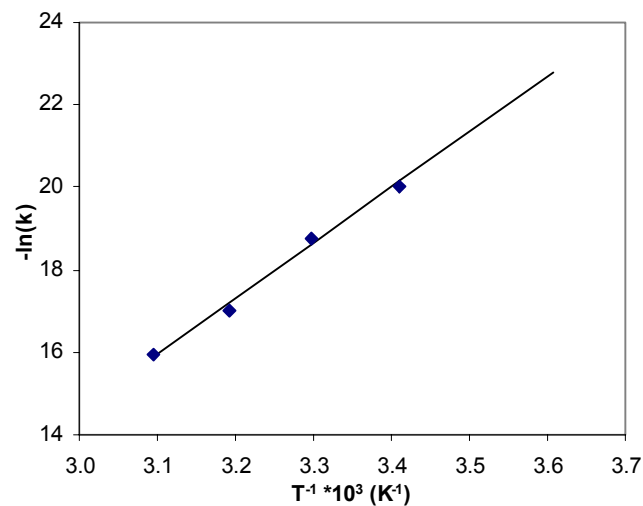


Figure 4.7- Dependence of the rate constant of the zero-order model on temperature, for browning. The \blacklozenge symbols represent parameters obtained with the individual fit and the solid line indicates the global fit.

Equation 4.10 was fitted to the experimental data and the parameter estimates are presented in Table 4.3. The collinearity between model parameters was below 0.96 and the fit had a high R^2_{adj} (0.976). Examples of the global model fit are also presented in Figure 4.6. Further examples are presented in Figures C.9, Appendix C. Further information on the quality of the fit is included in Appendix C (Figure C.10 illustrates the agreement between predicted and experimental data, the lack of residual tendency for predicted values, and the frequency distribution of the residuals).

Table 4.3- Estimates of rate constant of the zero-order model, for the individual (Eq. 4.9) and global (Eq. 4.10) fitting of browning data.

(°C)	INDIVIDUAL FITTING	GLOBAL FITTING	
	$k \times 10^9 \text{ (s}^{-1}\text{)}$	$k_{\text{ref}} \times 10^9 \text{ (s}^{-1}\text{)}$	Ea (kJ/mol)
4	-	5.2 ± 0.2	112 ± 2
8	-		
20	2.0 ± 0.2		
30	7.1 ± 0.4		
40	42 ± 2		
50	122 ± 3		

$T_{\text{ref}} = 27 \text{ }^\circ\text{C}$

Although the zero-order model yields good results, a more careful analysis of the data shows a pattern that could be described by an exponential increase followed by a standstill period and then a linear increase period (see Figure 4.8 and Figure C.11 (Appendix C)). In order to mathematically model the kinetics, the first

increase and the standstill period can be described by a first-order kinetic and the second increase period by zero-order kinetics:

$$C_{Br} = C_{Br}^{\infty} + (C_{Br}^i - C_{Br}^{\infty}) \times e^{-k_1 \times t} \quad t \leq t_c \quad (4.11)$$

$$C_{Br} = C_{Br}^c + k_2 \times (t - t_c) \quad t > t_c \quad (4.12)$$

where C_{Br}^i , C_{Br} , C_{Br}^c and C_{Br}^{∞} are, respectively, concentrations of browning (abs. 420 nm) at time zero, at any time t , at time t_c (the time when the zero-order kinetics starts) and at the standstill period, k_1 and k_2 are the rate constants of both reactions.

At 50 °C only the linear phase is noticeable as the reaction is very fast while at 20 °C the reaction is very slow and the rate constant of the first phase is very low, nearly zero, leaving few points to model the second reaction. The time at which the reaction changes from first to zero-order, t_c , decreases with temperature while C_{Br}^{∞} increases.

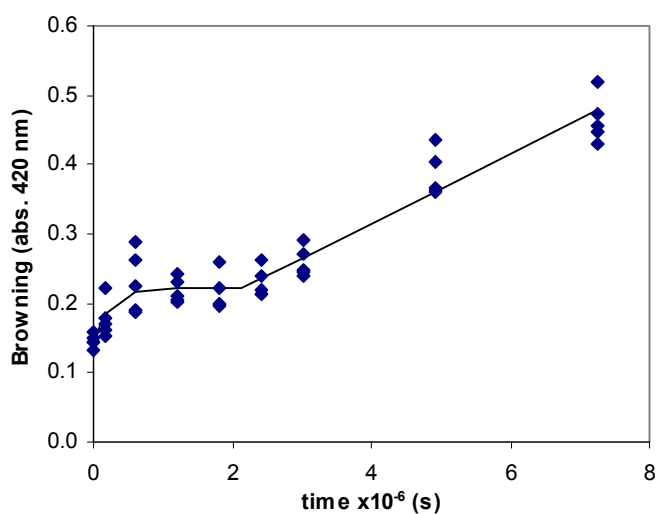


Figure 4.8- Fit of Equations 4.11 and 4.12 (solid line) to browning at (◆) 40 °C.

The parameters of the model individual fit are presented in Table 4.4. Several attempts were made to find a relation between the rate constants and temperature, using Arrhenius and WLF equations (Peleg, 1992), or even linear and polynomial relations, and although the result of the global model seemed quite good there were not enough points and/or temperature levels to achieve parameters with statistical significance. A validation of this model requires more experimental data.

Table 4.4- Estimates of the parameters for the two-consecutive reaction model (first followed by zero-order) fitting (Eq. 4.11 and 4.12) of browning data.

T (°C)	C_{BR}^{∞}	t_c (s)	$k_1 \times 10^6$ (s ⁻¹)	$k_2 \times 10^9$ (s ⁻¹)	$R^2_{adj.}$
20				124 ± 2	0.98
30	0.222 ± 0.008	2134080 ± 259200	4.3 ± 1.7	50 ± 4	0.96
40	0.21 ± 0.02	9288000 ± 2557440	0.31 ± 0.17	7.5 ± 0.7	0.92
50	0.156	29462400	0.012	18.5	0.90

4.4.3. HYDROXYMETHYL-2-FURFURALDEHYDE

An analysis of variance (significance level of 95%) showed no significant differences in HMF concentration for batches with high and low initial dissolved oxygen content, except for data at 50 °C. Taking into consideration the general trends, the kinetic analysis was performed using the different batches for each temperature as replicates.

Production of HMF was modelled as two consecutive zero-order reactions kinetic:

$$C_{HMF} = k_1 \times t \quad t < t_c \quad (4.13)$$

$$C_{HMF} = k_1 \times t_c + k_2 \times (t - t_c) \quad t \geq t_c \quad (4.14)$$

where C_{HMF} is the concentration of HMF at any time t , t_c is the critical time of behaviour change, and k_1 and k_2 are the rate constants of the slower and faster (first and second) reactions.

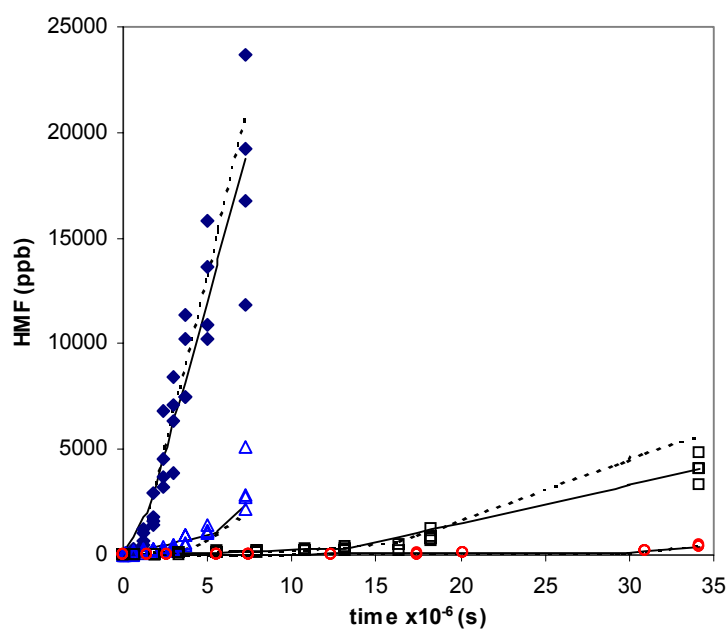
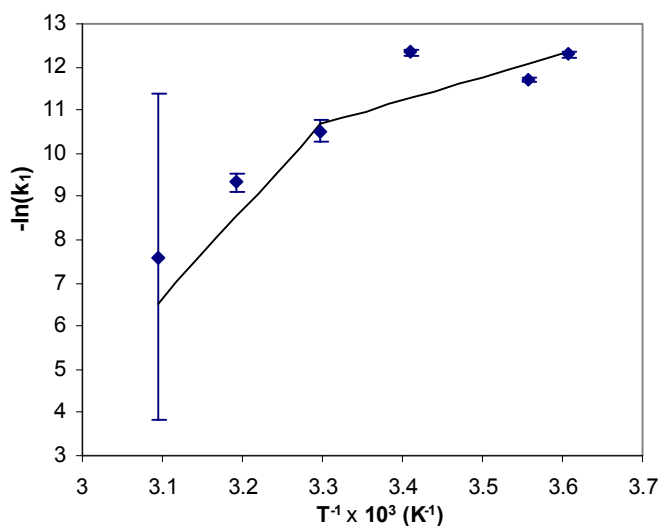


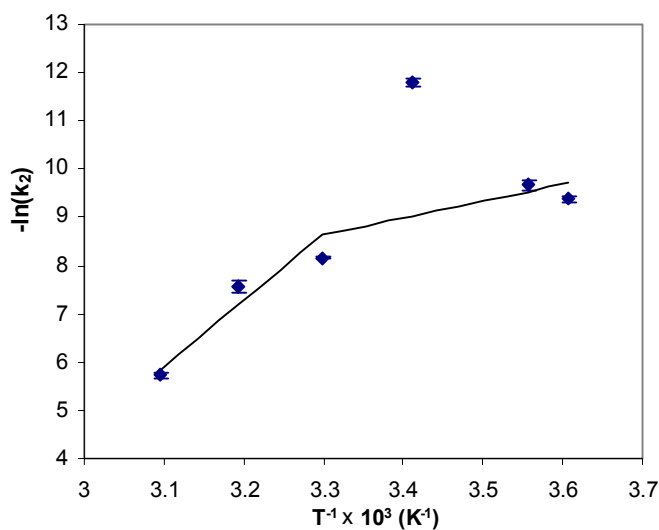
Figure 4.9- Fit of the two consecutive zero-order reactions kinetic model to HMF data, at (◆) 50, (△) 40, (□) 30, and (○) 4 °C. The dashed and the solid line indicate, respectively, the individual and global fit.

Figure 4.9 shows typical examples of the fit of this model to the experimental data ($R^2_{adj} > 0.92$, correlation coefficients < 0.938) (for further examples, see Figure C.12, Appendix C). Table 4.5 shows the model parameter estimates. The reaction rate constants from both phases followed two distinct Arrhenius profiles with

temperature (see Figure 4.10), one for temperature range of 50 to 30 °C, and another for 30 to 4 °C.



(a)



(b)

Figure 4.10- Dependence of the reaction rate constants of the two consecutive zero-order reaction kinetics on temperature for HMF formation: (a) rate constant of the first reaction (k_1); (b) rate constant of the second reaction (k_2). The \blacklozenge symbols represent parameters estimated by individual fits and the solid line indicates the global fit.

The critical time of behaviour change showed a sinusoidal decrease with temperature and therefore the Weibull model was used to describe this relationship (Figure 4.11). One could say a linear relationship would describe this dependence as well, but that was not the case, as it would lead to higher t_c values for 50 and 40 °C, which would yield very poor global fits to the experimental data.

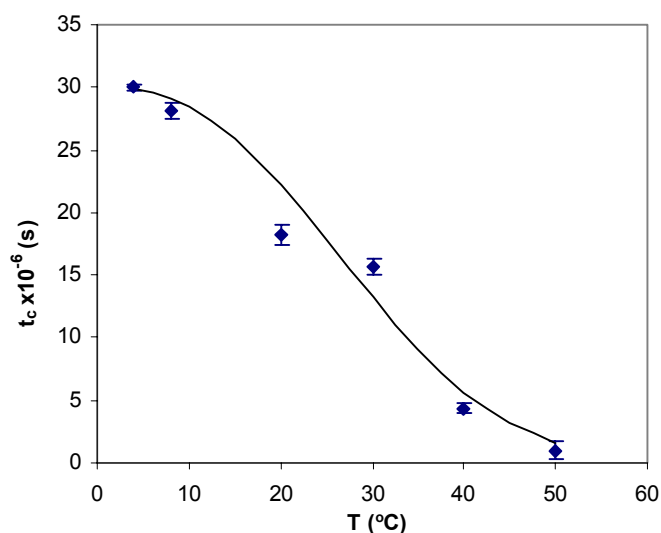


Figure 4.11- Relation of the time at which the reaction behaviour (HMF) changes with temperature. The \blacklozenge symbols represent parameters estimated with individual fits and the solid line indicates the global fit.

These relationships of the reaction constants and critical times and concentration with temperature were then incorporated in Equations 4.13 and 4.14, to build a global model:

$$C_{HMF} = k_{1ref} \times e^{-\frac{Ea_{11}}{R} \times \left(\frac{1}{273.15+T} - \frac{1}{273.15+T_{ref}} \right)} \times t \quad T < T_{ref} \text{ and } t < t_c \quad (4.15)$$

$$C_{HMF} = k_{1ref} \times e^{-\frac{Ea_{12}}{R} \times \left(\frac{1}{273.15+T} - \frac{1}{273.15+T_{ref}} \right)} \times t \quad T \geq T_{ref} \text{ and } t < t_c \quad (4.16)$$

$$C_{HMF} = k_{1ref} \times e^{-\frac{Ea_{11}}{R} \times \left(\frac{1}{273.15+T} - \frac{1}{273.15+T_{ref}} \right)} \times t_c +$$

$$+ k_{2ref} \times e^{-\frac{Ea_{21}}{R} \times \left(\frac{1}{273.15+T} - \frac{1}{273.15+T_{ref}} \right)} \times (t - t_c) \quad T < T_{ref} \text{ and } t \geq t_c \quad (4.17)$$

$$C_{HMF} = k_{1ref} \times e^{-\frac{Ea_{12}}{R} \times \left(\frac{1}{273.15+T} - \frac{1}{273.15+T_{ref}} \right)} \times t_c +$$

$$+ k_{2ref} \times e^{-\frac{Ea_{22}}{R} \times \left(\frac{1}{273.15+T} - \frac{1}{273.15+T_{ref}} \right)} \times (t - t_c) \quad T \geq T_{ref} \text{ and } t \geq t_c \quad (4.18)$$

$$\text{and } t_c = t_0 \times e^{-\left(\frac{T}{\alpha}\right)^\beta} \quad (4.19)$$

where k_{1ref} and k_{2ref} are rate constants at a reference temperature T_{ref} , Ea_{11} , Ea_{12} , Ea_{21} and Ea_{22} are activation energies regarding the dependence of the rate constants with temperature, R is the universal gas constant, and t_0 , α and β are the parameters of the Weibull model regarding the relation of the time of reaction/behaviour change with temperature (T).

Equations 4.15 to 4.19 showed to fit well the experimental data (Figure 4.10). Table 4.5 shows the global model parameter estimates. The global fit had an R^2_{adj} of 0.948 and the collinearity between the model parameters was below 0.83. Further information on the quality of the fit is included in Appendix C (Figure C.13 shows the fair agreement between predicted and experimental data, the lack

residual tendency and the approximately normal frequency distribution of the residuals).

Table 4.5- Estimates of the parameters for two consecutive zero-order reaction model individual (Eq. 4.13 and 4.14) and global (Eq. 4.15 to 4.19) fitting of HMF data.

INDIVIDUAL FITTING									
T (°C)	t_c (s)			$k_1 \times 10^6$ (s⁻¹)			$k_2 \times 10^3$ (s⁻¹)		
4	29980800 ± 259200			4.6 ± 0.5			0.084 ± 0.006		
8	28080000 ± 604800			8.4 ± 0.5			0.063 ± 0.006		
20	18230400 ± 864000			4.4 ± 0.3			0.0075 ± 0.0007		
30	15638400 ± 604800			27 ± 7			0.29 ± 0.01		
40	4320000 ± 518400			93 ± 23			0.51 ± 0.07		
50	1036800 ± 691200			498 ± 1887			3.3 ± 0.2		
GLOBAL FITTING									
t_0	α	β	T_{ref}	k_{1ref}	Ea_{11}	Ea_{12}	k_{2ref}	Ea_{21}	Ea_{22}
(day)	(°C)		(°C)	(day⁻¹)	(kJ/mol)	(kJ/mol)	(day⁻¹)	(kJ/mol)	(kJ/mol)
348 ± 6	32 ± 1	2.5 ± 0.4	30 ± 2	2.0 ± 0.4	45 ± 5	169 ± 16	15 ± 1	29 ± 3	114 ± 8

4.4.4. 2-FURFURALDEHYDE

As mentioned in §2.3, 2-furfuraldehyde (furfural) data was not affected by the initial level of dissolved oxygen (significance level of 95%), therefore the different batches were treated as replicates.

As mentioned in §2.1, furfural data is highly correlated with browning, and it was verified that its behaviour could also be described by a zero-order kinetic. When applied to furfural, it can be described by the following equation:

$$C_F = k \times t \quad (4.20)$$

where C_F is the concentration of furfural at any time t , and k is the rate constant.

This equation yielded fair fits to the data ($R^2_{\text{adj.}} > 0.834$). The parameter estimates are presented in Table 4.6 and examples of the individual fit are depicted in Figure 4.12.

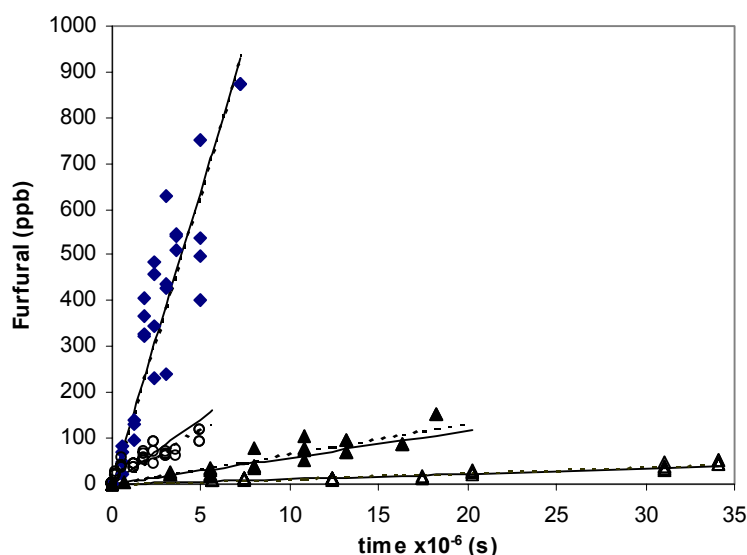


Figure 4.12- Fit of the zero-order model to furfural data, at (◆) 50, (○) 40, (▲) 30, and (△) 4 °C. The dashed and the solid line indicate, respectively the individual and global fit.

The reaction rate constants of furfural development increased with temperature according to two Arrhenius profiles, one in the range of temperature from 50 to 30 °C and another from 30 to 4 °C (Figure 4.13). This relationship was then incorporated in Equation 4.20 to build a global model:

$$C_F = k_{ref} \times e^{-\frac{Ea_{11}}{R} \left(\frac{1}{273.15+T} - \frac{1}{273.15+T_{ref}} \right)} \times t \quad T < T_{ref} \quad (4.21)$$

$$C_F = k_{ref} \times e^{-\frac{Ea_{12}}{R} \left(\frac{1}{273.15+T} - \frac{1}{273.15+T_{ref}} \right)} \times t \quad T \geq T_{ref} \quad (4.22)$$

where k_{ref} is the rate constant at a reference temperature T_{ref} , Ea_{11} and Ea_{12} are the activation energies regarding the dependence of the rate constant with temperature and R is the universal gas constant.

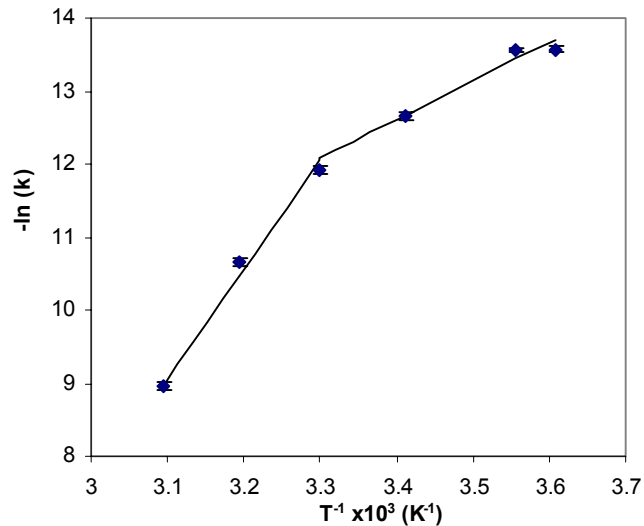


Figure 4.13- Dependence of the rate constants of the zero-order model on temperature, for furfural. The \blacklozenge symbols represent parameters obtained with the individual fit and the solid line indicates the global fit.

Equations 4.21 and 4.22 were fitted to the experimental data and the parameter estimates are presented in Table 4.6. The collinearity between model parameters was below 0.97 and the fit had a fair R^2_{adj} (0.919). Examples of the global model fit are also presented in Figure 4.13. Further examples are presented in Figures C.14, Appendix C. Further information on the quality of the fit is included in Appendix C (Figure C.15 illustrates the agreement between predicted and experimental data, the lack of residual tendency for predicted values, and the frequency distribution of the residuals).

Table 4.6- Estimates of the parameters for the zero-order model individual (Eq. 4.20) and global (Eq. 4.21 and 4.22) fitting of furfural data.

	INDIVIDUAL FITTING		GLOBAL FITTING			
	$k \times 10^6$ (s^{-1})		T_{ref} ($^{\circ}\text{C}$)	$k_{\text{ref}} \times 10^6$ (s^{-1})	E_{a11} (kJ/mol)	E_{a12} (kJ/mol)
4	1.27 ± 0.05		30 ± 3	5.7 ± 2.8	44 ± 14	126 ± 5
8	1.28 ± 0.03					
20	3.1 ± 0.1					
30	6.7 ± 0.3					
40	23 ± 1					
50	128 ± 6					

$T_{\text{ref}} = 27 \text{ }^{\circ}\text{C}$

4.4.5. 4-VINYL GUAIACOL

As 4-vinyl guaiacol has native fluorescence (maximum excitation at 320 nm and emission at 353 nm), an HPLC method using fluorescence detection was used to

quantify its concentration as it had much more sensitivity to this compound than a conventional UV detection. Fluorescence detection possesses sufficient sensitivity to detect as low as 10 ppb for PVG and can detect as low as one-fifth the flavour threshold value reported in literature for orange juice (Tatum *et al.*, 1975). Therefore when values of PVG concentration lower than 10 ppb were measured, they were not considered for modelling purposes.

It was found that PVG formation could be well described by first-order reaction kinetics:

$$C_P = C_P^\infty + (C_P^i - C_P^\infty) \times e^{-k \times t} \quad (4.23)$$

where C_P^i , C_P and C_P^∞ are the PVG concentrations at time zero, at any time t and at the equilibrium, and k is the rate constant.

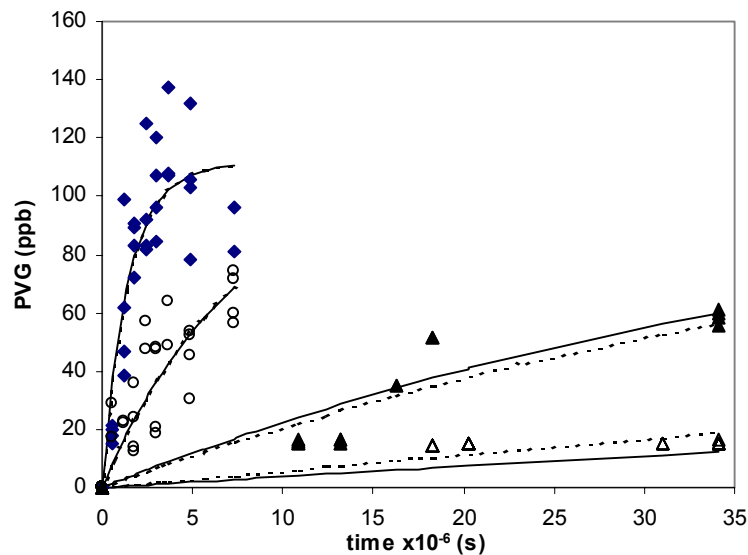


Figure 4.14- Fit of the first-order model to PVG data at (◆) 50, (○) 40, (▲) 30 and (△) 20 °C. The dashed and the solid line indicate, respectively the individual and global fit.

Figure 4.14 shows typical examples of the fit of first-order model to the experimental data ($R^2_{\text{adj}} > 0.853$, correlation coefficients < 0.96) (more detailed examples are presented in Figures C.16, Appendix C).

The concentration of PVG at the equilibrium was considered to be equal for all temperatures (see Figure 4.15), and the reaction rate constants followed an Arrhenius relation with temperature (see Figure 4.16).

The relationship of the rate constant with temperature was then incorporated in Equations 4.23 to build a global model:

$$C_P = C_P^\infty + (C_P^i - C_P^\infty) \times e^{-k_{ref} \times t} \times \left(\frac{1}{273.15+T} - \frac{1}{273.15+T_{ref}} \right) \quad (4.24)$$

where k_{ref} is the rate constants at a reference temperature T_{ref} , Ea is the activation energy regarding the dependence of the rate constant with temperature and R is the universal gas constant. The average temperature of the range tested, 27 °C (300.15 K), was chosen as the reference temperature.

Equation 4.24 was fitted to the whole set of data and Table 4.7 shows the parameter estimates. This global fit had an R^2_{adj} of 0.881 and the collinearity between the model parameters was below 0.65. Further information on the quality of the fit is included in Appendix C (Figure C.17 illustrates the agreement between predicted and experimental data, the lack of residual tendency for the predicted values, and the frequency distribution of the residuals). A better assessment of the validity of the model would require experimental data for longer storage periods.

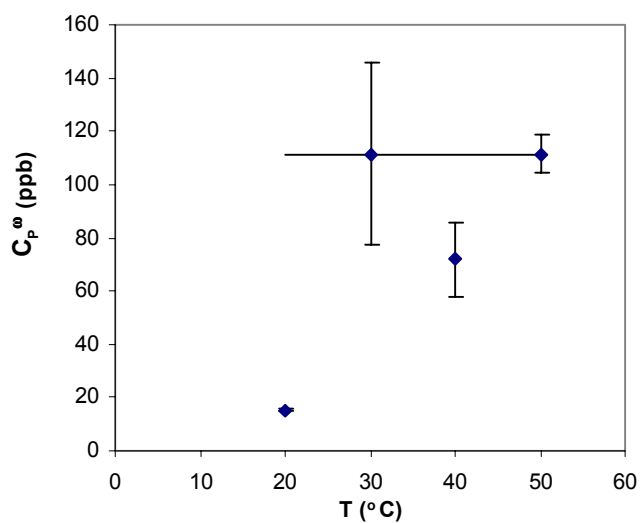


Figure 4.15- Dependence of the equilibrium PVG concentration on temperature. The \blacklozenge symbols represent parameters obtained with each individual fit and the solid line indicates the global fit.

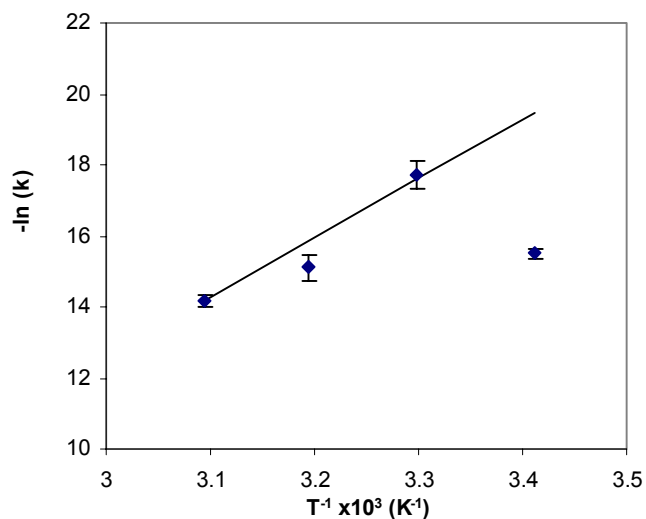


Figure 4.16- Dependence of the reaction rate constant of the first-order reaction kinetics on temperature for PVG. The \blacklozenge symbols represent parameters estimated with individual fits and the solid line indicates the global fit.

Table 4.7- Estimates of the parameters for the first-order model individual (Eq. 4.23) and global (Eq. 4.24) fitting of PVG data.

T (°C)	Individual Fitting		Global Fitting		
	C_P^∞ (ppb)	$k \times 10^6$ (s ⁻¹)	C_P^∞ (ppb)	$k_{ref} \times 10^6$ (s ⁻¹)	Ea (kJ/mol)
20	15.4 ± 0.2	0.19 ± 0.02	111 ± 5	0.013 ± 0.001	139 ± 5
30	112 ± 34	0.021 ± 0.008			
40	72 ± 14	0.3 ± 0.1			
50	112 ± 7	0.7 ± 0.1			

$T_{ref} = 27$ °C

4.5. CONCLUSIONS

Empirical mathematical models were developed for the compounds under study and showed to be adequate to describe the changes in orange juice quality during storage.

L-AA degradation can be either modelled by the Weibull model or by a two consecutive first-order models kinetic. The later has a higher number of parameters, and from the point of view of prevision the first can be used with similar results.

Browning index and Furfural were modelled using zero-order kinetics. A two consecutive first-order models kinetic described HMF formation, while PVG was explained using a first-order model kinetic levelling off to an equilibrium value. These models showed in general a fair agreement to experimental data.

L-AA degradation was much higher at small than at longer times, due to oxygen depletion in the earlier stages of storage.

The rate constants increased with temperature according to an Arrhenius type equation, in some case with a lower sensitivity to temperature (activation energy) at temperatures below app. 30 °C than at temperatures above this value.

Part III

Modelling dehydroascorbic acid, L-ascorbic acid and browning in controlled conditions

CHAPTER 5

Effect of ascorbic acid addition on L-ascorbic acid degradation and browning during storage of orange juice

Ascorbic acid (L-AA) degradation is often the critical factor for orange juice shelf life, which may be overcome by addition of L-AA (Chapter 2). The objective of this work was to study the effect of adding L-AA on kinetics of L-AA degradation and browning in orange juice during storage, in a range of temperatures. Single strength orange juice with different added L-AA contents and a control without added L-AA were stored during 2 months, protected from light, and monitored for L-AA, dehydroascorbic acid (DA), browning, O₂ and pH. Experiments were conducted at 20, 25, 30, 35, 40 and 45 °C. The results showed that addition of L-AA to orange juice slows down its degradation rate but promotes browning, especially at high storage temperatures. The Weibull model was found to fit well the data. Its rate constant showed an Arrhenius type relationship with temperature, and the reciprocal of the rate constant at a reference temperature decreased linearly with added L-AA concentration. The shape parameter, which relates to the mechanisms underlying the process, increased linearly with temperature, as observed in the previous chapter.

The L-AA degradation was also well described by a two consecutive first-order kinetics. The rate constant for the first reaction followed an Arrhenius relationship

with temperature while the second followed two distinct Arrhenius profiles with a discontinuity at 39.7 ± 0.4 °C. Both rate constants at the reference temperature of 39.7 ± 0.4 °C decreased exponentially with added L-AA concentration.

Browning was well described by zero-order kinetics. The rate constant showed an Arrhenius type relationship with temperature and the reciprocal of the rate constant at a reference temperature showed to increase linearly with added L-AA concentration.

L-AA was found to be the critical factor that limits orange juice shelf life, except when reasonable amounts of L-AA are added to the juice (≥ 400 mg/L at 20 and 25 °C; ≥ 300 mg/L at 30 °C). Regarding L-AA degradation, the Weibull model was found to be the most suitable for accelerated shelf life testing (ASLT), as the rate constant does not show any discontinuity with temperature. Shelf life was however systematically over-estimated, with errors between 2 and 62 %, indicating that ASLT must be used cautiously.

5.1. INTRODUCTION

Ascorbic acid is an important indicator of orange juice quality, because its decrease in concentration to levels lower than those required by legislation often defines orange juice shelf life. This is commercially overcome by addition of ascorbic acid, and therefore it would be most important to assess and model the

effects of added ascorbic acid on the degradation kinetics. Published studies focusing on added ascorbic acid in fruit juices are scarce. Saguy et al. (1978) in a study on concentration of grapefruit juice (with different initial L-AA contents) reported that initial L-AA concentration has no significant effect either on rate of deterioration or mechanism. Sakai et al. (1987), using aqueous solutions with added L-AA, reported that ascorbic acid degradation rate constants are independent of initial L-AA content.

The main objective of this work was to study the kinetics of L-AA degradation and browning in orange juice with added L-AA, in a range of temperatures, having in mind the importance of these models particularly for shelf-life estimation using accelerated tests.

5.2. MATERIALS AND METHODS

5.2.1. EXPERIMENTAL DESIGN

Single strength orange juice (Minute Maid™ premium) was bought from a local supermarket. All juice was part of the same batch. Using juice from a single batch minimized variations due to the processing conditions and to the fruit variability (agronomic factors). The juice was strained and divided into 6 batches, and different amounts of L-AA (Merck- 1.00127.0250) were added to each batch (I=0, J=100, K=200, L=300, M=400, and N=500 mg/L). Hard-thick screw capped tubes (1400 units), ≈33mL volume, were filled with juice, screwed without headspace,

sealed with silicone, and immersed in six thermostatic bath (Julabo SW-21C, Julabo Labotechik GMBH, Seelbach – Germany), which were protected from light (Figure 5.1). Twelve (2 replicates x 6 [AA]_{added}) tubes were randomly collected from each thermostatic bath at different time intervals, and analysed for L-ascorbic acid, dehydroascorbic acid, dissolved oxygen concentration and pH. Experiments were conducted at 20, 25, 30, 35, 40 and 45 °C (± 0.5 °C) for up to two months. Sampling times depended on temperature. Experimental data are presented in Table D.1 (Appendix D).

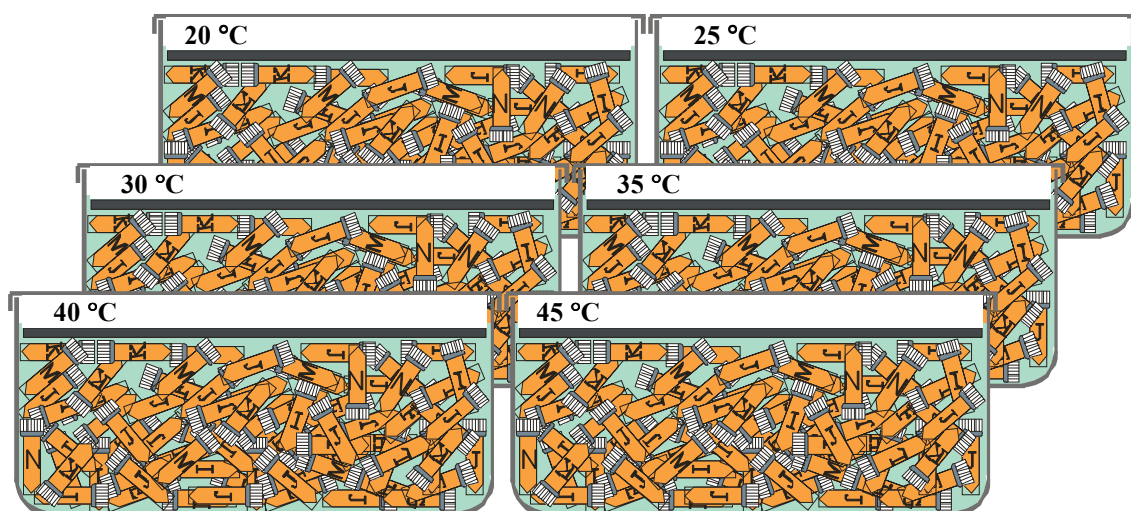


Figure 5.1- Representation of the conditions used for the experimental design.

5.2.2. ANALYTICAL DETERMINATIONS

Dissolved oxygen content was measured with an Oxi 340 oxygen electrode, equipped with a CelOx 325 probe and an air calibration beaker oxicall-SL (WTW Wissenschaftlich Technische, Weinheim, Germany). The initial oxygen content was 4.98 ± 0.73 ppm (variations within batch <6%) and the final content was 0.1

± 0.05 ppm. Brix degree was measured with an Atago hand refractometer. pH was measured with a Crison micropH-meter 2001 instrument, and its value varied from 3.79 ± 0.01 to 3.91 ± 0.06 .

Browning was measured as light absorbance at 420 nm (Meydav *et al.*, 1977) using a spectrometer (Unicam 8630 UV/VIS, Cambridge, U.K.).

Simultaneous L-ascorbic and dehydroascorbic acid analysis was performed by HPLC with the method described by Zapata & Dufour (1992) in a Beckman System Gold HPLC (Beckman Instruments, Inc. San Remo, California) equipped with a Beckman Model 168 Diode Array detector. One mL sample and 1 mL of freshly prepared internal standard solution (0.3 g/L isoascorbic acid, Sigma, I-0502) were diluted in ultra-pure water:methanol (95:5 v/v) in a 10 mL volumetric flask. The solution was centrifuged at 10,000 rpm for 5 minutes at 4 °C. One mL of OPDA (1,2-phenylenediamine dihydrochloride, 0.5 g/L) was added to 3 mL of the centrifuged solution in order to transform the dehydroascorbic acid into its derivatized form DFQ (fluorophore 3-(1,2-dihydroxyethyl)furo[3,4-b]quinoxaline-1-one). The solution was filtered through a C-18 sep pak cartridge (Waters, Millipore Corporation), and then through 0.45 microm Nucleopore Filters (Syrfil 25mm 0.45 micrometers FN). The first millilitre of the solution was discarded and the remaining solution was kept for 37 minutes in the dark at ambient temperature, and finally 10 μ L of the solution were injected into the HPLC. The mobile phase was water:methanol (95:5 v/v) with 6.82 g/L dipotassium phosphate (Sigma P-3786) and 1.86 g/L Cetrimide (Sigma T-4762) at

a flow rate of 1.8 mL/min. A Spherisorb ODS 18 (250 x 4.6 mm) column was used. The detector (166 Beckman UV-VIS detector) wavelength was set at 348 nm and after the elution of DFQ it was shifted to 261 nm for L-AA and IAA detection.

5.2.3. DATA ANALYSIS

The models tested were fitted by non-linear regression to the experimental data in order to estimate the models parameters. Fits were performed for each experiment carried out at a given temperature and for each batch, in order to assess the quality of the fit of the models, and to further analyse the dependence of the model parameters on temperature and added L-AA: these will be further referred to as “individual fits”. The kinetic equations were then combined with the equations that relate the model parameters to temperature and the resulting model was fitted to the whole set of experimental data to improve parameter estimation: this will be further referred to as "global fits".

Non-linear regression was performed with the STATISTICA™ '99 Edition software (StatSoft, Inc. (1999), STATISTICA for Windows (computer program manual), Tulsa, OK: 2300 East 14th St., Tulsa OK 74104, USA, WEB: <http://www.statsoft.com>).

5.3. RESULTS AND DISCUSSION

5.3.1. L-ASCORBIC ACID DEGRADATION

Figure 5.2 shows the fractional decrease in L-AA concentration at 35 °C, for samples with different initial L-AA contents, and similar results were obtained at the other temperatures tested.

The results show that the addition of L-AA slows down the degradation process (Figure 5.2). The rate of L-AA degradation in the control samples (no added L-AA) was app. 10 times the one reported in Chapter 4 for orange juice packaged in TBA packages. As earlier concluded differences in the initial oxygen content do not justify this result and as the samples were immersed in water and protected from light this difference in rate may be due to differences in the juice characteristics.

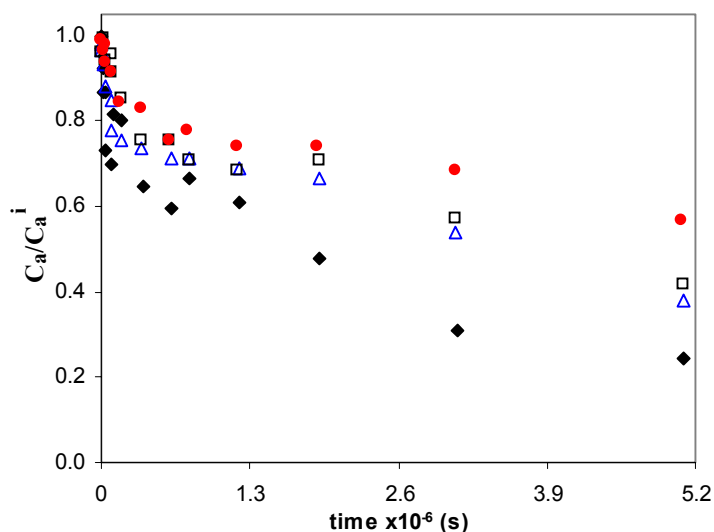


Figure 5.2- Fractional decrease of L-ascorbic acid at 35 °C, for different levels of L-AA addition: (◆) batch I- no addition, (△) K- 200 mg/L, (□) L- 300 mg/L, and (●) N- 500 mg/L.

Modelling L-AA degradation with the two consecutive first-order model

As observed in Chapter 4, §4.3, L-AA degradation could also be well described by two consecutive first order reaction kinetics (Eq. 4.1 and 4.2).

Figure 5.3 shows typical examples of the fit of this model to the experimental data and the parameters estimates are presented in Table 5.1 ($R^2_{adj} > 0.914$, correlation coefficients < 0.899) (for further examples, see Figures D.1 to D.6, Appendix D).

The reaction rate constants from the first reaction follow an Arrhenius relation with temperature whereas the reaction rate constants from the second reaction follow two distinct Arrhenius profiles, one for temperature range of 50 to 40 °C, and another for 30 to 20 °C. Both reaction rate constants at a reference temperature showed to decrease exponentially with added L-AA content, as can be seen in Figure 5.4.

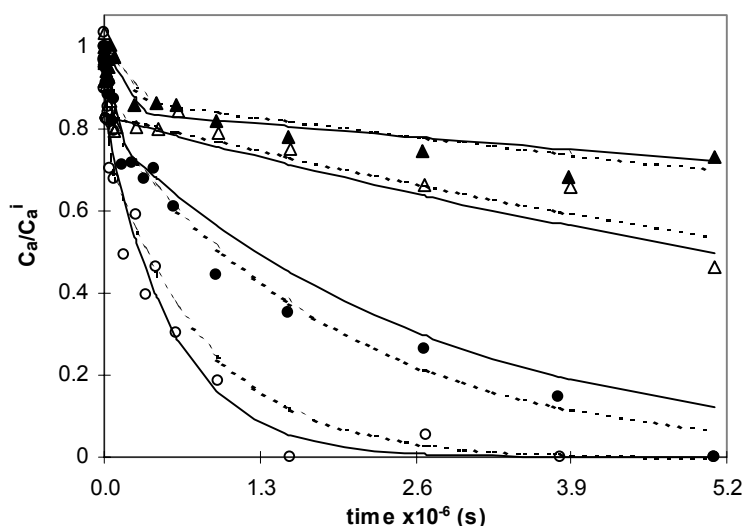
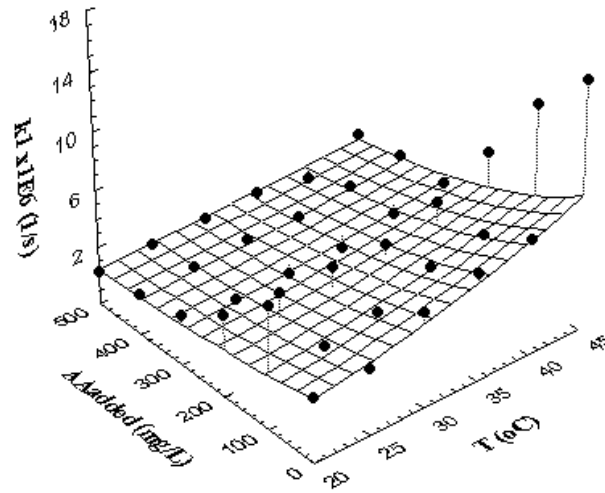
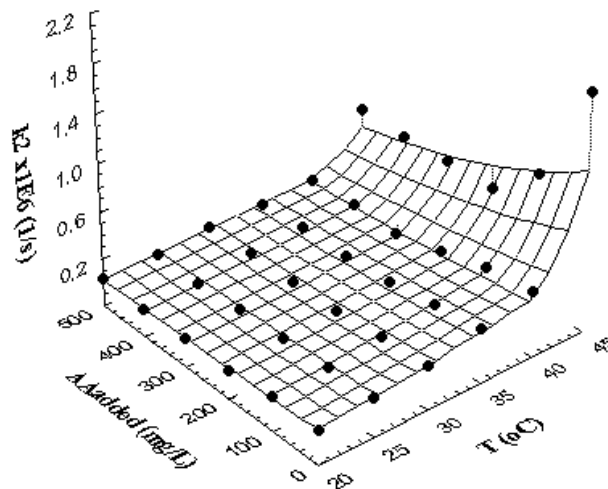


Figure 5.3- Fits of the two consecutive first-order reaction model to L-ascorbic acid at (○) 45°C -batch I, (●) 45°C -batch N (500 mg/L), (Δ) 20°C -batch I (no added L-AA) and (▲) 20°C -batch N (500 mg/L). The dashed and the solid lines indicate, respectively the individual and global fit.



(a)



(b)

Figure 5.4- Dependence of the reaction rate constants of the two consecutive first order reaction model on temperature and added L-AA concentration, for L-AA degradation: (a) rate constant of the first reaction (k_1); (b) rate constant of the second reaction (k_2). The symbol \bullet represents parameters estimated with individual fits and the surface indicates the global fit.

The logarithm of the time required for oxygen depletion (change from the first to the second reaction) was found to decrease exponentially with temperature and to increase linearly with added L-AA content (Figure 5.5).

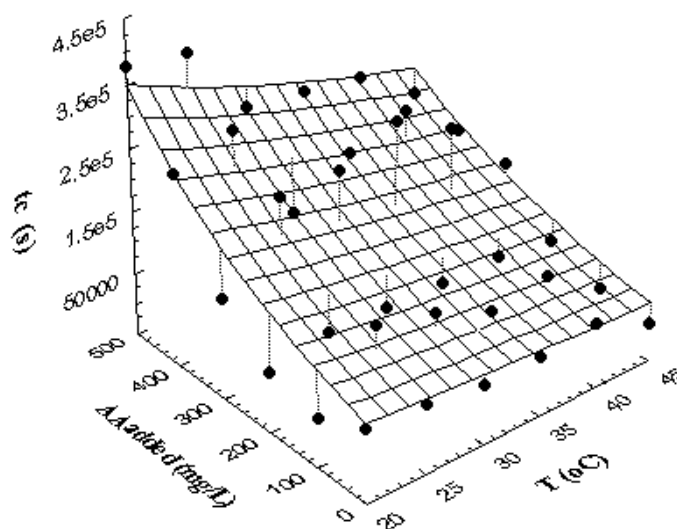


Figure 5.5- Dependence of the time required for oxygen depletion with temperature and added L-AA content. The symbol ● represents parameters estimated from individual fits and the surface indicates the global fit.

The value of the dissolved oxygen concentration at the time when reaction rate changes (t_c) was on average 0.76 ± 0.44 ppm (values for each condition tested are presented in Table 5.2). Dissolved oxygen content dropped to an equilibrium concentration in a very short time, as can be seen in Figure 5.6.

Table 5.2- Dissolved oxygen concentration (ppm) at the time when reaction rate changes (t_c).

Batch added AA conc. (mg/L)	TEMPERATURE (°C)					
	45	40	35	30	25	20
I - 0	1.1	0.6	0.9	1.8	1.7	1.5
J - 100	1.5	0.8	1.0	0.9	0.7	0.7
K - 200	0.6	0.7	0.4	0.7	0.8	2.0
L - 300	0.4	0.4	0.5	0.4	0.7	0.8
M - 400	0.4	0.4	0.4	0.4	0.7	0.9
N - 500	0.4	0.3	0.5	0.5	0.5	0.4

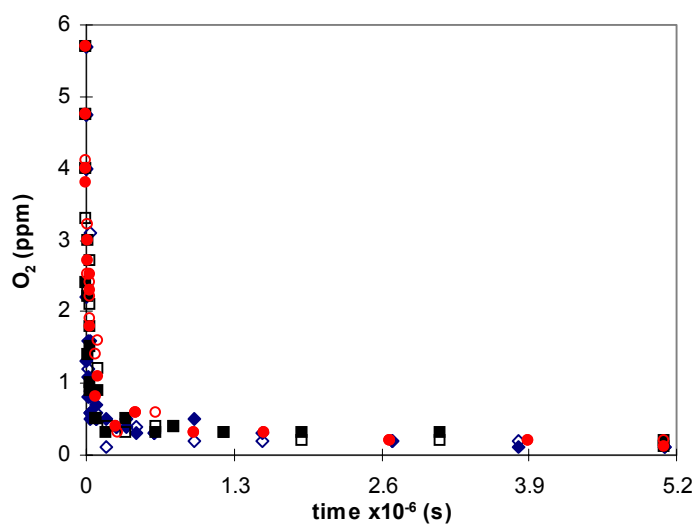


Figure 5.6- Decrease of dissolved oxygen with time (batch I - no added L-AA) at: (◆) 45, (◇) 40, (■) 35, (□) 30, (●) 25 and (○) 20 °C.

The relationships of the rate constants and time of oxygen depletion with temperature and added L-AA content were then incorporated in Equations 4.1 and 4.2 to build a global model:

$$C_a = C_a^i \times e^{\left[- \left(A_{k1ref} \times e^{-B_{k1ref} \times C_{add}} \right) \times e^{-\frac{Ea_1}{R} \left(\frac{1}{273.15+T} - \frac{1}{273.15+T_{ref}} \right)} \times t \right]} \quad t \leq t_c \quad (5.1)$$

$$C_a = C_a^i \times e^{\left[- \left(A_{k1ref} \times e^{-B_{k1ref} \times C_{add}} \right) \times e^{-\frac{Ea_1}{R} \left(\frac{1}{273.15+T} - \frac{1}{273.15+T_{ref}} \right)} \times t_c \right]} \times e^{\left[- \left(A_{k2ref} \times e^{-B_{k2ref} \times C_{add}} \right) \times e^{-\frac{Ea_{21}}{R} \left(\frac{1}{273.15+T} - \frac{1}{273.15+T_{ref}} \right)} \times (t-t_c) \right]} \quad t > t_c, T \geq T_{ref} \quad (5.2)$$

$$C_a = C_a^i \times e^{\left[- \left(A_{k1ref} \times e^{-B_{k1ref} \times C_{add}} \right) \times e^{-\frac{Ea_1}{R} \left(\frac{1}{273.15+T} - \frac{1}{273.15+T_{ref}} \right)} \times t_c \right]} \times e^{\left[- \left(A_{k2ref} \times e^{-B_{k2ref} \times C_{add}} \right) \times e^{-\frac{Ea_{22}}{R} \left(\frac{1}{273.15+T} - \frac{1}{273.15+T_{ref}} \right)} \times (t-t_c) \right]} \quad t > t_c, T < T_{ref} \quad (5.3)$$

and

$$t_c = e^{\left(D_{t_c,ref} + m_{t_c,ref} \times C_{add} \right) \times e^{b \times (T - T_{ref})}} \quad (5.4)$$

where A_{k1ref} and A_{k2ref} are k_{1ref} and k_{2ref} values for juice with no added L-AA, and B_{k1ref} and B_{k2ref} are the constants of the dependence of both rate constants at T_{ref} with added L-AA content (C_{add}), Ea_1 , Ea_{21} and Ea_{22} are activation energies regarding the dependence of the rate constants with temperature, R is the universal gas constant, $D_{t_c,ref}$ is the time for O_2 depletion for juice with no added

L-AA at T_{ref} and $m_{t_{c,ref}}$ is the slope of the linear relation of time of oxygen depletion at T_{ref} with C_{add} and b is the argument of the dependence of the time of oxygen depletion on temperature.

Equations 5.1 to 5.4 were fitted to the whole set of data and Table 5.3 shows the parameter estimates. This global fit had an R^2_{adj} of 0.952 and the collinearity between the model parameters was below 0.85, with the exception of two parameters of the relation of depletion of oxygen time with added L-AA content (0.98). Nonetheless, values below 0.99 are considered acceptable (Bates & Watts, 1988; Van Boeckel, 1996). Some examples of the global fit are presented in Figure 5.3, and the remaining in Appendix D, Figures D.7 to D.12. Further information on the quality of the fit is included in Appendix D (Figure D.13 illustrates the quality of the global fit, showing the good agreement between predicted and experimental data, the lack of residual tendency and an approximate normal distribution of the residual, for all the temperatures tested).

Modelling L-AA degradation with the Weibull Model

The Weibull model (Eq. 4.7) was also found to fit well the experimental L-AA data ($0.982 < R^2_{adj} < 0.889$) and the parameter estimates are presented in Table 5.4. The fits for some of the temperatures tested can be seen in Figure 5.7 and further examples are depicted in Appendix D (Figures D.1 to D.6).

Table 5.1- Estimates of the parameters of the individual fitting of the two consecutive first order model (Eq. 4.1 and 4.2) to L-AA data.

INDIVIDUAL FITTING									
T (°C)	Batch I (0 mg/L)			Batch J (100 mg/L)			Batch K (200mg/L)		
	$k_1 \times 10^6$ (s ⁻¹)	$k_2 \times 10^6$ (s ⁻¹)	$t_c \times 10^3$ (s)	$k_1 \times 10^6$ (s ⁻¹)	$k_2 \times 10^6$ (s ⁻¹)	$t_c \times 10^3$ (s)	$k_1 \times 10^6$ (s ⁻¹)	$k_2 \times 10^6$ (s ⁻¹)	$t_c \times 10^3$ (s)
45	15.0±9.8	1.8±0.2	12.7±8.8	11.5±3.3	0.88±0.06	18±5	6.3±0.9	0.52±0.04	46±7
40	6.1±1.4	0.35±0.05	56±12	4.4±1.4	0.30±0.04	82±25	4.6±1.8	0.19±0.03	61±22
35	5.5±1.2	0.25±0.03	47±11	3.8±1.1	0.20±0.02	67±18	3.4±1.7	0.13±0.02	62±29
30	4.6±1.1	0.17±0.02	47±11	2.5±0.5	0.15±0.02	109±25	3.4±1.2	0.11±0.02	63±20
25	2.7±1.3	0.13±0.02	64±30	2.0±0.3	0.12±0.01	133±22	3.5±1.9	0.09±0.02	68±36
20	2.6±9	0.09±0.01	70±21	6.5±2.0	0.10±0.01	30±9	3.6±0.8	0.044±0.008	49±10
T (°C)	Batch L (300 mg/L)			Batch M (400 mg/L)			Batch N (500 mg/L)		
	$k_1 \times 10^6$ (s ⁻¹)	$k_2 \times 10^6$ (s ⁻¹)	$t_c \times 10^3$ (s)	$k_1 \times 10^6$ (s ⁻¹)	$k_2 \times 10^6$ (s ⁻¹)	$t_c \times 10^3$ (s)	$k_1 \times 10^6$ (s ⁻¹)	$k_2 \times 10^6$ (s ⁻¹)	$t_c \times 10^3$ (s)
45	2.3±0.5	0.52±0.07	125±39	2.2±0.4	0.50±0.04	132±31	1.8±0.4	0.50±0.04	148±46
40	1.7±0.2	0.10±0.01	222±27	1.7±0.2	0.11±0.01	202±26	1.3±0.3	0.08±0.01	212±42
35	1.0±0.2	0.11±0.01	273±61	1.2±0.3	0.11±0.02	175±48	0.9±0.2	0.07±0.01	227±52
30	0.9±0.2	0.09±0.02	234±67	1.2±0.2	0.089±0.007	117±21	0.7±0.2	0.065±0.009	238±55
25	0.8±0.4	0.08±0.01	234±115	1.1±0.3	0.04±0.02	288±87	0.5±0.2	0.04±0.02	364±132
20	0.15±0.05	0.05±0.02	114±41	0.8±0.3	0.03±0.01	259±107	0.4±0.1	0.04±0.01	380±163

Table 5.3- Estimates of the parameters of the global fitting of the two consecutive first order model (Eq. 5.1 to 5.4) to L-AA data.

GLOBAL FITTING					
$A_{k1ref} \times 10^6$ (s ⁻¹)	B_{k1ref} (L/mg)	E_{a1} (kJ/mol)	$A_{k2ref} \times 10^6$ (s ⁻¹)	B_{k2ref} (L/mg)	E_{a21} (kJ/mol)
5.8±0.3	0.0031±0.0002	35±2	0.29±0.02	0.0023±0.0001	212±9
E_{a22} (kJ/mol)	T_{ref} (°C)	$D_{tc,ref}$ (s ⁻¹)	$m_{tc,ref} \times 10^3$ (L/(mg.s))	b (°C ⁻¹)	R^2_{adj}
42±4	39.7±0.4	10.85±0.06	2.9±0.2	-0.0020±0.0002	0.952

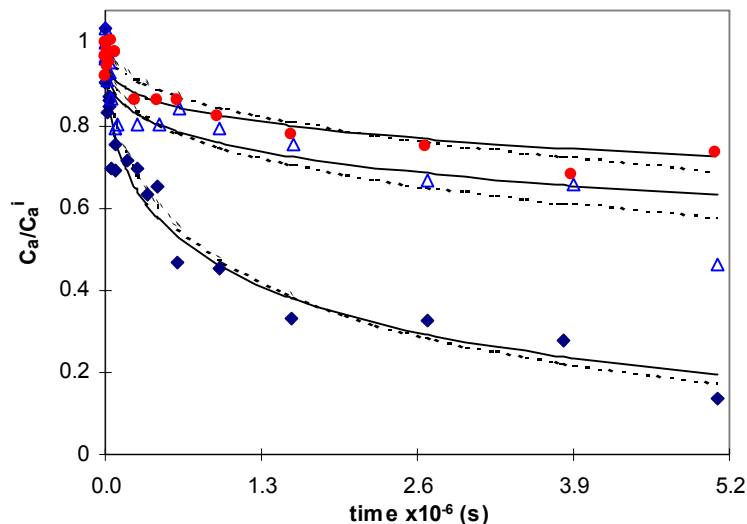
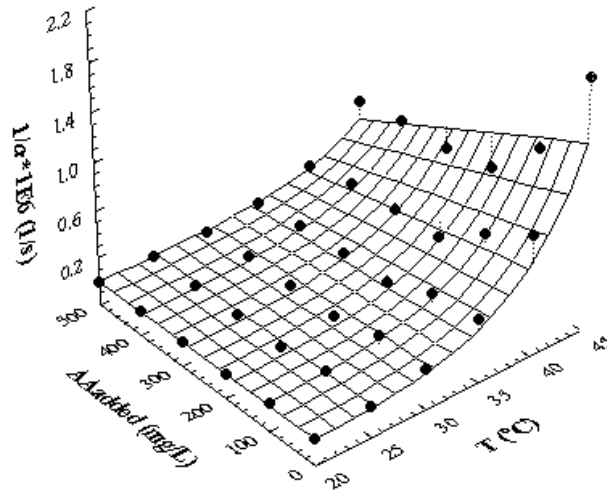
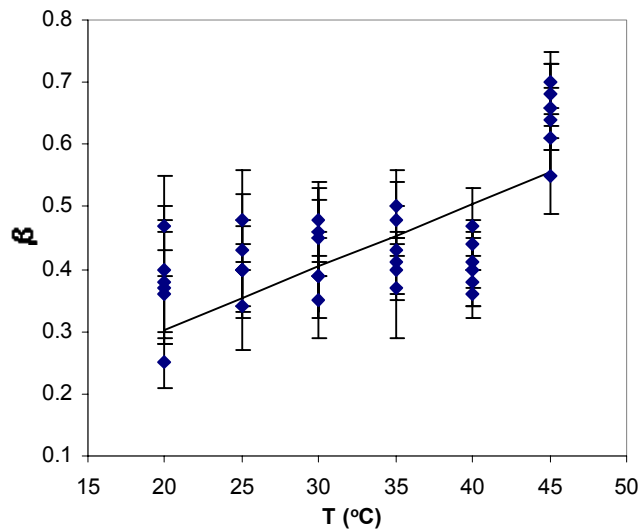


Figure 5.7- Fit of the Weibull model to L-ascorbic acid data at (◆) 40°C-batch I (no added L-AA), (△) 20°C-batch I (no added L-AA) and (●) 20°C -batch N (500 mg/L). The dashed lines indicate the individual fit and the solid lines the global fit.

The model rate constant ($1/\alpha$), which represents the time required to reach one log-cycle degradation, showed an Arrhenius type relationship with temperature. The rate constant at a reference temperature (32.5 °C - average temperature in the range tested), $(1/\alpha)_{\text{ref}}$, decreased linearly with added L-AA content while the activation energy maintained an approximately constant value (Figure 5.8). The shape constant (β), which relates to the mechanism underlying the process, increased linearly with temperature (Figure 5.8). (This increase was more obvious when a pre-global fit imposing an Arrhenius-type dependency of $1/\alpha$ with temperature was performed for each batch separately.)



(a)



(b)

Figure 5.8- Dependence of the Weibull model parameters on temperature and added L-AA content, for L- AA degradation: (a) rate constant ($1/\alpha$); (b) shape constant (β). Symbols \bullet and \blacklozenge represent parameters estimated with individual fits, and the solid line and surface indicate the global fit.

The above-mentioned relationships of $1/\alpha$ and β with temperature and added L-AA content were then incorporated in Equation 4.7 to build a global model:

$$C_a = C_a^i \times e \left[\left(\frac{1}{\alpha} \right)_0 + m_{1/\alpha} \times C_{add} \right] \times e^{-\frac{Ea}{R} \left(\frac{1}{273.15+T} - \frac{1}{273.15+T_{ref}} \right) \times t} \left. \right] \beta_{ref}^{+m \times (T - T_{ref})} \quad (5.5)$$

where $(1/\alpha)_0$ is the rate constant at the reference temperature when no L-AA is added, $m_{(1/\alpha)}$ is the slope of the linear variation of the rate constant at a reference temperature T_{ref} with added L-AA concentration (C_{add}), Ea is the activation energy regarding the dependence of the rate constant with temperature, β_{ref} is the shape constant at the reference temperature, m is the slope of the dependence of the shape constant with temperature, and R is the universal gas constant.

Equation 5.5 was fitted to the whole set of data and Table 5.3 shows the parameter estimates. Some examples of this fit are depicted in Figure 5.6 and fits for the remaining data are presented in Appendix D, Figures D.7 to D.12. This global fit had a fair R^2_{adj} (0.985) and the collinearity between the model parameters was below 0.95. Further information on the quality of the fit is included in Appendix D (Figure D.14 illustrates the quality of the global fit, showing a fair agreement between predicted and experimental data, the lack of tendency and an approximate normal distribution of the residual values).

Table 5.4- Estimates of the parameters of the individual (Eq. 4.7) and global fitting (Eq. 5.5) of the Weibull model to L-AA data.

INDIVIDUAL FITTING												
T (°C)	Batch I - no added L-AA		Batch J – 100 mg/L		Batch K – 200 mg/L		Batch L – 300 mg/L		Batch M – 400 mg/L		Batch N – 500 mg/L	
	$1/\alpha \times 10^6$ (s ⁻¹)	β	$1/\alpha \times 10^6$ (s ⁻¹)	β	$1/\alpha \times 10^6$ (s ⁻¹)	β	$1/\alpha \times 10^6$ (s ⁻¹)	β	$1/\alpha \times 10^6$ (s ⁻¹)	β	$1/\alpha \times 10^6$ (s ⁻¹)	β
45	2.2±0.2	0.66±0.07	1.1±0.1	0.61±0.05	0.77±0.09	0.55±0.06	0.75±0.08	0.64±0.05	0.72±0.06	0.68±0.05	0.69±0.05	0.70±0.05
40	0.60±0.08	0.44±0.04	0.54±0.09	0.47±0.06	0.23±0.05	0.40±0.06	0.16±0.03	0.38±0.04	0.16±0.03	0.41±0.04	0.07±0.02	0.36±0.04
35	0.29±0.06	0.43±0.07	0.21±0.04	0.41±0.05	0.09±0.03	0.37±0.08	0.13±0.02	0.50±0.06	0.10±0.02	0.48±0.06	0.04±0.01	0.40±0.05
30	0.13±0.04	0.39±0.07	0.15±0.04	0.39±0.06	0.06±0.02	0.35±0.06	0.08±0.02	0.46±0.07	0.05±0.01	0.48±0.06	0.04±0.01	0.45±0.06
25	0.09±0.03	0.43±0.09	0.11±0.02	0.40±0.04	0.05±0.02	0.34±0.07	0.06±0.02	0.48±0.08	0.06±0.03	0.40±0.08	0.2±0.01	0.40±0.07
20	0.04±0.02	0.37±0.09	0.05±0.02	0.36±0.07	0.004±0.003	0.25±0.04	0.018±0.015	0.38±0.10	0.02±0.01	0.4±0.1	0.02±0.01	0.47±0.08
GLOBAL FITTING												
$1/\alpha_0 \times 10^6$ (s ⁻¹)	$m_{1/\alpha} \times 10^9$ (L/(mg.s ⁻¹))		Ea (kJ/mol)	β_{ref}		m (°C ⁻¹)		$R^2_{adj.}$				
0.16±0.01	-0.22±0.02		139±5	0.429±0.008		0.0101±0.0007		0.985				

T= 32.5 °C

As earlier observed in Chapter 4, the two consecutive first-order model provided a better fit to the experimental data, both in terms of residuals (1.695 for Weibull model and 1.227 for two-consecutive first-order model) and in terms of goodness of fit (the AIC test (AKAIKE information criterion (Sakamoto et al., 1986)) revealed that the two-consecutive first-order has a slighter better result (higher value) than the Weibull model (two-consecutive: AIC=-786.77, Weibull: AIC=-712.46)).

5.3.2. BROWNING INDEX

Browning data at the end of this experiment (59 days) yielded comparable values with the ones produced in the storage of TBA packages: in juice stored in TBA packages browning had a value of 0.387 ± 0.033 and 0.198 ± 0.017 , respectively, after, 57 days at 40°C and 64 days at 30 °C, and in juice stored in tubes, without L-AA addition, browning values of 0.353 ± 0.001 and 0.235 ± 0.001 were measured after 59 days at 40 and 30 °C, respectively.

Non-enzymatic browning was modelled using zero-order kinetics (Eq. 4.9). This equation yielded good fits to the experimental data ($0.941 < R^2_{\text{adj}} < 0.974$) and examples of the individual fit are depicted in Figure 5.9. Further examples are presented in Figures D.15 to D.20 (Appendix D). The estimates of the rate constants are shown in Table 5.5.

They showed to increase with temperature according to an Arrhenius-type equation, and the rate constant at a reference temperature (32.5 °C – average temperature in the range tested) proved to increase linearly with added L-AA content (Figure 5.10).

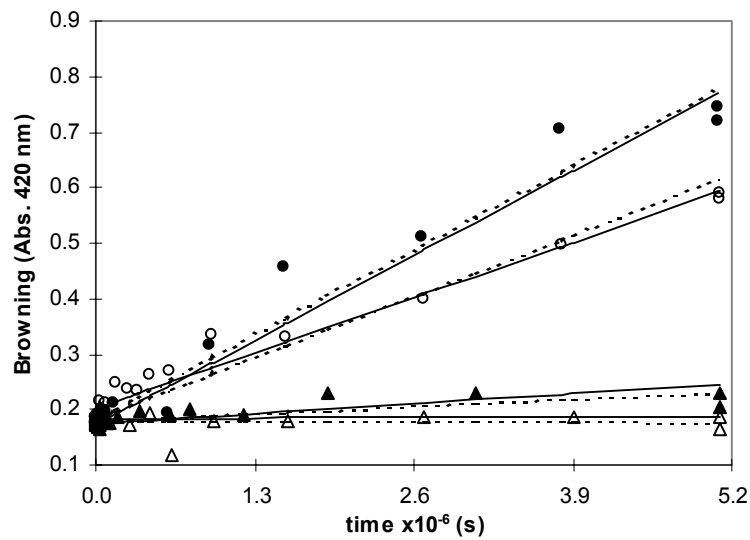


Figure 5.9- Fits of the zero-order model to browning index data at (○) 45°C -batch I (no added L-AA), (●) 45°C -batch N (500 mg/L), (▲) 35°C -batch K (200 mg/L) and (△) 20°C -batch I (no added L-AA). The dashed and the solid lines indicate, respectively the individual and global fit.

These relationships were then included in Equation 4.9 to build a global model:

$$C_{Br} = C_{Br}^i + (k_0 + m_k \times C_{add}) \times e^{-\frac{Ea}{R} \left(\frac{1}{273.15+T} - \frac{1}{273.15+T_{ref}} \right)} \times t \quad (5.6)$$

where k_0 is the rate constant for juice without added L-AA at the reference temperature, m_k is the slope of the linear relation of the rate constant at a reference temperature (T_{ref}) with added L-AA content (C_{add}), Ea is the activation energy

regarding the dependence of the rate constant on temperature and R is the universal gas constant.

Equation 5.6 was fitted to the experimental data and the parameter estimates are presented in Table 5.5. The collinearity between model parameters was below 0.96 and the fit had a fair $R^2_{adj.}$ (0.951).

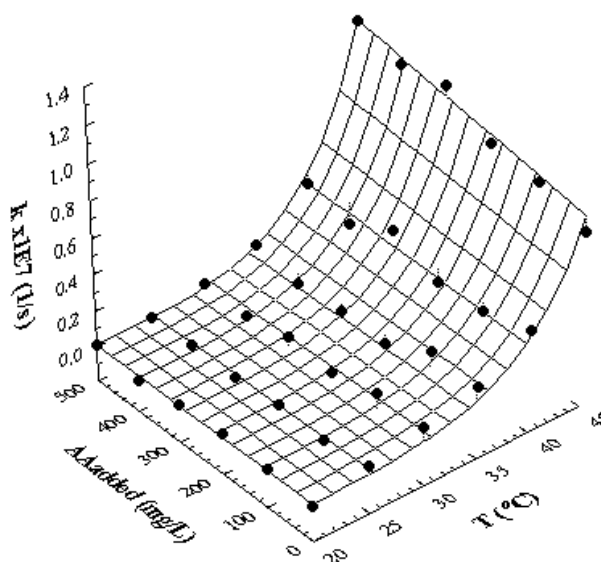


Figure 5.10- Dependence of the rate constant of the zero-order model on temperature and added L-AA content, for browning index. The symbol ● represent parameters estimated with individual fits and the surface indicates the global fit.

Table 5.5- Estimates of the parameters of the individual (Eq. 4.9) and global fitting (Eq. 5.6) of the zero-order model for browning data.

INDIVIDUAL FITTING						
	Batch I - no added AA	Batch J – 100 mg/L	Batch K – 200 mg/L	Batch L – 300 mg/L	Batch M – 400 mg/L	Batch N – 500 mg/L
T (°C)	$k \times 10^7$ (s ⁻¹)	$k \times 10^7$ (s ⁻¹)	$k \times 10^7$ (s ⁻¹)	$k \times 10^7$ (s ⁻¹)	$k \times 10^7$ (s ⁻¹)	$k \times 10^7$ (s ⁻¹)
45	0.77±0.03	0.87±0.03	0.93±0.04	1.10±0.04	1.07±0.03	1.17±0.05
40	0.36±0.03	0.31±0.02	0.31±0.02	0.43±0.02	0.32±0.02	0.39±0.03
35	0.20±0.02	0.22±0.01	0.10±0.02	0.11±0.02	0.11±0.012	0.17±0.01
30	0.12±0.03	0.14±0.02	0.08±0.02	0.11±0.02	0.06±0.01	0.08±0.01
25	0.06±0.01	0.02±0.01	0.04±0.02	0.02±0.01	0.04±0.01	0.02±0.01
20	-	0.011±0.009	0.025±0.009	0.02±0.01	-	0.005±0.005

GLOBAL FITTING				
C_{Br}^i -Batch I (abs.420nm)	$k_0 \times 10^7$ (s ⁻¹)	$k_m \times 10^{10}$ (L/(mg.s ⁻¹))	Ea (kJ/mol)	R ² _{adj.}
0.1806±0.0007	0.065±0.004	0.047±0.004	166±4	0.951

T= 32.5 °C

Examples of the global model fit are presented in Figure 5.9. Further examples of the global fit are presented in Figures D.15 to D.20 (Appendix D). Further information on the quality of the fit is included in Appendix D (Figure D.21 illustrates the good agreement between predicted and experimental data, the lack of residual tendency for predicted values, and the approximately normal distribution of the residuals).

It was noticed that at temperatures lower than 30 °C, no significant changes in orange juice colour occurred, while at high temperature the juice becomes quite brown in a short storage time, as expected because of the magnitude of the activation energy value. The addition of L-AA has a major effect on browning at the higher temperatures tested, while for ambient and slightly higher than ambient temperatures that effect is not significantly noticed.

5.3.3. SHELF LIFE PREDICTION BY ACCELERATED TESTING

To simulate ASLT the parameters of the mathematical models earlier reported were re-estimated, considering only the data gathered in abusive temperature conditions (35 to 45 °C). The values of the rate constants for these temperatures and for each different added L-AA content were estimated separately, and new values of reaction rate at the reference temperature and activation energies were calculated. Those values were used to estimate the time necessary to reach the compound threshold value at ambient temperature. “True” shelf life was estimated with the mathematical models developed with the data gathered in the full range

of temperature tested (20 to 45 °C). The threshold values used to define shelf life are those reported in Chapter 2.

Figure 5.11 shows the comparison of “true” shelf life and shelf life estimated by accelerating testing. The results show that at normal storage conditions L-AA degradation is the critical factor that limits shelf life, except when reasonable amounts of L-AA are added to the juice (≥ 400 mg/L at 20 and 25 °C; ≥ 300 mg/L at 30 °C).

As would be expected, the use of the two consecutive first-order reaction model to predict the time at which L-AA threshold content would be reached, raises problems, because of the different sensitivities of the reaction rate at abusive and ambient temperatures. The predicted reaction rate at ambient temperatures will be severely underestimated (the degree of underestimation depends on the difference of activation energies in the two ranges of temperatures), which will yield an estimated shelf life much longer than the real one. The Weibull model, in spite of its simplicity, does not show any discontinuity of the reaction rate in the whole range of temperature tested, and thus yields better results. Nevertheless, the model also overestimates shelf life, with errors that may reach 62%. These larger errors may be due to the small range of temperatures used to evaluate the model parameters (35 to 45 °C), as the precision of the model estimates is inversely related to the width of the temperature range tested (Box & Lucas, 1959).

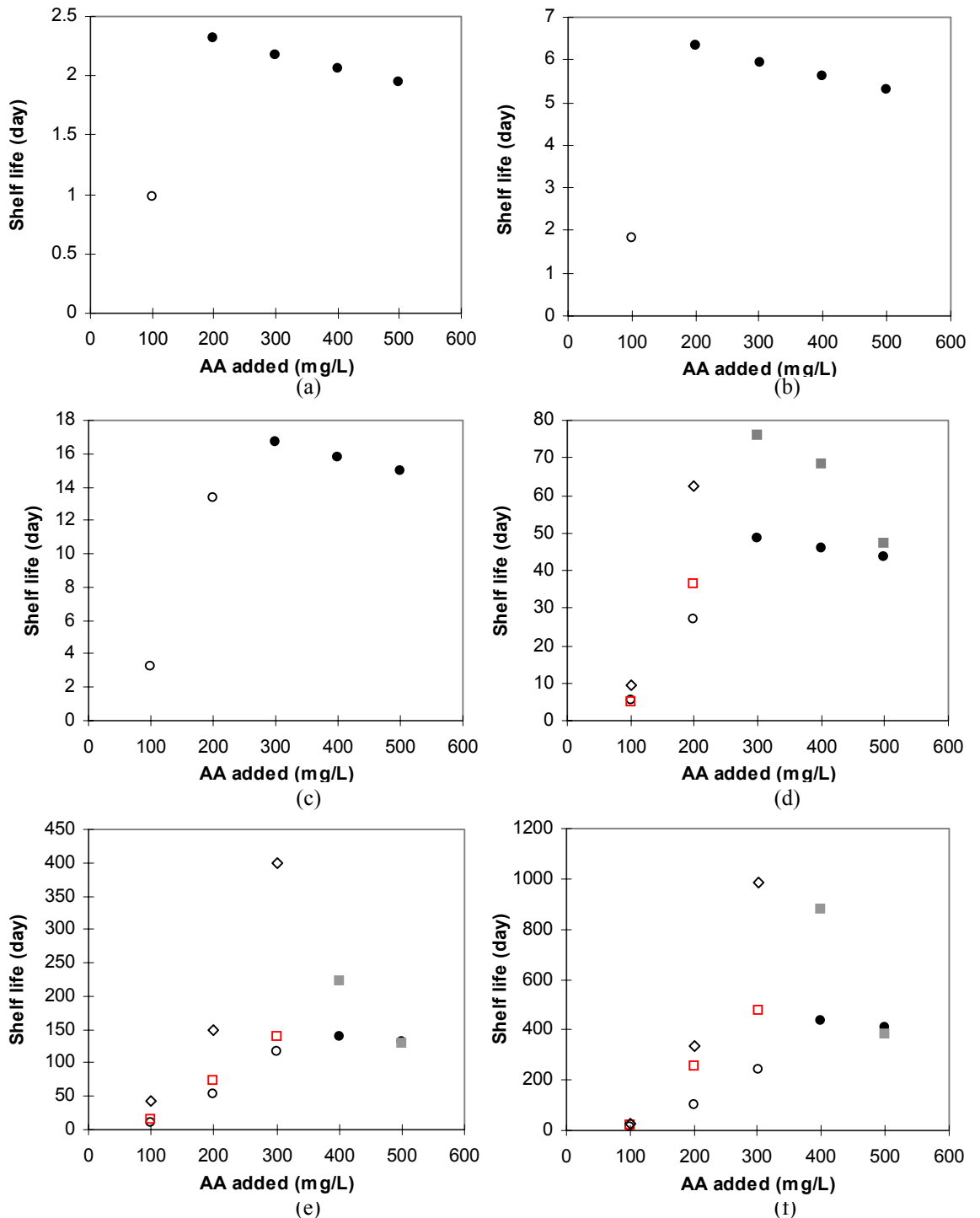


Figure 5.11- Comparison of “true” shelf life and shelf life estimated by accelerated testing at (a) 45, (b) 40, (c) 35, (d) 30, (e) 25 and (f) 20 °C. The dots represent the “true” shelf life, calculated with the mathematical models developed with the data gathered in the full range of temperatures tested (20 to 45 °C). The squares and diamonds represent the shelf life estimated using a mathematical model developed on the basis of data gathered in the high temperature range only (35 to 45 °C) considering, respectively, the Weibull or the two first-order consecutive reactions model for L-AA degradation. Open symbols indicate that L-AA is the factor limiting shelf life, whereas full symbols indicate that shelf life is limited by browning.

Figure 5.12 shows estimation errors when the Weibull model and the zero-order reaction are applied for L-AA degradation and browning, respectively. One can see that in general estimation errors decrease with increasing temperature. The smaller predicted errors were observed for the batch with the highest added L-AA content (500 mg/L).

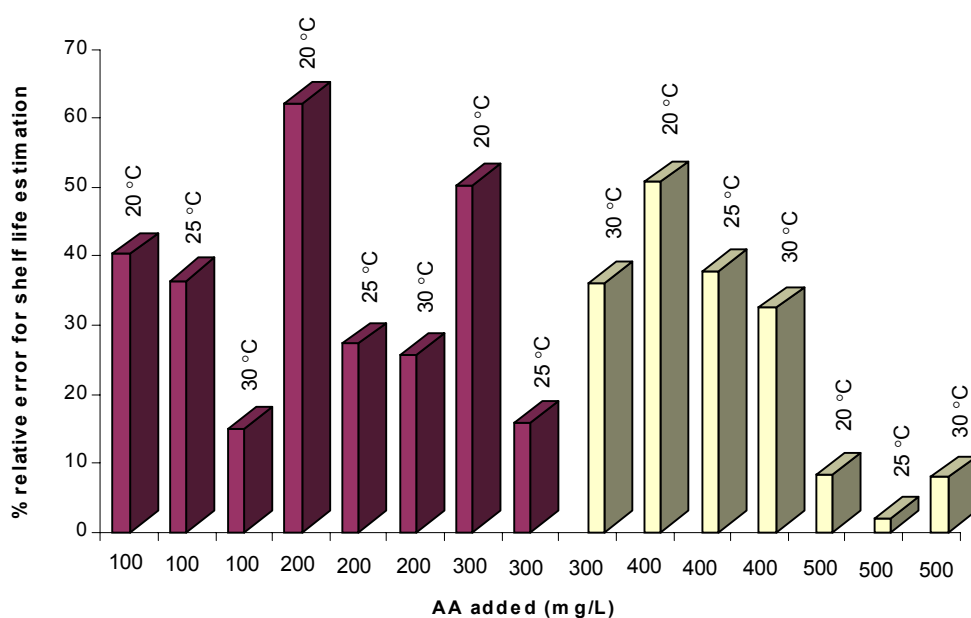


Figure 5.12- Estimation errors (%) when the Weibull model and the zero-order reaction are applied for L-AA degradation (dark grey bars) and browning (light grey bars), respectively.

5.4. CONCLUSIONS

The results show that addition of L-AA to orange juice slows down its degradation rate. Both the Weibull and the two consecutive first-order models provided a good description of the kinetics of degradation of ascorbic acid in the range of temperatures, added L-AA content and times tested. Nevertheless, the Weibull model is much simpler, with a smaller number of parameters, and showed to be more suitable for accelerated shelf life testing, as the rate constant did not show any discontinuity with temperature. The second reaction of the two consecutive first-order model shows a much higher sensitivity to temperature in abusive conditions (35 to 45 °C) than in normal storage temperatures, which hinders its use in ASLT.

Browning was well described by a zero-order kinetic, and appears to follow a single reactive pathway in the range of temperatures and added L-AA content tested. Browning rate increased with added L-AA content.

L-AA was found to be the critical factor that limits orange juice shelf life, except when reasonable amounts of L-AA are added to the juice (≥ 400 mg/L at 20 and 25 °C; ≥ 300 mg/L at 30 °C).

CHAPTER 6

Kinetics of L-ascorbic acid degradation and browning under excess oxygen and anaerobic conditions

The aerobic degradation of ascorbic acid (L-AA) in orange juice was determined in the 20-45 °C temperature range. Dehydroascorbic acid (DA), pH and browning were also monitored. Excess oxygen was maintained in the juice by continuous aeration. For low conversion the L-AA degradation followed first-order kinetics, but an analysis up to low L-AA retention showed a sigmoidal pattern. The Weibull model was found to describe this pattern. The rate constant increased with temperature according to an Arrhenius-type relationship whereas the shape constant decreased linearly with temperature. Before the time when maximum degradation rate occurred, pH, DA concentration and browning remained fairly constant, and then increased. It was found that this behaviour, as well as the dependence of the shape constant on temperature, might be explained by (i) the reconversion of DA into L-AA, following first-order kinetics in relation to DA and second order kinetics in relation to L-AA, and by (ii) different sensitivities of the reaction rate constants to temperature. Browning was also well described by the Weibull model, with a temperature independent shape parameter and an Arrhenius dependency of the rate constant on temperature. Under anaerobic conditions, obtained by nitrogen flushing, L-AA degradation came to an halt. This

suggests that the residual oxygen plays a major role in L-AA degradation in storage conditions referred to as anaerobic in earlier Chapters.

6.1. INTRODUCTION

The existence of two consecutive or parallel pathways, aerobic and anaerobic, involved in the degradation of ascorbic acid in orange juice is widely accepted. Several authors (Lee *et al.*, 1977; Hughes, 1985; Khan & Martell, 1967a; Khan & Martell, 1967b; Sakai *et al.*, 1987; Singh *et al.*, 1976) presented possible pathway schemes for ascorbic acid degradation. Most models reported on the literature were developed based on data gathered for relatively small L-AA conversions and/or under varying oxygen concentration, as the depleted oxygen was not replaced during storage. Modelling of aerobic L-AA degradation was earlier presented in Chapters 4 and 5, but the fast consumption of O₂ would not allow for a detailed study.

The complexity of the degradation mechanisms (Tannenbaum *et al.*, 1985; Liao & Seib, 1988) hinders the development of mechanistic models and pseudo kinetic models of zero, first or second orders are often applied, yielding a good fit to the experimental data. Sakai *et al.* (1987) applied a kinetic model consisting of two consecutive reactions (the first of order zero and the second of first-order) to describe the ascorbic acid oxidation in an aqueous solution, with different initial ascorbic acid concentration in which dissolved oxygen was held at a constant

level. These authors showed that this reactive mechanism might be perceived as either apparent first or zero-order kinetics, depending on the initial concentration of ascorbic acid and on the ratio of the rate constants of the sequential reactions.

The main objectives of this work were to further study and model the kinetics of aerobic L-ascorbic acid degradation in orange juice under extreme conditions: oxygen excess and total absence of oxygen. Browning was also studied because of its role on shelf life.

6.2. MATERIALS AND METHODS

6.2.1. EXPERIMENTAL DESIGN

Single strength orange juice (Minute Maid™ premium) was bought at a local supermarket. All juice used in the present study, as well as the juice used on the study described in the previous Chapter was part of the same batch. The juice was strained and 750 mL were poured into a 1L Buckner flask (Schott Duran, Germany), protected from light and immersed in a thermostatic bath (Julabo SW-21C, Julabo Labotechik GMBH, Seelbach – Germany). After the juice temperature reached the bath temperature, the time was set to zero, a sample (10-mL) was removed for analysis and aeration was switched on. The juice was continuously aerated for up to 36 hours and samples (10 mL) were removed at regular intervals and analysed for L-ascorbic acid, dehydroascorbic acid, browning and pH (Figure 6.1). At sampling times, the O₂ dissolved in the juice

contained in the Erlenmeyer flask and the °brix were also measured. Experiments were conducted at 20, 25, 30, 35, 40 and 45 °C ($\pm 0.5^\circ\text{C}$). The oxygen content varied between 4.70 to 5.67 ppm for different experiments, and variations during a given experiment were in general smaller than 10%. pH values varied from 3.69 to 3.77, being the increase during a given experiment smaller than 2.5%. The °brix was constant throughout the experiments with a value of 11.0. Experimental data is included in Appendix E, Table E.1.

Additional experiments with continuous aeration being replaced by nitrogen (N_2) flushing were performed to study L-AA degradation and browning in anaerobic conditions. Data is conveyed in Table E.2, Appendix E.

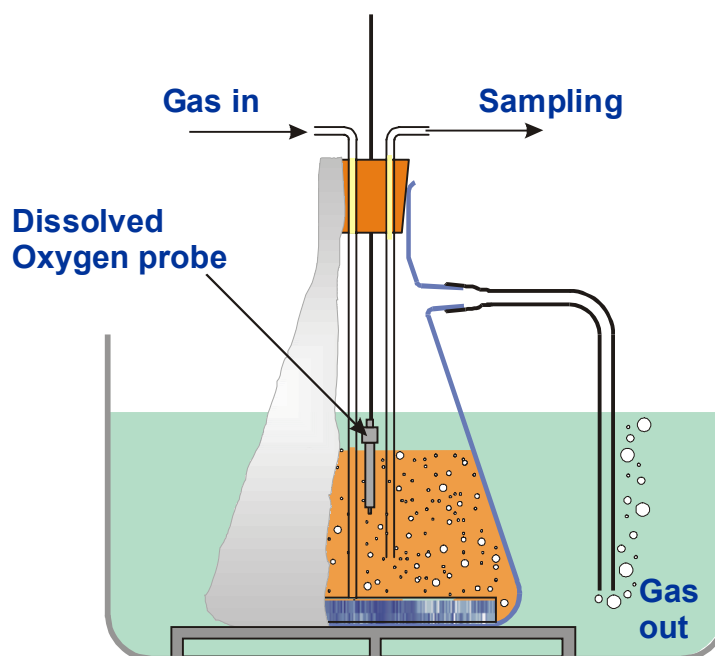


Figure 6.1- Schematic representation of the experimental set-up.

6.2.2. ANALYTICAL DETERMINATIONS

All analytical determinations were performed according to the description given on §5.2.2.

6.2.3. DATA ANALYSIS

The models tested were fitted by non-linear regression to the experimental data in order to estimate the models parameters, as described previously in §5.2.3.

Non-linear regression of integrated equations was performed with the Stata™ 5.0 software (Computing Resource Centre, Texas, USA).

Non-linear regression of ordinary differential equations (ODE) was performed using the least squares subroutine of ODRPACK (Boggs et al., 1992). The simulation of the ODE system was performed with a LSODE pack (Hindmarsh, A. C., Computing and Mathematics Research Div., 1-136 Lawrence Livermore National Laboratory, Livermore, CA 94550).

The Mathematica® 3.0 Nonlinear Fit package software (Wolfram Research, Illinois, USA) was used to evaluate the parameter curvature and maximum relative parameter effects. These determinations are useful for checking the reliability of the confidence intervals and confidence regions calculated for model parameters, because most statistical packages base these calculations on expressions that are only valid for linear regressions, even when the models are nonlinear. If the maximum relative intrinsic curvature (Max Intrinsic) is much smaller than the confidence region relative curvature (95% conf. region), the

solution locus is approximately linear over the confidence region, and the parameter effects curvature (Max parameter effects) is below the critical value (95% conf. region), the estimates are said to have a "nearly" linear behaviour and the confidence regions are reliable (Wolfram, 1996). Otherwise, they just provide asymptotic approximations.

6.3. RESULTS AND DISCUSSION

6.3.1. L-ASCORBIC ACID DEGRADATION UNDER EXCESS OXYGEN

The results showed that the decrease of L-AA concentration with time follows a sigmoidal pattern (Figure 6.1). This pattern may also be noticed in some data reported in literature (Kebede et al., 1998, and Sakai et al., 1987). A number of sigmoidal models, such as the Logistic, Gompertz, Richards Morgan and Weibull models (Seber & Wild, 1989) were fitted to the data (results not shown) but while the fits to the individual experiments were very good for all the models tested, the kinetic parameters did not show a logical relation with temperature, varying very erratically, with the exception of the Weibull model.

Modelling L- AA degradation with the Weibull Model

Figure 6.1 shows typical examples of the fit of the Weibull model (Eq. 4.7) to the experimental data ($R^2_{adj} > 0.995$) (for further examples, see Figures E.1 and E.2,

Appendix E, where the individual and global fits of the Weibull model are depicted).

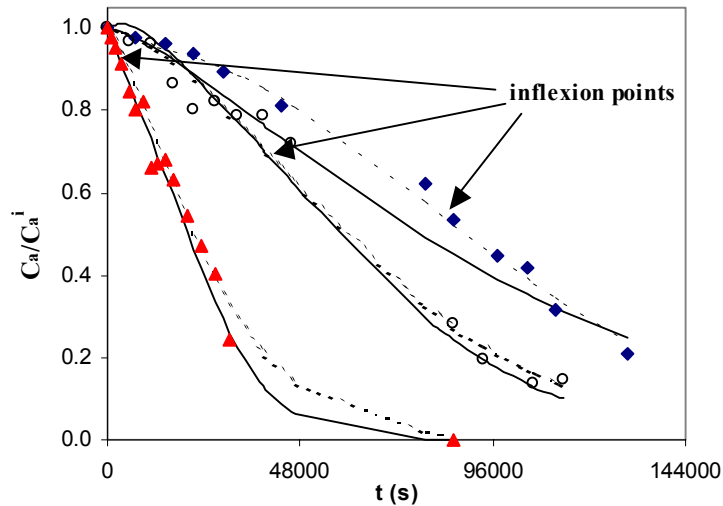


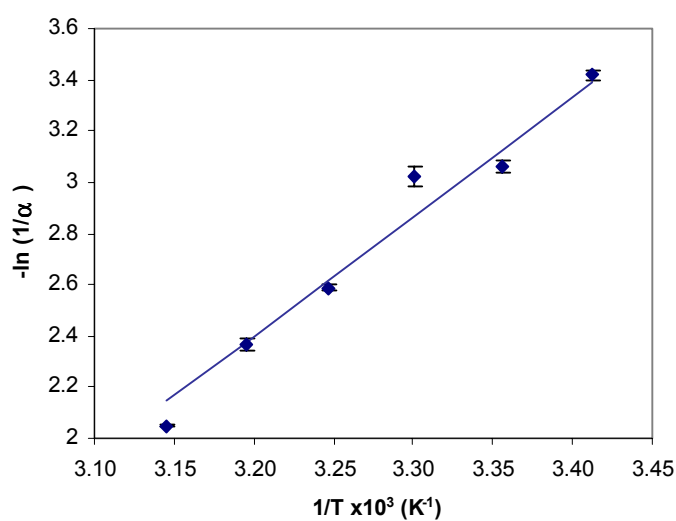
Figure 6.2- Fits of the Weibull model to L-ascorbic acid data at \blacklozenge 20, \circ 30 and \blacktriangle 45 °C. The dashed and the solid lines indicate, respectively, the individual and global fits.

The rate constant increased with temperature according to an Arrhenius-type relationship (Figure 6.3 a) whereas β appeared to decrease approximately linearly with temperature (see Figure 6.3 b), which shows that the degradation patterns differ with temperature.

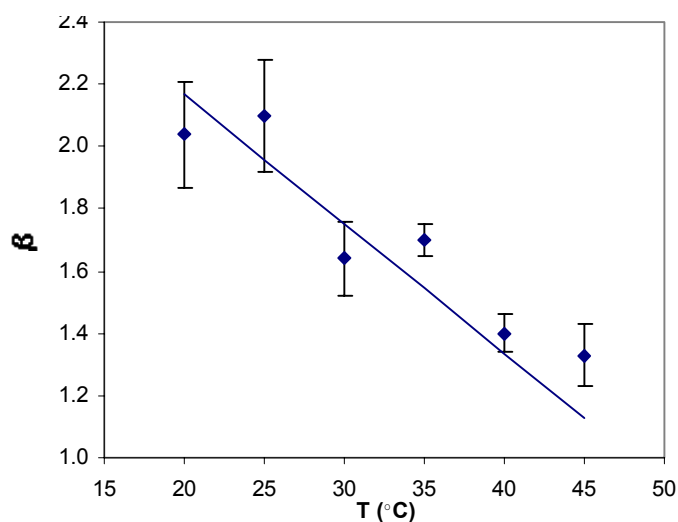
The said relationships of $1/\alpha$ and β with temperature were then incorporated in equation 1 to build a global model:

$$C_a = C_a^i \times e^{\left[\left(\frac{1}{\alpha} \right)_{ref} \times e^{-\frac{E_a}{R} \left(\frac{1}{273.15+T} - \frac{1}{273.15+T_{ref}} \right)} \right] \times t} \left. \right\}^{\beta_{ref} - m \times (T - T_{ref})} \quad (6.1)$$

where $(1/\alpha)_{\text{ref}}$ is the rate constant at a reference temperature T_{ref} , E_a is the activation energy regarding the dependence of the rate constant with temperature, β_{ref} is the shape constant at T_{ref} , m is the slope of the dependence of the shape constant on temperature and R is the universal gas constant.



(a)



(b)

Figure 6.3- Dependence of the Weibull model parameters on temperature, for ascorbic acid degradation: (a) rate constant ($1/\alpha$); (b) shape constant (β). The \blacklozenge symbols indicate the parameters obtained with individual fits and the line indicates the global fit.

The average temperature of the range tested, 32.5 °C, was chosen as the reference temperature. Equation 6.1 was fitted to the whole set of data and Table 6.1 shows the parameter estimates. This global fit had a high R^2_{adj} (0.995) and the collinearity between the model parameters was below 0.51, except between β_{ref} and m (coefficient of correlation 0.97). However, values below 0.99 are considered acceptable (Bates & Watts, 1988; Van Boeckel, 1996).

Further information on the quality of the fit is included in Appendix E (Figures E.3 a) and E.4 a) illustrate the quality of the global fit - good agreement between predicted and experimental data and lack of residual tendency for predicted values- for all the temperatures tested).

The location of the inflexion points of the degradation curves relates to the time, $t_{w_{\text{max}}}$, when the degradation rate is maximum w_{max} . At this time the first derivative, with respect to time (dC_a/dt), is zero, and one can obtain:

$$t_{w_{\text{max}}} = \alpha \left[\frac{(\beta - 1)}{\beta} \right]^{\frac{1}{\beta}} \quad (6.2)$$

$$w_{\text{max}} = -C_a^i \times \frac{\beta}{\alpha} \times e^{\left(-\frac{\beta-1}{\beta} \right)} \times \left(\frac{\beta-1}{\beta} \right)^{\left(\frac{\beta-1}{\beta} \right)} \quad (6.3)$$

These times decreased exponentially with temperature, as shown in Table 6.1 and correspond fairly well to those when the values of dehydroascorbic acid, browning and pH start to increase (Figure 6.4).

Table 6.1- Estimates of the parameters of the individual (Eq. 4.7) and global fitting (Eq. 6.1) of the Weibull model to L-AA data.

T (°C)	INDIVIDUAL FITTING			GLOBAL FITTING						
	$1/\alpha \times 10^6$ (s ⁻¹)	β	R ² _{adj.}	$1/\alpha_{ref} \times 10^6$ (s ⁻¹)	Ea (kJ/mol)	β_{ref}	m	R ² _{adj.}	$t_{w_{max}} \times 10^{-3}$ (s)	$w_{max} \times 10^3$ (mg/(l*s))
20	9.08 ± 0.2	2.04 ± 0.17	0.998	17.9 ± 0.3	39 ± 2	1.65 ± 0.35	-0.0415 ± 0.0071	0.996	80.3	2.61
25	13.0 ± 0.3	2.10 ± 0.18	0.998						56.9	3.61
30	13.6 ± 0.5	1.64 ± 0.12	0.995						39.2	4.58
35	20.9 ± 0.3	1.70 ± 0.05	0.999						25.2	5.33
40	26.1 ± 0.6	1.40 ± 0.06	0.998						13.7	5.92
45	35.8 ± 0.1	1.33 ± 0.10	0.997						4.3	7.83

T_{ref} = 32.5 °C

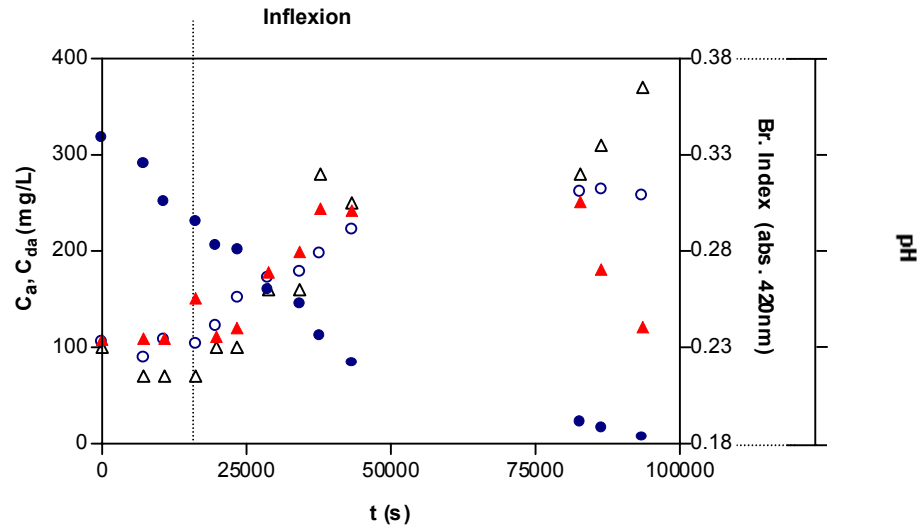


Figure 6.4- Evolution of experimental data of L-AA (●), DA (▲), browning (○) and pH (△) at 40 °C.

Before these times, the juice pH, dehydroascorbic acid concentration and browning index remained fairly constant, respectively, 3.7, 113 mg/L and 0.24 (absorbance at 420 nm). An example is shown in Figure 6.4, for dehydroascorbic acid, browning index and pH values at 40 °C.

It was possible to notice that for small conversions (experimental times ≤ 8 h, corresponding to conversions $<60\%$ at 45°C, $<30\%$ at 35°C and $<14\%$ at 20°C), the ascorbic acid degradation curves could be well described by first-order kinetics (Eq. 4.1), with the rate constant following an Arrhenius dependency on temperature (see Figure 6.5) ($R^2_{adj} > 0.999$, correlation coefficient < 0.845), as reported by several authors, and described in the previous Chapters:

$$C_a = C_a^i \times e^{-k_{ref} \times t} \times e^{-\frac{E_a}{R} \left(\frac{1}{273.15+T} - \frac{1}{273.15+T_{ref}} \right)} \quad (6.4)$$

where k_{ref} is the rate constant at a reference temperature $T_{\text{ref}} = 32.5 \text{ }^\circ\text{C}$ (for further examples, see Figures E.1 and E.2, Appendix E, where the individual and global fits of the first-order model are represented. Further information on the quality of the fit is included in Appendix E (Figures E.3 b) and E.4 b) illustrate the quality of the global fit - good agreement between predicted and experimental data and lack of tendency of the residual values- for all the temperatures tested).

The parameter estimates are presented in Table 6.2. The activation energy of the first-order model was almost twice that of the Weibull model owing to the change of degradation patterns with temperature, which in the later model is accounted for by the β constant. Both for the first-order and for the Weibull model, the analysis of the fit curvature (respectively, Table 6.2 and 6.1) shows that the confidence intervals calculated for the different parameters are reliable.

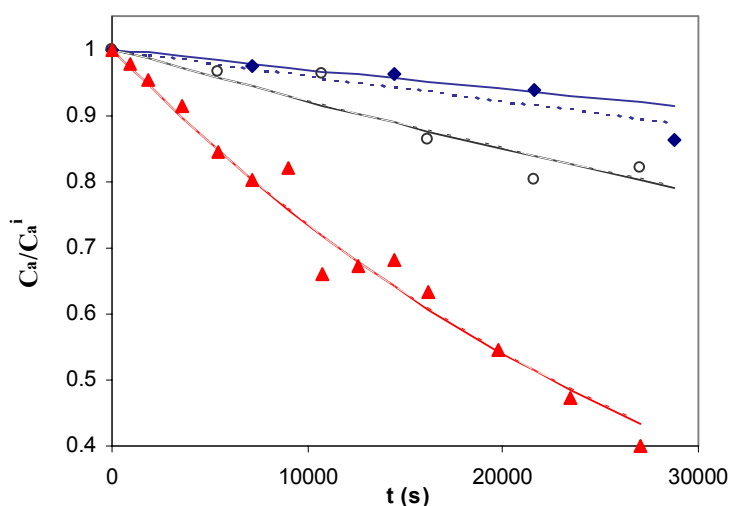


Figure 6.5- Fits of the first-order model to L-ascorbic acid data for times smaller than 8 hours at \blacklozenge 20, \circ 30 and \blacktriangle 45 $^\circ\text{C}$. The dashed and the solid lines indicate, respectively, the individual and global fits.

Table 6.2- Estimates of the parameters of the individual (Eq. 4.1) and global fitting (Eq. 6.4) of the first-order model to L-AA data.

T (°C)	INDIVIDUAL FITTING		GLOBAL FITTING		
	k x10 ⁶ (s ⁻¹)	R ² _{adj.}	k _{ref} x10 ⁶ (s ⁻¹)	Ea (kJ/mol)	R ² _{adj.}
20	4.0 ± 0.6	0.999	10.5 ± 0.5	71 ± 4	0.999
25	5.3 ± 0.9	0.999			
30	8.1 ± 0.8	0.999			
			FIT CURVATURE		
35	11.1 ± 1.2	0.998	Max Intrinsic	Max parameter effects	95% conf.region
40	21.1 ± 1.0	0.999	0.023	0.13	0.52
45	30.8 ± 1.0	0.999			

$$T_{\text{ref}} = 32.5 \text{ }^{\circ}\text{C}$$

Modelling L-AA and DA degradation with a Mechanistic Model

The inflexion points observed in the L-AA degradation curves suggest that the degradation kinetics might be reversible. Indeed, under aerobic conditions the ascorbic acid is degraded to dehydroascorbic acid, which in turn can be reconverted to ascorbic acid by mild reduction as well as hydrolysed into 2,3-diketogluconic acid (DKGA), which will lead to the formation of browning pigments (Tannenbaum *et al.*, 1985):



As at the inflexion time dehydroascorbic acid, browning and pH increase, one may infer that at this time the rate of reversion of dehydroascorbic acid to ascorbic acid lowers considerably. This might be explained by a dependence of the reversion of dehydroascorbic acid into ascorbic acid on the concentration

of the latter component. In this case, the differential equations relating the changes of ascorbic acid and dehydroascorbic acid (C_{da}) with time might be written as:

$$\frac{dC_a}{dt} = -k_1 C_a + k_2 C_a C_{da} \quad (6.6)$$

$$\frac{dC_{da}}{dt} = k_1 C_a - k_2 C_a C_{da} - k_3 C_{da} \quad (6.7)$$

where k_1 , k_2 and k_3 are the rate constants of, respectively, the degradation of L-AA, the reversion of dehydroascorbic acid and the degradation of dehydroascorbic acid.

It was however found that these equations were not able to describe the sudden increase on dehydroascorbic acid concentration, and thus they were slightly altered by making the reversion of dehydroascorbic acid a second order reaction in relation to ascorbic acid concentration. Equations 6.6 and 6.7 thus become:

$$\frac{dC_a}{dt} = -k_1 C_a + k_2 C_a^2 C_{da} \quad (6.8)$$

$$\frac{dC_{da}}{dt} = k_1 C_a - k_2 C_a^2 C_{da} - k_3 C_{da} \quad (6.9)$$

A multivariate analysis was performed fitting Equation 6.8 and 6.9 to L-ascorbic acid and dehydroascorbic acid data. The fits were fairly good and the rate constants also increased with temperature according to an Arrhenius-type equation:

$$\begin{aligned} \frac{dC_a}{dt} = & -k_{1ref} \times e^{-\frac{Ea1}{R} \left(\frac{1}{273.15+T} - \frac{1}{273.15+T_{ref}} \right)} \times C_a + \\ & + k_{2ref} \times e^{-\frac{Ea2}{R} \left(\frac{1}{273.15+T} - \frac{1}{273.15+T_{ref}} \right)} \times C_a^2 \times C_{da} \end{aligned} \quad (6.10)$$

$$\begin{aligned} \frac{dC_{da}}{dt} = & k_{1ref} \times e^{-\frac{Ea1}{R} \left(\frac{1}{273.15+T} - \frac{1}{273.15+T_{ref}} \right)} \times C_a - k_{2ref} \times e^{-\frac{Ea2}{R} \left(\frac{1}{273.15+T} - \frac{1}{273.15+T_{ref}} \right)} \times \\ & \times C_a^2 \times C_{da} - k_{3ref} \times e^{-\frac{Ea3}{R} \left(\frac{1}{273.15+T} - \frac{1}{273.15+T_{ref}} \right)} \times C_{da} \end{aligned} \quad (6.11)$$

where k_{1ref} , k_{2ref} and k_{3ref} are the rate constants at T_{ref} of, respectively, the degradation of L-AA, the reconversion of dehydroascorbic acid and the degradation of dehydroascorbic acid and Ea_1 , Ea_2 and Ea_3 are the corresponding activation energy values.

The estimates of the model parameters, obtained by global fitting of Equations 6.10 and 6.11 to the whole set of L-AA and DA data are summarised in Table 6.3. Figure 6.6 shows examples of the global fit for L-AA and DA data. The estimates of all parameters were statistically different from zero.

Further examples can be viewed in Appendix E, Figures E.1 and E.2 for the individual and global model fits to L-AA. Further information on the quality of the fit is included in Appendix E (Figures E.5 and E.6 illustrate the good quality of the global fit, for all the temperatures tested).

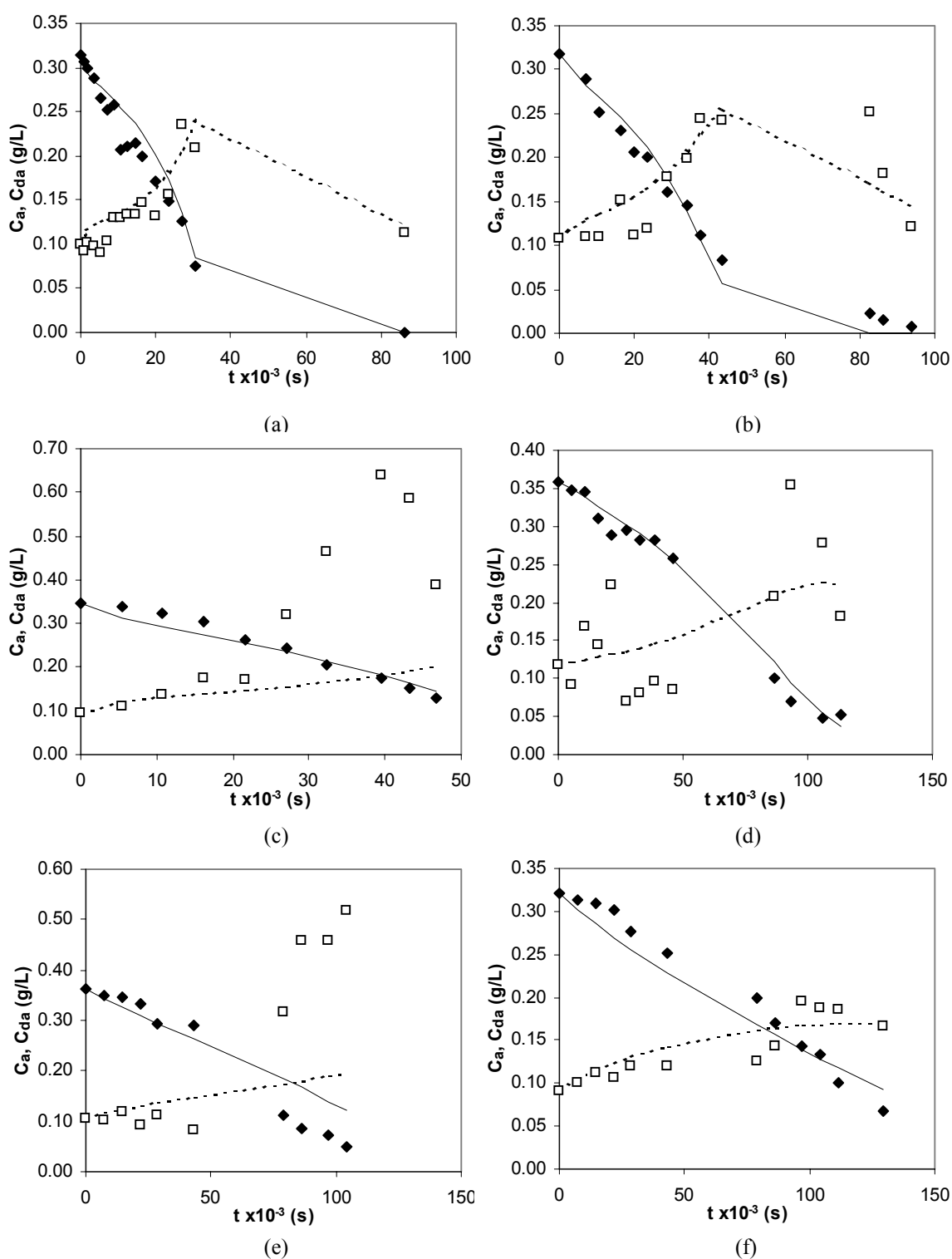


Figure 6.6- Fits of the mechanistic model to (\blacklozenge) L-ascorbic acid (C_a) and (\square) dehydroascorbic acid (C_{da}) data at (a) 45, (b) 40, (c) 35, (d) 30, (e) 25 and (f) 20 °C. The dashed and the solid lines indicate, respectively, the global fit to C_{da} and C_a .

The degradation kinetics of dehydroascorbic acid showed a much smaller sensitivity to temperature than the degradation kinetics of ascorbic acid and the reconversion of dehydroascorbic acid to ascorbic acid. The rate constant of this reaction was also much smaller.

Although this may be considered a mechanistic model, one should however take into consideration that there is no real evidence that the dehydroascorbic acid degradation follows a second order kinetics in relation to ascorbic acid concentration, and as such this model also relies on empiricism to a great extent. Furthermore, the parameter estimates of this model show a large confidence interval, in some cases of the order of magnitude of the estimates themselves, which is due to the inability of the model to separate the influence of the different reactions on the concentration changes. The Weibull model, although lacking any theoretical basis, provides good fits and a much better statistical significance. The changes of the shape constant (β) on temperature might be explained by the different sensitivity of the three reactions to temperature.

Table 6.3- Estimates of the parameters of the global fit of the mechanistic model (Eq. 6.10 and 6.11) to L-ascorbic acid and dehydroascorbic acid data.

Parameter	Estimate	95% Confidence Interval
$k_{1\text{ref}} \times 10^6 \text{ (s}^{-1}\text{)}$	93 ± 19	54 to 132
$k_{2\text{ref}} \times 10^6 \text{ (s}^{-1}\text{)}$	2100 ± 539	1011 to 3184
$k_{3\text{ref}} \times 10^6 \text{ (s}^{-1}\text{)}$	12 ± 1	10 to 15
$Ea_1 \text{ (kJ/mol)}$	94 ± 11	71 to 117
$Ea_2 \text{ (kJ/mol)}$	107 ± 13	81 to 133
$Ea_3 \text{ (kJ/mol)}$	27 ± 9	8 to 45

$T_{\text{ref}} = 32.5 \text{ }^\circ\text{C}$

The proposed mechanistic model was tentatively applied to the data reported in Chapter 5, taking into consideration the effect of oxygen concentration on the reaction kinetics, by assuming the L-AA degradation to be first-order in relation to L-AA and either first or second-order in relation to oxygen (data not shown). Although the prediction errors were relatively small, the model predictions were clearly biased, showing that this model cannot be applied in normal storage conditions.

6.3.2. BROWNING UNDER EXCESS OXYGEN

In the conditions tested in this work browning was much faster and could be measured to greater levels than in Chapters 4 and 5. The results showed that as time increases browning kinetics deviate from a zero-order, as might be expected. It was found that this pattern might also be adequately described by the Weibull model adapted to growth kinetics and considering that browning levels off at an equilibrium value,

$$\frac{C_{Br} - C_{Br}^{\infty}}{C_{Br}^i - C_{Br}^{\infty}} = 1 - e^{-\left[\left(\frac{t}{\alpha}\right)^{\beta}\right]} \quad (6.12)$$

Figure 6.7 shows the fits for some of the temperatures tested. Further examples can be viewed in Appendix E, Figure E.7 with the individual and global model fits, and Figure E.8 illustrate the quality of the global fit, good relation between predicted and observed values and lack of residual value tendency, for all the temperatures tested ($0.992 < R^2_{adj} < 0.999$).

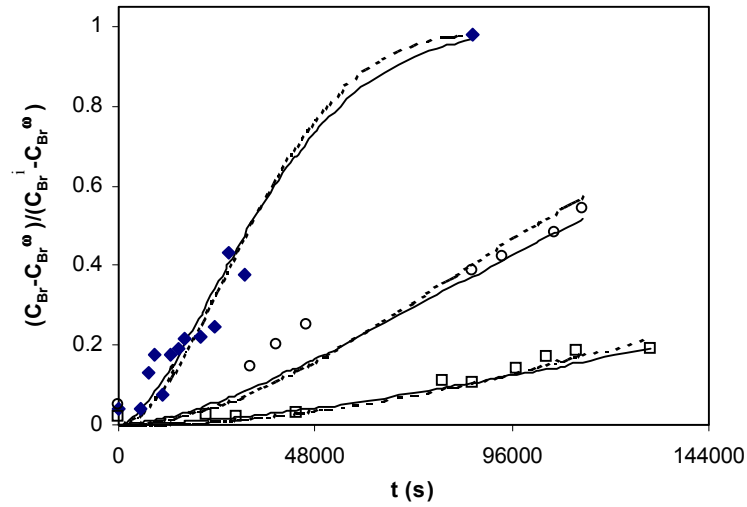


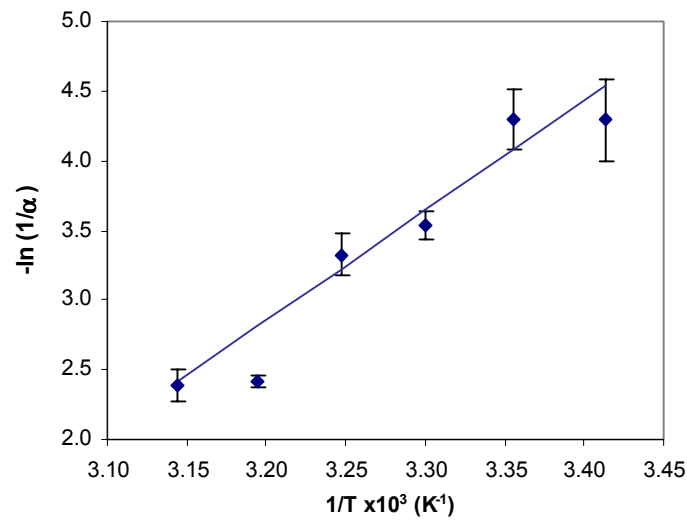
Figure 6.7- Fit of the Weibull model to browning index data at (□) 20, (○) 30 and (◆) 45 °C. The dashed line indicates the individual fit and the solid line the global fit.

The rate constant ($1/\alpha$) increased with temperature according to an Arrhenius-type equation (Figure 6.8 a), whereas the equilibrium concentration and the β parameter were temperature independent (Figure 6.8 b):

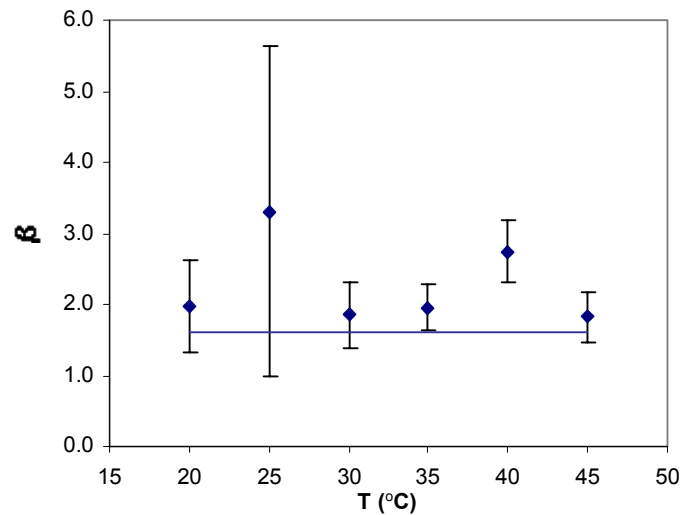
$$\frac{C_{Br} - C_{Br}^{\infty}}{C_{Br}^i - C_{Br}^{\infty}} = 1 - e^{-\left[\left(\frac{1}{\alpha} \right)_{ref} \times e^{-\frac{E_a}{R} \left(\frac{1}{273.15+T} - \frac{1}{273.15+T_{ref}} \right)} \right]^{\beta}} \quad (6.13)$$

The estimates of this model parameters, obtained by the global fitting of Equation 6.13 to the whole set of data, are summarised in Table 6.4. The fit had a very high R^2_{adj} (0.999) and the correlation between parameters was generally low (correlation coefficient < 0.89). The activation energy value is in the range of others reported in literature for the cases of zero (e.g. Saguy *et al.* (1978), Stamp & Labuza (1983), Cohen *et al.* (1994) reported, respectively, values of 62.7, 92,

and 89 kJ/mol) or first-order kinetics (e.g. Toribio & Lozano (1986) reported a value of 105 kJ/mol). The lack of dependence of the β parameter on temperature agrees with the earlier finding that, when modelling browning with zero-order kinetics, the activation energy does not change with temperature.



(a)



(b)

Figure 6.8- Dependence of the Weibull model constants on temperature, for browning index (a) rate constant; (b) shape constant. The \blacklozenge symbols represent parameters estimated with each individual fit and the line indicates the global fit.

Table 6.4- Estimates of the parameters of the individual (Eq. 6.12) and global fitting (Eq. 6.13) of the Weibull model to browning data, as well as the maximum growth rate and the time at which it occurs, calculated based on the global fitting parameters.

T (°C)	INDIVIDUAL FITTING			GLOBAL FITTING						
	$1/\alpha \times 10^6$ (s ⁻¹)	β	R ² _{adj.}	$(1/\alpha)_{\text{ref}} \times 10^6$ (s ⁻¹)	E _a (kJ/mol)	β	C [∞] (mg/L)	R ² _{adj.}	$t_{w_{\text{max}}} \times 10^{-3}$ (s)	$w_{\text{max}} \times 10^6$ (s ⁻¹)
20	3.8 ± 1.1	2.0 ± 0.6	0.993	8.9 ± 0.9	66 ± 3	1.6 ± 0.1	0.328 ± 0.007	0.999	185.04	0.44
25	6.0 ± 1.3	3.3 ± 2.2	0.998						117.36	0.64
30	8.1 ± 0.8	1.9 ± 0.5	0.989						75.96	1.22
				FIT CURVATURE						
				Max Intrinsic	Max parameter effects	95% conf. region				
35	10.1 ± 1.5	2.0 ± 0.3	0.999	0.20	1.06	0.63			49.68	1.69
40	24.7 ± 1.0	2.7 ± 0.4	0.992						32.76	2.97
45	25.6 ± 3.1	1.8 ± 0.4	0.993						31.96	4.58

T_{ref} = 32.5 °C

The maximum relative intrinsic curvature and the parameter-effects curvature were greater than the confidence region relative curvature (Table 6.4), showing that in this case the confidence intervals can only be considered as asymptotic approximations, what may be due to the fact that the model was applied in concentration ranges quite below equilibrium. The maximum browning rates also occurred at times that decreased exponentially with temperature, their values being approximately twice of those for ascorbic acid degradation (Table 6.4 and 6.1, respectively).

6.3.3. L-AA DEGRADATION IN ANAEROBIC CONDITIONS

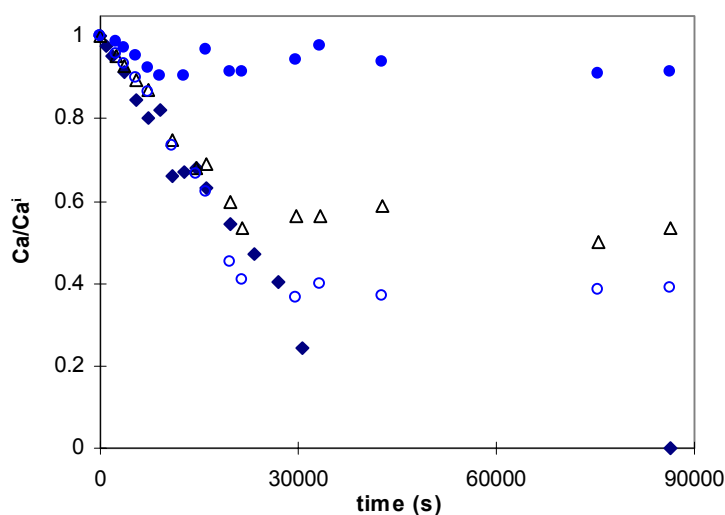


Figure 6.9- Effect of replacing aeration by N_2 flushing on L-AA degradation ($T=45\text{ }^\circ\text{C}$): (●) after 2 hours, (Δ) after 4 hours (\circ) after 6 hours and (\blacklozenge) control (continuous aeration).

Figure 6.9 shows that when the flow of air (oxygen) is stopped and the oxygen is removed from the juice matrix (substituting this flux of air by nitrogen) L-AA degradation comes to an halt, independently of the level of L-AA retention at that time. This suggests that the residual oxygen plays a major role in L-AA degradation in storage conditions referred to as anaerobic in earlier Chapters.

6.4. CONCLUSIONS

The Weibull model provided a good description of the kinetics of degradation of ascorbic acid in the range of temperatures and conversions tested under excess oxygen. A first-order model could also be applied to the data satisfactorily, but only for lower conversions (experimental times up to 8 hours) as for greater conversions degradation curves show a sigmoidal pattern. The inflexion points of L-AA degradation curves roughly coincided with the time when the concentration of dehydroascorbic acid starts to increase, together with the pH and the browning index. The temperature dependency of the rate constants was well described by the Arrhenius law. The shape constant of the Weibull model was temperature independent for browning kinetics but decreased with temperature for ascorbic acid degradation. The later observation shows that the pattern of L-AA degradation is temperature dependent. This might be explained by (i) the reconversion of DA into L-AA, following first-order kinetics in relation to DA and second order kinetics in relation to L-AA, and by (ii) different sensitivities of the different reactions rate constants to temperature. Browning was also well

described by the Weibull model levelling off at an equilibrium value, and appears to follow a single reactive pathway in the range of temperatures tested.

In absence of oxygen L-AA does not degrade, which highlights the importance of the residual oxygen for L-AA degradation under storage conditions referred to as anaerobic in earlier Chapters.

CHAPTER 7

Effect of ascorbic acid addition on L-ascorbic acid degradation and browning under excess oxygen conditions

Chapter 5 analyses the effect of added L-AA on L-AA degradation and browning during storage of pasteurised orange juice. Chapter 6 reports the mathematical modelling of the same quality indicators under aerobic conditions. In the later chapter a mechanistic model was proposed for L-AA degradation, that might be able to describe the stabilizing effect of L-AA addition, as it assumes that reconversion of DA to L-AA depends on L-AA concentration. This Chapter builds on Chapters 5 and 6, aiming at studying the effect of added L-AA under aerobic conditions, and particularly at assessing the applicability of the said mechanistic model in these conditions.

Single strength orange juice with different added ascorbic acid (L-AA) contents (J=100, K=200, L=300, M=400, and N=500 mg/L) was protected from light, continuously aerated for up to 48 hours and monitored for L-ascorbic acid, dehydroascorbic acid, oxygen, pH, and browning. Experiments were conducted at 20, 25, 30, 35, 40, and 45 °C.

The mechanistic model developed in the previous chapter was found to describe fairly well L-AA and DA degradation in the whole range of conditions tested. Some of the estimates of the model parameters were significantly different from

those reported in the previous Chapter, probably owing to a high correlation between those parameters.

The Weibull model was also found to fit the L-AA data fairly well, but the dependence of the model parameters on temperature and added L-AA was more complex than observed in previous Chapters, the model requiring a larger number of parameters when compared to the mechanistic model.

Browning was described by the zero-order model, with an activation energy linearly dependent on added L-AA content, while the rate constant at the reference temperature showed to be constant.

7.1. INTRODUCTION

Several authors presented possible pathway schemes for ascorbic acid degradation. The schemes for anaerobic degradation are speculative while the aerobic mechanisms are better understood. Most of the studies were conducted in model systems at low pH (Tannenbaum *et al.*, 1985) and because of that the degradation mechanisms may differ from those in a particular food product containing ascorbic acid. In addition, most of the models reported in literature were developed based on data gathered during short periods and/or under varying oxygen concentration, as the depleted oxygen was not replaced during storage. Very little information regarding the influence and modelling of the aerobic ascorbic acid degradation with added ascorbic acid is given in literature and even

less on orange juice. Because ascorbic acid is an important indicator of orange juice quality and its degradation may be the critical factor for orange juice shelf-life it is important to check if that may be overcome by addition of ascorbic acid even under aerobic conditions. On the other hand nonenzymatic browning is one of the main reasons for the loss of commercial value in citrus products as it is the first visible quality defect to be detected at ambient temperature storage. As browning is related to ascorbic acid degradation (among other compounds) it would be very important to see how the addition of ascorbic acid would influence the formation kinetics of brown pigments under aerobic conditions.

The objectives of this study were to study L-ascorbic acid aerobic degradation as well as dehydroascorbic acid kinetics and browning in orange juice with added ascorbic acid, in a range of temperatures and to develop mathematical models that may be used for predictive purposes. The influence of continuous deaeration was also studied.

7.2. MATERIAL AND METHODS

7.2.1. EXPERIMENTAL DESIGN

Single strength orange juice (Minute Maid™ premium) from the same batch as the juice used for the two previous studies was used for this experimental work. The procedure used in the previous Chapter (§6.2.1) was adopted for this study. The only difference lays on the addition of L-AA to the juice. After the juice

temperature reached the bath temperature different amounts of L-AA were added (J=100, K=200, L=300, M=400, N=500 mg/L), aeration was switched on and the juice was continuously aerated for up to 48 hours. The experimental data is displayed in Table F.1, Appendix F.

Additional experiments were carried out with continuous N₂ flushing, as explained in the previous Chapter. Two levels of addition of L-AA were tested in this set of experiments: I= 0 and N= 500 mg/L. The experimental data is included in Table F.2, Appendix F.

Oxygen content was maintained fairly constant throughout the experiments, ranging from 4.22 to 5.93 ppm, depending on the batch and temperature, and pH values showed a slight increase from 3.66 to 3.77 (Figure F.30 and F.31, Appendix F).

7.2.2. ANALYTICAL DETERMINATIONS

Analytical determination procedures are described in §5.2.2.

7.2.3. DATA ANALYSIS

As described in §6.2.3.

7.3. RESULTS AND DISCUSSION

7.3.1. L-ASCORBIC ACID DEGRADATION UNDER EXCESS OXYGEN

Modelling L-AA and DA degradation with the Mechanistic Model

A multivariate analysis was performed fitting Equations 6.10 and 6.11 to L-ascorbic acid and dehydroascorbic acid data, separately for each batch. It was observed that the rate constants and activation energies were not significantly different between batches with added L-AA content. The batch with no addition of L-AA presented greater values for the reaction rate estimates of reaction 1 and 2, which were statistically different from the other five batches, as can be seen in Figure 7.1. This may however be due to a high correlation between these parameters, as different combinations of parameters yielded similar results in terms of prediction of both L-AA and DA degradation.

Thus, it was assumed that L-AA addition would not affect the model constants and Equations 6.10 and 6.11 were used to perform a global fit simultaneously to all six batches. The residuals were normally distributed (Shapiro-Wilk test) and the estimates of the parameters were statistically different from zero (with the exception of the activation energy of the third reaction), but it was observed that the fit for L-AA was poor for the longer experimental times. Another aspect to take into consideration is that the experimental error in the determination of DA is considerably larger than that of L-AA data. This is clear in Figure 7.2 and is reflected in the variance of the residuals of DA, that is approximately 3 times that of L-AA (Figure F.1c, Appendix F).

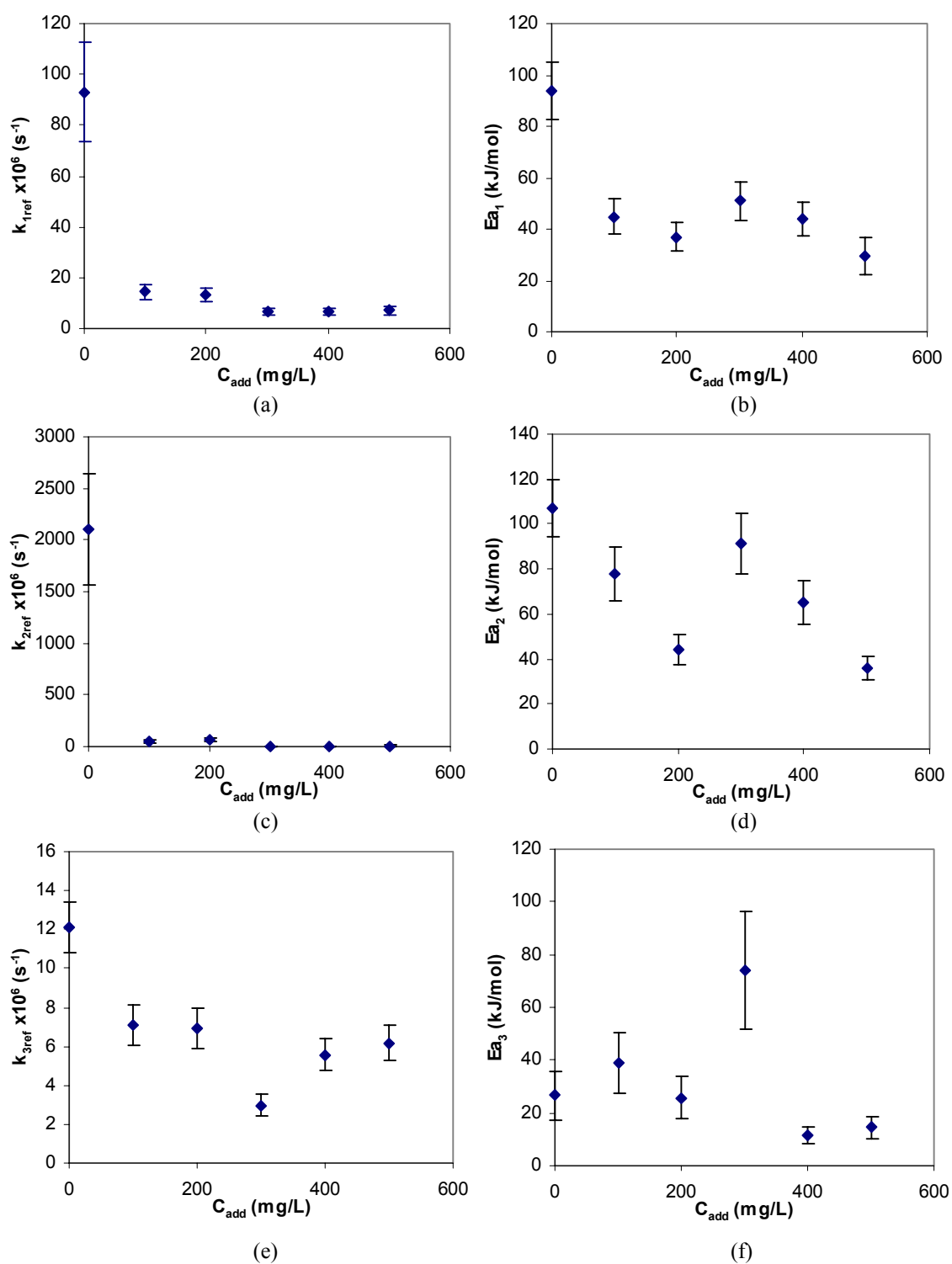


Figure 7.1- Dependence of the parameter estimates, reaction rate at the reference temperature and activation energy, of Eq. 6.10 and 6.11 on added L-AA content (C_{add}).

Another fit was then performed, using weighted regression (the DA residuals were divided by 3, in order to achieve a variance of the residual values of the same order of magnitude for both L-AA and DA), and a logarithmic transformation was applied for L-AA data (in order to give a relatively higher importance to data at longer times/lower values of concentration). The estimates of the model parameters, thus obtained are summarised in Table 7.1. Figure 7.2 shows examples of this global fit for L-AA and DA data. Further examples can be analysed in Figures F.3 to F.8 (Appendix F).

Table 7.1- Estimates of the parameters of the global fit of the mechanistic model (Eq. 6.10 and 6.11) to L-ascorbic acid and dehydroascorbic acid data.

Parameter	Estimate	95% Confidence Interval
$k_{1\text{ref}} \times 10^6 \text{ (s}^{-1}\text{)}$	13.8 ± 0.4	13 to 15
$k_{2\text{ref}} \times 10^6 \text{ (s}^{-1}\text{)}$	45 ± 3	39 to 52
$k_{3\text{ref}} \times 10^6 \text{ (s}^{-1}\text{)}$	7.0 ± 0.7	6 to 8
$Ea_1 \text{ (kJ/mol)}$	53 ± 3	47 to 59
$Ea_2 \text{ (kJ/mol)}$	78 ± 8	62 to 95
$Ea_3 \text{ (kJ/mol)}$	48 ± 10	27 to 68

($T_{\text{ref}}=32.5 \text{ }^\circ\text{C}$)

The residuals showed to be normally distributed (Shapiro-Wilk test), and the “runs test” (Cromwell *et al.*, 1994) showed that there is no autocorrelation for DA residuals, although the residuals of L-AA were slightly auto-correlated. Further information on the quality of the global fit is included in Appendix F (Figure F.9 and F.10 illustrate the quality of the global fit - good agreement between predicted

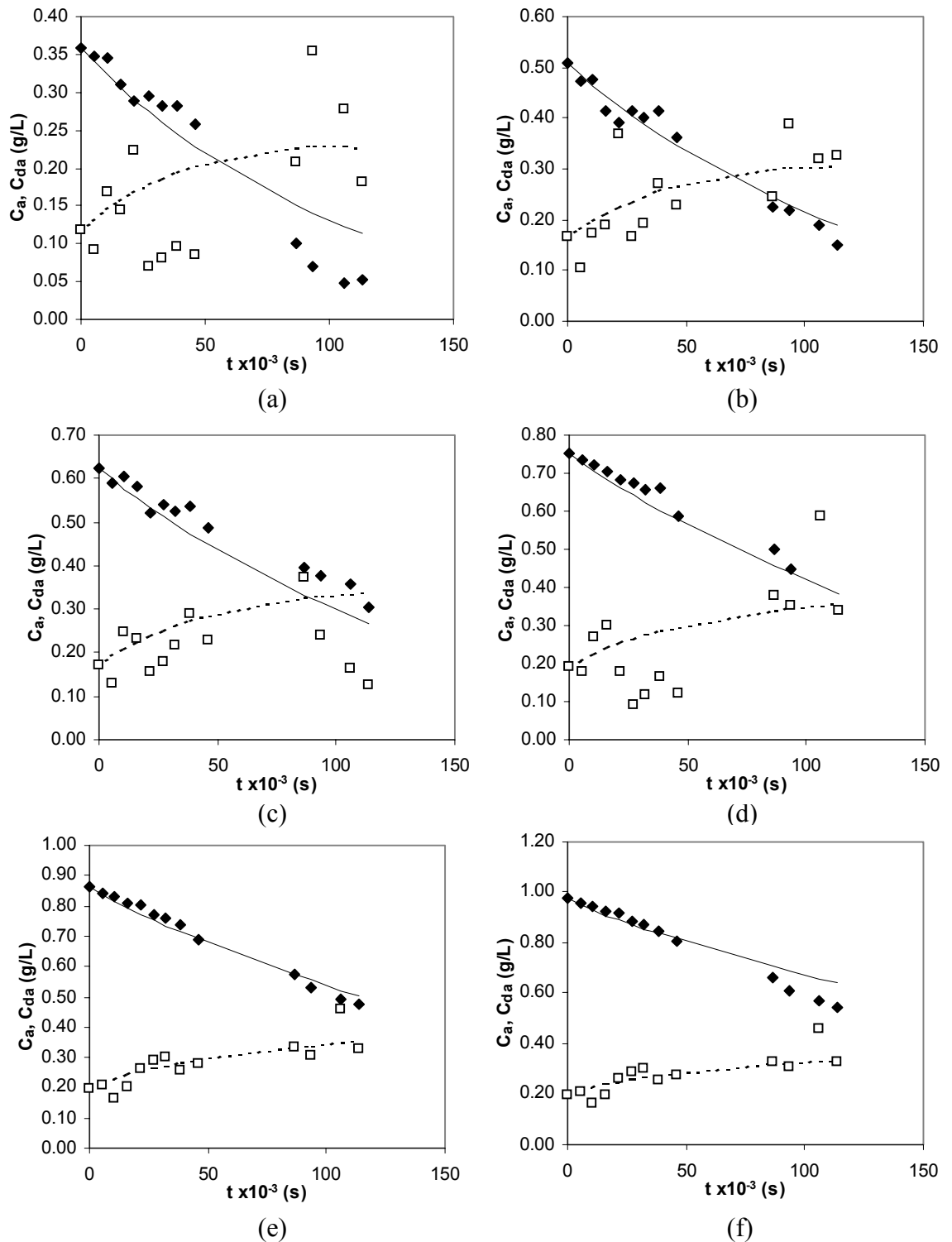


Figure 7.2- Fit of the mechanistic model to (\blacklozenge) L-ascorbic acid (C_a) and (\square) dehydroascorbic acid data (C_{da}) at 30 °C, for (a) batch I (no added L-AA), (b) batch J (100 mg/L), (c) batch K (200 mg/L), (d) batch L (300 mg/L), (e) batch M (400 mg/L) and (f) batch N (500 mg/L). The dashed and the solid lines indicate, respectively, the global fit to C_{da} and C_a .

and experimental data and lack of residual tendency for predicted values- for all the batches and temperatures tested).

Modelling L-AA degradation with the Weibull Model

The sigmoidal pattern observed for L-AA data in the previous Chapter was also evident in the results gathered in this work (Figure 7.3). The Weibull model (Eq. 4.7) was then used to model the degradation of L-ascorbic acid and was found to fit well the data. Figure 7.3 shows typical examples of the fit ($R^2_{adj} > 0.998$) (for further examples, see Figures F.16 to F.20, Appendix F).

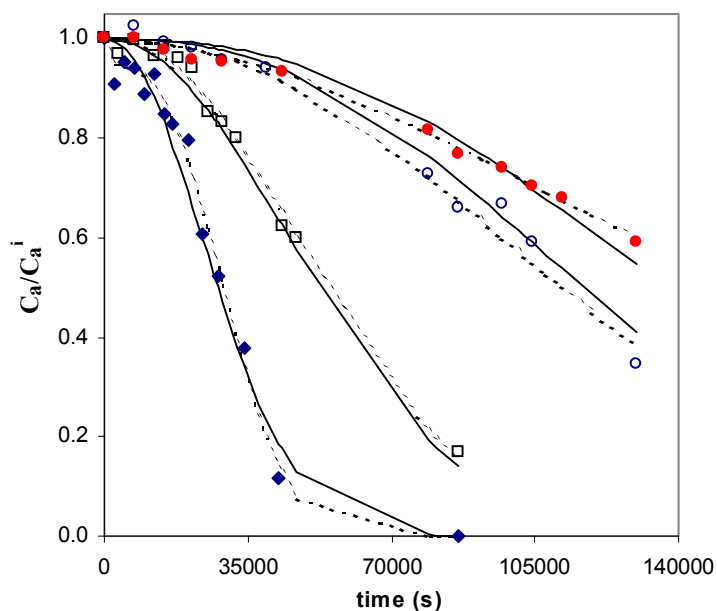


Figure 7.3- Fit of the Weibull model to ascorbic acid data at (◆) 45°C - Batch J (100 mg/L), (□) 45°C -N (500 mg/L), (○) 20°C -J (100 mg/L) and (●) 20°C -N (500 mg/L). The dashed and solid lines indicate, respectively, the individual and the global fit of the Weibull model.

The dependence of the model parameters on temperature and added L-ascorbic acid concentration was more complex than that observed in previous Chapters. The scale constant (α) decreased exponentially with temperature rather than following an Arrhenius-type relationship:

$$\alpha = \alpha^i + (\alpha^\infty - \alpha^i) \times (1 - e^{-\gamma \times (45 - T)}) \quad (7.1)$$

where α^i and α^∞ are the scale constants at the highest (initial) and lowest (final) temperature (T) and γ is the constant of the dependence on temperature.

The scale parameter at the highest temperature (α^i) showed to increase linearly with added L-AA content, and the same was verified for the constant γ :

$$\alpha^i = \alpha|_{T=45} + m \times C_{add} \quad (7.2)$$

$$\gamma = a_\gamma + b_\gamma \times C_{add} \quad (7.3)$$

where $\alpha|_{T=45}$ is the value of the scale parameter at 45 °C, a_γ is the value of the constant γ for juice with no added L-AA, and m and b_γ are, respectively, the slopes of the linear dependence of the scale parameter at the highest temperature and of the constant γ with added L-AA content (C_{add}). The dependence of the scale constant on temperature and added L-AA is illustrated in Figure 7.4a).

The shape parameter, β , showed to have a minimum around 35 °C and was not dependent on the amount of added L-AA, as can be seen in Figure 7.4b). Its dependence on temperature can be described as:

$$\beta = \beta_a + \beta_b \times (T - T_{ref}) + \beta_c \times (T - T_{ref})^2 \quad (7.4)$$

With these Equations, a global fit could then be applied, yielding:

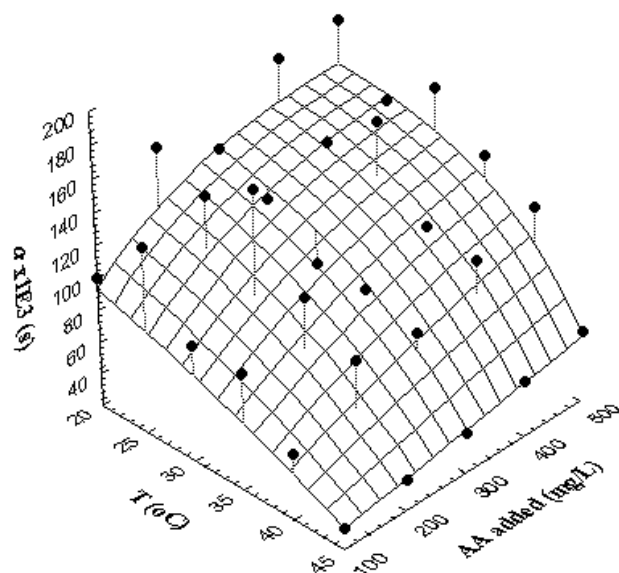
$$C_a = C_a^i \times e \left\{ \left[\frac{1}{(\alpha|_{T=45} + m \times C_{add}) + [\alpha^\infty - (\alpha|_{T=45} + m \times C_{add})]} \right] \times \left[\frac{1}{1 - e^{-(a_\gamma + b_\gamma \times C_{add}) \times (45 - T)}} \right] \right\}^{\beta_a + \beta_b \times (T - T_{ref}) + \beta_c \times (T - T_{ref})^2} \quad (7.5)$$

Equation 7.5 yielded a good fit to the whole set of data as can be seen in Figure 7.3. Further examples of the global fit are depicted in Figures F.11 to F.15 (Appendix F). The parameter estimates are summarised in Table 7.2. This global fit had a high R^2_{adj} (0.998) and the collinearity between the model parameters was below 0.855. Further information on the quality of the fit is included in Appendix F (Figure F.21 illustrates the quality of the global fit (agreement between predicted and experimental data, the lack of residual tendency for the predicted values, and the frequency distribution of the residuals), for all the batches and temperatures tested).

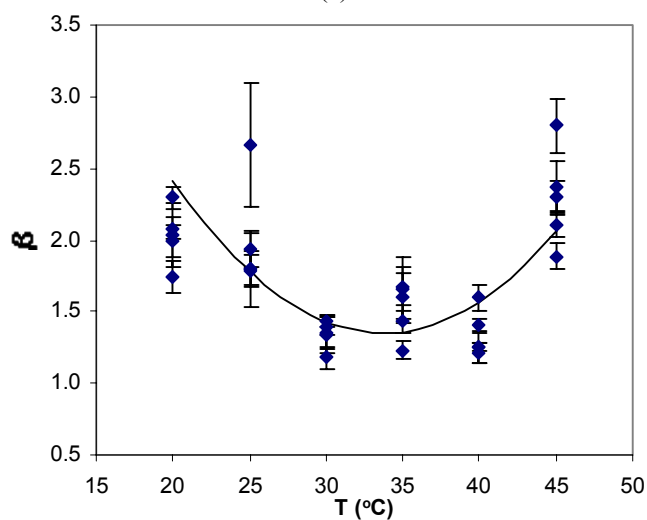
Table 7.2- Estimates of the parameters of the individual (Eq. 4.7) and global fitting (Eq. 7.5) of the Weibull model to L-AA data.

INDIVIDUAL FITTING																
T (°C)	Batch J (100 mg/L)			Batch K (200 mg/L)			Batch L (300 mg/L)			Batch M (400 mg/L)			Batch N (500 mg/L)			
	$\alpha \times 10^3$ (s)	β	$R^2_{adj.}$	$\alpha \times 10^3$ (s)	β	$R^2_{adj.}$	$\alpha \times 10^3$ (s)	β	$R^2_{adj.}$	$\alpha \times 10^3$ (s)	β	$R^2_{adj.}$	$\alpha \times 10^3$ (s)	β	$R^2_{adj.}$	
20	133±5	2.1±0.2	0.998	160±5	1.7±0.1	0.999	161±2	2.30±0.08	1	177±4	2.08±0.08	1	183±6	2.0±0.1	0.999	
25	136±3	1.8±0.1	0.999	146±11	1.8±0.3	0.994	124±6	2.7±0.4	0.998	140±3	1.9±0.1	0.999	147±4	1.8±0.1	0.998	
30	108±5	1.4±0.1	0.996	165±12	1.3±0.1	0.998	171±2	1.18±0.08	0.989	167±5	1.40±0.06	0.999	169±4	1.43±0.04	0.999	
35	92±4	1.6±0.2	0.992	117±6	1.6±0.2	0.989	100±2	1.43±0.07	0.998	118±4	1.7±0.1	0.998	143±6	1.23±0.07	0.999	
40	61±2	1.6±0.1	0.997	96±5	1.2±0.1	0.997	90±4	1.21±0.07	0.998	113±2	1.23±0.03	0.999	126±3	1.41±0.04	0.999	
45	33.7±0.7	2.8±0.2	0.999	39.9±0.7	2.3±0.1	0.999	15±1	2.4±0.2	0.997	55±1	1.89±0.09	0.999	64±1	2.11±0.09	0.999	
GLOBAL FITTING																
$\alpha _{T=45} \times 10^3$ (s)	$m \times 10^5$ (s.L/mg)	$\alpha^\infty \times 10^3$ (s)	$a_\gamma \times 10^3$ (°C ⁻¹)	$b_\gamma \times 10^4$ (L/(°C.mg))	β_a	β_b (°C ⁻¹)	$\beta_c \times 10^3$ (°C ⁻²)	$R^2_{adj.}$								
25.8±1.4	7.3±0.5	162±4	4.3±0.5	2.1±0.3	0.95±0.02	-0.025±0.004	5.7±0.4	0.998								

$T_{ref}=32.5$ °C



(a)



(b)

Figure 7.4- Dependence of the Weibull model parameters on temperature for L-ascorbic acid degradation: (a) scale constant (α); (b) shape constant (β). Symbols \bullet and \blacklozenge represent parameters estimated with individual fits and the line and/or surface these estimated with the global fit.

Modelling L-AA degradation for low conversions

A earlier reported in Chapter 6 (§6.3.1), it was observed that for relatively low conversions, corresponding to times smaller than 8 hours, the ascorbic acid degradation curves could be well described by first-order kinetics (Eq. 4.1). The fits for some of the temperatures and batches tested can be seen in Figure 7.5. Further examples are presented in Figures F.16 to F.20 (Appendix F).

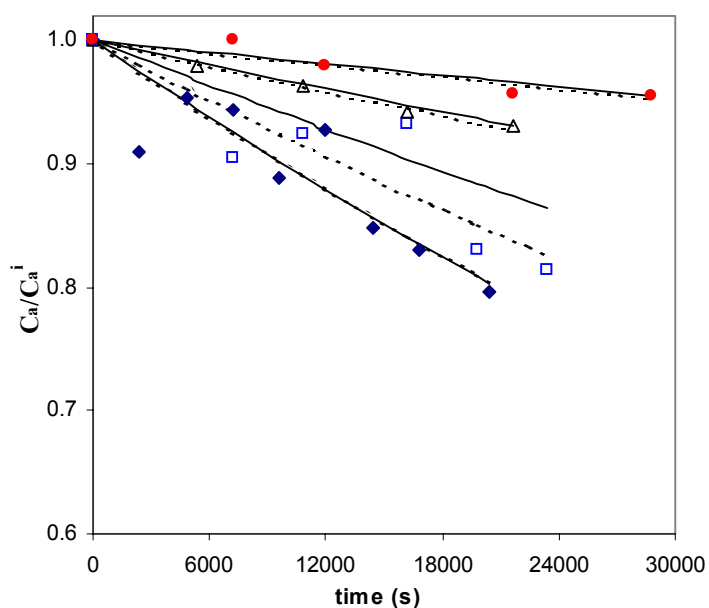


Figure 7.5- Fit of the first-order model to L-ascorbic acid data for times smaller than 8 hours: (◆) 45°C - Batch J (100 mg/L), (□) 40°C -L (300 mg/L), (△) 30°C -M (400 mg/L) and (●) 20°C -N (500 mg/L). The dashed and solid lines indicate, respectively, the individual and the global fit.

For these low conversions, the rate constant followed an Arrhenius type dependency on temperature, and the rate constant at a reference temperature of 32.5 °C showed to decrease linearly with added L-AA content (see Figure 7.6):

$$C_a = C_a^i \times e \left[(a_k - b_k \times C_{add}) \times e^{-\frac{E_a}{R} \left(\frac{1}{273.15+T} - \frac{1}{273.15+T_{ref}} \right)} \right] \quad (7.6)$$

where k_{ref} is the rate constant at a reference temperature T_{ref} (32.5 °C), E_a is the activation energy regarding the dependence of the rate constant with temperature, and R is the universal gas constant; parameters a_k and b_k are the factors of the dependence of the reference rate constant with added L-AA content.

Equation 7.6 was used to fit the experimental data yielding good results, as can be seen in Figure 7.5. More examples of the global fit can be analysed in Figures F.11 to F.15 (Appendix F). Further information on the quality of the fit is included in Appendix F (Figure F.22 (Appendix F) shows the good agreement between experimental and predicted data, the lack of residual tendency with predicted values and the approximately normal distribution of those residuals).

Estimates of the model parameters, both for individual and global fittings are presented in Table 7.3.

The activation energy is similar to that obtained for the first reaction of the two consecutive first-order model earlier applied when the juice was not aerated (§5.3), and parameters a_k and b_k are of the same order of magnitude of those reported in Chapter 5, which shows that during short storage times O_2 concentration does not limit L-AA degradation. The model parameters showed very low collinearity (correlation coefficients below 0.344), with the exception of the two parameters

that relate k_{ref} with added L-AA content (coefficient of correlation 0.94). However, values below 0.99 are considered acceptable (Bates & Watts, 1988; Van Boeckel, 1996).

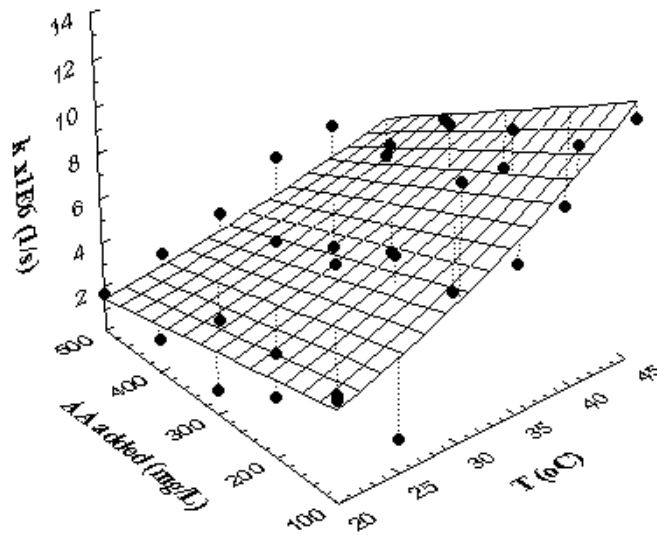


Figure 7.6- Dependence of the reaction rate constant of the first-order model on temperature and added L-AA. The ● symbols represents parameters estimated with individual fits and the surface those estimated with the global fit.

Table 7.3- Estimates of the parameters of the individual (Eq. 4.1) and global fitting (Eq. 7.6) of the first-order model to L-AA data.

INDIVIDUAL FITTING										
T (°C)	Batch J (100 mg/L)		Batch K (200 mg/L)		Batch L (300 mg/L)		Batch M (400 mg/L)		Batch N (500 mg/L)	
	k x10 ⁶ (s ⁻¹)	R ² _{adj}	k x10 ⁶ (s ⁻¹)	R ² _{adj}	k x10 ⁶ (s ⁻¹)	R ² _{adj}	k x10 ⁶ (s ⁻¹)	R ² _{adj}	k x10 ⁶ (s ⁻¹)	R ² _{adj}
20	4.5±0.4	0.999	2.7±0.3	0.999	1.06±0.05	1.00	1.5±0.1	1.00	1.7±0.2	0.999
25	1.5±0.1	1.00	1.5±0.1	0.999	1.5±0.1	0.999	1.1±0.4	0.999	2.4±0.1	1.00
30	11.3±1.2	0.998	6.5±1.2	0.998	4.3±0.2	1.00	3.5±0.1	1.00	3.0±0.1	1.00
35	6.7±1.4	0.998	3.6±1.0	0.999	3.6±1.0	0.999	2.1±0.8	0.999	4.5±0.9	0.999
40	10.6±0.9	0.999	9.6±1.1	0.998	8.2±1.0	0.998	5.6±0.3	0.999	4.8±0.4	0.999
45	10.6±1.0	0.998	5.1±1.3	0.998	5.1±1.3	0.998	5.7±0.9	0.999	2.3±0.4	0.999
GLOBAL FITTING										
a x10 ⁶ (s ⁻¹)		b x10 ⁹ (L/(s.mg))				Ea (kJ/mol)		R ² _{adj}		
8.1±0.5		11.2±1.3				31± 4		0.999		

T_{ref}=32.5 °C

7.3.2. BROWNING UNDER EXCESS OXYGEN

The Weibull model was fitted to browning index data, as in §6.3.2, but the estimates of the model parameters were found not to be reliable because in many experiments the maximum browning index measured falls too short of equilibrium. A zero-order model (Eq. 4.9) was then used to fit the data. This model produced fair fits to the experimental data ($0.782 < R^2_{\text{adj}} < 0.995$). The model parameters are presented in Table 7.4, and examples of the fit can be seen in Figure 7.7. Further examples are shown in Figures F.23 to F.28 (Appendix F).

The rate constants showed to increase with temperature according to an Arrhenius type equation. Then, when a pre-global fit was performed for each batch separately imposing an Arrhenius dependency with temperature, the rate constants at a reference temperature showed to be independent of added L-AA, while activation energies increased linearly with added L-AA content (see Figure 7.8). As temperature increases the effect of adding L-AA is more perceptible, which can explain the increase of the activation energy values. This relationship was the included in Equation 4.9 to build a global model:

$$C_{Br} = C_{Br}^i + k_{ref} \times e^{-\frac{Ea_0 + m_{Ea} \times C_{add}}{R} \left(\frac{1}{273.15 + T} - \frac{1}{273.15 + T_{ref}} \right)} \times t \quad (7.7)$$

where k_{ref} is the rate constant at a reference temperature (T_{ref}), Ea_0 is the activation energy value considering juice without added L-AA, m_{Ea} is the slope of the linear relation of the activation energy with added L-AA content (C_{add}), and R is the universal gas constant. The reference temperature (32.5 °C, average value of the

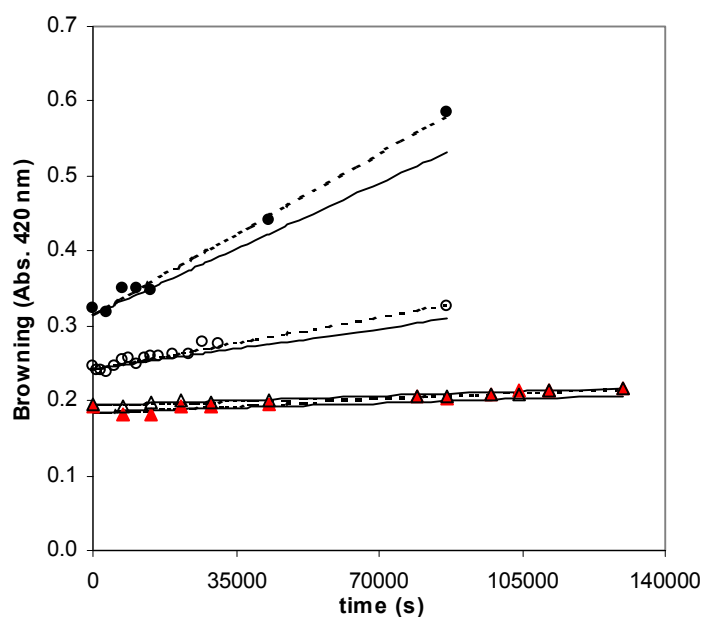


Figure 7.7- Fit of the zero-order model to browning at (Δ) 20 °C -batch I (no added L-AA), (\blacktriangle) 20 °C -batch N (500 mg/L), (\circ) 45 °C -batch I (no added L-AA), and (\bullet) 45 °C -batch N (500 mg/L). The dashed and solid lines indicate, respectively, the individual and global fits.

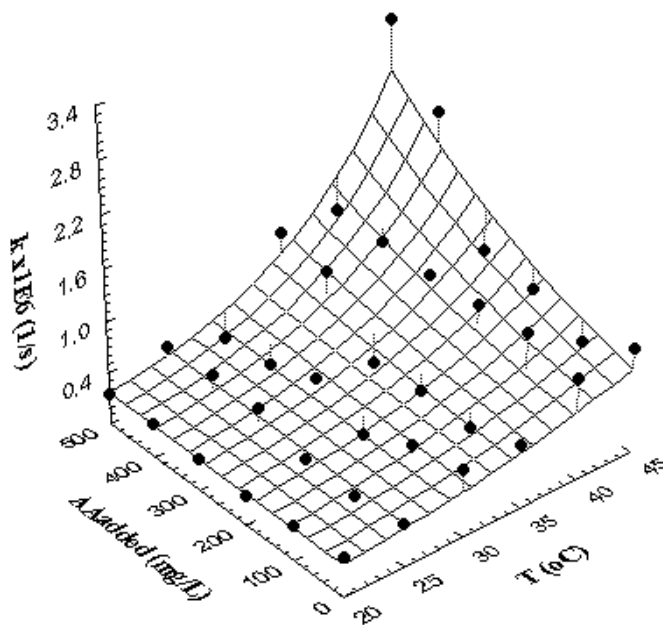


Figure 7.8- Dependence of the zero-order model rate constants on temperature and added L-AA content, for browning. The \bullet symbol represent parameters estimated with individual fits and the solid surface/line indicates the global fit.

Table 7.4- Estimates of the parameters of the individual (Eq. 4.9) and global fitting (Eq. 7.7) of the zero-order model to browning index data.

INDIVIDUAL FITTING												
T (°C)	Batch I (no added L-AA)		Batch J (100 mg/L)		Batch K (200 mg/L)		Batch L (300 mg/L)		Batch M (400 mg/L)		Batch N (500 mg/L)	
	$k \times 10^6$ (s ⁻¹)	R ² _{adj.}	$k \times 10^6$ (s ⁻¹)	R ² _{adj.}	$k \times 10^6$ (s ⁻¹)	R ² _{adj.}	$k \times 10^6$ (s ⁻¹)	R ² _{adj.}	$k \times 10^6$ (s ⁻¹)	R ² _{adj.}	$k \times 10^6$ (s ⁻¹)	R ² _{adj.}
20	0.25±0.02	0.956	0.19±0.02	0.959	0.14±0.02	0.892	0.17±0.03	0.930	0.19±0.01	0.969	0.16±0.01	0.930
25	0.30±0.05	0.956	0.22±0.02	0.938	0.243±0.008	0.995	0.44±0.04	0.800	0.44±0.04	0.962	0.41±0.06	0.800
30	0.57±0.05	0.912	0.46±0.09	0.955	0.19±0.05	0.762	0.46±0.09	0.855	0.25±0.02	0.918	0.21±0.03	0.855
35	0.53±0.06	0.964	0.33±0.04	0.835	0.40±0.05	0.891	0.35±0.04	0.941	1.05±0.05	0.971	1.16±0.09	0.941
40	0.98±0.09	0.960	1.11±0.09	0.906	1.1±0.2	0.874	1.1±0.2	0.782	1.1±0.2	0.823	1.1±0.2	0.782
45	1.00±0.05	0.949	0.71±0.04	0.965	1.0±0.1	0.931	1.1±0.41	0.990	2.3±0.1	0.990	3.1±0.1	0.990

GLOBAL FITTING			
$k_{ref} \times 10^6$ (s ⁻¹)	Ea ₀ (kJ/mol)	m _{Ea} (kJ.L/(mol.mg))	R ² _{adj.}
0.17±0.01	46±4	0.073±0.006	0.891

T_{ref}= 32.5 °C

temperature range under study) was used to improve parameter estimation.

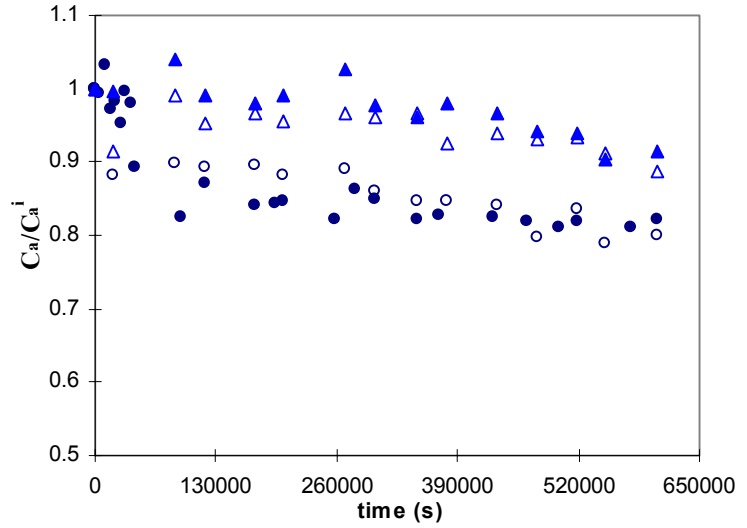
Equation 7.13 was then fitted to the experimental data. Figure 7.7 shows some of the results obtained and additional examples can be analysed in Figures F.23 to F.28 (Appendix F).

The estimates of the model parameters are summarised in Table 7.4. The fit was not very good ($R^2_{\text{adj}}=0.891$) but correlation between parameters was generally low (correlation coefficient < 0.89). Further information on the quality of the fit is included in Appendix F (Figure F.29 shows the agreement between experimental and predicted data, the lack of residual tendency with predicted values and the approximately normal distribution of those residuals).

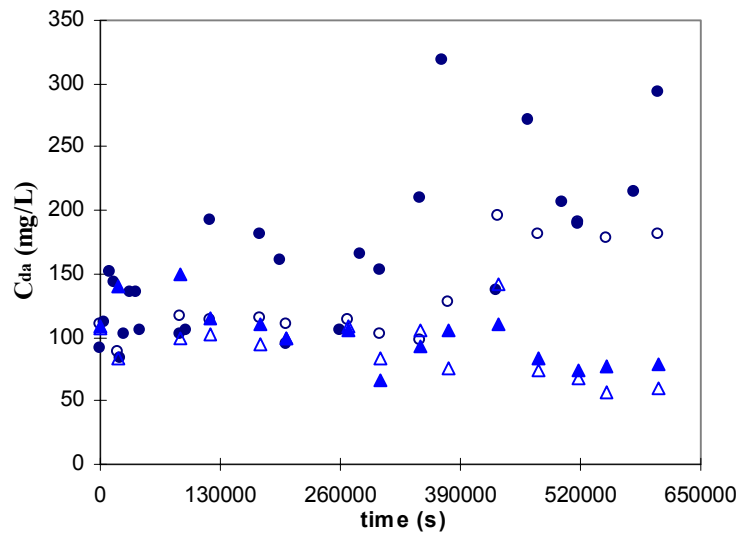
7.3.3. L-ASCORBIC ACID DEGRADATION IN ANAEROBIC CONDITIONS

Degradation of L-AA in the absence of oxygen was studied by flushing continuously nitrogen through orange juice. Anaerobic degradation of L-AA is very slow, as can be seen in Figure 7.9.

Unfortunately data could not be collected for longer times, as the juice started to concentrate, and conversions just up to 20% were obtained. Although modelling was not used, due to the high retentions obtained, the data (Figure 7.9) allows visualizing the effect of storage temperature on anaerobic degradation velocity, while there is no evident effect from the addition of L-AA.



(a)



(b)

Figure 7.9- Effect of continuous nitrogen flushing on (a) L-AA degradation and (b) dehydroascorbic acid formation/degradation in orange juice, at \triangle 20 °C -batch I (no added L-AA), \blacktriangle 20 °C -batch N (500 mg/L), \circ 45 °C -batch I (no added L-AA), and \bullet 45 °C -batch N (500 mg/L).

7.4. CONCLUSIONS

The results show that, under aerobic conditions, addition of ascorbic acid to orange juice slows down its degradation rate whereas it increases the browning rate, especially at high temperatures. Under anaerobic conditions L-AA degradation was very slow.

The mechanistic model developed in the previous chapter was found to describe fairly well L-AA and DA degradation in the whole range of conditions tested. Some of the estimates of the model parameters were significantly different from those reported in the previous Chapter, probably owing to a high correlation between those parameters.

A first-order model could also be applied to the data satisfactorily, but only for lower conversions (experimental times up to 8 hours) as for greater conversions degradation curves show a sigmoidal pattern. L-AA degradation rate in this period was similar to that earlier observed in the aerobic pathway when the juice was stored in tubes. This suggests that L-AA degradation rate in the aerobic pathway depends on the availability of oxygen but does not depend on its concentration.

The Weibull model was also found to fit the L-AA data fairly well, but the dependence of the model parameters on temperature and added L-AA was more complex than observed in previous Chapters, the model requiring a larger number of parameters when compared to the mechanistic model.

Browning was described by the zero-order model, with an activation energy linearly dependent on added L-AA content, while the rate constant at the reference temperature showed to be constant.

**General conclusions and
recommendations for
further work**

General Conclusions and Recommendations for Further Work

This section summarises the main conclusions of the work performed in the framework of this thesis, with the aim of providing an integrated perspective and stressing the major outcomes. Recommendations for further work are also presented.

General Conclusions

Experiments carried out with orange juice packed in TBA, under isothermal conditions covering a wide range of temperatures (4 to 50 °C), showed that L-AA, browning, and flavour compounds were greatly affected by temperature whereas initial dissolved oxygen content did not show a significant effect during storage. This limits the use of high initial oxygen contents as an accelerating factor for shelf life studies. The package permeability to oxygen proved to be sufficiently low to limit oxidative reactions, yet a residual oxygen concentration was maintained during the whole storage period (up to 13 months).

Empirical mathematical models were developed to describe the degradation kinetics of a number of quality indicators during storage of orange juice in the conditions above described. Browning and 2-furfuraldehyde were well described by a zero-order model whereas 4-vinyl-guaiacol followed a first-order model.

Formation of 5-Hydroxymethyl-2-furfuraldehyde showed a discontinuity with time, which was modelled by two consecutive zero-order reactions, the second being much faster than the first. The reverse was observed for L-ascorbic acid, which degradation rate was much faster at short times. This was attributed to two different reactive pathways: an aerobic mechanism dominating while oxygen was available, followed by a slower anaerobic reaction when oxygen concentration was very small. It was however found that the later mechanism was not truly anaerobic, as in the complete absence of oxygen L-AA does not degrade. The Weibull model was also found to provide a good description of L-AA degradation, with the advantage of being much simpler and requiring less model parameters. The rate constants of the models above described, increased with temperature according to an Arrhenius-type equation, in some case with a lower sensitivity to temperature (activation energy) at temperatures below approximately 30 °C than at temperatures above this value.

L-AA was found to be the critical shelf life quality indicator, closely followed by browning. Supplementation of orange juice with L-AA led to increased shelf life, as addition of L-AA to orange juice slows down its degradation rate. However, L-AA remained the critical factor that limits orange juice shelf life, except when reasonable amounts of L-AA were added to the juice (≥ 400 mg/L at 20 and 25 °C; ≥ 300 mg/L at 30 °C). Both the Weibull and the two consecutive first-order models provided a good description of the kinetics of degradation of L-AA during storage of L-AA supplemented juice under normal and abusive temperature conditions. Nevertheless, the Weibull model showed to be more suitable for

accelerated shelf life testing, as the rate constant did not show any discontinuity with temperature. The second reaction of the two consecutive first-order reactions model shows a much higher sensitivity to temperature in abusive conditions (35 to 45 °C) than in normal storage temperatures, which hinders its use in ASLT. Browning rate increased with added L-AA content and was well described by zero-order kinetics.

Studies on L-AA and dehydroascorbic acid (DA) degradation in orange juice with excess oxygen allowed to develop a mechanistic model that could describe the stabilizing effect of added L-AA on its degradation. This mechanism assumes that L-AA conversion into DA is reversible, the reconversion of DA into L-AA being dependent on L-AA concentration, and that DA decomposes irreversibly into degradation products. The rate constants of these reactions were found to increase with temperature according to an Arrhenius-type relationship, being the reaction of reconversion of DA into L-AA more sensitive to temperature than the others. L-AA degradation in these conditions could also be well described by the Weibull model, although it would require a large number of parameters to account for temperature and added L-AA effects. Browning appears to follow a Weibull model levelling off to an equilibrium value, although this model could not be thoroughly tested because in most situations the extension of browning was too small to allow to a detailed analyses of its kinetics. Browning rate increased linearly with initial L-AA contents.

Recommendations for Further Work

Shelf life prediction of pasteurised orange juice is a very complex field of research because of the complexity of the product matrix, chemical reactions involved in quality degradation, and their dependence on environmental factors. This work provides some insight into shelf life limiting factors, but there is a need for developing comprehensive research work. Based on the results obtained, several recommendations for further work may be drawn.

- The aerobic pathway for L-AA and DA degradation in orange juice should be further understood. This would require a study of the degradation kinetics in a different range of constant dissolved oxygen concentration. The influence of oxygen on the so-called “anaerobic” pathway should also be further explored.
- A better understanding is required regarding the influence of supplementing the juice with L-AA on the kinetics of quality indicators degradation. It would be of interest to extend the analysis carried out in this work to other quality indicators, and to develop a more comprehensive mathematical model that might describe not only L-AA and AA degradation but also the accumulation of the compounds produced by these reactions.
- Studies should be conducted in non-isothermal conditions, to simulate the temperature variations the packaged juice is normally subjected to in the distribution chain. Tests conducted at constant temperature often fail to adequately predict the process behaviour in dynamic conditions.

- It would be necessary to define optimal experimental designs for ASLT so that they can be used to accurately predict shelf life in normal storage conditions. Otherwise, its utilisation will remain risky.

**List of Communications
based on thesis work**

List of Communications based on thesis Work

[RCB#]- Refereed chapter of a book

[RP#]- Refereed paper

[NRP#]- Non-refereed paper

[O#]- Oral presentation

[PT#]- Poster presentation

Chapter 2

[O1] **Manso, M. C.**, Oliveira, F. A. R., Ahmé, L. M., Poças M. F. and Öste, R.
Selection of quality indicators and test conditions for predicting shelf-life
of aseptically packaged orange juice by application of accelerated tests.
Oral presentation in: 10th IAPRI World Conference on Packaging,
March 20-23, 1997, Melbourne, Australia.

[NRP1] **Manso, M. C.**, Oliveira, F. A. R., Ahmé, L. M., Poças M. F. and Öste, R.
1997. Selection of quality indicators and test conditions for predicting
shelf-life of aseptically packaged orange juice by application of
accelerated tests. Proceedings of the 10th IAPRI World Conference on
Packaging, p. 327-334, Melbourne, Austrália.

Chapter 3

- [RP1] L. M. Ahrné, F.A.R. Oliveira, **M. C. Manso**, M. C. Drumond, , R. Öste, V. Gekas. 1997. Modelling of Dissolved Oxygen Concentration during Storage of Packaged Liquid Foods. *Journal of Food Engineering*. 34: 213-224.
- [PT1] **M. C. Manso**, L. M. Ahrné, R. E. Öste & F. A. R. Oliveira. Dissolved Oxygen Concentration Changes during Storage of Packaged Orange Juice. Poster presentation in: 1996 IFT Annual Meeting & FOOD EXPO, June 22-26, 1996, New Orleans, USA.

Chapter 4

- [PT2] **Maria C. Manso**, Lília Ahrné, Fernanda Oliveira, Rikard Öste. Modelling Furfural Production in Aseptically Packaged Orange Juice. Poster presentation in: Livsmedel 95, October 18-19, 1995, Uppsala, Sweden.
- [RCB1] L. M. Ahrné, **M. C. Manso**, E. Shah, F.A.R. Oliveira, R. E. Öste. 1996. Shelf-life Prediction of Aseptically Packaged Orange Juice. Chemical Markers for Processed and Stored Foods, Ed. Tung-Ching Lee and Hie-Joon Kim, ACS Symposium Series 631, Ch. 10, p.107-117.

- [O2] **Manso, M. C.**, Oliveira, F. A. R., Ahrné, L. M., Öste, R. *Modelagem da Produção de 5-Hidroximetil-2-Furfuraldeído em Sumo de Laranja Embalado Assepticamente*. Oral presentation in: *3º Encontro de Química de Alimentos*, March 23-26, 1997, Faro, Portugal.
- [NRP2] **Manso, M. C.**, Oliveira, F. A. R., Ahrné, L. M., Öste, R. 1997. *Modelagem da Produção de 5-Hidroximetil-2-Furfuraldeído em Sumo de Laranja Embalado Assepticamente*. Proceedings of the *3º Encontro de Química de Alimentos*, p. 24-26, Faro, Portugal.
- [O3] **Manso, M. C.**, Oliveira, F. A. R., Ahrné, L. M., Öste, R. Ascorbic Acid Degradation During Storage of Aseptically Packaged Orange Juice. Oral presentation in: 1997 IFT Annual Meeting & FOOD EXPO, June 15-18, 1997, Orlando, USA.

Chapter 5

- [RP2] **Manso, M. C.**, Oliveira, F. A. R., Fitzpatrick, J. 2000. Modelling ascorbic acid degradation in orange juice with added ascorbic acid. Proceedings of the Eighth International Congress on Engineering and Food (ICEF-8), Puebla, Mexico.
- [PT3] **Manso, M. C.**, Oliveira, F. A. R., Fitzpatrick, J. Modelling ascorbic acid degradation in orange juice with added ascorbic acid. Poster presentation in: Eighth International Congress on Engineering and Food (ICEF-8), April 9-13, 2000, Puebla, Mexico.

Chapter 6

- [RP3] **Manso, M. C.**, Oliveira, F. A. R., Oliveira, J. C., Frías, J. M. Modelling Ascorbic Acid Thermal Degradation and Browning in Orange Juice under aerobic conditions. In press: International Journal of Food Science and Technology.
- [PT4] **Manso, M. C.**, Oliveira, F. A. R., Oliveira, J. C. Modelling aerobic ascorbic acid degradation in orange juice. Poster presentation in: 10th World Congress of Food Science and Technology (IUFOST), October 3-8, 1999, Sydney, Australia.

Chapter 7

- [PT5] **Manso, M. C.**, Oliveira, F. A. R., Oliveira, J. C. Modelling aerobic ascorbic acid degradation in orange juice with added ascorbic acid. Poster presentation in: 1999 IFT Annual Meeting & FOOD EXPO, July 24-28, 1999, Chicago, USA.

References

References

Electronic References

Anonymous. 1949. The Florida Citrus Code of 1949. [Cited 9 June 2000]

Available from: <http://www.leg.state.fl.us/citizen/documents/statutes/1999/ch0601/tit10601.htm>

Anonymous. 2000. Glossary of juicy terms. [Cited 3 March 2000] Available from:

<http://www.floridajuice.com/floridacitrus/ojterms.htm>

Hui, S. 1999. Sweet oranges: the biogeography of *Citrus sinensis*. Canada. [Cited

6 June 2000] Available from: <http://www.sfu.ca/~shui/resources/orange.html>

Morris, A. 1996. The orange Juice production Process and Product Forms. In:

Morris Citrus Economics Newsletter, 1(8), [Cited 5 June 2000] Available from:

<http://www.ultimatecitrus.com/oj.html>

Tetra Pak. 2000. Products and services [Cited 14 June 2000] Available from:

<http://www.tetrapak.com/>

Bibliography

- Ahmed, A. A., Watrous, G. H., Hargrove, G. L. and Dimick, P. S. 1976. Effects of fluorescent light on flavour and ascorbic acid content in refrigerated orange juice and drinks. *Journal of Milk Food Technology*. 39: 323.
- Anonymous. 1995. Centers for Disease Control, Outbreak of *Salmonella* Hartford infections among travellers to Orlando, Florida, EPI-AID report. Pp. 62. Florida.
- AOAC. 1965. Official Methods of Analysis. Ed. Horwitz, W., 10th ed., Pp. 764, Washington, D.C.
- Atkins, C. D., Rouse, A. H., Huggart, R. L., Moore, E. L. and Wenzel, F. W. 1953. Gelation and clarification in concentrated juices. III. Effect of heat treatment of Valencia oranges and Duncan grapefruit juices prior to concentration. *Food Technology*. 7: 62.
- Barron, F. H., Harte, B., Giancin, J. and Hernandez, R. 1993. Modelling of oxygen diffusion through a model permeable package and simultaneous degradation of vitamin C in Apple juice. *Packaging Technology and Science*. 6: 301.
- Bates, D. M. and Watts, D. G. 1988. Nonlinear regression analysis and its applications. John Willey and Sons. New York.

- Beuchat, L. R. 1982. Thermal inactivation of yeasts in fruit juices supplemented with food preservatives and sucrose. *Journal of Food Science*. 47: 1679.
- Bisset, O. W., Veldhuis, M. K. and Rushing, N. B. 1953. Effect of heat treatment temperature on the storage life of Valencia orange juice. *Food Technology*. 7: 258.
- Bissett, O. W. and Berry, R. 1975. Ascorbic acid retention in orange juice as related to container type. *Journal of Food Science*. 40: 178.
- Blair, J. S., Godar, E. M., Masters, J. E. and Riester, D. W. 1952. Exploratory experiments to identify chemical reactions causing flavor determination during storage of canned acid juice. *Food Research*. 17: 235.
- Boggs, P. T., Byrd, R. H., Rogers, J. E. and Schnabel, R. B. 1992. User's Reference Guide for ODRPACK Version 2.01 Software for Weighted Orthogonal Distance Regression. National Institute of Standards and Technology, Gaithersburg, MD 20899, USA.
- Box, G. E. P. and Lucas, H. L. 1959. Design of experiments in non-linear situations. *Biometrika*. 46: 77.
- Bruemmer, J. H. 1980. Relationship of citrus enzymes to juice quality. In: Citrus Nutrition and Quality. S. Nagy and J. A. Attaway (Ed.), ACS Symposium Series 143. Pp. 151, American Chemical Society, Washington, D.C.

- Buettner, G. R. 1988. In the absence of catalytic metals ascorbate does not oxydize at pH 7: ascorbate as a test for catalytic metals. *Journal of Biochemical and Biophysical Methods*. 16: 27.
- Cameron, R. G., Baker, R. A. and Grohmann, K. 1997. Citrus tissue extract affect juice cloud stability. *Journal of Food Science*. 62 (2): 242.
- Cameron, R. G., Baker, R. A. and Grohmann, K. 1998. Multiple forms of Pectinmethylesterase from citrus peel and their effects on juice cloud stability. *Journal of Food Science*. 63 (2): 253.
- Cameron, R. G., Niedz, R. P. and Grohmann, K. 1994. Variable heat stability for multiple forms of pectin methylesterase from citrus tissue culture cells. *Journal of Agri. Food Chem*. 42: 903-908.
- Castaldo, D., Laratta, B., Loiudice, R., Giovane, A., Quagliuolo, L. and Servillo, L. 1997. Presence of Residual Pectin Methylesterase Activity in Thermally Stabilized Industrial Fruit Preparations. *Lebensmittel Wissenschaft und Technologie*. 30: 479-484.
- Cohen, E., Birk, Y., Mannheim, C. H. and Saguy, I. S. 1994. Kinetic parameter estimation for quality change during continuous thermal processing of grapefruit. *Journal of Food Science*, 59, 155.
- Costa, R. M., Oliveira, F. A. R. and Boutcheva, G. 2000. Structural changes and shrinkage of potato during frying. *International Journal of Food Science and Technology*, In press.

- Cromwell, J. B., Labys, W. C. And Terraza, M. 1994. Univariate tests for time series models. Pp. 28. Sage, Thousand Oaks, CA.
- Cunha, L. M. S. R. L. 1998. Improved Parameter Estimation by Means of Experimental Design for Non-linear Modelling of Kinetic Mechanisms. Ph.D. thesis, Escola Superior de Biotecnologia, Universidade Católica Portuguesa, Porto, Portugal.
- Cunha, L. M., Oliveira, F. A. R. and Oliveira, J. C. 1998. Optimal experimental design for estimating the kinetic parameters of processes described by the weibull probability distribution function. *Journal of Food Engineering*. 37: 175.
- Deinhard, G., Blanz, P., Poralla, K. and Altan, E. 1987. *Bacillus acidoterrestris* sp. Nov., a new thermotolerant acidophile isolated from different soils. *Systematic and Applied Microbiology*, 10: 47.
- Devore, J. L. 1995. Probability and statistics for Engineering and the Sciences. 4th Ed. Pp. 174-175. Duxbury Press. New York.
- Eison-Perchonok, M. H. and Downes, T. W. 1982. Kinetics of ascorbic acid autoxidation as a function of dissolved oxygen concentration and temperature. *Journal of Food Science*. 47: 765.
- FDA (Food and Drug Administration). 1993. FDA Nutritional Labelling Manual: a Guide for Developing and using Data Bases. Washington DC: Food and Drug Administration, Center of Food Safety and Applied Nutrition. USA

- Fellers, P. J. 1988. Shelf life and quality of freshly squeezed, unpasteurized, polyethylene-bottled citrus juice. *Journal of Food Science*. 53: 1699.
- Fennema, O. 1985. Water and ice. In Principles of food science. Chap.2. Marcel Dekker, Inc. New York.
- Fernández, A., Salmerón, C., Fernández, P.S. and Martínez, A. 1999. Application of a frequency distribution model to describe the thermal inactivation of two strains of *Bacillus cereus*. *Trends in Food Science and Technology*. 10: 158.
- Fiddler, W., Parker, W. E., Wasserman, A. E. and Doerr., R. C. 1967. Thermal decomposition of Ferrulic acid. *Journal of Agricultural and Food Chemistry*. 15(5): 757.
- Fors, S. 1983. Sensory properties of volatile Maillard reaction products and related compounds: a literature review. In: The Maillard Reaction in Foods and Nutrition. G. R. Waller and M. S. Feather (Ed.), Pp.185. ACS Symposium series 215. Washington, D.C.
- Fu, B. and Labuza, T. P. 1993. Review: Shelf life prediction: theory and application. *Food Control*. 4(3): 125.
- Gacula Jr., M. C. 1975. The design of experiments for shelf life study. *Journal of Food Science*. 40: 399.
- Gacula Jr. and M. C., Kubala, J. J. 1975. Statistical models for shelf life failures. *Journal of Food Science*. 40: 404.

- Gamel, J. W., Weller, E. A., Wesley, M. N. and Feuer, E. J. 2000. *Parametric cure models of relative and cause-specific survival for grouped survival times. Computer Methods and Programs in Biomedicine. 61: 99.*
- Garrote, R. L., Silva, E. R. and Bertone, R. A. 1988. Effect of freezing on diffusion of ascorbic acid during water heating of potato tissue. *Journal of Food Science. 53: 473.*
- Giles, G. A. 1998. Packaging materials. In: The Chemistry and Technology of Soft Drinks and Fruit Juices. Chap. 5. Pp. 103. P. R. Ashurst (Ed). CRC Press.
- Gnanasekharan, V. and Floros, J. D. 1993. Shelf-life prediction of packaged Foods. In: Shelf-life studies of foods and beverages. Pp.1081. Elsevier Science Publishers B. V.
- Graumlich, T. R., Marcy, J. E. and Adams, J. P. 1986. Aseptically packaged orange juice and concentrate: A review of the influence of processing and packaging conditions on quality. *Journal of Agriculture and food Chemistry. 34: 402.*
- Gregory, J. F. 1993. Ascorbic acid bioavailability in foods and supplements. *Nutrition Reviews. 51(10): 301.*
- Gross, J. 1977. Carotenoid pigments in citrus. In: Citrus Science and Technology. Vol. 1. S. Nagy, P. E. Shaw and M. K. Veldhuis (Ed). AVI Publishing Co., Westport, CT.
- Gross, J. 1987. Pigments in Fruits. Academic Press, New York.

- Guyer, R. B., Miller, W. M., Bissett, O. W., and Veldhuis, M. K. 1956. Stability of frozen concentrated orange juice. I. The effect of heat treatment on enzyme inactivation and cloud stability of frozen concentrate made from Pineapple and Valencia oranges. *Food Technology*. 10: 570.
- Hahn, G. J., Shapiro, S. S., 1967. Statistical Models in Engineering. Wiley, New York.
- Hahn, H. 1988. Packaging material for aseptic packaging. Chapter 5. In. Aseptic Packaging of Food. H. Reuter (Ed.), Pp. 228. Technomic Publishing Company, Inc., USA.
- Handwerk, R. L. and Coleman, R. L. 1988. Approaches to citrus browning problem. A review. *Journal of Agricultural and Food Chemistry*. 36: 231.
- Haralampu, S. G., Saguy, I. and Karel, M. 1985. Estimation of Arrhenius model parameters using three least-square methods. *Journal of Food Processing and Preservation*. 9(3): 129.
- Heinz, V. and Knorr, D. 1996. High pressure inactivation kinetics of *Bacillus subtilis* cells by a three-state-model considering distributed resistance mechanisms. *Food Biotechnology*. 10: 149.
- Hendrix, C. M. and Redd, J. B. 1995. Chemistry and Technology of citrus juices and by-products. In: Production and Packaging of non-carbonated fruit juices and fruit beverages. P. R. Ashurst (Ed). Chap. 2. Pp. 53. Blackie Academic and Professional, Glasgow.

- Hertlein, J., Singh, R. P. and Weisser, H. 1995. Prediction of oxygen transport parameters of plastic packaging materials from transient state measurements. *Journal of Food Engineering*. 24: 543.
- Hill, C. J. and Grieger-Block, R. A. 1980. Kinetic data: generation, interpretation and use. *Food Technology*. (2): 56.
- Hsieh, Y. P. and Harris, N. D. 1993. Effect of sucrose on oxygen uptake of ascorbic acid in a closed aqueous system. *Journal of Agricultural and Food Chemistry*. 41: 259.
- Huelin, F. E. 1953. Studies on the anaerobic decomposition of ascorbic acid. *Food Research*. 18: 633.
- Huelin, F. E., Coggiola, I. M., Sidhu, G. S. and Kennett, B. H. 1971. The anaerobic decomposition of ascorbic acid in the pH range of foods and in more acid solutions. *Journal of the Science of Food Agriculture*. 22: 540.
- Hughes, D. E. 1985. Irreversible reaction kinetics of the aerobic oxidation of ascorbic acid. *Analytical Chemistry*. 57: 655.
- IFST. 1993. Shelf life of Foods- Guidelines for its determination and prediction. Institute of Food Science and Technology, London, UK.
- Ilincanu, L. A., Oliveira, F. A. R., Drumond, M. C., Machado, M. F. and Gekas, V. 1995. Modelling moisture uptake and soluble solids losses during rehydration of dried apple pieces. In. Proceedings of the First Main Meeting of

- the Copernicus Programme Project “Process Optimisation and Minimal Processing of Foods”. Vol. 3: Drying, J. C. Oliveira (Ed.), Pp. 64, Escola Superior de Biotecnologia- Universidade Católica Portuguesa, Porto, Portugal.
- Johnson, M. L. and Frasier, S. G. 1985. Nonlinear least-squares Analysis. Methods in Enzymology. 117: 301.
- Jonhson, J. R., Bradock, R. J. and Chen, C. S. 1995. Kinetics of Ascorbic Acid Loss and Nonenzymatic Browning in Orange Juice Serum: Experimental Rate Constants. Journal of Food Science. 60(3): 502.
- Kaanane, A., Kane, D. and Labuza, T. P. 1988. Time and temperature effect on stability of maroccan processed orange juice during storage. Journal of Food Science. 53: 1470.
- Kacem, B., Cornell, J. A., Marshall, M. R., Shireman, R. B. and Mathews, R. F. 1987. Nonenzimatic browning in aseptically packaged orange drinks: Effect of ascorbic acid, aminoacids and oxygen. Journal of Food Science. 52: 1668.
- Kanner, J., Fishbein, J., Shalom, P., Hanel, S. and Ben-gera, I. 1982. Storage stability of orange juice concentrate packaged aseptically. Journal of Food Science. 43: 429.
- Karel, M. 1974. Packaging protection for oxygen-sensitive products. Food Technology. (8): 50.

- Karel, M. 1979. Prediction of nutrient losses and optimization of processing conditions. In Nutritional and safety aspects of food processing. Chapt. 8. S.R. Tannenbaum (Ed.), Marcel Dekker, Inc. New York.
- Karel, M., 1983. Quantitative analysis and simulation of food quality losses during processing and storage. In: Computer-aided Techniques in Food Technology. Chap. 5. Pp. 117. Israel Saguy (Ed). Marcel Dekker, Inc. New York.
- Kawamura, S. 1983. Seventy years of the Maillard reaction. In: The Maillard reaction in Foods and Nutrition. Chap. 1. Pp. 3. G. R. Waller and M. S. Feather (Ed). ACS Symposium series 215. Washington, D.C.
- Kebede, E., Mannheim, C. H. and Miltz, J. 1998. Ascorbic acid retention in a model food packed in barrier plastic trays and cans. *Lebensmittel Wissenschaft und Technologie*. 31: 33.
- Kennedy, J. F., Rivera, Z. S., Lloyd, L. L., Warner, F. P. and Jumel, K. 1992. L-ascorbic acid stability in aseptically processed orange juice in TetraBrik cartons and the effect of oxygen. *Food Chemistry*. 45: 327.
- Khan, M. M. T. and Martell, A. E. 1967a. Metal ion and metal chelate catalysed oxidation of ascorbic acid by molecular oxygen. I. Cupric and ferric ion catalysed oxidation. *Journal of the American Chemical Society*. 89: 4176.

- Khan, M. M. T. and Martell, A. E. 1967b. Metal ion and metal chelate catalysed oxidation of ascorbic acid by molecular oxygen. II. Cupric and ferric chelate catalysed oxidation. *Journal of the American Chemical Society*. 89: 7104.
- Komitopoulou, E., Boziaris, I. S., Davies, E. A., Delves-Broughton, J. and Adams, M. R. 1999. Alicyclobacillus acidoterrestris in fruit juices and its control by nisin. *International Journal of Food Science and Technology*. 34: 81.
- Körmendy, I., Pátkai, G., Sényi, J. and Gion, B. 1994. Examination of the Usefulness of Empirical Kinetic Equations for Describing the Formation of 5-HMF in Grapefruit Juice. *Journal of Food Engineering*. 23: 519.
- Labuza, T. P. and Kamman, J. K. 1983. Reaction kinetics and accelerated tests - simulation as a function of temperature. In: Computer-aided Techniques in Food Technology. Chap. 4. Pp. 71. Israel Saguy (Ed). Marcel Dekker, Inc. New York.
- Labuza, T. P. 1982. Open Shelf Life Dating of Foods. Food and Nutrition Press, Westport, Conn.
- Labuza, T. P. and Riboh, D. 1982. Theory and application of Arrhenius Kinetics to prediction of nutrient losses in foods. *Food Technology*. (10): 66.
- Labuza, T. P. and Schmidl, M. K. 1985. Accelerated shelf-life testing of foods. *Food Technology*. (9): 57.

- Laing, B. M., Shlueter, D.L. and Labuza, T.P. 1978. Degradation kinetics of ascorbic acid at high temperature and water activity. *Journal of Food Science*, 43: 1440.
- Lathrop, P. J. and Leung, H. K. 1980. Rates of ascorbic acid degradation during thermal processing of canned peas. *Journal of Food Science*. 45:152.
- Lee, H. S. and Coates, G. A. 1999. Vitamin C in frozen, fresh squeezed, unpasteurised, polyethylene bottled orange juice: a storage study. *Food Chemistry*. 65: 165.
- Lee, H. S. and Nagy, S. 1990. Formation of 4-Vinyl guaiacol in adversely stored orange juice as measured by an improved HPLC method. *Journal of Food Science*. 55 (1): 162.
- Lee, H. S. and Nagy, S. 1996. Chemical degradative indicators to monitor the quality of processed and stored citrus products. In: *Chemical markers for processed and stored foods*. Chap. 9, Pp.86. ACS Symposium Series 631, Ed. Tung-Ching Lee and Hie-Joon Kim.
- Lee, H. S., Rouseff, R. L. and Nagy, S. 1986. HPLC determination of furfural and 5-hydroxymethyl-furfural in citrus juices. *Journal of Food Science*. 51(4): 1075.
- Lee, S. H. and Labuza, T. P. 1975. Destruction of ascorbic acid as a function of water activity. *Journal of Food Science*. 40: 370.

- Lee, Y. C., Kirk, J. R., Bedford, C. L. and Heldman, D. R. 1977. Kinetics and computer simulation of ascorbic acid stability of tomato juice as function of temperature, pH and metal catalyst. *Journal of Food Science*. 42: 640.
- Lemos, M. A., Oliveira, J. C., van Loey, A. and Hendrickx, M. E. 1999. Influence of pH and High pressure on thermal inactivation kinetics of horseradish peroxidase. *Food Biotechnology*. 13 (1): 13.
- Lenz, M. K. and Lund, D. B. 1980. Experimental procedures for determining destruction kinetics of food components. *Food Technology*. (2): 51.
- Liao, M-L. and Seib, P. A. 1988. Chemistry of L-ascorbic acid related to foods. *Food Chemistry*, 30, 289.
- Linton, M., McClements, J. M. J. and Patterson, M. F. 1999. Inactivation of *Escherichia coli* O157:H7 in orange juice using a combination of high pressure and mild heat. *Journal of Food Protection*, 62(3): 277.
- Machado, M. F., Oliveira, F. A. R., Gekas, V. and Singh, R. P. 1999a. Kinetics of moisture uptake and soluble-solids loss by puffed breakfast cereals immersed in water. *International Journal of Food Science and Technology*, 33 (3): 225.
- Machado, M. F., Oliveira F. A. R. and Cunha L. M. 1999b. Effect of milk fat and total solids concentration on the kinetics of moisture uptake by ready-to-eat breakfast cereals. *International Journal of Food Science and Technology*, 34 (1): 47.

- Mack, T. E., Heldman, D. R. and Singh, R. P. 1976. Kinetics of oxygen uptake in liquid foods. *Journal of Food Science*. 41: 309.
- Marcotte, M., Stewart, B. and Fustier, P. 1998. Abused thermal treatment impact on degradation products of chilled pasteurized orange juice. *Journal of Agricultural and Food Chemistry*. 46: 1991.
- Marcy, J. E., Hansen, A. P. and Graumlich, T. R. 1989. Effect of storage temperature on stability of aseptically packed concentrated orange juice and concentrated orange drink. *Journal of Food Science*. 54: 227.
- Marshall, M., Nagy, S. and Rouseff, R.L. 1986. In. The Shelf Life of Fruits and Beverages. Elsevier Science Publishers, Amsterdam.
- McIntyre, S., Ikawa, J. Y., Parkinson, N., Haglund, J. and Lee, J. 1995. Characteristics of an Acidophilic *Bacillus* strain isolated from shelf-stable juices. A research note. *Journal of Food Protection*, 58(3): 319.
- McLaughlin, N. B. and Pitt, R. E. 1984. Failure characteristics of apple tissue under cyclic loading. *Transactions of the ASAE*. 27: 311.
- Melnick, R. L. and Kohn, M. C. 2000. Dose-response analyses of experimental cancer data. *Drug Metabolism Reviews*. 32(2): 193.
- Meydav, S., Saguy, I. and Kopelman, I. J. 1977. Browning determination in citrus products. *Journal of Agricultural and Food Chemistry*. 25: 602.

- Mizrahi, S. and Karel, M. 1977a. Accelerated stability tests of moisture-sensitive products in permeable packages by programming rate of moisture content increase. *Journal of Food Science*. 42(4): 958.
- Mizrahi, S. and Karel, M. 1977b. Accelerated stability tests of moisture-sensitive products in permeable packages at high rates of moisture gain and elevated temperatures. *Journal of Food Science*. 42(4): 1575.
- Mizrahi, S., Labuza, T. P. and Karel, M. 1970a. Computer aided prediction on extent of browning in dehydrated cabbage. *Journal of Food Science*. 35: 799.
- Mizrahi, S., Labuza, T. P. and Karel, M. 1970b. Feasibility of accelerated tests for browning in dehydrated cabbage. *Journal of Food Science*. 35: 804.
- Mohr Jr., D. H. 1980. Oxygen mass transfer effects on the degradation of vitamin C in foods. *Journal of Food Science*. 45: 1432.
- Moshonas, M. G. and Shaw, P. E. 1987. Quantitative analysis of orange juice flavour volatiles by direct injection gas chromatography. *Journal of Agricultural and Food Chemistry*. 35: 161.
- Moshonas, M. G. and Shaw, P. E. 1994. Quantitative determination of 46 volatile constituents in fresh unpasteurized orange juices using dynamic headspace gas chromatography. *Journal of Agricultural and Food Chemistry*. 42: 1525.
- Nagy, S. and Rouseff, R. L. 1986. Citrus fruit juices. In: Handbook of food and beverage stabilization. Pp. 719. Academic Press, New York.

- Nagy, S. 1980. Vitamin C content of citrus fruit and their products: a review. *Journal of Agricultural and Food Chemistry*. 28: 8.
- Nagy, S., Chen C. S. and Shaw, P. E. 1993. Fruit Juice Processing Technology. Pp. 124. AGScience, Inc. Auburndale, Florida.
- Nagy, S. and Dinsmore, H. L. 1974. Relationship of furfural to temperature abuse and flavor change in commercially canned single strength orange juice. *Journal of Food Science*. 39: 1116.
- Nagy, S., Lee, Y., Wainish, Rouseff, R. L. and Lin, J. C. C. 1990. Nonenzymatic browning of commercially canned and bottled grapefruit juice. *Journal of Agricultural and Food Chemistry*. 38(2): 343.
- Nagy, S. and Randall, V. 1973. Use of furfural content as an index of storage temperature abuse in commercially processed orange juice. *Journal of Agricultural and Food Chemistry*. 21(2): 272.
- Nagy, S. and Smoot, J. M. 1977. Temperature and storage effects on percent retention and percent U.S. recommended dietary allowance of vitamin C in canned single strength orange juice. *Journal of Agricultural and Food Chemistry*. 25(1): 135.
- Naim, M., Striem, B. J., Kanner, J. and Peleg, H. 1988. Potencial of ferrulic acid as a precursor of off-flavours in stored orange juice. *Journal of Food Science*. 53(2): 500.

- Naim, M., Wainish, S., Zehavi, U., Peleg, H., Rouseff, R. L. and Nagy, S. 1993. Inhibition by thiol compounds of off-flavor formation in stored orange juice. 2. Effect of L-Cystaine and N-acetyl-L-cystaine on p-vinylguaiacol formation. *Journal of Agricultural and Food Chemistry*. 41: 1359.
- Nelder, J. A. and Mead, R. 1965. A Simplex method for function minimization. *The Computer Journal*. 7: 308.
- Nelson, P. R. 1983. Stability prediction using the Arrhenius Model. *Computer Programs in Biomedicine*. 16: 55.
- Nelson, W. 1969. Hazard plotting for incomplete failure data. *Journal of Quality Technology*. 1: 27.
- Nielsen, T. J. 1994. Limonene and Myrcene Sorption into Refillable Polyethylene Terephthalate Bottles, and Washing Effects on Removal of Sorbed Compounds. *Journal of Food Science*. 59(1): 227.
- Nielsen, T. J. and Giacini, J. R. 1994. The Sorption of Limonene/Ethyl Acetate Binary Vapour Mixtures by Biaxially Oriented Polypropylene Film. *Packaging Technology and Science*. 7: 247.
- Nispieros-Carriedo, M., and Shaw, P. E. 1990. Comparison of volatile flavor components in fresh and processed orange juices. *Journal of Agricultural and Food Chemistry*. 38: 1048.

- Palakow, D. A. and Dunne, T. T. 1999. Modelling fire-return interval T: stochastic and censoring in two-parameter Weibull model. *Ecological Modelling*. 121: 79.
- Parish, M. E. 1997. Public Health of Nonpasteurized Fruit Juices. *Critical Reviews in Microbiology*, 23(2): 109.
- Parish, M. E., Narciso, J. A. and Friedrich, L. M. 1996. Incidence of coliforms, *E. coli* and *Salmonella* associated with a citrus-processing facility. Presented at the 1996 IFT annual meeting, New Orleans, USA.
- Peleg, 1992. On the use of WLF model in polymers and foods. *CRC Critical Reviews in Food Science and Nutrition*. 32: 59.
- Peleg, H., Naim, M., Zehavi, U., Rouseff, R.L. and Nagy, S. 1992. Pathways of 4-vinylguaiacol formation from ferrulic acid in model solutions of orange juice. *Journal of Agricultural and Food Chemistry*. 40: 764.
- Peleg, H., Naim, M., Rouseff, R. L. and Zehavi, U. 1991. Distribution of Bound and Free Phenolic Acids in Oranges (*Citrus sinensis*) and Grapefruits (*Citrus paradisi*). *Journal of Science of Food and Agriculture*. 57: 417.
- Peraza, A. L., Pena, J. G., Segurajauregui, J. S. and Vizcarra, M. 1986. Dehydration and separation of grape pomace in a fluidized bed system. *Journal of Food Science*. 51: 206.
- Pettipher, G. L., Osmundson, M. E. and Murphy, J. M. 1997. Methods for the detection and enumeration of *Alicyclobacillus acidoterrestris* and investigation

- of growth and taint in fruit juice and fruit containing drinks. *Letters in Applied Microbiology*. 24: 185.
- Pieper, G., Borgudd, L., Ackermann, P. and Fellers, P. 1992. Absorption of aroma volatiles of orange juice into laminated carton packages did not affect sensory quality. *Journal of Food Science*. 57(6): 1408.
- Pinhatti, M. E. M. C., Variane, S., Eguchi, S. Y. and Manfio, G. P. 1998. Detection of acidothermophilic bacilli in industrialized fruit juices. *Fruit-Processing*. 7(9): 350.
- Poças, M. F. F. and Oliveira, F. A. R. 1998. *A Embalagem de Produtos Alimentares*. Federação das Indústrias Potuguesas Agro-Alimentares. Portugal.
- Potter, R. H., Bertels, J. R. and Sinki, J. 1985. Proc.Asetipak 85, Schotland Business Research, Inc., Princeton, N.J. In. Shelf Life Studies of Fruits and Beverages. Pp.755. Elsevier Science Publishers B.V.
- Quast, D. G. and Karel, M. 1972a. Effects of environmental factors on the oxidation of potato chips. *Journal of Food Science*. 37: 584.
- Quast, D. G. and Karel, M. 1972b. Computer simulation on storage life of foods undergoing spoilage by two interacting mechanisms. *Journal of Food Science*. 37: 679.

- Quast, D. G., Karel, M. and Rand, W. M. 1972. Development of a mathematical model for oxidation of potato chips as a function of oxygen pressure, extent of oxidation and equilibrium relative humidity. *Journal of Food Science*. 37: 673.
- Ragnarsson, J. O. and Labuza, T. P. 1977. Accelerated shelf-life testing for oxidative rancidity in foods - Review. *Food Chemistry*. 2: 291.
- Ramaswany, H. S. and Abbatemarco, C. 1996. Thermal processing of fruits. In: Processing of Fruits, Science and Technology. Vol.1 Biology, Principles and Applications. Somogyi, L. P., Ramaswany, H. S., Hui, Y. H. (Ed), Chap.2, Pp. 25. Technomic Publishing Co.
- Reuter, H. 1988. Aseptic packaging systems. In. Aseptic Packaging of Food. H. Reuter (Ed.). Chap.4. Pp. 110. Technomic Publishing Company, Inc., USA.
- Robertson, G. L. and Samaniego, C. M. L. 1986. Effect of Initial Dissolved Oxygen Levels on the Degradation of Ascorbic acid and the Browning of Lemon Juice during Storage. *Journal of Food Science*. 51(1): 184.
- Rodger, G., Hastings, R., Cryne, C. and Bailey, J. 1984. Diffusion properties of salt and acid into herring and their subsequent effect on muscle tissue. *Journal of Food Science*. 49: 714.
- Roig, M. G., Bello, J. F., Rivera, Z. S. and Kennedy, J. F. 1994. Possible additives for extension of shelf life of single strength reconstituted juice aseptically packaged in laminated cartons. *International Journal of the Food Science and Nutrition*. 45: 15.

- Rojas, A. M. and Gerschenson, L. N. 1997. Ascorbic acid destruction in sweet aqueous model systems. *Lebensmittel Wissenschaft und Technologie*. 30: 567.
- Sadler, G.D. 1984. A mathematical prediction and experimental confirmation of food quality loss for products stored in oxygen permeable polymers. PhD thesis, Purdue University, USA.
- Sadler, G. D., Parish, M. E. and Wicker, L. 1992. Microbial, Enzymatic and Chemical changes during storage of fresh and processed orange juice. *Journal of Food Science*. 57: 1187.
- Saguy, I. and Karel, M. 1980. Modeling of quality deterioration during food processing and storage. *Food Technology*. (2): 78.
- Saguy, I., Kopelman, J. and Mizrahi, S. 1978. Extent of Nonenzymatic Browning in Grapefruit Juice During Thermal and Concentration Processes: Kinetics and Prediction. *Journal of Food Processing and Preservation*. 2: 175.
- Saguy, I., Kopelman, J. and Mizrahi, S. 1978. Simulation of ascorbic acid stability during heat processing and concentration of grapefruit juice. *Journal of Food Processing and Preservation*. 2: 213.
- Sahbaz, F. and Somer, G. 1993. The effect of citrate anions on the kinetics of cupric ion-catalysed oxidation of ascorbic acid. *Food Chemistry*. 47: 345.

- Sakai, Y., Watanabe, H., Takai, R. and Hasegawa, T. 1987. A kinetic model for oxidation of ascorbic acid and beta-carotene. *Journal of Food Processing and Preservation*. 11: 197.
- Sawhney, R. L., Pangavhane, D. R. and Sarsavadia, P. N. 1999. Drying kinetics of single layer Thompson seedless grapes under heated ambient air conditions. *Drying Technology*. 17(1-2): 215.
- Schmidt, K. and Bouma, J. 1992. Estimating shelf-life of cottage cheese using hazard analysis. *Journal of Dairy Science*. 75: 2922.
- Seber, G. A. F and Wild, C. J. 1989. Growth models. In: Nonlinear regression. Chap. 7. Pp. 325. John Wiley and Sons, New York.
- Shaw, P. E., Buslig, B. S. and Moshonas, M. G. 1993a. Classification of commercial orange juice types by pattern recognition involving volatile constituents quantified by gas chromatography. *Journal of Agricultural and Food Chemistry*. 41: 809.
- Shaw, P. E., Nagy, S. and Rouseff, R. L. 1993b. The Shelf Life of Citrus Products. In. Shelf Life Studies of Fruits and Beverages. Pp. 755. Elsevier Science Publishers B.V.
- Shepherd, H. and Bhardwaj, R. K. 1988. Thin layer drying of pigeon pea. *Journal of Food Science*. 53: 1813.

- Singh, R. P. 1974. Computer simulation of liquid food Quality during storage. PhD thesis. Michigan State University. USA.
- Singh, R. P. and Heldman, D. R. 1976. Simulation of Liquid Food Quality During Storage. Transactions of the ASAE. 19: 178.
- Singh, R. P, Heldman, D. R. and Kirk, J. R. 1976. Kinetics of quality degradation: Ascorbic acid oxidation in infant formula during storage. Journal of Food Science. 41: 304.
- Snir, R., Koehler, P. E., Sims, K. A. and Wicker, L. 1996. Total and Thermostable Pectinesterases in Citrus Juices. Journal of Food Science. 61(2): 379.
- Solomon, O. 1994. Effect of oxygen and fluorescent light on the quality of orange juice during storage at 8 °C. MSc. thesis. Department of Food Science. Göteborg University, Sweden.
- Solomon, O., Svanberg, U. and Sahlström, A. 1995. Effect of oxygen and fluorescent light on the quality of orange juice during storage at 8 °C. Food Chemistry. 53: 363.
- Spittstoesser, D. F., Lee, C. Y. and Churey, J. J. 1998. Control of Alicyclobacillus in the juice industry. Dairy, Food and Environmental Sanitation. 18(9): 585.*
- Stamp, J. A. and Labuza, T. P. 1983. Kinetics of the maillard reaction between aspartame and glucose in solution at high temperatures. Journal of Food Science. 48: 543.

- Stein, E. R., Brown, H. E. and Cruse, R. R. 1986. Seasonal and storage effects on colour of red fleshed grapefruit juice. *Journal of Food Science*. 51: 574.
- Stewart, I. 1980. Color as related to quality in citrus. In: Citrus Nutrition and Quality. S. Nagy and J. A. Attaway (Ed.). ACS Symposium Series 143. American Chemical Society, Washington, D.C.
- Tannenbaum, S. R., Young, V. R. and Archer, M. C. 1985. Vitamins and Minerals. In: Food Chemistry. O. R. Fennema (Ed.). Pp. 489. 2nd Ed. New York: Marcel Dekker, Inc.
- Tatum, J. H., Nagy, S. and Berry, R. E. 1975. Degradation products formed in canned Single Strength orange juice during storage. *Journal of Food Science*. 40: 707.
- TetraPak. 1998. The Orange Book. Tetra Pak Processing Systems AB, Lund, Sweden.
- Toledo, R. T. 1986. Post processing changes in aseptically packed beverages. *Journal of Agricultural and Food Chemistry*. 34: 405.
- Toribio, J. L. and Lozano, J. E. 1986. Heat induced browning of clarified apple juice at high temperatures. *Journal of Food Science*. 51: 172.
- Trammell, D. J., Dalsis, D. E., and Malone, R. T. 1986. Effect of oxygen on taste, ascorbic acid loss and browning for HTST-pasteurized, single strength orange juice. *Journal of Food Science*. 51 (4): 1021.

- Van Boekel, M. A. J. S. 1996. Statistical aspects of kinetic modeling for food science problems. *Journal of Food Science*. 61(3): 477.
- Versteeg, C., Rombouts, F. M. and Pilnik, W. 1978. Purification and some characteristics of two pectinesterase isoenzymes from orange. *Lebensmittel Wissenschaft und Technologie*. 11: 267.
- Versteeg, C., Rombouts, F. M., Spaansen, C. H. and Pilnik, W. 1980. Thermostability and orange juice cloud destabilizing properties of multiple pectinesterases from orange. *Journal of Food Science*. 45: 969.
- Vieira, M. C., Teixeira, A. A. and Silva, C. L. M. 2000. Mathematical modeling of the thermal degradation kinetics of vitamin C in cupuaçu (*Theobroma grandiflorum*) nectar. *Journal of Food Engineering*. 43: 1.
- Villota, R. and Hawkes, J. G. 1992. Reaction Kinetics in Food Systems. Chap. 2. In: Handbook of Food Engineering. Dennis Heldman and Daryl Lund (Ed). Pp. 39. Marcel Dekker Inc., N.York.
- Walls, I. and Chuyate, R. 1998. Alicyclobacillus – historical perspective and preliminary characterization study. *Dairy, Food and Environmental Sanitation*. 18(8): 499.
- Walpole, R. E. and Myers, R. H. 1978. Probability and Statistics for Engineers and Scientists. 2nd Ed. Pp. 133. MacMillan Publishing Co, Inc. New York.

- Wang, X. Y., Seib, P. A. and Ra, K. S. 1995. L-ascorbic acid and its 2-phosphorylated derivatives in selected foods: vitamin C fortification and antioxidant properties. *Journal of Food Science*. 60(6): 1295.
- Weibull, W. 1951. A statistical distribution function of wide applicability. *Journal of Applied Mechanics*. 18: 293.
- White, D. R., Lee, H. S. and Kruger, R. E. 1991. Reverse phase HPLC/EC determination of folate in citrus juice by injection with column surtching. *Journal of Agricultural and Food Chemistry*. 39: 714.
- Wicker, L. and Temelli, F. 1988. Heat inactivation of pectinesterase in orange juice pulp. *Journal of Food Science*. 53: 162.
- Wilkes, J. G., Conte, E. D., Kim, Y., Holcomb, M., Sutherland, J. B. and Miller, D. W. 2000. Sample preparation for the analysis of flavours and off-flavours in foods- a review. *Journal of Chromatography A*. 880: 3.
- Wisotzkey, J. D., Jurtshuk, P., Fox, G. E., Deinhard, G. and Poralla, P. 1992. Comparative sequence analyses on the 16SrRNA (rDNA) of *Bacillus acidocaldarius*, *Bacillus acidoterrestris* and *Baccilus cycloheptanicus* and proposal for creation of a new genus, *Alicyclobacillus* gen. nov. *International Journal of Systematic Bacteriology*. 42: 263.
- Wolfram, S. 1996. The Mathematica Book. Pp. 467. 3rd Ed. Wolfram Media, Cambridge University Press.

Zapata, S. and Dufour, J.-P. 1992. Ascorbic acid, dehydroascorbic and isoascorbic acid simultaneous determinations by reverse phase ion interaction HPLC. *Journal of Food Science*. 57: 506.